Motor Learning Based Real-Time Control for Dexterous Manipulation of Prosthetic Hands

A thesis submitted to The University of Manchester for degree of

Doctor of Philosophy

In the Faculty of Science and Engineering

2022

Kemal Balandiz

School of Engineering

Department of Mechanical, Aerospace and Civil Engineering

Table of Contents

List of Figures

List of Tables

List of Abbreviations

Abbreviations	Meaning
ADL	Activity of Daily Living
ANN	Artificial Neural Network
AR	Autoregressive
BCI	Brain-Computer Interface
CNS	Central Neural System
DC	Direct Current
DIP	Distal Interphalangeal
DoF	Degrees of Freedom
DWT	Discrete Wavelet Transform
ECoG	Electrocorticography
ED	Extensor Digitorum
EEG	Electroencephalography
EI	Extensor Indicis
EMG	Electromyography
ENG	Electroneurogram
EPB	Extensor Pollicis Brevis
EPL	Extensor Pollicis Longus
ESI	Electrical Source Imaging
FDP	Flexor Digitorum Profundus
FDS	Flexor Digitorum Superficialis
FPL	Flexor Pollicis Longus
GMM	Gaussian Mixture Model
HMI	Human-Machine Interface
HMM	Hidden Markov Model
IAV	Integrated Absolute Value
IEEG	Intracranial Electroencephalographic
IMES	Implantable Myoelectric Electrode System
IP	Interphalangeal
KF	Kalman Filters
K-NN	K-Nearest Neighbours
LDA	Linear Discriminant Analysis

LWPR	Locally Weighted Projection Regression
MAV	Mean Absolute Value
MCP	Metacarpophalangeal
MCV	Muscle Contraction Value
ML	Machine Learning
MNN	Multilayer Neural Network
MSE	Mean Squared Error
NB	Naïve Bayes
NLR	Nonlinear Logistic Regression
PCA	Principal Component Analysis
PIP	Proximal Interphalangeal
PNI	Peripheral Nervous Interface
PNS	Peripheral Nervous System
QDA	Quadratic Discriminant Analysis
RBFN	Radial Basis Function Network
RFS	Random Forests
R-LLGMN	Recurrent Log-Linearized Gaussian Mixture Network
RMS	Root Mean Square
RMSE	Root Mean Squared Error
SC	Status Changes
SPM	Spectral Power Magnitudes
SSC	Slope Signal Changes
STFT	Short-Time Fourier Transform
SVM	Support Vector Machines
TC	Threshold Crossing
TD	Time Domain
TMR	Targeted Muscle Reinvention
WL	Wavelet Length
WLT	Wavelet Transform
WPT	Wavelet Packet Transform
WT	Wavelet Transform
ZC	Zero Crossing

Abstract

Myoelectric controlled prosthetic hands represent an effective tool to restore functionality and enhance the quality of life for upper limb amputees. Such devices provide sensing, multifunctionality and more natural control. In the current state of the art solutions, the control is mainly accomplished through sophisticated motions encoding by using machine learning algorithms for residual forearm muscles. Offline analysis and evaluation of motion detection accuracy for such algorithms on data sets are the main focus of current studies. However, there is a significant gap between laboratory evaluations and system integration in the complicated real-time environment. Because a sufficient and comprehensive analysis of complete prostheses requires a sophisticated synchronisation of data acquisition, motion classification, and timely prosthetic actuation with a wearable compact system, most prosthetic control lack the robust interface to facilitate all required functionalities in an acceptable manner for the majority of users. Even if advancements in data integration and computational power enable high prediction accuracy, the practical implementation of such technology is still being challenged by various influences, particularly those related to the fact that the signal sources are biological signals that change considerably by limb position, variations on muscle contraction, electrode shifting and amputation level. Therefore, most of the existing prostheses are passive, and their dexterity properties remain fixed with limited object grasping and hand gestures.

This research presents the design of a bypass socket and integrated real-time control system based on pattern recognition algorithms to control a prosthetic hand. This study covers a compact system development beginning with investigating the anatomy and natural dexterity of the human hand, motor control, and human-like physical manipulation for data collection, going through the sEMG feature extraction and finally implementing adequate embedded pattern recognition on a prosthesis prototype.

A wide range of techniques such as sEMG signals, data gloves, and force sensors was employed to collect data from able-bodied subjects. Popular pattern recognition algorithms such as k-Nearest Neighbours (k-NN), support vector machines (SVM), linear discriminant analysis (LDA) and artificial neural network (ANN) were used to differentiate individual finger manipulations and hand motions. The performance of classifiers with different muscle observation approaches and a variety of feature extraction methods with two windowing sizes and the various number of the electrode was compared against the publicly available data sets and similar studies.

The offline analysis results led to a novel bypass socket design to minimise electrode shifting, causing difficulty to use during model training and inconsistencies between users, which increases motion detection errors between the desired and performed motions. New electrode arrangement by socket prototype ensured the transmission of the most significant input from all muscles and standardised data acquisition between sessions, particularly considering the real-time conditions with a limited source of signals to stump and dynamic arm orientation. It provides a sufficient approximation to pattern recognition since it resists elbow rotation and provides immense practicality to achieve an intuitive embedded system.

A combined dynamic data acquisition and control approach that yields high accuracy and robustness were implemented as the final strategy and tested in real-time with an able-bodied subject. The development of control architecture is based on how humans maintain control stability during dynamic arm orientation over time, particularly in different amputation levels. The system performance was tested with real-time evaluation metrics such as motion completion rate, motion detection accuracy, reach and grasp experiments and timing of the system to detect and execute the intended motion. A significant improvement was observed in path efficiency, motion completion rate and motion completion time.

The findings suggested that combining machine learning algorithms and dynamic data collection demonstrates high accuracy, almost 94% completion rate to predict the intended hand movement with 0.23 seconds of data processing and prediction in real-time. The real-time tests results from healthy subjects indicated that the applied control architecture enables users to intuitively and smoothly control prostheses based on EMG data without significant delay. This advancement suggests that significant gains in the robustness from the use of the dynamic control system alleviate the standalone classification approach.

In summary, data collection from dynamic arm posture and embedded control system with proposed bypass socket appears to be a promising approach for enhancing prostheses. The preliminary results demonstrated adaptability, facilitation, and simultaneous control of multiple joints without the requirement for retraining and switching between sessions.

Declaration

I declare that no portion of the work referred to in the thesis has been submitted to support any application for another degree or qualification of this or any other university or other institutes of learning.

Copyright Statement

Acknowledgements

I would like to acknowledge and thank all my experiment participants for their willingness and patience, and also those who have made significant contributions to the success of this research. I would like to especially thank my supervisor, Dr Lei Ren, for his support, guidance, and faith in me during this research and for allowing me to work in his fascinating research environment.

All members of the Ren group, past and present, who contributed, have created this fantastic atmosphere are much appreciated. Thanks to Dr Wei Guowu for his guidance, support, and constant encouragement through my PhD and special thanks to Dr Tingting Mu for her help and for guiding me to develop myself professionally.

This research would not have been possible without support from the Ministry of National Education, The Republic of Turkey. I am genuinely grateful to the committee member who awarded me the scholarship and made my doctoral study possible.

Other than the research group, there are few names I would like to send my sincere thanks to, for their support and friendship (and apologise to those who deserve to be called out but were missing); Yusuf Kurt, Tugrul Nalbantoglu, Embiya Yusufoglu, Mesut Bekirogullari, Lutfi Ozturk, Ulvi Karaca, Enes Aslan, Pinar Urhal, Mehmet Cagatay, Eda Arikan, Irem Kilic, Alvaro D Gaticadiaz, Celal Tiltay, Naim Deniz, Sibel Sari, Halil Yilmaz, Esmanur Baltaci, Oguz Yakut, Cagri Kaymak, Emre Ozyurt.

A special thanks to Emily Kendall, for her care and patience and her family for their support and encouragement over these years. I am thankful to Dr Lynne Kendall for her guidance and her role as a proofreader.

Most of all, I would like to thank my family for their unwavering love and support. To them, I dedicate this thesis.

Chapter 1 Introduction

The human hand demonstrates extraordinary dexterity to explore, control, and modify objects and their environment. It shows remarkable behaviour to execute a variety of movements precisely with the help of complex kinematic structure, tactile sensory system and bidirectional communication with the brain. On the other hand, upper limb amputation significantly limits human autonomy, and severe amputation can result in a range of psychological and physical difficulties among amputees [1].

In the past, as sensory technology and control techniques became more advanced, developing the dexterities of robotic hands has evolved and become more prominent. Whereas the ergonomic and cosmetic aspects remain important issues for most researchers, the priority of regaining prosthetic hand properties is ongoing in many studies. Many companies (e.g., CyberHand, Otto Bock, SmartHand, and Michelangelo Hand) and research centres have recently focused on offering active robotic hands for patients. Several studies have developed myoelectric prostheses by combining muscle groups/muscle synergies hypotheses. This approach has enabled to control the wrist and fingers by measuring EMG signals generated as a sequence of muscle contraction, indicating patterns related to intended hand functions. However, such devices suffer from limited dexterity, low degree of freedom, and underperformed in real-life conditions. Consequently, according to research, up to 30% to 50% of amputees cannot properly use their prostheses [2],[3].

Due to the complexity of dynamic and under-actuation, dexterous object manipulation with a high degree of freedom remains one of the significant challenges. In order to control sophisticated prostheses, the system needs a more advanced human-machine interface (HMI), including electromyography (EMG), electroneurogram (ENG) approaches, and appropriate data acquisition to interpret the raw data to robotics [4]. Furthermore, to mimic human hand behaviours and achieve high skills, a prosthetic hand must be capable of manipulating joints and simultaneously controlling independent fingers without significant time delay [5].

Several mechanically sophisticated myoelectric prosthetic hands have been presented to users by using the muscle synergies hypothesis [6], [7]. In this context, the robotic learning control approach has been obtained using various modern classification and regression methods such as artificial neural networks (ANN) and support vector machines (SVM) [8]. This new approach has influenced pattern recognition to be improved beyond basic activities such as close and open the hand, wrist flexion, and extension. It has moved further to a new trend to simultaneously identify muscle actions to control individual fingers. Such an approach can provide robust control and teach the robotic hand to adjust to unknown circumstances when required. However, it has been indicated that the pattern recognition technique associated with laboratory results to the real real world is not satisfying. According to the research [9] , the completion rate of real-time control by transradial amputees was 55%, while the classification accuracy was 85%. Thus, it has been suggested that the robust system in these algorithms is complicated and unreliable unless the real-time conditions are employed during model training.

This study presents a control system approach to overcome the main drawback connected to dexterous manipulation as proposed by [10],[11]: limited functionality, poor user interface, the accuracy of movement selection and response time delay.

The functionality of the prothetic was improved by detecting the thumb abduction and independent fingers motions led by small muscles group using new sensory distribution. This is important since, in most research, the collaboration of thumb muscles is disregarded, particularly during precision grasping, because it is difficult to detect and separate from other muscle groups. The compactness and real-time control are key points that significantly affect controllability and response time, eventually the patient's satisfaction. In this study, with the help of a synchronised embedded system, data acquisition, data processing, prediction and motion execution was achieved within 0,23 seconds.

In general, prediction accuracy is the most crucial performance parameter in prostheses. However, the majority of studies have used offline assessments such as accuracy, recall, and precision to verify their findings, which only evaluates the performance of algorithms rather than prostheses. Furthermore, these laboratory results do not satisfy real-time conditions because it is challenging to synchronise all devices in a physical world. Real-time validation tests were carried out using a bionic hand to assess motion selection and motion completion time in this research. In addition, to enhance the prediction performance of the prosthetic, sEMG data were collected from the subjects while performing several dynamic and static arm postures.

Finally, in particular, for individuals with a high level of amputations, the capability of performing a large variety of finger and hand motions is limited due to the lack of muscles and incompatibility of data collection. A machine learning model with appropriate parameters on sEMG with new sensory modality and the embedded system was developed to improve the finger and grasps classification (>90%) and improve the robustness of the prosthetic hand for high-level amputation. The developed bypass socket with the embedded control to conduct real-time tests is shown in Figure 1.1.

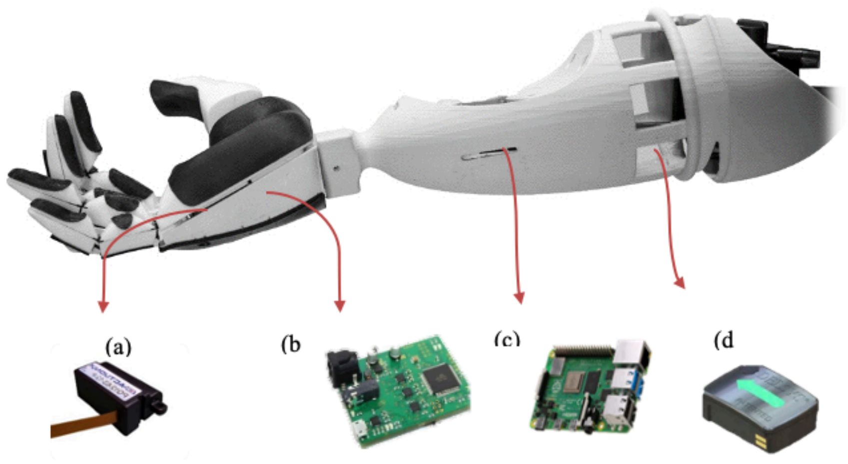

Figure 1:1: The main parts of the system: (a) linear actuator, (b) the mini controller, (c) mini PC, (d) EMG electrodes, custom-made prosthetic socket.

This study's original contribution was as follows:

1. Demonstrating that the generic approach with machine learning algorithms and feature extraction methods yielded the best prediction accuracy when using the proposed sensory modality and embedded control system.
2. Controlling a high degree of freedom prosthetic hand solely using sEMG data from upper limb muscles in real-time.
3. Creating a live pipeline between components to deliver real-time data (0.23 sec) and continuously producing human-like behaviour for prostheses.
4. Developing and testing a potential low-cost multifunctional prosthesis control with novel sensory distribution and wearable socket.

1.1 Research Aim and Objectives

This research aims to develop a motor learning-based control system that differentiates independent finger/hand motions and enables users to manage a multifunctional prosthetic hand in real-time.

The objectives to achieve the proposed aim are:

1. Investigate human hand physiology, biomechanics, motor control, and discover the interaction and basic logic between components for continuous control.
2. Research machine learning algorithms and feature extraction methods to discover how to transfer human hand skills to a system.

3. Design and conduct experimental protocol to examine the influence of sensory placements, number of electrodes, number of subjects and feature extraction methods on the pattern recognition performance.
4. Develop an alternative sensory modality and bypass socket prototype, and test its general applicability and robustness with dynamic arm orientations.
5. Create an embedded control architecture capable of collecting, processing, and differentiating user intentions and executing the projected motion with minimal time delay.
6. Validate the dexterity and robustness of the developed control method on a prototype using real-time performance metrics such as motion completion accuracy and motion completion time.

1.2 Thesis Outline

The structure of this thesis is organised as follows.

Chapter 1 provides an introduction of this study, stating the aim and objectives of the presented research and providing the outline of this dissertation.

Chapter 2 presents the studies that have been conducted in the field of upper limb prostheses to date, with the focus on electromyography-based prostheses. The literature review provides fundamental knowledge of anatomy and motor control of the human hand, and some control methods implemented in motion detection and prosthetic hand designs. This chapter also covered the fundamental paradoxes faced in this literature and their continuous improvement regarding stability and robustness.

Chapter 3 describes the methodology followed, including the experimental setup, instruments, and automated used methods. Detailed information on data collection, feature extraction, and labelling of data are provided.

Chapter 4 gives general reviews of appropriate data acquisition and popular machine learning methods for hand manipulation. This chapter's focus is evaluating eight different time-domain features for data acquisition and four classification techniques to map the kinematic and dynamic motions of the human hand. A comparative approach was taken to demonstrate the effectiveness of classifiers and extracted features regarding high accuracy and low computational cost in various static arm positions. The effects of windowing length on classification accuracy is also presented in this section. This chapter is quite important, since this data representation underlines stochastic control in the following chapters.

Chapter 5 introduces the ideal testing conditions to improve the classification accuracy of myo-signals, mostly affected by interferences in real amputees' lives. Considering the classification accuracy concerning different arm positions and feature extractions methods, we analysed the direct effects of electrode placement on motion detection with a designed custom-made socket to identify the uncertainties. In particular, the main motivation behind dexterous manipulation and the necessity of stochastic control in the field is emphasised. The need for the new socket design with positive and negative points are presented and discussed.

Chapter 6 presents testing and validation results of control strategy on a developed prototype, a combination of commercially existing devices and new modifications. The performance of the real-time data acquisition and control in various iteration and learning approaches are analysed. This chapter provides real-time testing metrics and detailed evaluation of acquired data on a tendon driver robotic hand. The main purpose of this chapter is to achieve robust control that imitates motions from human counterparts.

Finally, **Chapter 7** presents the study's implications and highlights the links between research objectives and their answers. It addresses overall contributions, work carried out in this research and summarises the raised question drawing from the study's limitation. It brings a conclusion to this thesis and provides an outlook for possible future works. The above structure and the relations among the chapters are illustrated in Figure 1.2.

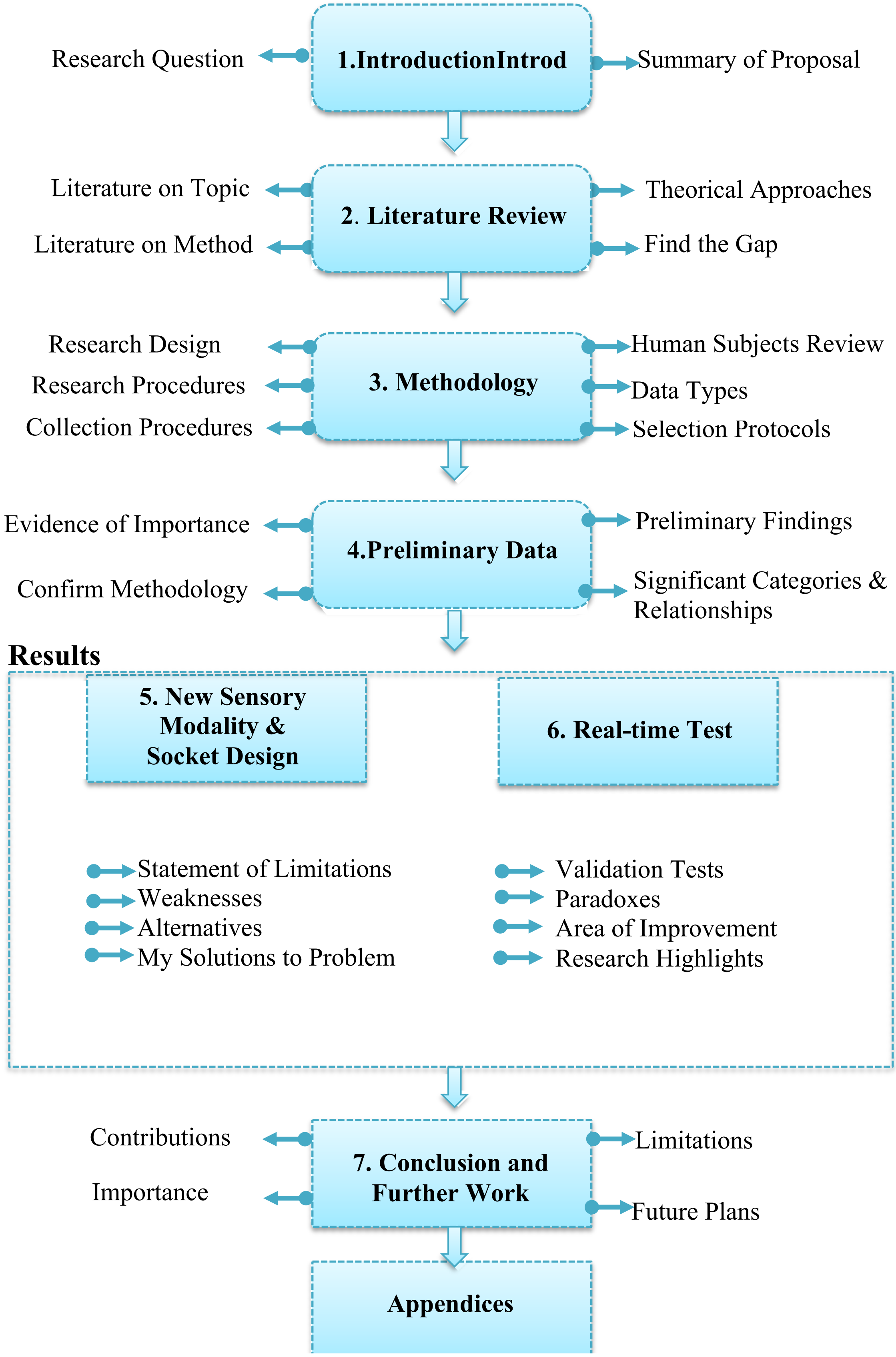

Figure 1:2: Flow chart of the research.

Chapter 2 Literature Review

2.1 Introduction

There have always been attempts to develop a multifunctional robotic hand to provide the human hand's full functions. There was no particular effort or funding to develop multifunctional prostheses from the beginning of the 21st century until World War II. In the 1960s and 1970s, there has been more investigation and funding to develop externally driven dexterous arm-hand systems. In general, upper limb prostheses have advanced significantly; however, because of the human-computer interface (HCI) limitation, the existing devices have significant challenges in providing the flexibility and function of biological hands. The statistic indicated that the electrical prostheses rejecting rate are around 30% [12] due to lack of reliability, high cost, and poor functionality [13].

According to a survey, nearly 2 million amputees live in the USA [3], which was estimated to be doubled by 2050 [14]. The arm amputation levels are 57% for transradial and 23% for transhumeral, respectively, with the right limb being more frequently affected due to work-related injuries or illnesses [15]. Although some advanced prosthetics hand have been developed, the cost of these devices varies from $25,000 to $75,000 [16], [17]. Considering these highlighted statistics, it is not surprising that a vast amount of researchers are focusing on improving the intuitiveness and robustness by working towards EMG based dexterous manipulation with sensory feedback.

While numerous concepts and attempts have been made in the field of prosthetics, only a few procedures and technologies have been widely accepted and moved from laboratories to everyday clinical usage. Whereas most commercially available devices are based on (on/off) control or basic proportional control, modern multifunctional and hybrid prostheses now satisfy the demands of users. In multifunctional dexterous prostheses, classifiers are offline trained by collecting data while repeating the number of specified movement's classes. The trained models are established sequentially in either online or offline implementation, in which the user takes action based on sets of EMG features. When the user gesture is identified, a control command from the prediction is sent to the controller, which then executes the full motion [18].

This chapter discusses the current methods used for upper limb prostheses control and their potential improvements. First, human hand biomechanics and the central nervous system (CNS) were presented and thoroughly examined. Furthermore, most studies on the integration of human-machine interface and advancement in clinical and real-time control, particularly related to EMG-based assistive devices and their foundation formed the prostheses, were investigated. The most critical challenges and gaps in existing devices, such as the complexity of human-machine interfaces, signal acquisition and operating modes, were also introduced. Finally, the potential solution with particular attention to muscle synergy and ML-based pattern recognition that mainly operate with either EMG, iEMG or both were discussed. The purpose is to enlighten the reasons initiating the development directions adopted in developing the control architecture presented in this thesis.

2.2 Biomechanics of Human Hand

The human hand has 27 major bones, at least 18 joint articulations and more than 30 active muscles performing with 27 degrees of freedom (DoF). It empowers people to interact with objects, manipulate and modify their surroundings. In all of these capabilities, the human brain efficiently deals with the complexity of the degree of freedom of the kinematic system and the complications of mechanoreceptors, which play a critical part in encoding the timing, quantity of torque, and magnitude of distribution in finger joints.

In humans, control and manipulation abilities are associated with advanced sensory (receptor) and actuator (muscle) systems. Mimicking this synergy is a challenging and time-consuming undertaking. In robotics, the concept of advancing prosthesis control using haptic technologies that contribute to the effective management of desired activities has gained popularity. The majority of current researches aim to maximise the effectiveness of limited inputs while minimising duplication in order to identify the natural performance of the human hand [19].

The hand movements are guided by a succession of muscular contractions that provide the necessary force. The hand muscles are multi-articulate, which implies that each muscle may command more than one degree of freedom. When the person moves his/her fingers, the tendon slips across the bones, producing a range of hand movements. The human hand can move at a rate of more than 40 rad/s (2290 degrees/s), and a healthy hand gripping can use up to 400N (90 lbs) of muscular strength. The average speed of daily living tasks (picking and placing) has been measured in an average range of 4rad/s (172 degrees/s to 200 degrees/s). The prehension force activity of daily living tasks (ADL) varies up to 67 N (15lbf). These properties are reliant on the interaction between the grasping surface and objects [3].

Studies in neuroscience [20], [21] have suggested that the central neural system (CNS) has a control mechanism that links the inner world of our motor system to the physical environment. The brain's perception and knowledge, which transfer through the motor system to muscles to create force and trajectory in the physical environment, infer human intention for the unknown environment. The sensory feedback recreates the human response simultaneously while natural movements are performed in a close control loop. This sophisticated control offers new insights for understanding human hand behaviours and new perspectives for unique designs concepts that could be employed in the robotics system. A control model that includes intricacies of the physical environment may enhance the naturalness of prostheses.

Although some anatomical properties of the human hand and motor behaviours were successfully reproduced in several pioneering research, conventional concepts of these designs have been challenged by experimental results. Compared to the human hand's performance, currently presented artificial mechanisms and learning methods are far from ideal properties such as speed and force can achieve clinical performance speeds of of 3 rad/s and forces of 110 N (25 lbs), none of these devices can reach human-like manipulation and control level.

2.3 Upper Limb Prostheses

Prostheses are devices that have been developed to replace the loss of a specific limb in the human body. A considerable proportion of commercial prostheses for hands and legs with feet are in the early stages have been created for aesthetic objectives. However, with rapid advancements in robotics and control, it has become possible to improve functionality and construct articulated dexterous prostheses. Thus, according to the interaction between patient and devices, prostheses can generally be divided into two groups as active and passive prostheses. The passive prostheses have been further subdivided into two categories as aesthetic and functional. Prostheses have been designed as aesthetic is accompanied by the healthy hand in such tasks requiring two hands. The passive functional hands have been designed to perform such specific tasks where users can use various end effectors [5]. On the other hand, body-powered active prostheses can be controlled by body activation, in which either body motion or electrical activation actuates the mechanism. Electrically powered prostheses can also be subdivided into three types, based on the control method:

a. ***Myoelectric Prostheses*,** group of electrically activated devices controlled by the electromyographic (EMG) signal determined from the surface of muscles through electrodes placed on the muscle belly [9];
b. ***Button controlled prostheses***, types of recently introduced devices in which different functions and motions are manually activated by buttons or software applications with the help of the remaining hand or muscles [9];

c. ***Multifunctional hybrid prostheses,*** which are high-performance prostheses, combine different data acquisition methods and machine learning techniques for sophisticated control and precise manipulation [22].

Figure 2.1 illustrates a diverse group of prostheses based on activation and control policies. Passive prostheses have a simple man-machine interface without any direct information from the user's body, and intended activation is sent to devices that do not have any feedback and may or may not affect prostheses performance. However, active prostheses use different activation approaches and complex man-machine interfaces. This group of prostheses was separately discussed in the next section (section 2.3.2.2). To simplify the variety of concepts, methods, and implementations of different approaches, another section (section hybrid prosthesis) was created.

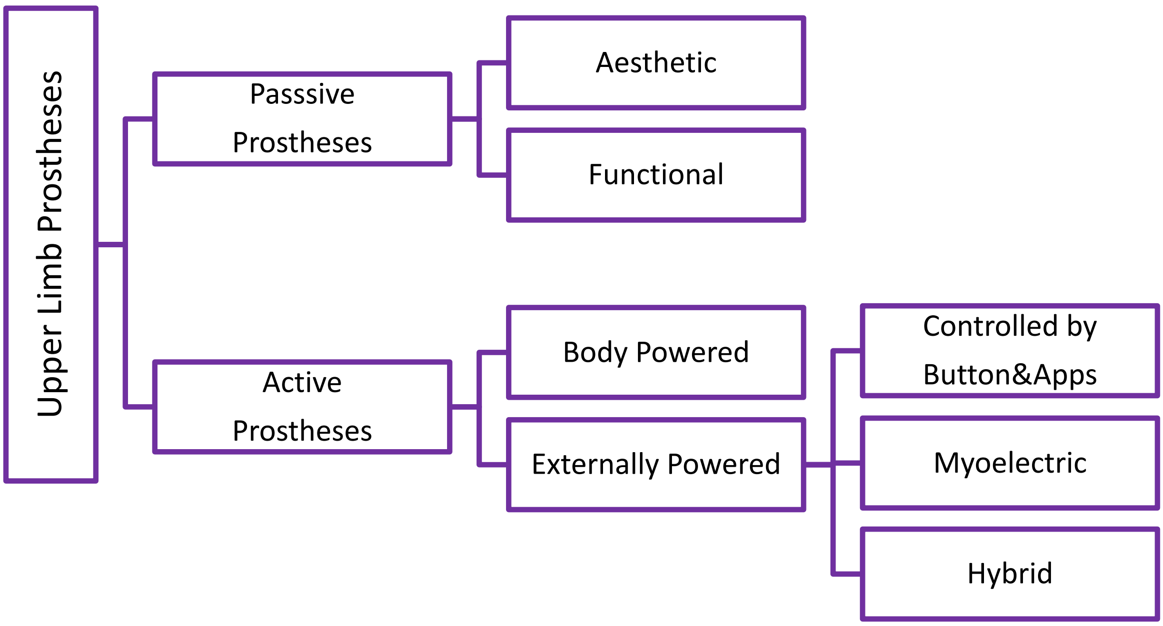

Figure 2:1: The diagram of different types of prostheses.

2.3.1 Passive-Unpowered Prostheses

Passive prostheses are a group of prostheses and instruments that are either static or adjustable and do not provide users a wide variety of functions. Devices in this category include semi-active hands and customised tools. There are numerous varieties of passive prostheses described in the literature, and they are frequently referred to by various names and phrases. Passive prostheses are classified into two types: aesthetic and functional. The main advantage and disadvantage of passive protheses is presented in table 2.1.

2.3.1.1. Functional Prostheses

Regarding cosmetic purposes, these passive hands are covered with a cosmetic outer glove and soft plastic. Highly realistic hands are preferably painted and individualised for different sizes and colours. These custom designed passive prostheses serve only one function or incorporate specialised features to assist a specified task. This group of devices can adapt from tools and may lead to more than one function. In the past, due to the lack of sophisticated control, amputees operated their devices for non-prehensile work, pushing and pulling objects. Device capacity is frequently defined as the mode of prehension functions that are mainly employed in daily life. Figure 2.2 demonstrates prehension patterns and equivalent passive devices (tools) [3].

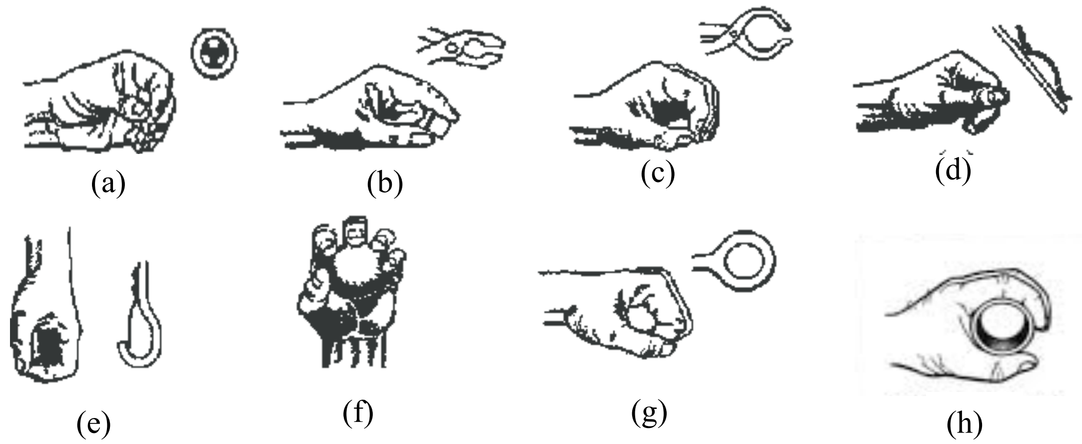

Figure 2:2: Schematic of the prehension patterns of the passive prostheses (a,b) palmar prehension, (c) tip prehension, (d) lateral prehension, (e) hook prehension, (f) spherical prehension, (g,h) cylindrical prehension (Reproduced from [3]).

2.3.1.2. Aesthetic Prostheses

According to the literature, this class of prosthesis has been classified into two groups: static and dynamic appearances. The surface's shape, colour, and finish were assigned to the static group. On the other hand, the dynamic group is associated with the mechanical device's motions and determines which functions are carried out. This form of prosthetic hand required manual labour, with the aesthetic aspect taking precedence over the functional aspect. According to Biddis *et al.* [12], this type of prosthesis must have two qualities: first, it must be undetectable, and second, it must make the user feel comfortable while wearing it. The role of this prosthesis in regular life is described as passive adaptive, meaning it provides stability, pushing, pulling, and holding in a passive manner. According to Kejlaa *et al.* [23], the primary motivations for using aesthetic prostheses are mental comforting rather than daily activities. Aesthetic prostheses are commonly utilised in social situations because they boost self-esteem and allow users to engage in both professional and social activities.. Figure 2.3 shows an example of the aesthetic passive prosthesis.

Figure 2:3: Passive aesthetic prosthetic had [reproduced from [24]].

Aesthetic prostheses are lightweight, and the socket system is only required to keep them in place. However, regardless of functioning, various dissatisfaction has been reported for this group of prostheses, such as heat issues on the socket part, glove complications, and difficulties wearing clothes. The primary prostheses design, as well as their pros and limitations, are summarised in table 2.1.

Table 2:1: Variety in Upper Limb Prostheses

Type	**Main Advantages**	**Main Disadvantages**
Passive	Lightweight. Best cosmetic appearance. Less harnessing.	High cost due to custom made design. No function or least function. Low cost glove strain easily.
Body Powered (Active)	Moderately costly. Moderately lightweight. High durability. Various prehensor is available for a number of activities.	The number of body activities needed to operate. High harnessing. Least user satisfaction for cosmetic appearances. Limited sensory feedback.
Battery Powered & Hybrid	Least or no harnessing. Moderate body motion required for operation. Moderate satisfaction for cosmetic appearances. Maximum functionality.	Heaviest. High cost. Complex maintenance. Long therapy time for training.

2.3.2 Active Prostheses

2.3.2.1 Body Powered Prostheses

The body-activated or body-powered prostheses are designed to perform such specific movements mechanically. The user operates the device by a cable attached to the shoulder or torso, and the planned action is translated directly into the remaining limb. The main drawback of this interface type is that the user can only open and close a claw as an end effector. The advantage of these prostheses is that it provides simple and intuitive control in a low degree of freedom [22]. In most body-activated devices, the user uses his/her muscles to operate the device, generally by a cable known as Bowden cable. This device has two parts, housing and an inner tension cable. The housing part connects two endpoints as a flexible bridge. The cable is custom-designed with constant length regardless of motion and slides through the housing part.

After World War II, the Bowden cable was improved to design active prostheses for the United States veterans. In the terminal fitting, the cable pass through the prosthetic joints between two endpoints, and the physiological joint actuate the prosthetic joint. Some simple modification on the Bowden cable has been done over the years and is still used nowadays [3]. Figure 2.4 illustrates the body-powered prostheses based on the activation and control scheme.

(a)

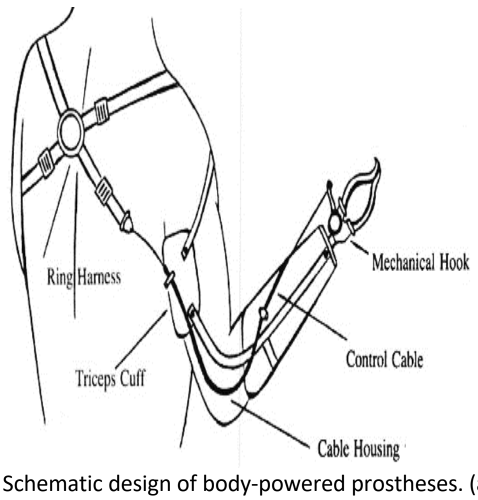

(b)

Figure 2:4: Schematic design of body-powered prostheses. (a) flexion by body forward motion, (b) shoulder depression for extension control (Reproduced from [3]).

2.3.2.2 Multifunctional Prostheses

2.3.2.2.1 **Myoelectric Prostheses**

Myoelectric control has been extensively used since it was introduced in the 1940s, and there is comprehensive literature outlining the different approaches of using EMG's characteristics and properties. Historically, this has been considered a new age for prostheses technology. It has been improved as an intuitive method for natural control of prostheses since the same principle is applied to the mammalian to command their physiological limb. The basis of this approach is that it captures electromyographic signal (EMG) from electrical actions of muscles through sensors from the skin surface (non-invasive) or directly implements into muscles (invasive method). The process transforms a set of impulses and stretches in muscles fibres into physical actions, each of which could be modelled with a machine learning model or a transfer function.

Numbers of processing methods of EMGs, such as amplification, rectification, and thresholding, have been applied to provide a DC signal representing the muscle contraction level to control the prosthesis. Traditional myoelectric control has one or two electrodes and reference electrodes, and EMG electrodes are positioned on the surface of the skin near the agonist and antagonist pair of muscles. One of the most positive points of this method is that it acts as a natural control of limbs, even there is only one way of information translation (from user to prosthesis).

However, some drawbacks of the non-invasive method have been emphasised in the literature. For example, EMG data collection can be affected by several factors, such as the placement of electrodes, noise from the line, and skin surface. Training time, misclassification rate, and amputation level, such as unilateral and bilateral, are other negative points of this interface. The alternative data collection method (invasive method) can provide some advantages since it receives information directly from muscles. However, this alternative method is costly and for some clinical issues, such as infection and healing time, so it is unfeasible and cannot be applied to all users [22].

Chronologically, the first samples of electronically actuated hand prostheses were introduced by Reinhold Reiter in 1948 after the Second World War [25]. These early-stage myoelectric hands used on/off control to initiate actions. To determine a suitable activation threshold from a group of muscles, engineers have used the various intensity of muscular contractions. The magnitude of sEMG rises as muscle tension increases. The correlation is complex nonstationary, non-linear and associated with many factors, including the position and orientation of sensors and noise. Although the electromyographic signal is non-linear, broadly monotonic, the user recognises this response as linear with the help of some signal processing techniques. This method has been used in literature with different control methods such as on/off, proportional control, or finite state machines.

The simple control approach of the method allows some actions, such as a slight contraction to flex fingers, stronger contraction to extend fingers, and no muscle contraction, to bring the device to initiate position [8]. Figure 2.5 and figure 2.6 demonstrate the processed signal to control prostheses.

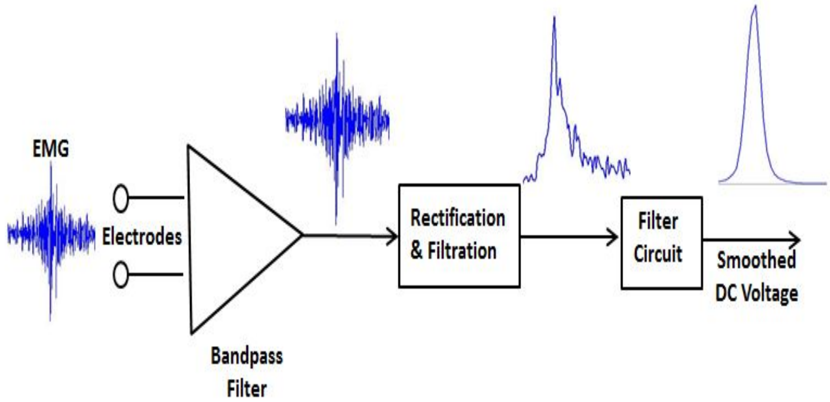

Figure 2:5: Conventional myoelectric signal processing with one channel sEMG.

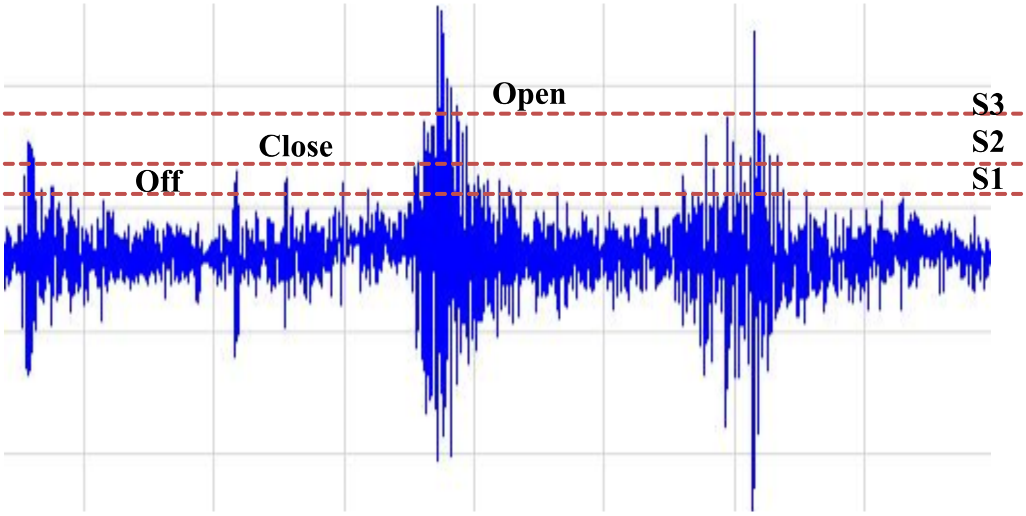

Figure 2:6: One channel EMG amplitude-based prosthesis control scheme.

The same control logic has been applied to two opposing muscle groups, such as flexor and extensor muscles in prosthetic devices [11]. Several thresholds have been used to differentiate which EMG activity is relevant and eliminate unwanted noises. Even though both methods are fast and applicable to real-time control, the number of movements is limited, and the control is unlike smooth action to the human hand. Figure 2.7 demonstrates the processed EMG signals to control the prosthesis from two sides of the myoelectric.

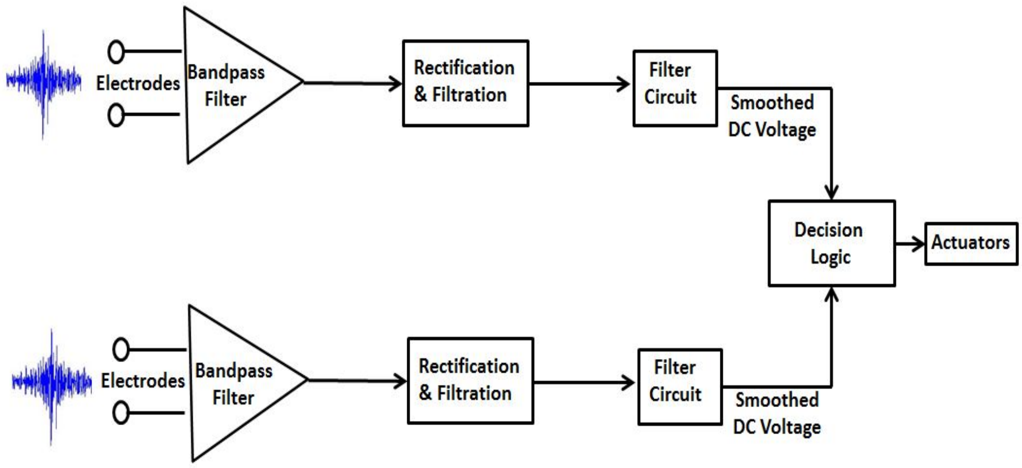

Figure 2:7: Standart myoelectric processing scheme in two sites of myoelectrical control.

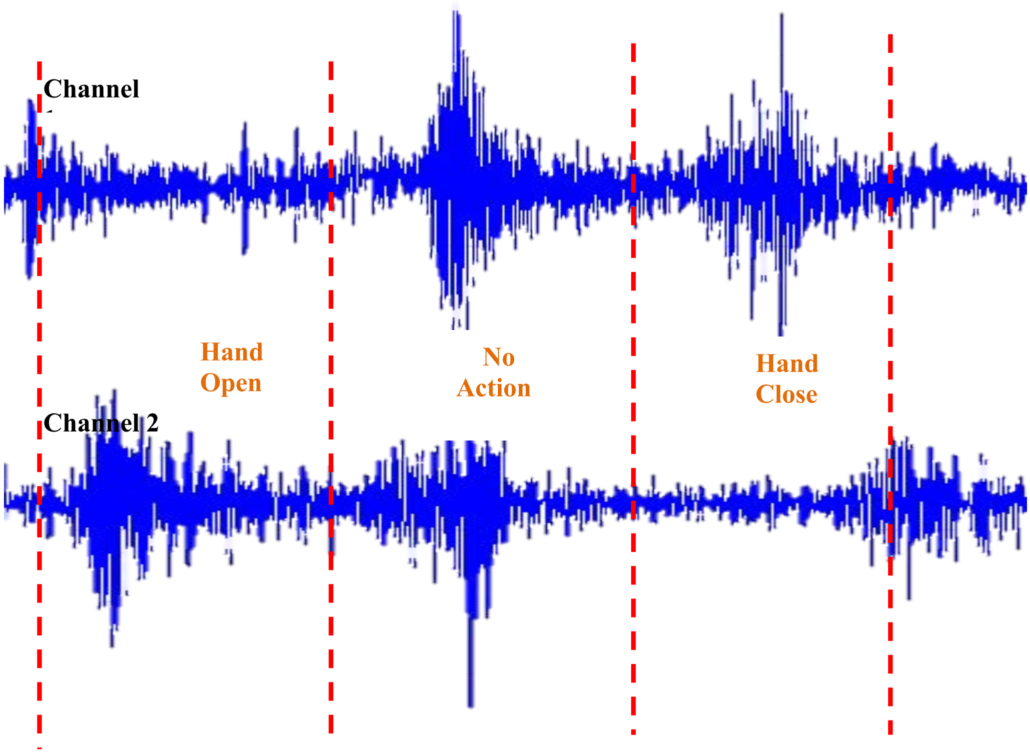

Figure 2:8: Two-channel sEMG based prostheses control scheme.

An alternative method to on/off control has been proposed by [15] and [16]. The aim was to vary the device action's velocity and force continuously and proportionally to the recorded EMG signals from opposing muscle groups. This method has been recently used as proportional control. One of the mechanical outputs, such as force, velocity, or position, varies by user input within an essential continuous interval. This approach is being used in many clinical devices [17]. Although this method is mainly accepted for several movements, it is unsuitable for dexterous manipulation, such as individual finger manipulations.

Since surface EMG signals are very weak at approximately 100 mV, these signals have been amplified and ranged between 1 to 5 V before they have been used. Amplifiers have been used to remove common signals and leave signals with capacity differences between two sensors. A DC signal is created after main EMG signals have been amplified and bandlimited using some non-linear signal processing, such as rectification or squaring. In order to obtain an on/off control, voltage is smoothed and compared with a logic circuit. The activation command is sent to the actuator when the amplitude is higher than a threshold value; otherwise, it remains off

Most of the traditional upper limbs use pair muscles, as shown in figure 2.8. The described control method allows one degree of the freedom movement to be activated at a time. Another technique, called direct control, has been developed by [18] to accomplish more delicate movements by mapping individual EMG signals to the particular prosthetic activities. However, this technique needs to overcome the interference of many muscles contracting together, which causes crosstalk of the EMG signal and reduces individual muscle force [19].

This method performs well if one degree of freedom is expected, such as transradial amputee. On the other hand, if the wrist rotation is required, the patient must externally shift as described in the previous method or co-contract the forearms muscles to switch from one state to another. This method is not recommended since switching mode is slow and not robust. Other techniques, such as target muscle reinforcement or EEG control, have been used in those circumstances. Furthermore, using the same muscle pairs to control different joints is not straightforward for users to learn because the employed muscle might not be autonomously correlated with the joint's degree of freedom. For example, biceps and triceps muscles could be associated to control finger motions [26].

In another alternative control approach, muscles' amplitude from a relaxed state to a fully contracted state is distributed to three different segments, as described in figure 2.8. Each of these segments is associated with different specific activities. This method is inappropriate because users need to keep muscle contraction in the constant amplitude, which is biologically not straightforward.

Nowadays, considerable progress in multifunctional prostheses with high degrees of freedom has been made. Several active prostheses with wrist articulations are under improvement or in clinical tests. Touch Bionic has introduced a multifunctional prosthetic device with individually controlled joints for finger and thumb manipulation. Otto Bock and CyberHand have also been offering various functions to users. However, these new devices do not offer human-like robustness without sophisticated control methods that allow users to control joints individually. Figure 2.9 shows the advanced poliarticulated myoelectric hands.

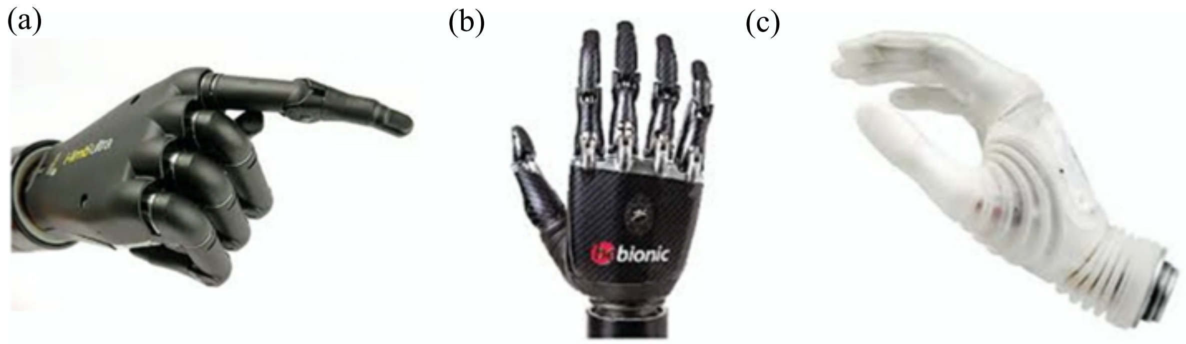

Figure 2:9: Commercially available prosthetic hands. (a) i-Limb [27], (b) Be-bionic [7] and (c) Mihellangelo hand[28] .

Recently, I-LIMB [6] has introduced a multi-articulated five fingers hand. This device is one of the most advanced prostheses with individual finger manipulation mode. However, in the control aspect, the prosthesis is controlled traditionally with two inputs EMG signal, switches into different modes via a mobile application that is not different from other commercial devices. Furthermore, another drawback of these prosthetic hands is that there is no sensory or tactile feedback to improve the users' experience, and the only sensory system is based on the user's vision. As aforementioned, these limitations influence device acceptability significantly [7], [8].

Consequently, existent upper limb prostheses are mostly limited to previously described simple functions, such as power grip or flexion, extension, significantly far from dexterous and multifunctional control. From this perspective, a new pattern recognition control approach, hybrid control, has been introduced to overcome these multifunctional control limitations [23], by offering more functions, even using the same number of sEMG channels [26].

One of the factors causing the rejection of EMG based control prostheses is the unsatisfactory user interface and lack of robustness. Many attempts have been made to improve the robustness of prostheses [29]. They have improved the motion recognition rate by using a mixture model with feature extraction to classify several hand grasps and individual finger manipulations. This group of prostheses require external control activation to drive various motors in joint movement. The number of active joints can be increased or decreased manually via buttons/switches, software applications, or a pressure sensor placed on the muscle to trigger different functions (see Figure 2.10). They suggested that this switching mode could address some main challenges related to the non-linearity of EMG signals and dynamic arm orientations. Recently, mobile applications have commonly been used to easily and quickly change the prosthesis configuration without having a computer connection. These communications methods have advantages in the degree of freedom; however, the training time is long and is not robust [22].

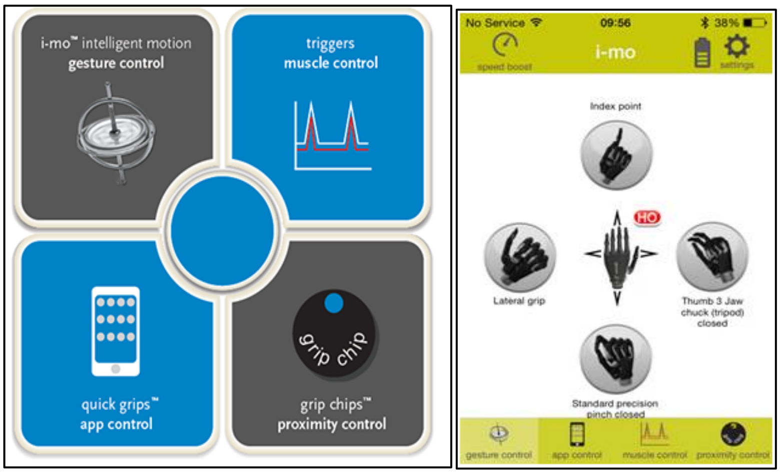

Figure 2:10: Gesture control of i-limb quantum upper limb prosthesis (Reproduced from [6]).

2.3.2.2.2. **Hybrid Prostheses**

Design and control of dexterous hands for multifunctional manipulation are exceedingly difficult due to dynamic complexity, under-actuation and control states. Although some multifunctional devices have been proposed in the past, most of these devices are controlled by direct control methods or on/off control [30]. Improving signal quality and providing prostheses for high-level arm amputation (such as transhumeral amputation or shoulder disarticulation) shown in figure 2.11 requires sophisticated and additional methodologies.

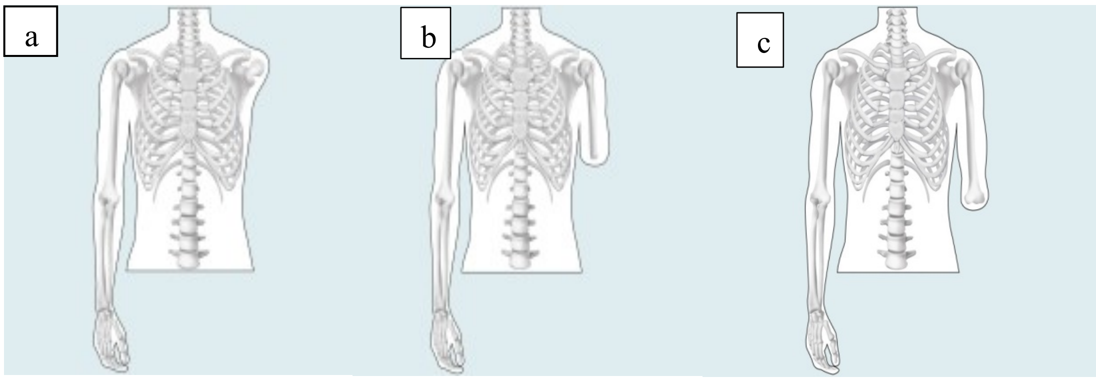

Figure 2:11: Different levels of amputations (a) Shoulder disarticulation, (b) Transhumeral amputation, (c) Elbow disarticulation (Reproduced from [6]).

This section presents the most commonly used methods to address operating and learning dexterous manipulation problems for hybrid data collection. They are (as shown in Figure 2.12) peripheral neural interface (PNI), targeted muscle reinvention (TMR) and brain-computer interface (BCI) [31].

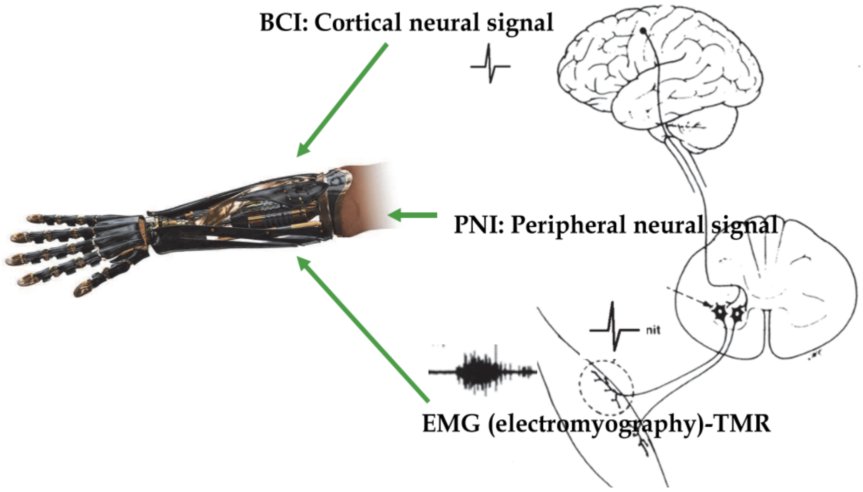

Figure 2:12: Three neural machine interfaces of neuroprostheses (Reproduced from [18]).

2.3.2.2.2.1 Neural Control Prostheses

The traditional myoelectric control method has major restrictins for controlling high-level arm amputetion due to the lack of control signals associated with arm movements. Furthermore, many patients have difficulty repeating muscular contractions or producing isolated EMG signals, and also electrode shifting and skin conditions can affect sEMG, making control unreliable. A new approach called neuroelectric control has been considerably investigated and used for neural control of multifunctional prostheses [32]. In a neural-based control prosthetic hand system, the subject's intention for movements is detected from neural or invasive muscular signals using epimysial or superficial electrodes. Extraction of a neural signal can be detected around or inside the nerve. Several of the challenges associated with surface EMG recordings can possibly be alleviated by implanted electrodes. They can resist many external influences surface readings, allowing for more reliable data sources and continuous management. Furthermore, these implanted sensors can collect prioritised EMG signals from muscles, enabling intuitive control of prostheses.

After discovering activities related to limb movements are operated in the brain (M1 and S1) cortical area, the pioneering work by [33] was conducted to control a prosthetic hand through the intraneural electrodes. Rossini *et al.* [34] have used electroneurographic (ENG) signals to operate a robotic hand and deliver sensory feedback by implementing a classification technique. Recently, Raspopovic *et al.* [35] have implemented intrafascicular electrodes into the nerve of amputees to acquire data to control the robotic hand and elicit sensation for force control. Young *et al*. [36] have achieved significant progress in developing implanted EMG recording for prostheses control. The critical point in this research is that the electrodes are wirelessly powered by magnetic field energy. A similar approach was followed by [37] using 32 electrodes; however, the test was done on the animal model rather than the human. The full functional prosthetic hand have been developed by Posquina *et al.* [38], using implantable electrodes. After six months of training, the participant who received the implants has managed to successfully perform 22 motions in real-time. Pioneering research has been conducted by Polasek *et al*.[39]. They have implanted the first chronically implant into the nerve cuff of and upper limb amputees for pattern recognition. More recently, George *et al.* [40] have developed bidirectional neuromyoelectric prostheses with close feedback sensory systems implanted. The EMG signals were collected from the residual arm to manipulate six degrees of freedom prosthetic hand independently. The design mimics the natural sensory feedback of human motor control. Figure 2.13 represents nerve intraneural interface for implanted sensor for prostheses control.

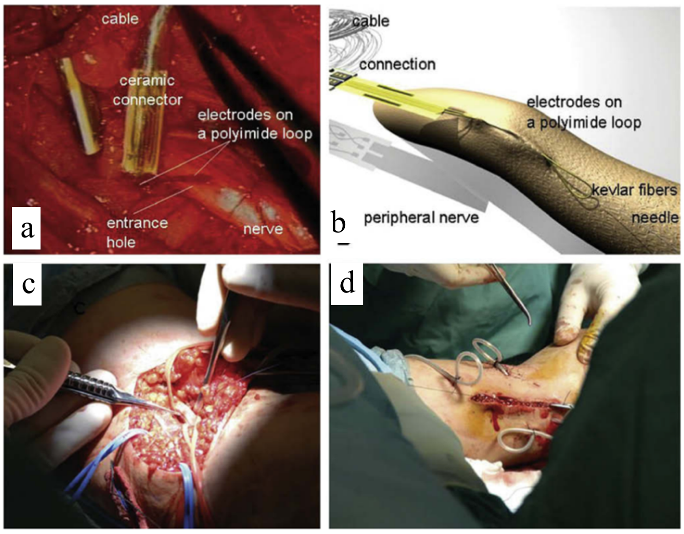

Figure 2:13: Implantation procedure of intrafascicular microelectrodes into nerve fibre. (a)microphotographic view (b)illustration of the method, (c)exposed median nerve (d)signal transit cable (reproduced from [34]).

Besides commanding prostheses, engineers and neuroscientists have developed a neural interface to enhance control abilities by ENG signals and by stimulating the PNS. Although the new concept improves control and sensory feedback efficiency, there are some significant concept problems, such as the nerve's size, sensors' performance, and recording difficulties. In addition, this method is only feasible for laboratory studies because of surgical issues and contamination by various noises in a surrounding environment.

There are some further problems in this method while transmitting the signal out of the body. Generally, percutaneous wires are used in this method, which can be easily infected by interferences. Finally, prosthetic hand control is required to perform for a long time (several years); however, the implanted hardware are not durably in service (maximum six months to one year), this is one of the critical issues [18].

2.3.2.2.2.2 Targeted Muscles Reinvention (TMR)

Implementing a multifunctional prostheses strategy to people with above elbow amputation is not straightforward since the remaining muscles in the residual arm for control are not accessible. To address this problem, the connection between prostheses and remaining muscles has been made by surgery, and this new surgical method is called targeted muscle reinvention (TMR). The arm muscles do not biomechanically function at any amputation level because of limb loss, but the nerve attached to those muscles is still active. With the TMR surgical method, the remaining nerves are transferred and reused as a motor command in myoelectric control. Firstly, the myoelectric signal muscle source is reinvented, and then it determines the nerve corresponded to intended movements [41]. Figure 2.14 schematically illustrates TMR techniques on the patient with shoulder disarticulation. This method is one of the most powerful man-machine interfaces, since users can intuitively and simultaneously control their prostheses. It has been proposed that patients who have TMR surgery can perform 16 different motions of the elbow, wrist, thumb, and fingers [22]. As an alternative method obtaining EMG signals and isolating and amplify signals to enhance amplitude, this method can overcome the problem of shoulder disarticulation. This method allows patients to manipulate multiple arm's degrees, using the standard reconstructive method without the need for implantable devices [42]. The method is now a clinically available medical procedure for upper-limb amputees, with more than 40 patients undergoing it around the world [43]. A recent study [44] has revealed the potential of TMR combined with pattern recognition methods in allowing people with above-elbow amputations to control a multifunctional prosthetic in real-time. After the surgery, the performance of the prostheses was evaluated using real-time control metrics such as block transfer, clothespin test. In order to compare the effectiveness of TMR method, Hargrove *et al.* [45] have conducted a series of real-time and virtual tests on Southampton hand using combined pattern recognition and TMR methods. With both virtual and physical tests, all 8 participants displayed the capacity to perform elbow/ wrist rotation and dynamic object manipulation. They claimed that subjects who have TMR surgery have statistically achieved better performance than direct control.

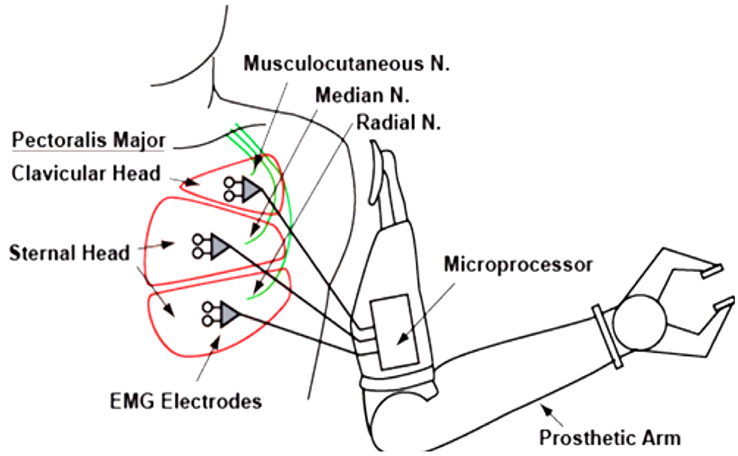

Figure 2:14: The targeted muscle reinvention method (Reproduced from [46]).

Notably, the TMR method does not only provide multifunctional control but also optimises the signal for focal control [47]. Clinical research showed that TMR contributes to a rich source of the external control signal, which improves classification accuracy and good repeatability [48]. Furthermore, some other promising technologies, such as implantable myoelectric electrode systems (IMES), could benefit from TMR. This telemeter system can alleviate some surface EMG signal issues to stabilise and make robust operation easier for advanced prosthetic hand systems [47].

Although TMR provides significant advantages over direct sEMG, some issues with myoelectric prosthesis control still exist. For example, current commercial systems depend on EMG volume and separating the surface EMG signals of distinct muscles is challenging. Furthermore, while the consistency of the EMG signal is still critical for a successful control, the TMR technique adapts the human brain to recognise that the prosthesis is a property of the body and provides an efficient interface to the user for self-development.

2.3.2.2.2.3 Brain-Machine Interfaces (BMIs)

The last sophisticated source of control information for prosthetic hands is BCI. The majority of current research in this field aims to provide control and communication to people with severe spinal cord injury or critical motor signal translation impairments. As technology advances and the hazards of implant placement reduced, such procedures can offer the opportunity for individuals in the future [49]. The brain-machine interface is a physical environment where electrical signals from the brain are detected and processed to control the prosthesis. Two commonly used methods in these interfaces are electroencephalography (EEG) and electrocorticography (ECoG). The first method (EEG) is a non-invasive approach that provides the brain's electrical activity via wearable electrodes individually from the scalp [50]. Even though the second technique (ECoG) is a very similar method [51], because the electrodes are placed in the brain specified location, directly connected to the cerebral cortex, it is an invasive method. The data acquired with this method has been used to control the multifunctional prosthesis without the intermediate muscle requirement (see Figure 2.15).

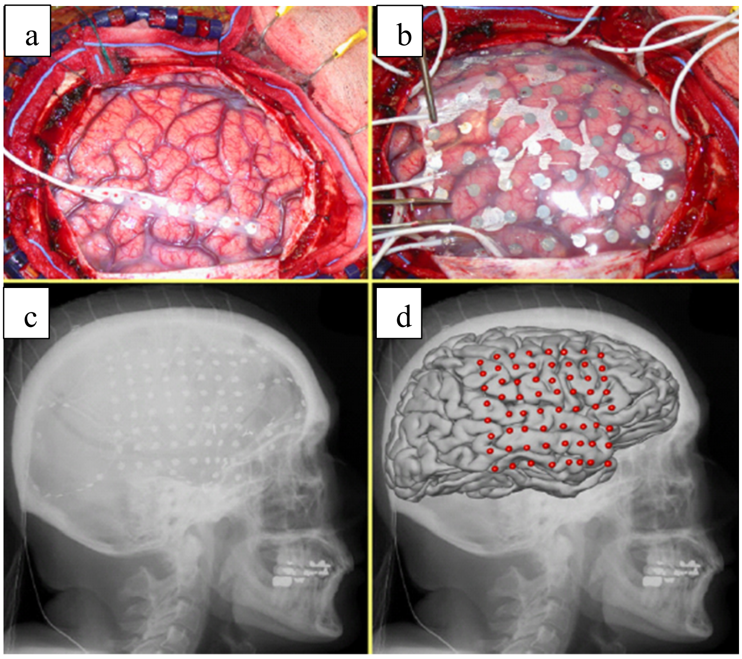

Figure 2:15 The electrode implanted on brain with ECoG electodes. (a), before placement, (b) after placement, radiograph (c) the location of electrode grid (d) (reproduced from[52])

The common implantation of BCIs is to interpret changes from the EEG signals since it reflects the activation changes at a certain point in the brain and does not need surgery [53]. However, identifying those regions is a big challenge, as the measurement may represent the sum of brain signals travelled from many disparate brain regions. McMullen *et al.* [54] have demonstrated a harmonic system to record grasp types, hand posture, and reaching parameters and decode the signal from synchronised intracranial electroencephalographic (iEEG) signals to control a robotic arm system. The movement-related iEEG signal has been used to develop a simultaneous and individual online control of dexterous manipulation. Recently, ECoG signals have been gathered directly form subject's cortex to manipulate multifunctional robotic system [55]. Simlarly, Osborn *et al.*[49] have demonstrate the efficacy of targeted neuromuscular electrical stimulation to enhance neuropathic sensation and motion decoding in the amputee subject. The BCIs is an alternative method to classical EMG control because of the potentiality of finer long-time signal stability.

The safety and stability of the interface are two of the most problematic aspects of the iEMG approach. Furthermore, it is challenging to acquire required or reproducible signals because of iEMG records single or multi signals from hundreds of individual fibres. The interface requires extensive signal processing and deep learning algorithms that are not straightforward in real-time control to deal with massive datasets.Therefore it is suggested that pattern recognition techniques are necessary to improve prosthesis control [22],[56].

2.3.2.3 Prostheses Feedback

This section provides a summary of the mechanical and somatosensory feedback. Particularly, the recording techniques, the state-of-the-art applications on neural and sEMG based prostheses, and their current challenges from clinicians, engineers, and rehabilitation perspectives are summarised.

Multifunctional systems have been tested, identifying independent movements up to 16 classes using EMG, EEG, and some other BCI method. High-level amputees such as bilateral shoulder disarticulation patients have achieved higher than 92% accuracies in pattern recognition trials [15]. Following these advances, the goal of many researchers is to reduce the number of electrodes to a reasonable number for a different level of amputations while achieving similar or higher accuracy. Early presented works have demonstrated advancement in functionality, speed, and quality of signal acquisition for prostheses control. Users have reported that their prostheses are more convenient when they perform tasks with their hybrid hand than traditional control [47], [57]. This man-machine interface has enhanced somatosensory further, in which the received signals were directly connected to median and ulnar nerves.

Although current hybrid methods have improved prostheses' performance, lack of sensory feedback to perform independent movements for close loop in a prosthetic hand is a significant obstruction. Most of the current prostheses rely on visual feedback by carefully observing the device rather than knowing any descriptive detail of grip force or position [58]. Therefore, to establish human human-like dexterity, neurological impulses from the central nervous system for prosthetic devices is critical. There are various sensory feedback interfaces to provide intuitive control for prostheses, and these can be summarised in the following.

Sensory information can be decoded in a variety of methods, including somatosensory stimulation to mechanical or electrical vibration. For example, the first method is “vibrational”, in which the sensory information from tactile pressure is converted into an electrical current pulse that stimulates patients’ residual skin through vibration. It was proposed to enhance prosthetic devices performance controlled via EMG signals [59]. Secondly, “force sensory” has a similar logic to vibrational approach with one exception: when the pressure increases, it causes a series of pressures on the subject's skin. Lastly, “electrical” refers to the sensory information provided by a low level electrical impulse to stimulate and simulate the feeling of touch when skin-object connection is accomplished [60]. Figure 2.16 shows sensory feedbacks for the control system and user.

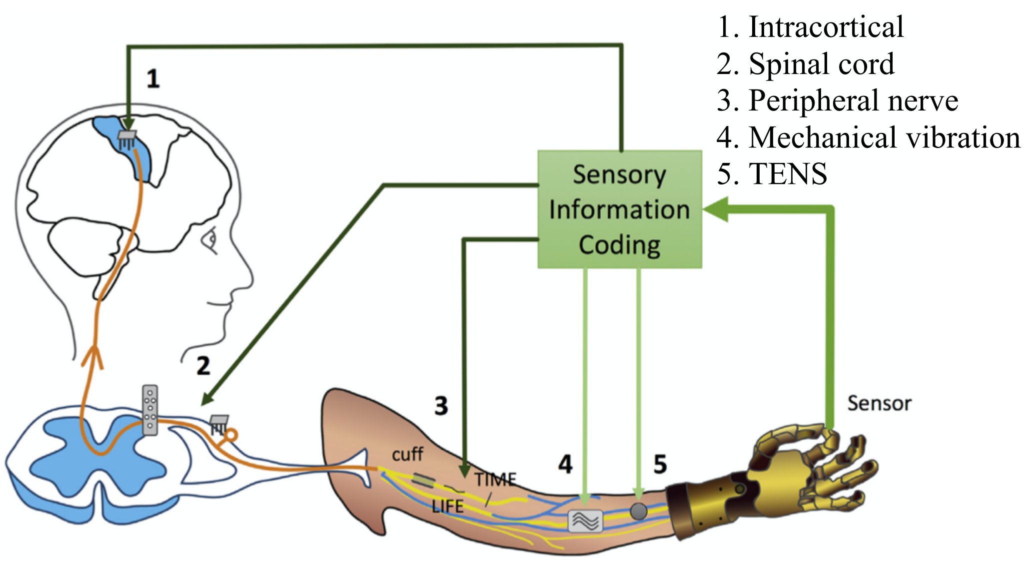

Figure 2:16: Block scheme of sensory-based control systems to deliver haptic information. (Reproduced from [61]).

Recent approaches intended to imitate tactile receptors’ nature by using skin behaviour and the receptor's neuromorphic model. A neuromorphic model was presented by Thakor *et al.* [62], with a biologically inspired epidermis receptor to provide stimuli sensory feedback to users. They have added force sensors to a myoelectric prosthesis’s fingertip to control the strength and stability of object grasping. In this work, the system was tested on subjects, and specified objects were gripped without any damage.

Non-invasive vibrotactile feedback was developed by Clemente *et al.* [63], to address some challenges regarding continuous control. An embedded control system and sensory were added to the fingertip to inform users and upgrade the effectiveness of robust control[64]. Whilst in some other study on close feedback Farina *et al.* [65], have compared vibrotactile feedback of the previous research using Michelangelo commercial prosthetic hand. They have presented that by using electrotactile feedback, the presicion control can be improved by 23%.

In the studies of Raspopovic *et al.* [35] and Ciancio *et a* [66], they have proposed that the ideal multifunctional prosthetic hand should be controlled by peripheral sensory interface to precisely characterise motion and contact with objects. The researches have shown that amputees can induce the sensation of missing hands and even fingers by stimulating specific sensory systems, either invasive or skin surface in their remaining stump, using mechanical or somatosensory stimuli [40], [67].

Somatosensory is an alternative approach to the aforementioned traditional force and pressure-based sensors. In this method, the communication is derived between the artificial hand and the peripheral nervous system (PNS). It is the newest form of sensory system for protheses control and rehabilitation of motor disease. However, there are some limitations for further studies since it is not straightforward to control the stimuli signal, and it needs a surgical procedure [35], [66], [68]. Furthermore, the dimension and geometry of the electrode inside the nerve play an essential role in selecting a specific sensory response.

2.4 Machine Learning Methods and Pattern Recognition

Many studies have been conducted to design and develop dexterous prostheses for several decades. Priority has been given from the mechanic system to haptic, from control algorithms and machine learning to raise degrees of freedom. Most of the studies have been done to improve movement speed and force generation capacity to make the robotic hand convenient for multifunctional manipulation.

The traditional perspective for electromyography prostheses control is employing two input EMGs pattern recognition to directly operate a limited degree of freedom (moving from one state to another). This control approach has been commercially available for a powered prosthesis for upper-limb amputees. However, this classical control model is not reliable and functional as expected due to the instability of EMG signals and lack of functionality.

In contrast to the simple EMG classification approach, to improve a prosthetic hand's performance and manipulation skills, a new control method with multiclass classification has been proposed in up to 27 different classes [37]. This newly proposed control method called sEMG pattern recognition-based control includes conducting EMG signal acquisition, feature extraction, multi-label classification, and multifunctional prosthesis control.

Pattern recognition was proposed to the prosthetic research community in the 1970s. The aim was to provide a sequence of muscle actions. The raw EMG signals are pre-processed, such as windowing and feature extraction, for multifunctional control by classifying different muscle activation [69]. However, this approach was not widespread until the 1990s when it became possible to obtain more new content of EMG signal; the ideas based on pattern recognition control algorithms have been rising [46].

This method is based on the theory that EMG signals accommodate detailed information of intended motions. Different feature extraction methods have been deployed, and classification techniques have been used to identify several arm and hand manipulations. While the pattern has been discriminated against in different classes, a responsible command is delivered to the controller to execute motion, as illustrated in figure 2.17. This new control method's main benefit is that the user has intuitive control, and the classifier has fast differentiation for each multiple movements.

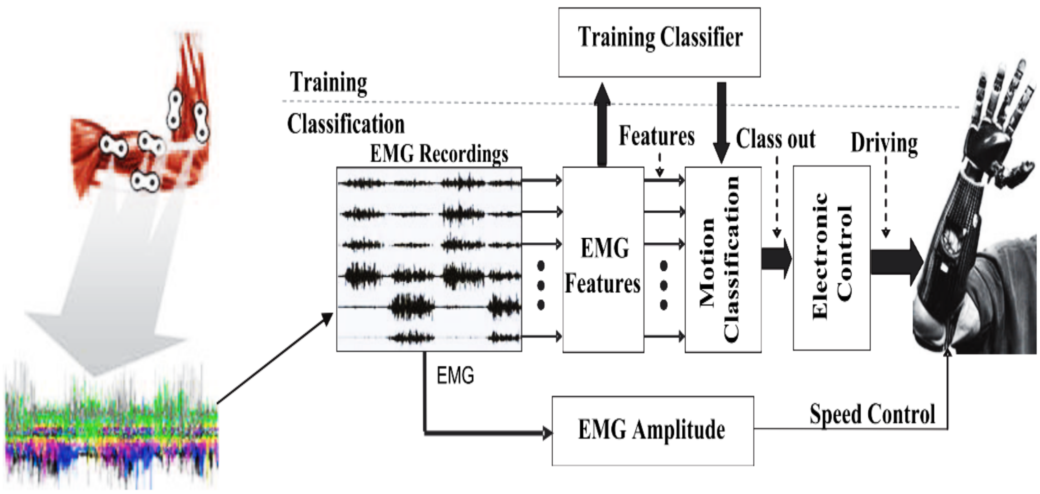

Figure 2:17: Schematic of EMG based prosthesis control (Reproduced from [18]).

Although several practical implementation problems are awaited, much research has been done to investigate next-generation technology's practicality for microprocessor-driven myoelectric prosthesis [18]. The progress has been improved by increasing the number of EMG signals, which enhanced the classification's accuracy and allowed multifunctional control [70]. This has influenced pattern recognition to be developed beyond basic movements such as close and open hands, wrist flexion, and extension. It has moved further to a new trend in identifying muscle actions to control individual fingers [71].

Whilst there has been a significant advancement in pattern recognition, there are several drawbacks when users have control and interaction in real-life situations. The main challenge is the degradation in classification and motion execution when the user performs the wrong movements since pattern recognition is only capable of one exercise in sequence and corresponds to the introduced pattern. Also, during the movement execution, the effect of displacement of electrodes, muscle size, muscle fatigue can significantly affect the EMG signal quality and, eventually, classification accuracy [72].

The previous attempts have improved the classification and control methods by using different feature sets and classifiers through surface EMG recording. Some studies have discovered that invasive EMG detection may have advantages over non-invasive methods for dealing with non-stationary EMG signals. The complexity of invasive methods and their superiority have been discussed in [37], [73]. They have examined and compared surface and intramuscular methods using data recorded from the untargeted and targeted surface to achieve the superior method.

The studies showed that the association of pattern recognition methods in laboratory results to the real world is insufficient. It has been suggested that the completion rate of real-time control in pattern recognition by transradial amputees was 55%, while the classification accuracy for offline data was 85% [74], [75]. Thus it was shown that limited studies had achieved a sophisticated real-time control and the robust system in these algorithms is complicated and unreliable for most of the studies [26].

The most explicit statement regarding using the EMG signal for controlling a multifunctional prosthetic hand is given in section 2.3, and further details are presented in section 2.4. The following sections go through the comprehensive method of pattern recognition control and the various machine learning strategies.

2.4.1 Data Acquisition and Feature Extraction

The surface electromyography (sEMG)-based control system has been employed in several studies and has demonstrated the capacity to operate a high degree of DoF prostheses. The control scheme is associated with the amplitude of limbs' muscles described with features extracted from EMG measurements. Different feature extraction strategies have been shown to improve the number of states from EMG data and solve issues with nonstationary muscle signals. Figure 2.18 depicts the formal content of data capture and interpretation of the EMG signal.

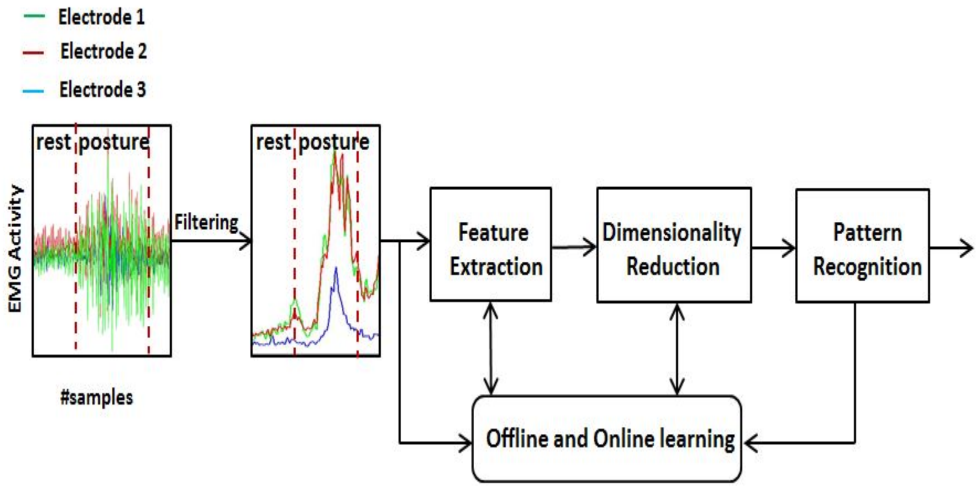

Figure 2:18: Stages of signal processing for electromyography and pattern recognition.

The feature selection has a significant effect on the achievement of EMG based pattern recognition. In the early version of commercially available prosthetic hands, the steady amplitude of EMG signals has only been used as their features. After data acquisition technology has been improved, signals have been filtered, generally utilising bandpass filters to minimise noise (low pass) and motion effect to eliminate undesired effects and improve signal quality (high pass). Most EMG signals, accounting for approximately 90% of the power spectrum, ranging from 20 Hz to 450 Hz. The lower cut-off frequency varies, but the most commonly utilised range is 10 Hz to 200 Hz.

In order to provide more informative signals and enhance classification performance, multivariate feature sets have been suggested. For more intuitive control, the EMG signals of the upper limbs are often pre-processed based on time-domain features, such as root mean square, mean absolute value and variance of the electromyographic signal. Although the autoregressive model has been used in some researches [76]–[79], time-domain features have been widely favoured since they need less computation and perform better in real-time control than frequency domain features [77], [80], [81].

Electromyography signal features are employed on windowed raw sEMG data. The recorded EMG signals from the subject have been segmented into various analysing windows. The window size is generally 100-300 ms. Occasionally, overlapping is applied to maximise the value of continuous data in terms of computer capability [82]. However, the progress delay in real-time control because the signal buffering causes duration. Figure 2.19 depicts the visualisation of feature extraction from window length and associated overlaps. Windowing provides a way to evaluate only necessary data, reducing analysis, computing memory, and eliminating superfluous information (redundancy). However, increasing training window length may cause bias problems and underfitting of the data.

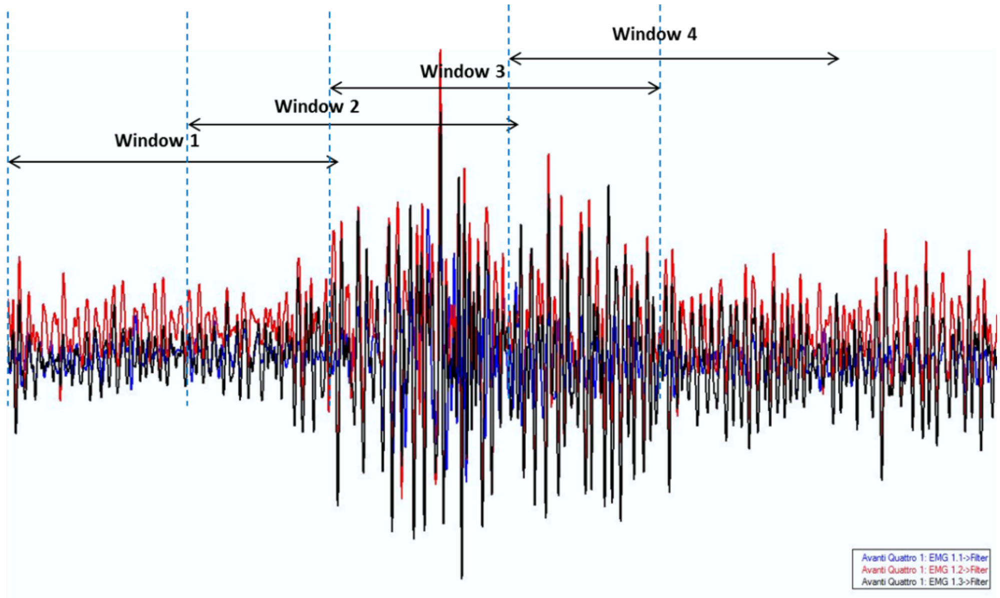

Figure 2:19: Segmentation of windows analysis of EMG signal

The ideal control performance for rapid prehensor prosthesis has been recommended to be 100 ms, while delays of more than 200 ms have been reported to be detrimental to users [83]. However, laboratory research on pattern recognition has usually reported their findings in 300 ms for high pattern recognition accuracy. The efficiency of prostheses generally degrades as window length is reduced because of time delay [26]. Furthermore, in order to reduce disparities between electrodes, data is often normalised, and the mean zero and standard deviation of each dimension or electrodes are determined [5].

According to a recent study, attempts to map sEMG signals to finger and hand motions have been successful (up to 80-95 %) [84]. Even though there is a remarkable approach for processing EMG signals, there is no standard protocol for extracting data from experiments [85]. Likewise, there is no strict rule governing the types of filters and machine learning approaches [86]. Therefore, each research group has taken a unique strategy to achieve high accuracy and sophisticated control.

The majority of recent research on pattern recognition-based control has employed classification accuracy as the performance metric. To increase classification accuracy, researchers explored a variety of machine learning algorithms ranging from fuzzy logic classifiers [87], [88] to Gaussian mixture model[77], [89], [90], linear discriminant model[21], [91] to nearest-neighbour [81], [92] and recently multilayer neural network [31], [93]. Since this study aims to develop a control method for a dexterous prosthetic hand using EMG signals, the following sections contain substantial literature on current advanced ML approaches. All of the approaches covered in this and subsequent sections are summarised in Tables 2.3, which provide a summary by classifier type, feature extraction methods, and the number of subjects and electrodes.

According to recent studies, the sEMG pattern recognition based on deep learning can achieve higher detection performance than its competitors, such as LDA, SVM, LR, GMM and MLP. These sophisticated learning methods can achieve high accuracy in offline tests with large data sets and long enough training time; however, in the case of pattern recognition, the iteration time and generalisation capability are priorities. Furthermore, the performance of these deep learning methods relies on the size of accessible large data sets and computing processors, which in most case scenarios is not feasible on real-time control. Therefore in the following sections, the most practical and popular ML tools were analysed regarding their computational cost, practicality and feasibility of employing in real-time control.

2.4.2 Linear Discriminant Analysis

Linear discriminant analysis (LDA) is one of the most extensively used machine learning methods in pattern recognition for prostheses control. It has mostly been employed as a dimensionality reduction method for pre-processing. However, since it is capable of dealing with overfitting problems, it is often used as a linear pattern classifier. The first idea was proposed in 1948 to separate two classes, and then it was theorised as a multi-class linear discriminant [94]. LDA generally uses a method similar to the principal component analysis, but it secures class discrimination axes information for data categorisation. It defines the feature direction on new vector space (w), projects data from two groups and separates them as much as possible (see Figure 2.20). Therefore, it has been used as a classifier in some practical control problems since it reduces computation cost.

In order to create large datasets, researchers have employed additional electrodes/channels and feature extraction methods to recognise more patterns. However, this leads to high dimensionality and complexity. Thus, in the literature, LDA has been employed as a pre-processing step for dimension reduction and a classifier [95]. Figure 2.21 illustrates the control strategy for LDA methods in the study [74].

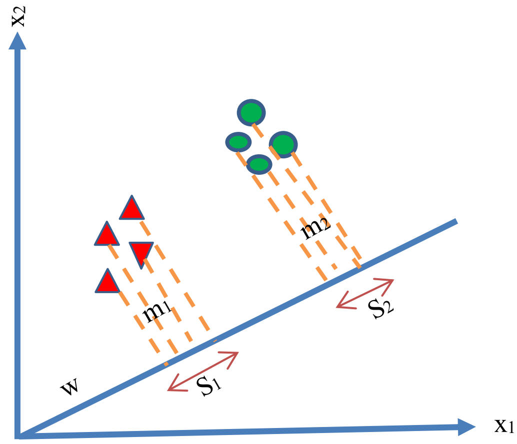

Figure 2:20: Illustration of two dimensional, two category data projected on w vector. S1 and S2 are the distance of each data group projected, and m1-m1 is the means of samples for each class.

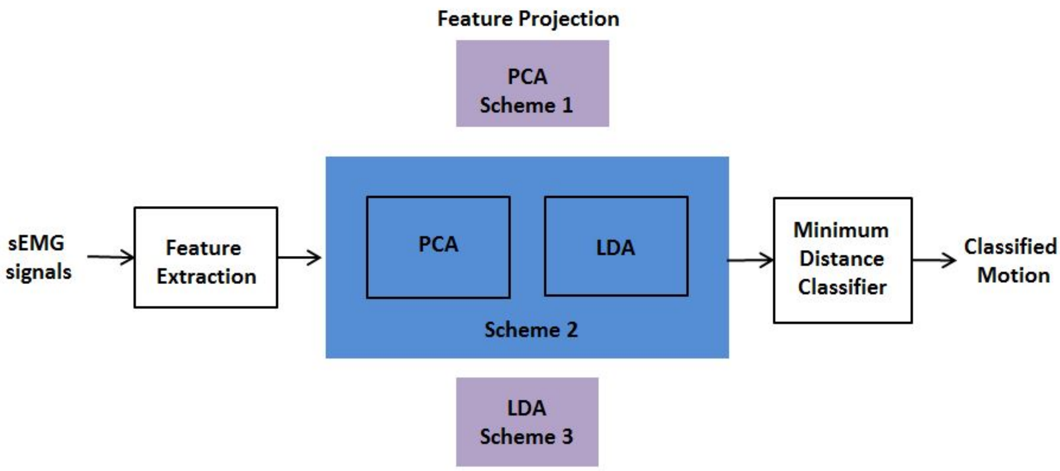

Figure 2:21: Schematic of three future projection methods (Reproduced from [95]).

After TMR surgery, a real-time feature extraction approach and classification were developed to control a virtual robotic hand [41]. The LDA has been used in their study as the main classifier for real-time control and clinical tests. The shape of the decision border is the main distinction between linear and nonlinear classifiers. In order to establish a parallel set of LDA classification to differentiate boundaries between similar motion classes, Zhao *et al.* [96] have suggested a classification technique for combined motions. Many studies [97],[98] have demonstrated the performance of LDA with TD characteristics for real-time control of prosthesis. A comprehensive classification performance evaluation of NLR, MLP, SVM and LDA has been done by Bellingegni *et al.* [99] with time domain features. Linear discriminant analysis has been used with high dimensional datasets because of its robustness properties. Its classification performance has been compared to that of more sophisticated classification methods such as SVM and ANN while needing less processing time in [100].

Reach and grasp movements are essential daily activities that require dynamic arm motions. An attempt to detect grasping intention from sEMG during dynamic arm orientation has been made by Batzianoulis *et al.* [97] with below elbow amputee. The classification performance of four popular methods has been compared regarding their practicality and computational cost [101]. Another research has been conducted using several variants of limb postures to define a feature chart for sEMG signals using TD and FD features [102]. A novel classification approach using LDA for muscular contraction was investigated by Patel *et al.*[103]. The authors compared online and offline control findings with LDA and PCA methods and claimed that this strategy might give more consistency and natural control during multifunctional dynamic tasks. Similary as in [104], it has been used in regression based approach to cotrol a prostheses in real-time. Since it is a practical method in term of model training and implementation without compromising classification in was used in [105] to compare the accuracy performance between able-bodeid and amputee participant. Batzianoulis *et al.* [97] have used LDA to compare the performance of three pattern recognition methods.

The main advantage of LDA is that it provides a straightforward approach for establishing a practical conclusion just by using input information based on biological properties of EMG signals, which are not consistently reproducible. Despite the fact that LDA does not require complexity in its methods and is pragmatic, LDA accuracy is limited by feature size. As a result, a comparison of the most often used classifiers with different factors such as computing cost, applicability, and robustness will offer insight into selecting a suitable classifier for real-time control.

2.4.3 Support Vector Machines

Support vector machine (SVM) has proven to be a supervised learning tool, with associated learning models that analyse features for classification and regression. They linearly build a model that distributes data into categories by creating a hyperplane between them (see Figure 2.22). Using kernel functions, the algorithms can be transformed into non-linear classification (see Figure 2.23). The kernel function can be polynomial, sigmoidal, and radial based functions [106]. The decision boundary is the primary distinction between these functions. The theory has been introduced in [107]. In the original algorithm, SVMs separate only two different data sets. However, adapted approaches for combining several SVM to classify multiclass data sets have been presented. The goal is to create a model that predicts unseen target tasks using known training data.

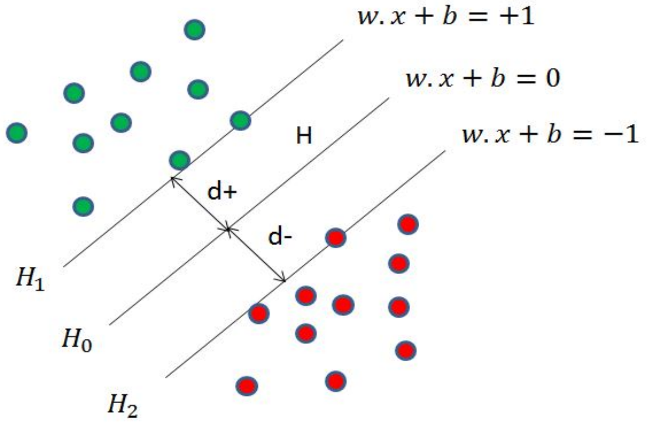

Figure 2:22: Schematic of Linear SVM optimal hyperplane.

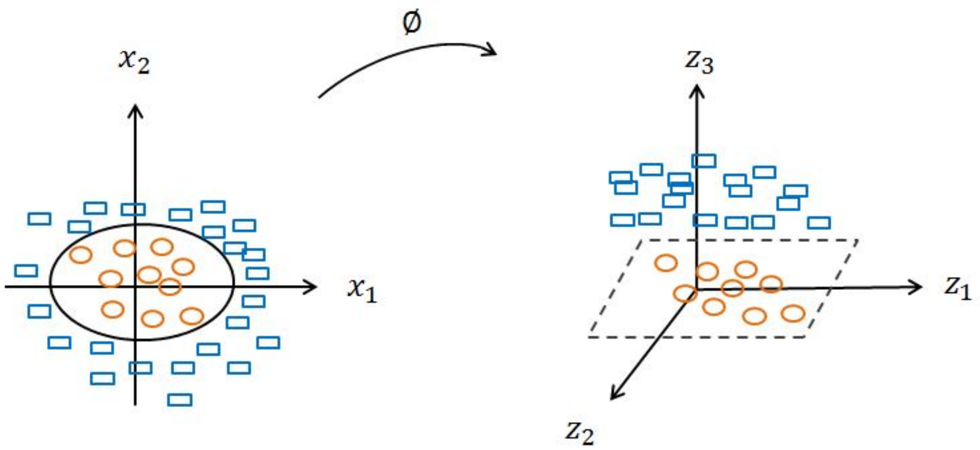

Figure 2:23: Schematic of non-linear SVM in high dimensional space.

Because of its processing efficiency on big and high-dimensional datasets, the SVM offers significant advantages as a classification method for biological signals. Only a subset of training data is used in the decision-making process for new classes; thus, only these points are maintained in memory, which improves memory efficiency and offers the capability for real-time control. Although the training process for this classifier takes a long time due to high dimensionality and non-linear datasets, the method achieves good classification performance with kernel functions [108], [109].

Precise prediction is one of the most important aspects of prosthetics control; hence SVM algorithms is a popular method and commonly used for offline and online classification of sEMG signals. SVM has been employed to control a four-finger hand with thirteen active DoFs to operate active prosthesis while minimising computational cost [3]. Another research has used SVM to control CyberHand through neural signal (ENG) and surface EMG signal [34].

In order to verify the reliability and compatibility of neural signals SVM has been used as a decisive method in [110]. Similary, Castellini *et al.* [111] have compared three machine learning methods on real-time control and has claimed that the SVM classifier's accuracy is over 90%. The performance of a real-time system with a novel socket has been tested in terms of end-to-end recognition and executing time by using SVM with able-bodied and healthy subjects. Several feature extraction methods and kernels have been evaluated with a multiclass LS-SVM to predict the classes of five repetitions of reported motions of 27 people in [86]. In another study Pizzolato *et al.* [112] have compared the performance of six EMG data acquisition setups on 41 similar hand motions using two classification algorithms, SVM and Random Forest.

Support vector machines have been demonstrated to be ideal classification algorithms. However, it has been proved empirically that accuracy is equivalent and is dependent on individuals, feature extraction methods, and the number of classes [113], [114]. Furthermore, since SVM has a high capacity to handle large data sets and its flexibility to adapt new information, it has been employed in numerous studies to categorise surface electromyography for neuromuscular disorders diagnosis [115]. Gu *et al.* [116] has tested and mapped eight different kernel functions for EMG pattern recognition for prostheses control.

Besides the extensive memory requirement during training sessions when large data sets are acquired, this method operates very efficiently once learning is completed. Even though the ideal sets of SVM rules and functions are challenging to be determined to characterise the system behaviour, the studies conducted in literature have suggested that the SVM has a high capability to imitate human decision making more accurately than other classifiers. For example, Guo *et al.* [117] has compared eight combinations of feature extraction methods by using two classifiers (SVM and ANN) and achieved 88% prediction accuracy. The authors also claimed that SVM performed better than ANN in real-time experiments. An sEMG based real-time reach and grasp tests have been taken in [97] by employing SVM. The authors have conducted a series of dynamic arm motions and successfully reduced the time delay between user intention and device response using practical SVM kernels.

Despite the fact that SVM is a common classification approach, there have been several concerns about SVM algorithms. Since it contains many kernel functions, it is challenging to choose an appropriate kernel and its parameters. Other disadvantages include algorithmic complexity and a lack of transparency. Additionally, the SVM technique necessitates greater system memory and processing time during the training stage since it memorises system samples based on rules in the membership functions; thus, the method is more prone to overfitting problems if the learning rate is not tuned appropriately. As a result, various more intelligent decision-making algorithms (such as ANN and TD learning) have been suggested as superior to SVM approaches by combining the benefits of detecting nonlinear and complicated data with flexible learning algorithms.

2.4.4 k-Nearest Neighbour

The k-nearest neighbour (k-NN) is an instance-based (memory-based) supervised method that has been used to address classification and regression problems. It is a straightforward approach that establishes the hypothesis directly from presented training data. As a result, when a new prediction is required from an unseen data instance, the most relevant instance is recalled from stored memory and returned to differentiate the new requested instance (see Figure 2.24). The classifier predicts test samples based on k training samples, where k is the number of test samples' nearest neighbours. As a result, the inclusion of k -values might degrade the performance of the k-NN method. If k is too small, the classifiers algorithm does not offer any advantages and may cause ovefititng. To avoid such issue, it is suggested that the ideal value of k be determined empirically by hiring different k -values. In nearest-neighbour learning, the targeted data can be either discrete or real-time. For real-time valued data, the Euclidean distance is employed as a similarity metric, whereas the Hamming distance is applied for discrete data. The strategy is particularly beneficial for real-time control after model training [8].

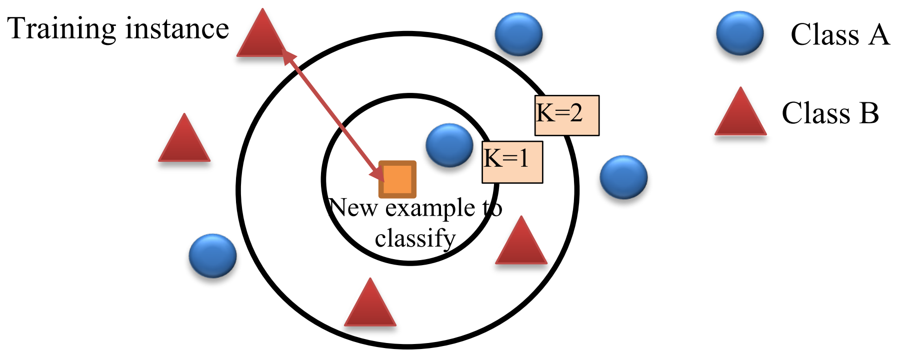

Figure 2:24: Schematic illustration of k-NN methods for k=2.

Although the high accuracy of surface EMG-based classifiers is necessary for prosthesis control, the computational cost is also critical for intuitive control [116]. Because k-nn provides substantial advantages in terms of practicality, it has been widely employed in prosthetics control. A combination of k-nearest neighbour (k-NN) and genetic algorithm (GA) to classify two pair of EMG signals placed on the superficial layer for finger flexion has been conducted in [76]. In another study, k-NN has been used for online control of a prosthetic hand [118]. As another example of individual finger decoding, data from 16 channels while performing 12 individual finger movements has been differentiated in [119]. In the study, they have achieved an accuracy rate of 80%. A detailed comparison between k-NN, LDA and quadratic discriminant analysis (QDA) for prostheses control has been made in [101]. Rasheed *et al.* [120] studied an adaptive fuzzy k-NN for classification of sEMG from four channels. They have incorporated diverse characteristics, using a modified classification approach, multiple kernels, and reached 91 % classification accuracy. Christodoulou *et al.* [121] have employed k-NN to extract sEMG features from 40 patients' for diagnosis. The purpose of the study was to distinguish between patients' movements that had neuromuscular problems and those that did not. Similarly, Atzori *et al.* [81] have investigated finger and wrist movement classification by employing various methodological approaches, features, and classification techniques. They have created data sets based on different measurement methods, features, and classification methods. Concerning numerous methodological aspects, 70% average accuracy has been achieved.

Although k-NN is an effective tool for classification in real-time control, it has some drawbacks. Because it saves training data, this learning method requires a larger memory, making it computationally infeasible for wearable technologies Furthermore, particularly for large data sets, this method takes a long time to search through the complete training data set to discover the nearest neighbour and extract the output. As a result, there is a delay and a lack of intuitiveness, especially if additional training is necessary for new users.

2.4.5 Artificial Neural Network

Neural networks (NN) are data modelling techniques inspired by the topology of human neural networks. They offer a robust error strategy for training data to approximate real, vector, and discrete test data. Algorithms have been effectively applied to EMG-based control for hand motion detection and exoskeletons, either by combining component analysis such as PCA, ICA or by considering raw signals. Backpropagation techniques like gradient descent and Adam optimiser have been used to optimise network parameters to match input-output training sets. Artificial neural networks (ANNs) offer considerable benefits in high-dimensional space and uncertainty, which are characteristics of EMG data[122]. Furthermore, it is suggested that ANN is a powerful tool for multiclass classification since it performs well with large data sets and hence does not need complicated feature extraction methods in the data processing.

Artificial neural networks (ANNs) are mathematical functions implemented on parallel processing units, and it employs statistical approaches comparable to those used in the previously presented machine learning method. The perceptron defines a hyperplane to divide the inputs into two spaces. By implementing different kernel functions, the perceptron separates multiclass by checking the inputs. Figure 2.25 illustrates a multilayer ANN with seven inputs. The weight values can be calculated offline by given data samples. By giving instances one by one instead of the whole sample, the neural network can adapt itself slowly in online learning.

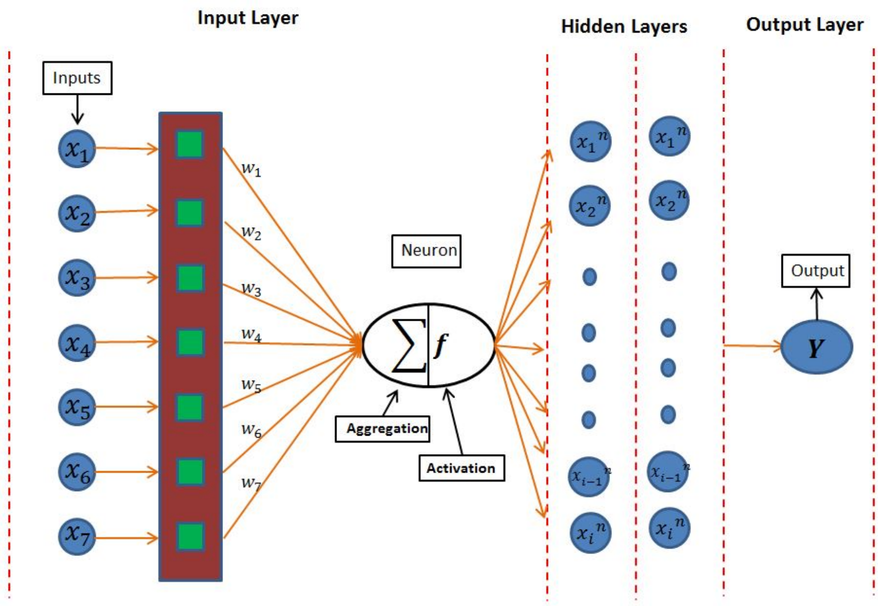

Figure 2:25: Schematic of ANN layers and neurons.

Developing an active prosthesis for a different level of amputation is a big challenge. Researchers have developed different electromyographic (EMG) measurement methods to acquire intended movement performed by users. Many machine learning techniques have been implemented to obtain control commands from limb activities. However, most of these approaches provide discrete motion control, despite the fact that daily human activities are continuous control. The fundamental disadvantage of the EMG signal as a control mechanism is its non-linearity and non-stationarity [123]. Therefore many studies have used neural network classifiers to tackle this issue since ANN can solve both linear and non-linear data mapped from EMG signals.

The data size, physical environment, and the user may need to be changed over time; therefore, the pattern recognition must be retrained depending on performance metrics. Thus, when working with big data and high-dimensional features, ANN provides substantial benefits in terms of robust control of prostheses since it eliminates the need to store training data. Furthermore, since they strengthen the robustness of extracted features, ANNs offer significant benefits in overcoming challenges during dynamic upper-limb motion control.

Recently, different ANN architectures have been used in several prosthesis research projects.. Hudgins *et al*. [124] have established one of the first examples to successful control a multifunctional prosthesis based on EMG signal classification using ANNs. In this groundbreaking work, they have increased the number of states per channel to minimise the user's effect. Gu *et al*. [116] have employed a probabilistic ANN with backpropagation to control a robotic arm simultaneously. Throughout the training, the novel adaptive approach efficiently updated classifiers in real-time. In order to estimate non-linear samples in real-time control, a multilayer perceptron (MLP) has been used in [83]. The study claimed that a real-time control had been achieved within 125 ms without any execution time delay. They also have investigated the influence of feature extraction and ML parameters, and the research outcome showed that feature size and signal processing methods have more effect on class separability than MLP parameters.

Motor control provides robust responses by analysing structural and functional changes. After movement is conducted, the input data are updated by correctness via sensory feedback. The integration of this topology into a robotic system has substantially improved the intuitiveness of prostheses. A notable attempt using this topology is presented in [125]. An adaptive neuroprosthetic controller to map data from neurological states to prosthetics to improve the robustness of devices has been developed. The research has employed Hebbian reinforcement learning (HRL) and claimed that the adaptive controller performance increased by 6% after the third day. It is suggested that the system must discover more postures and differentiate large EMG data sets in order to adjust a controller without the requirement of manual calibration. Thus, Zhao *et al.* [78] have presented a Levenberg-Marquart (LM) based framework for obtaining high-dimensional characteristics for real-time control of a bionic hand.

Data-driven learning has shown to be an effective method for performing multitask with minimum human involvement. A generative neural network approach has been employed in [31] to build a multifunctional arm-hand manipulator. Similarly, based on a dynamic probabilistic model, Bu *et al.* [126] have developed an innovative EMG pattern recognition system. They integrated Hidden Markov Model (HMM) techniques with NN to establish a stochastic strategy to differentiate six hand gestures.

ANN has been used to operate a multifunctional myoelectric prosthetic hand using a variety of alternate approaches. The majority of multifunctional myoelectric control system implementations have relied on assumptions derived from provided features, such as multichannel EMG signals or statistical datasets describing hand or finger motions. Once a pattern has been found from training data sets, other unknown patterns can be determined [114]. When a new specimen is received for real-time control, the incremental learning mechanism updates the model parameters while maintaining the original network topology. A number of reviews discussed deep learning algorithms for big data in detail [127]–[129].

Although the use of deep learning to sEMG is still in early stages, three types of model(Unsupervised Pre-trained Networks (UPN), Convolutional Neural Network (CNN) and Recurrent Neural Network (RNN)) have already been utilised to assess the biological signals and manipulate prostheses. A deep belief network (DBN) has been used as an alternative to conventional ML models to differentiate five hand motions [130]. A deep belief network (DBN) has been used as an alternative to conventional ML models to differentiate five hand motions. Geng *et al*. [131] have investigated the performance of CNN for recognition of independent finger raw data collected from EMG without preprocessing and feature extraction methods. Similarly, Cote-Allard *et al.* [132] have used the spectrograms feature of EMG signals collected from two subjects with eight electrodes to classify seven hand-arm gestures. Although this approach significantly benefits from large data sets, the method is significantly influenced by data size, model parameters, and computational cost. A detailed comparison of the CNN method with conventional methods has been made in [133] by usin publicly available Ninapro datasets.

In contrast to conventional ML methods, RNNs use time-series data to create feed-forward processing. It saves information of previous inputs and creates a model in the present. For sEMG based pattern recognition, this can provide a significant advantage to deal with dynamic arm orientation and non-linear biological signals. Laezza *et al.* [134] have evaluated the performance of three deep learning models for sEMG signal in this study. The research outcomes showed that RNN achieved 91.81%, higher than CNN and RNN (89%, 90.4%), respectively. Similarly, the performance of SVR and RNN has been compared for predicting upper limb joint rotation in [135].

Researchers have developed many alternative ANNs techniques for prosthesis control as a classification or regression method. Generalisation, working in high-dimensional space, learning directly from training data sets in real-time, and adaptability to varied situations are all key advantages of ANN. However, because of the long training period of ANN and the complexity in establishing the right size of the architecture and function parameters, various alternative approaches to ML have been deployed to deliver a straightforward solution with high precision and accuracy.

2.4.6 Principal Component Analysis

Principal component analysis (PCA) is a statistical approach widely used in various application fields, including computer vision, image compression and pattern recognition. It has been extensively employed in EMG signals to discover patterns in high-dimensional data when graphical representation is ambiguous. PCA is a practical tool that can compress data without sacrificing useful information. It does not remove features but instead transforms them with smaller dimensions by decreasing duplication and noise.

Many academics have used PCA to visualise data to find the association between motions and sEMG signals [56], [136], [137]. An exploratory investigation was carried out in [138] to command a 16 DoF robotic hand with a two-dimensional control signal by reducing sensory input from 50 distinct grab actions. To characterise the high degree of human hand synergies, researchers frequently investigate the reduced dimension to identify the pattern by the proportion of total variance determined by PCA [139]. As a pioneering study, Santello *et al.* [140] have conducted research to characterise the human hand by PCA. They have defined the number of degrees of freedom and hand posture distribution according to fingers that create force and synergy. In another work, Braido *et al.* [141] have used PCA to explore the behaviour and coordination of fingers by reducing the large dimensionality of the raw data into a more comprehensible and manageable format. Some other unique PCA approaches have been developed to enhance the classification accuracy of EMG-based control. Hargrove *et al.* [73] have used PCA, a set of motion-class-specific filters to correlate the acquired signals. In this approach, the decreased number of features is prioritised for classification. They compared the classification results of pre-processing and non -processing EMG features (see Figure 2.26).

In the previous work, Zhang *et al*. [95] have used five time-domain features for four-channel EMG data and compared the performance of Linear discriminant analysis (LDA) results with and without PCA. In the first step of the study, PCA was used for feature projection, and then LDA was used as a classifier. Similarly, Jun-Uk *et al.* [83] have employed PCA for four-channel EMG data to reduce dimensionality and simplify the progress of the classifier for real-time control.

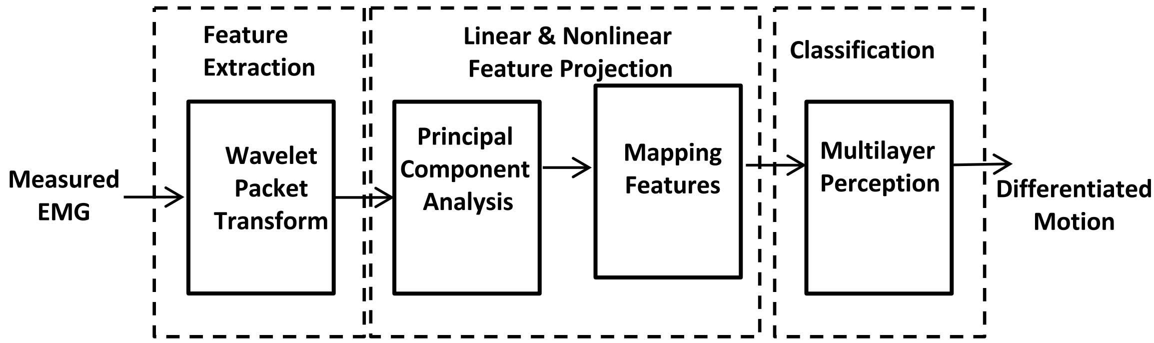

Figure 2:26: Schematic diagram of EMG pattern recognition with PCA dimensionality reduction.

The redundancy problem in control has been described in [142] as such a task that can be accomplished in several ways. For example, different finger joint combinations can bring the fingertip to the same final point. This is a characteristic problem of deciding one possible solution out of many. Such a decision can be made by the sensorimotor system robustly, but it is a problem in control to be addressed. The correlation of control signals determines control action direction, and PCA can always create a minimal number of represented components for large datasets. Thus, Gabiccini *et al.* [139] have employed this principle as fundamental control law in their motor control based research. In the circumstances of few inputs, it is relatively simple to distinguish the limb actions, as they spread different graph regions. On the other hand, combined high dimensional can only be separated by PCAs or ICA. Atzori *et al.* [86] have used a similar approach to distinguish data of 52 different movements from multiple subjects.

In order to increase motion recognition accuracy and differentiate more patterns, descriptive information of muscles and the number of features must be increased. This is likely to cause high dimensionality of the feature vector problem. Thus, the projection of movement's feature vectors using PCA gives some intuition about the mapping from high dimension into low dimension spaces. It reduces the processing time of classification and meets the demands of real-time control. Since PCA is one of the well-known methods to give insight into the connection between hand manipulation and sEMG signals, it has been used to reduce planning and learning complexity and generate well-defined features.

Considerable research is required to create and optimise learning algorithms and datasets to gather appropriate information from able-bodied to amputee participants. All of the ML approaches mentioned in this study show promise, provide inspiration and practicality in prostheses, and highlight the potential to develop a more sophisticated sEMG based pattern recognition system. Table 2.2 outlines the various learning approaches and feature extraction strategies available for prosthetic hand control.

Table 2:2: Summary of EMG-based protheses reseaches that have used ML techniques.

Ref.	**Year**	**Input Data**	**Number of Classes**	**Number of Electrodes**	**Machine Learning Model**	**Data Features**
[143]	2001	EMG	6-class	4-channel	PCA, LDA	STFT, WPT WT,
[126]	2003	EMG	6-class	6-channel	ANN	MAV
[77]	2005	EMG	6-class	4-channel	GMM, MV	AR, RMS
[113]	2005	EMG	8-class	7-channel	SVM	MCV
[78]	2005	EMG	3-class	2-channel	NN	AR, MAV
[144]	2005	EMG	6-class	5-channel	GMM, MLP, LDA	AR, RMS
[5]	2006	EMG	6-class	10-channel	SVM	MCV
[70]	2006	EMG	4-class	4-channel	MLP	STFT
[83]	2006	EMG	9-class	4-channel	PCA, MLP	WLT
[145]	2008	EMG	18-class	8-channel	SVM	MCV
[146]	2008	EMG	6-class	16-channel	SVM	WT
[111]	2009	EMG	5-class	10-channel	MLP, SVM, LWPR	MCV
[147]	2009	EMG	12-class	32-channel	MLP	MAV, WA, WL
[138]	2010	EMG	3-class	2-channel	PCA	MCV
[75]	2010	EMG	11-class	12-channel	LDA	MAV, ZC, WL, SSC
[118]	2011	EMG	7-class	9-channel	k-NN	MAV
[148]	2011	EMG	7-class	9-channel	SVM	MCV

Table 2:2: Continued

Ref.	Year	Input Data	Number of Classes	Number of Electrodes	Machine Learning Model	Data Features
[119]	2011	EMG	12-class	16-channel	LDA, SVM, k-NN	MAV, WL, ZC, SSC
[101]	2011	EMG	5-class	2-channel	k-NN, LDA, QDA	IAV, RMS
[149]	2012	EMG	6-class	2-channel	LDA	Multi feature
[86]	2012	EMG	52-class	10-channel	PCA, SVM	RMS
[71]	2012	EMG	10-class	2-cahannel	SVM, k-NN	WL, ZC, SSC, AR
[150]	2013	Ultrasound	6-class	-	PCA	-
[100]	2013	EMG	10- class	4-channel	LDA, QDA, RFS	RMS, WL
[151]	2013	EMG	9-class	4-channel	LDA, SVM, QDA, k-NN	MAV, ZC, WL
[96]	2013	EMG	3-class	6-channel	LDA	MAV, ZC, WL
[152]	2013	EMG	25-class	8-channel	LDA, SVM	MAV, ZC, SSC, WL
[54]	2014	ECoG	4-class	128-channel	PCA, LDA	MCV
[95]	2014	EMG	9-class	4-channel	PCA, LDA	MAV, RMS, ZC, WL, SSC,
[153]	2014	EMG	5-class	192-channel	ANN, NMF, LR	RMS
[154]	2014	iEEG	2-class	4-channel	LDA	AR
[155]	2015	EMG	6-class	12-channel	LDA	MAV, WL, AR, MV
[156]	2015	EMG	4-class	8-channel		MAV, ZC, MCV, RMS, WL,
[157]	2016	Ultrasound	11-class	-	k-NN	-
[158]	2016	EMG	8-class	8-channel	SVM	MAV

Table 2:2: Continued

Ref.	Year	Input Data	Number of Classes	Number of Electrodes	Machine Learning Model	Data Features
[56]	2017	EEG	2-class	-	MLP, NB, k-NN, PCA	DWT
[159]	2017	iEMG	3-class	8-channel	LDA, SVM	MAV, WL, ZC
[84]	2017	EMG	6-class	14-channel	RF (random forest)	MAV, WL
[116]	2018	sEMG	14-class	8-channel	LDA, SVM	DFT, WT, WPT
[103]	2018	EMG	5-class		PCA, LDA	MCV, MAV
[160]	2018	EMG	5-class	2-4 channel	LR, CC, SC	-
[161]	2018	EMG	8-class	8-channel	CNN, SVM	-
[162]	2019	EEG	4-class	57-channel	ESI	-
[64]	2019	iEMG, EMG	4-class	4-channel	k-NN	MAV
[17]	2019	EMG	10-class	5-channel	R-LLGMN, HMM	MAV
[163]	2019	EMG	3-classs	8-channel	SVM	TC, SC
[164]	2019	EMG	4-class	6-channel	NLR	RMS
[165]	2019	EMG	6-class	32-channel	N/A	KF
[166]	2019	EMG	4-class	8-channel	LDA	ACCmmg
[167]	2019	EMG	5-class	16-channel	RLS-DF	RMS
[168]	2020	sEMG	6-class	8-channel	SNN	RMS
[169]	2020	EMG	4-class	8-channel	LR	-
[170]	2020	EMG	4-class	8-channel	LR	RMS

Table 2:2: Continued

Ref.	Year	Input Data	Number of Classes	Number of Electrodes	Machine Learning Model	Data Features
[171]	2020	EMG	8-class	16-channel	CNN	-
[172]	2021	EMG	5-class	8-channel	CNN	RMS
[173]	2021	EMG	6-class	6-channel	CNN	MAV, SSC, ZC, WL
[174]	2021	iEMG	12-class	16-channel	CNN, RNN,	SC, SSC, WL, RMS, MAVS

2.5 Challenges and Research Scope

Since the 1970s sEMG has been employed as a popular control interface for upper limb prostheses. A variety of promising non-invasive, wearable myoelectric prosthetic hands have been created and are widely available. Despite mechanical and control systems developments, commercially available prostheses are far from human-like dexterity and intuitiveness. Comfort and functionality are the most common reasons for prosthesis dissatisfaction, according to the literature reviewed for this study. Some other research and reviews have also supported this viewpoint [10], [11], [175],[176]. Cosmetic appearance, lack of sensory system, lack of robustness, muscle contraction level, electrode shifting, variability in arm position, socket fitting problem, and high cost are other issues that must be addressed.

Following the review's findings, sEMG was frequently employed to detect muscle patterns for prostheses control. Innovative techniques, muscle reinvention, and neuromuscular signal recording have been devised to deliver muscle signals for different categories of users. These method have produced control signals for various functions, including anticipating individual finger flexion, object grabbing, and other qualities previously mentioned. However, most studies used limited hand and arm posture, and just a few studies used reaching and grasping actions to assess their control system. Furthermore, most existing research does not provide answers for amputees who retain a small number of biceps and triceps muscles.

As a result of the current findings, advanced data collecting and machine learning methodologies are necessary to meet the issues that have arisen due to the environment and subject availability. Despite the fact that some large datasets were created from various subjects and a significant number of hand and arm postures, most studies evaluated their research outcomes using metrics like accuracy, recall, precision, R^2, and F-Score. However, since real-time control requires adaption, non-stationary signal, synchronisation, and continuity, this analysis fails to represent online scenarios.

Currently, there are several studies using ML approaches to control sEMG-based prostheses; however, in many cases, these studies lack a standard for their concepts, parameters, signal processing, real-time validation testing, and type of hand/finger motions. Moreover, the majority of these studies are either unreplicable due to unrealistic settings or unfeasible due to being highly sophisticated and cannot be transferred from laboratories to real-world conditions. Therefore, there is a significant gap between laboratory research and clinical use of prostheses, despite all of the most remarkable advancements in machine learning and sensory advances [177]. Following this review, this study aims to develop a sEMG based pattern recognition to find answers for four main challenges presented in the literature as follows:

***User friendly*: **Any prostheses should be intuitive and natural. The user should be able to control it easily. This will be accomplished by the use of a bypass socket and a novel sensory modality.

Independent function's control: Multifunctional hand should have a high degree of freedom and should execute each function without the help of any external application or switching functions. Independent finger and thumb abduction control will be used to accomplish this.

***Simultaneous multifunction control (parallel control)*: **Amputees should be able to coordinate and perform multi joints simultaneously and effectively without damaging other functions. To do so, a regression method will be used to process several functions at the same time and separately.

***Fast Response*: **Prostheses should respond immediately after receiving command signals and sensory feedback. Data acquisition, processing, motion prediction, and execution were optimised to process in 0.23 seconds with the new embedded control in this study.

The literature studies outcomes were analysed based on surveys and reviews conducted in [176],[178],[179],[180]. This chapter summarises the primary control approaches based on the aforementioned main challenges (see Table 2.3), which were asked in the surveys to actual prostheses users.

Table 2:3: Comparision Between Some Approach for Control of Prosthetic Limbs

Approach	Main Advantages	Main Disadvantages
Surface Electromyography (sEMG)	Non-invasive. Easy implementation.	Non-natural control strategies without ML methods. Not easy to learn operating.
Implantable electromyography (iEMG)	Improve the quality of EMG signals. Provide focal information.	As an EMG. Costly.
Targeted Muscle Reinvention (TMR)	More natural control strategy. Effective sensory feedback. Focal data acquisition.	Require surgical process. More suitable for shoulder level amputation.
Implantable Peripheral Interfaces (PNI)	Potentially selective and versatile for natural sensory feedback.	Limitations regarding controllable DOFs. Invasiveness. Acquisition of noisy signals.

2.6 Summary

The myoelectrical (EMG) signal is one of the most extensively utilised sources for prediction and controlling upper limb prostheses. Sophisticated ML algorithms, considerable advancement in hardware systems and continuous development of large data have made remarkable progress in artificial prostheses in recent years. Deep learning significantly improved the accuracy of sEMG based pattern recognition and reduced the interferences caused by environmental conditions, and it boosted the robustness and intuitiveness.

This chapter investigated the applicability and efficiency of ML methods in sEMG based pattern recognition. It analysed the key approaches used in developing prosthetic hands, including signals processing, feature extraction techniques, different types of classifiers, socket design, sensory modality, and performance evaluation methods. Finally, the current problems and opportunities for clinical implementation of these approaches were identified and discussed.

Prostheses have gained greater capability over the years as wearable sensors and machine learning approaches have advanced. Studies have revealed that amputees may be able to restore at least several of their lost limb functions using sEMG based pattern recognition. Although non-invasive prostheses have shown promising results, several real-world problems must be addressed. To begin with, myoelectrical prostheses have limited control and intuitiveness. Secondly, control of prostheses is typically unnatural, with a poor human-machine interface (HMI). Finally, despite the fact that laboratory-based studies shown excellent accuracy (almost 96 %) in offline testing, real prostheses users reported frustrated dissatisfaction with their devices (about 65-75 %).

Studies have developed novel adaptive algorithms, unique approaches for sensory modalities, merging post-processing, and alternative model training. These strategies have all demonstrated varying levels of success in offline research and online control. Although computational skills have improved intuitiveness, the reliability of the EMG signal has remained one of the key challenges. The investigations have developed into alternative data collections, such as targeted muscle reinvestigation (TMR) and electroneurographic (ENG) signals, in order to discover and analyse more reliable EMG signals. The novel method has dominated research in the fields of pre-processing and removing artefacts in the real-time management of EMG data. Following these improvements, several researchers have attempted to mimic the nature of tactile receptors by combining the skin behaviour neuromorphic model of the receptor for sensory feedback.

However, although the recordings from focal locations improved pattern recognition accuracy, the stiff form and propagation of anchoring pressures can harm nerves and may cause significant damage. Early studies revealed that implanted electrodes could regenerate a reliable, though limited, capacity; on the other hand, it is far from worldwide use because it has some potential to nerve fibre loss and a resulting loss in cardiac response.

Furthermore, even though contemporary hybrid approaches have enhanced prosthetic performance with sensory feedback to execute the autonomous movement, they have also introduced new drawbacks, such as higher costs, design problems, and increased user training load. Lastly, in order to reduce the problem's complexity and give a dependable solution to instability, a compact combination of all compartments that enables permanent and continuous connection with users has been proposed. However, many systemic problems connected to human-machine interfaces, such as crosstalk, motion artefacts, limb position variations, muscle force, and especially processing time in real-time control, diminish the functionality of the prosthesis. In terms of classification performance, signal processing and feature extraction play an essential role in obtaining adequate performance for motion detection. Several domain characteristics have been proposed throughout the observation method, including signal amplitude, muscle conditions, and signal type.

This chapter highlighted the important parameters of feature extraction methods and pre-processing in each domain. Popular ML tools for enhancing sEMG based controlled prosthetic hand in considering highlighted rejection rate were also presented. Data collecting principles, sensory feedback, machine learning methodologies, and real-time controls were investigated to deal with myoelectrical instability. Finally, the most important notion of mechanical advances in terms of socket and electrode location was underlined in this chapter.

Chapter 3 Methodology: Forearm Muscle Activity and Electromyography

3.1 Introduction

Surface electromyography (sEMG) based control was first introduced in the early 1950s and 1960s as threshold-based control to simply control prostheses (open and close functions) for a primary degree of freedom grippers. The control method was introduced to regain at least the most basic tasks of daily life. For cost and convenience reasons, the proposed threshold-based control is still used in a substantial number of commercial prostheses. However, the idea of detecting multifunctions of the hand using pattern recognition algorithms for amputees has lately gained popularity. This concept has advanced thanks to a range of machine learning technologies. The researchers aim to comprehend amputees' intentions better and expand the possibilities for advanced multi-fingered prosthetics.

Despite considerable progress, clinical applications of these technologies remain limited due to the incapacity of some pattern recognition algorithms to deal with non-stationary myoelectrical (EMG) signals. Muscle fatigue, variable conductivity, electrode shifting, and user pattern change have all been seen to disturb sEMG signals. Furthermore, changes in arm position and velocity of motion change the data, resulting in degradations and the requirement to retrain a new model with varying arm orientations.

This chapter aims to undertake a series of experiments using the current popular techniques to better understand gripping and single finger patterns and build a sufficient real-time-control model and control interface for a prosthesis. Numerous experimental circumstances from the literature were employed to analyse EMG signal fluctuations, detect motions as precisely as possible, and minimise some of the previously-mentioned disadvantages in clinical and practical implementations.

3.2 Experiment Methodology

3.2.1 Participants

These EMG tests aim to assess the motor control strategy of human upper limbs and imitate its effectiveness for controlling upper limb prosthetics. This experiment's data was utilised to create a control method for transradial amputees. An able-bodied participant participated in EMG tests. The participant is 26 years old, a righthanded male. The participant has no musculoskeletal or motor control disease or limitation that could cause restraint of the self-selected activity speed or naturalness of manipulation. Five healthy males between the ages of 24 and 28 volunteered for this study's second part, which aimed to assess muscular fatigue and individual participant effect on classification performance. All of the participants were right-handed. The reason behind the right-hand decision is because, according to statistics, the arm amputation levels are 57% for transradial and 23% for transhumeral, respectively, with the right limb being more frequently affected due to work-related injuries or illnesses [15]. The contents of the trials were explained to volunteers, and they were instructed not to engage in any physical activity between their trials, due to physical exercise has been proven to generate muscle fatigue, and long-term muscle training has been shown to cause sEMG data to be misrepresented between trial sessions [181], [182]. A variety of issues, including the fact that each person has a varied muscle contraction level, range of arm motion, and limb size, challenge implementing real-time control systems.

Although there are no standards for experimental protocol or number of subjects, which makes it difficult to compare EMG results between studies, the majority of research has been conducted with healthy participants. Therefore, researchers have employed various subjects from 3 subjects [183], [184] to 220 subjects [185]. In fact, the number of subjects is more closely related to the type of MLs deployed and the purpose of the investigations. Some studies attempt to collect as much data as possible from various types of subjects in order to develop a publicly available database [186], [187]. Those research focused on specific activities with small number of individuals, which may lack generalisability in daily living activities in the literature have focused on real-time implementations of prostheses. Peerdeman *et al.* [188] conducted a systematic literature review and concluded that the majority of studies only conducted experiments on able-bodied subjects due to the difficulty of recruiting amputated subjects. Previous research has shown that control accuracy for amputees is comparable to that of able-bodied people, if not slightly lower and more unstable [189],[190]. It has been hypothesised that amputees suffer to obtain high accuracy and execute activities on time [191]. It is unclear if this is due to a lack of sensation or a lack of motor control. In [192], Al-Timeny *et al.* collected sEMG data from ten able-bodied and six below-elbow amputees. They achieved 98 % accuracy for able-bodied subjects and 90% accuracy for amputee subjects. More information about the number and type of subjects can be found in [175], [176].

3.2.2 Materials and Sensors

As the main data acquisition component, we recorded corresponding EMG signals using Delsys™ Trigno Wireless System®, with recently released Quattro sensors. These electrodes were developed with high accuracy and allow more precision muscle detection as they have a small size. As stated in the last chapter, there is a debate in the literature concerning the ideal electrode location on muscles and electrode crosstalk. As a result, thanks to the electrode's size, this newest electrode has removed electrode placement issues. To assess the kinematics of the human hand, a setup was employed to combine seven EMG sensors and a data glove. The wireless VMG 30™ data glove provides up to 30 high accurate joint angles, capturing all the human hand motions. More importantly, the flexion and extension of two joints and abduction/ adduction of each finger were illustrated on the computer screen for tracking purposes. Force sensors are included in the glove's fingerprint, allowing for the gathering of both force and pressure data. The VMG 30™ data acquisition sensory was used to minimise the uncertainties on the contact points in object manipulation and perform accurate repetition of each trial.

In the static arm trials, the subjects were instructed to establish their first natural position, which they could use to grab and hold objects. It may be feasible to check if the initial manipulation was detected and the fingers returned to their original place by measuring the force and posture of the trial. A workstation computer (Intel i7 @2.6 GHz with Windows 10) was used for data collection and storage. Delsys EMGWorks Analysis and Matlab tools were used to analyse the obtained data.

3.2.3 Equipment Calibration and Participant Preparation

The muscle activation signals (EMGs) from the participant's upper limb were captured to examine how the muscles were engaged during the finger and object manipulation trials. The Delsys system calibration was made via its patented software. The detail of the procedure is available in Delsys online documentation; under the section, calibrate a Delsys system [185]. The system stores the calibration information for each sensor that has been paired in default. When a new experiment is initiated, the calibration file is used to precisely display measured signals in most cases without manual calibration.

For data glove calibration, the VMG 30™ software provides an open API for the construction of hand simulation, visualisation, and calibration of kinematic outputs. Calibration takes less than a minute and is easy to implement. It displays calibrated sensor data in the MotionBuilder in an interface [193]. The participant's upper limb was equipped with EMG surface electrodes and a data glove. The electrode placement was made based on palpation, as recommended in [118]. The participant's skin surface was prepped for reliable data collecting since it is suggested to attach the electrodes to the user's skin with the hair removed and cleansed .

The EMG signals can be influenced by a variety of variables that, in most cases, are unrelated to finger position and behaviour [194]. Many of these aliasing signals have a negative impact on the quality of EMG signals, interfering with control and classification performance. The experiments were conducted while keeping all of these concerns in mind and researching ways to avoid them. The muscle contraction signals were recorded for muscle groups while participans were asked to contract muscles for ten seconds and maintain a steady contraction for at least three seconds. Several studies have investigated the effect of sampling rate, sessions duration and the number of repetitions. For example, Khushaba *et al*, [195] and Pizzolato *el at.* [112] have conducted their experiment with six repetitions with each trial in 5s. To avoid data biasing, the 3s time duration was decided to ensure maximum muscle contraction was recorded. The approach is comparable to previous biomechanics research investigations such as [81], [86], [112].

3.2.4 Electrode Placement

The data collection setup for each session was meticulously repeated in terms of the muscle architecture of the forearm. The electrodes were assigned after finding the best position of each muscle, which was accomplished using the palpation method while the user repeatedly contracted the inspected muscles and in accordance with the standard protocol provided for non-invasive (sEMG) signal detection [196].

The electrode orientation was determined by the place of the muscle observation. Due to the appropriate size of electrodes, four micro Quattro sensors were primarily planted to assess the dense sampling of muscles stationed in the proximal area of the forearm. The remaining three sensors were placed on the primary activity areas of the flexor digitorum superficialis and flexor digitorum profundus muscles. The precise placements of muscles were determined based on their importance in motor control of human hand motions. Furthermore, a high number of transradial amputees can still reach the majority of these muscles. The VMG 30™ system was used to collect hand manipulation sequences and finger motions, and this system was then used to analyse hand kinematic activity. This integrated system is not ideal for real-time control due to its complexity and interactive display of joint angle changes, but it is suitable for machine learning model training. Figure 3.1 displays the capture manipulation system and the placement of 7 electrodes on the arm to targeted muscles. The number of the sensor was decided after an extensive literature review such as [22], [191]. In another review Farell *et al.* [37] have compared different numbers of electrodes and their influence on pattern recognition. The compatibility of the system, number of subjects, experiment duration, ML methods and feasibility of employing the maximum number of the electrode have been effective in this decision. Numerous studies have been conducted with a different number of electrodes. A detailed review that compared the number of electrodes and sampling rate is given in [176]. Furthermore, the literature chapter discusses in depth the number of electrodes, ML algorithms, and feature extraction techniques (see table 2:2). Regarding classification accuracy, it has been suggested that using at least four electrodes is reasonable as employing less than four causes a large decrease in classification accuracy. It is recommended that the quantity of sensor must be kept at least in the range of 4 to 6 to ensure that it does not compromise the detection performance. It has been demonstrated that using more than 8 sensors does not significantly improve classification performance [37], [197].

The subjects were told to perform basic finger motions and manipulate all hand joint axes in accordance with the targets. The goal of this experiment was to explain static hand postures and identify the form synergy of the grasped items. These object gripping types were chosen as a form of "prioritisation" of grasps based on how frequently they are utilised in daily life [103],[198]; accordingly, sphere, tripod, and cylinder (prismatic) shapes were chosen. Appendix D represents the object specifications.

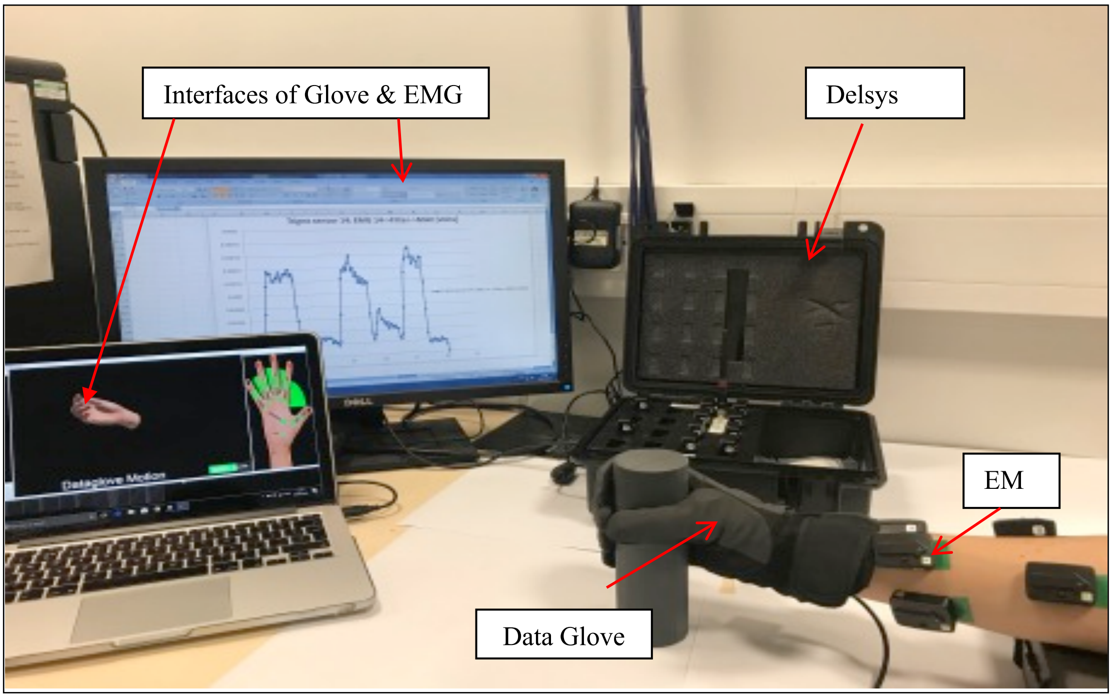

Figure 3:1: The experimental setup shows EMG data acquisition and data gloves for capturing finger orientations and postures.

Because the targeted muscles are so close together, a thorough examination of their structure and activity, as well as accurate EMG sensor positioning, is required. Each finger manipulation and object grabbing was investigated independently in the experiment using Delsys sEMG sensors on the required muscles. As indicated in table 3-1, we placed our seven electrodes over the right forearm muscles. These muscles were chosen since they are primarily in charge of controlling the actions of the fingers and wrist. In the experiment, individual flexion and abduction of the thumb, as well as extension and flexion of the index finger, middle finger, ring, and little fingers were conducted, as shown in table 3-1. Individual finger categorization is proposed in order to differentiate unlearned combined actions and control prosthetic hand fingers naturally.

Table 3:1: Description of Muscles and Joints Interested

Muscles	Examined Fingers and Joints		
	Affected Fingers	*Flexed Joints*	*Extended Joints*
Flexor Pollicis Longus	Thumb		
Extensor Policis Brevis	Thumb		MCP
Extensor Policis Longus	Thumb		IP
Extensor Indicis	Index finger		PIP, MCP
Extensor Digitorum	Index, Middle, Ring, Pinky		MCP, PIP
Flexor Digitorum Superficialis	Index, Middle, Ring, Pinky	PIP, MCP	
Flexor Digitorum Profundus	Index, Middle, Ring, Pinky	DIP, PIP	

Table 3:2: Conducted Experiment and Subject Number

Basic Finger Motions	
Number of sessions	5
sEMG (FPL, EPL, EPB, EI, ED, FDS, FDP)	7
Total number of movements	6
Number of repetitions	3
Hand Gesture	
Number of sessions	5
sEMG (FPL, EPL, EPB, EI, ED, FDS, FDP)	7
Total number of movements	3
Number of repetitions	3

3.2.5 Experiment Composition

The experiment setup was made up of four major components. The tests were designed to collect seven channels of sEMG signals from a subject's extrinsic muscles as they performed simple finger movements and object grabbing. At the start of the individual finger manipulation, the initial component aims to determine the relevant signal composition for model training. EMG signals were collected from precisely selected sites on the user's forearm.

The experiment was conducted in an indoor laboratory using a PC running Delsys EMGWorks Analysis software and DataGlove (VRML/Cosmo) software. The subjects repeated six-finger gestures three times as presented on the second computer screen for each trial. Five valid trials were obtained for each manipulation, yielding a total of 30 valid EMG trials for each participant. The participants were instructed to relax their muscles during the testing and were fully informed of the experiment outcomes. The participant was given the necessary time to become familiar with the trials. The trials were computed after DataGlove collected the finger's and hand's initial locations and confirmed the finger was in a natural posture. To track finger positions, a data glove and an EMG capture device were used to create a synchronised system. EMG data recording began when all sensors were linked and ended after the finger achieved the desired postures. The finger manipulation tests were aimed to collect data for ML training and validate the efficiency of varied electrode placements, variable arm postures, and muscle changes by different persons on healthy participants. After pre-processing, the data from each trial were saved as training data. Figure 3.2 depicts six distinct finger motions used for data collecting. The finger motions were chosen based on their frequency of employment in daily living activities as derived in [86] and [199]. The experiment does not need to follow any specific sequence because the datasets for the ML model were randomised to avoid biased data.

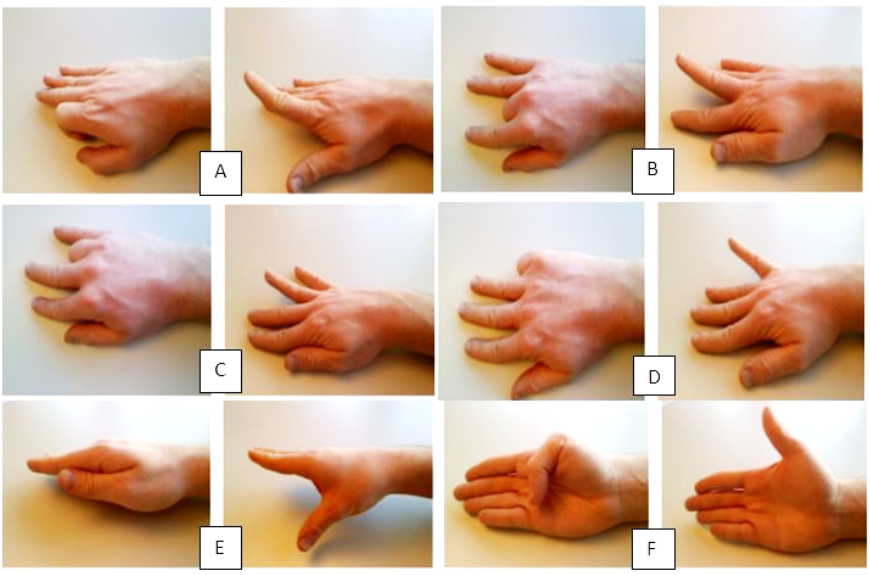

Figure 3:2: Different movement classes (individual finger) considered in this study.

The experiment aims to collect data from all finger motions, from flexion/extension through abduction/adduction, using forearm sEMG signals to create a dataset for pattern recognition. It has been reported that independent finger manipulation will significantly improve functionality and intuitiveness [147]. The methodology is best suited for natural control because it represents data from single fingers rather than a wrist or elbow to control prostheses. These datasets allow the control of active prostheses with a high degree of freedom. Independent finger detection can also improve the precision of object grabbing as presented in [187], [198].

The second part of the trails is based on motion prediction, with the subjects being asked to construct the finger configuration required for object grabbing by applying forces to the fingers and measuring their amplitude. The object gripping trials were carried out to collect training and testing data for three different types of motions (see Figure 3.3) and were paused by resting time to minimise muscular fatigue issues. The data collection approach resembled finger manipulation activities. The individuals were instructed to grip three described objects with the right hand as naturally as possible. The items for the gripping trials were 3D printed using the standards outlined in [198]. The subjects were asked to determine initial posture, which they could use if they were to grasp and hold the objects. After the initial manipulation, the subjects were asked to apply force and trials were recorded, and fingers returned to their initial position. Since the aim of experiments is to record data and mimic the fingers' kinematic motion, subjects were asked to concentrate on performing full-motion rather than applying force. In total, three manipulations were performed in each experiment, with five repetitions in a total of 15 trials per subject. The items were chosen from the literature to cover the most often used hand movements in daily life. Each activity set lasted 10 seconds, and participants were given sufficient rest time. The subject's forearm was simply supported throughout the trials to prevent any movement. Figure 3.3 depicts the setup for the object gripping trial. The type of motion (here represent three objects) were decided based on the literature that indicates these three motions are frequently used in daily household and working condition [198], [200]. Although there are no standards for object selection, most of the literature followed certain motions representing main muscle activities (see table 3.2) derived from [201], [202].

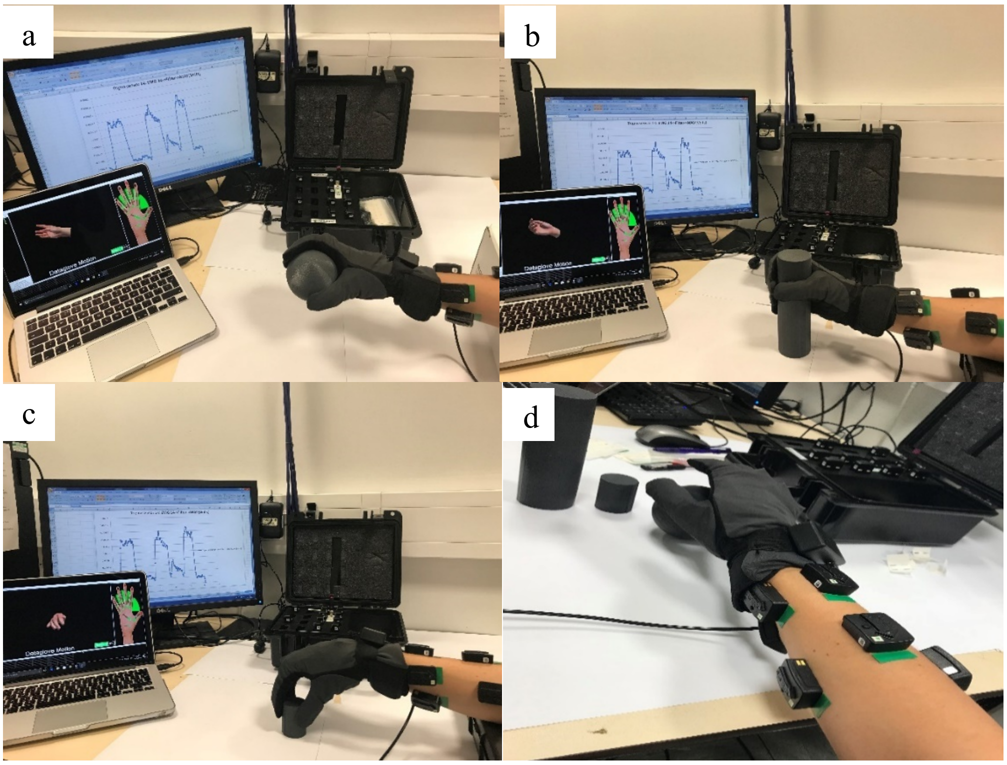

Figure 3:3: Presentation of three hand manipulations (objects grasping). Three objects are ball grasping (sphere), cylinder grasping, precision control pinch grasping, and hand open (relax) position.

Considerable efforts have been made to reduce the effect of arm mobility by using new training protocols that take into account independent parameters. In this methodology, a dynamic strategy for training a classifier with increased generalisation ability that incorporates different EMG changes in data collecting was taken. A total of three-arm postures were used in training methods, which affect elements such as upper-limb muscle tension and sEMG distribution. The literature shows that a large portion of data has been collected from static arm-hand posture is presented in [176].

The identical electrode array, finger, and hand grabbing actions were used in the third and fourth groups of experiments. In these trials, subjects were asked to hold their arm in three different positions in order to assess the effects of arm orientation on EMG signal amplitude and motion detection performance. The experimental setups were identified from the literature [118], [119]. EMG data representing different arm positions were collected for each class of motion and used for pattern classification. In this the last stage of the experiments, the subjects were asked to sit on a chair and start with their upper limb relaxed vertically (figure 3.4(a), and then the subjects were asked to perform a series of finger motions in this position. For the second arm position, after having maintained their arm in the horizontal position, the subjects were asked to flex his arm from the elbow to bring the forearm in the vertical (up) position (as shown in figure 3.4(b)). The third group of the experiment was conducted while the subject's arm was on the table in a horizontal position (figure 3.4(c)). In the forearm mobility experiments, the subjects were asked to relax their arm and flex/extend his finger to the maximum degree as they felt comfortable.

Figure 3:4: Experimental setup showing the arm's positions to perform finger motions and objects grasping with targeted muscle investigation. (a) the arm on the horizontal table position, (b) arm upright, (c) arm up-down (vertical).

3.3 Data Processing

The EMG data were collected using the aforementioned experimental settings to identify muscle activation patterns and amplitude from all channels in order to categorise the label of each window. Because it is difficult to classify samples from raw data and overcome some limitations of raw data, raw sEMG signals for Quattro and Trigno electrodes were pre-processed at 2 kHz before being used as a control command. Raw sEMG signals were band-pass filtered and normalised in relation to the muscle contraction levels promised. To minimise noise and movement artefacts, a 4th order Butterworth band-pass filter in the frequency range of 20-450 Hz was used, as the major energy of the EMG signal is stored at this frequency. EMG data segmentation enhances prediction accuracy and control precision. Therefore data processing and windowing size must also be chosen carefully since it has a considerable impact on real-time control performance, as inconvenient windowing size causes motion execution to be delayed.

Larger windowing sizes have been recommended for high classification performance in several machine learning algorithms, such as SVM and LDA; nevertheless, this causes classifier decisions to be delayed and results in high prostheses rejection rates. Windowing sizes ranging from 50 to 300 ms have largely been documented in the literature[176] . According to studies[100], [187], the best results have been obtained with small incremental windowing sizes. In this study, two distinct window sizes were used to evaluate alternative windowing sizes. Chapter 5 contains a detailed explanation of the influence of widowing size.

For comparison reasons, signals were firstly segmented at a windowing size of 125ms (window overlap: 0.0625 s). Because the intensity of sEMG signals varies from subject to subject, the level of the signals was adjusted using a variable gain amplifier. For performance comparison, a larger windowing size, 300 ms (with 150 ms overlap), was employed, and details are presented in chapter 5. Notably, the segment size must be greater than the processing and decision period in order to prevent the sliding window problem. Therefore, such a compromise in accuracy is essential to enable appropriate time for decision making while the new sample is gathered during continuous control.

Electromyography signals are generally derived in the form of time-domain (TD), frequency domain (FD), and time-frequency domain (TFD) features. Time-domain features have most commonly employed as they are derived from various signal magnitudes in a specified period. On the other hand, frequency domain (FD) features to utilise the power spectrum for feature extraction have been used in [100], [102]. Thus, the studies based on the sEMG signal have proved that the best results can be achieved in the time domain features [117], [176], since the delay for TD computation is less than for other domains such as FD and AR. Furthermore, autoregressive (AR), time-domain autoregression (TD-AR), and wavelet transform (WT) has also been employed as feature extraction methods. A detailed review of feature extraction methods and their implementation is given in chapter 2. In this chapter, six features of raw signal in time domain were computed for each window: Root Mean Square (RMS), Mean Absolute Value (MAV), Integrated Absolute Value (IAV), Waveform Length (WL), Simple Square Integration (SSI), and Average Amplitude Change (AAC). In order to compare different denoising methods and to improve comprehension of EMG data, two-periodic TD features, kurtosis analysing (KA)[203] and peak activation level [204] were also used . Some of these features have already been used in some earlier works [95], [199]. The type of feature extraction methods was chosen from the literature [112], [205] that highlight these processing methods are more practical for real-time control since they do not require high computational power. Figure 3.5 illustrates pre-processed sEMG data collected from the human counterpart (subject 1, male 26 years old, right handed) while the user exhibits sequences of inserted (flexion and extension) actions.The figure was created from one subject to illustrate the effect of feature extraction methods. The EMG signals were analysed in MATLAB using custom-written code, and a mathematical explanation is provided in Appendix B.

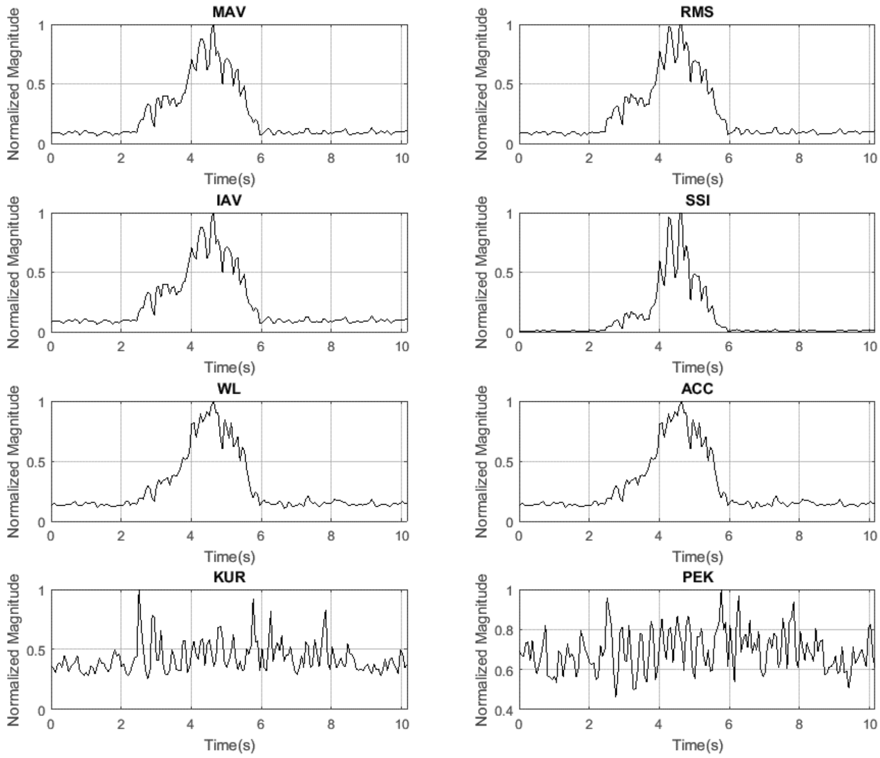

Figure 3:5: Illustration of eight feature extraction methods for ring finger manipulation.

Figures 3.6 and 3.7 (acquired from subject 1 during five trials for representation) illustrate the pre-processed and amplified EMG data for finger motion and object grasping trials. The divided sections depict the occurrence of motion throughout the course of 10 seconds per motion.

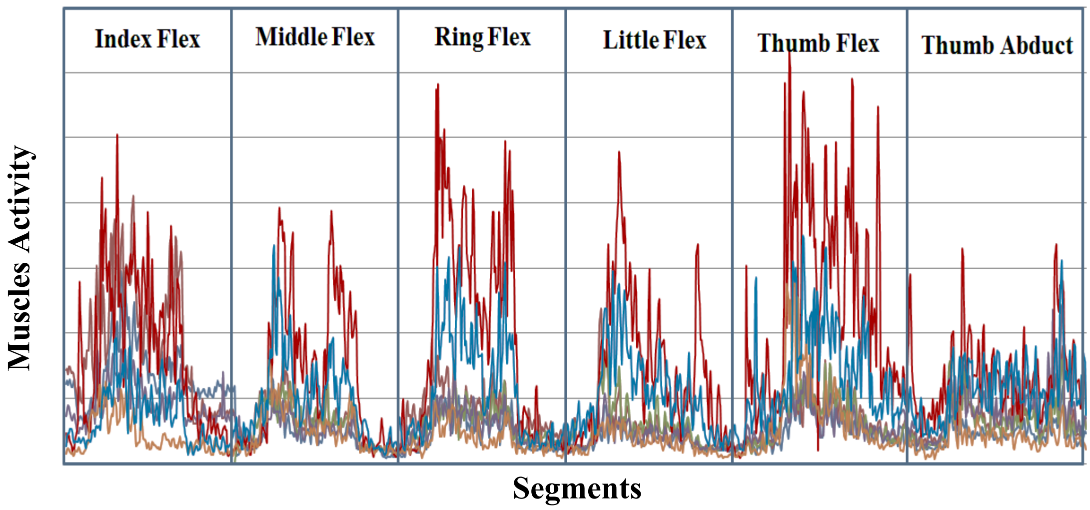

Figure 3:6: The composition of the sEMG signal from an able-bodied subject while performing six individual finger motions. Each colour represents the RMS value of the seven channels used in the experiment.

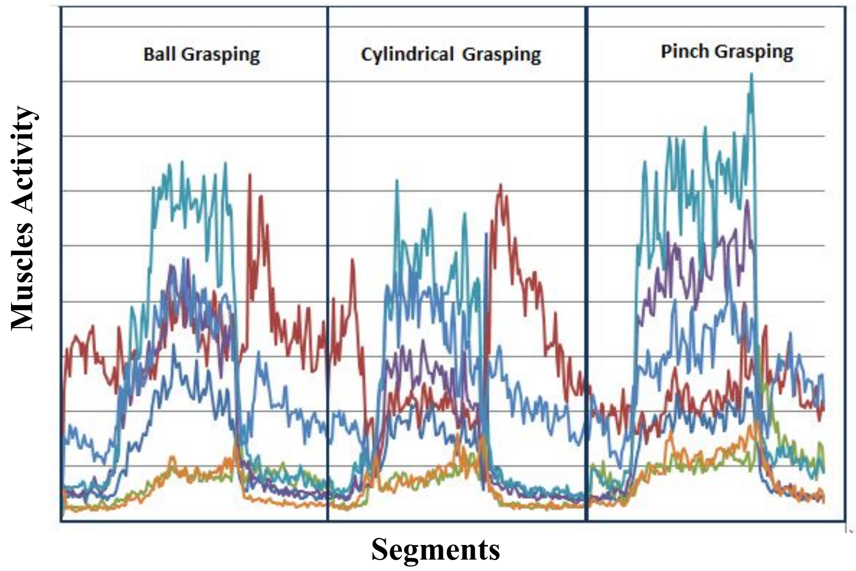

Figure 3:7: The composition of sEMG signal from an able-bodied subject while performing three objects grasping Each colour represents the RMS value of seven-channel used in the experiment

Training data points were normalised to obtain mean zero and standard deviation in each dimension or electrode. The data sets for each user was split into 70% training and 30% for testing sets. Consequently, feature representation is the value of each EMG signal (i.e., seven channels for six movements or three grasping) from each channel. As illustrated in figure 3.8, these feature vectors are provided as the input value of our classifier.

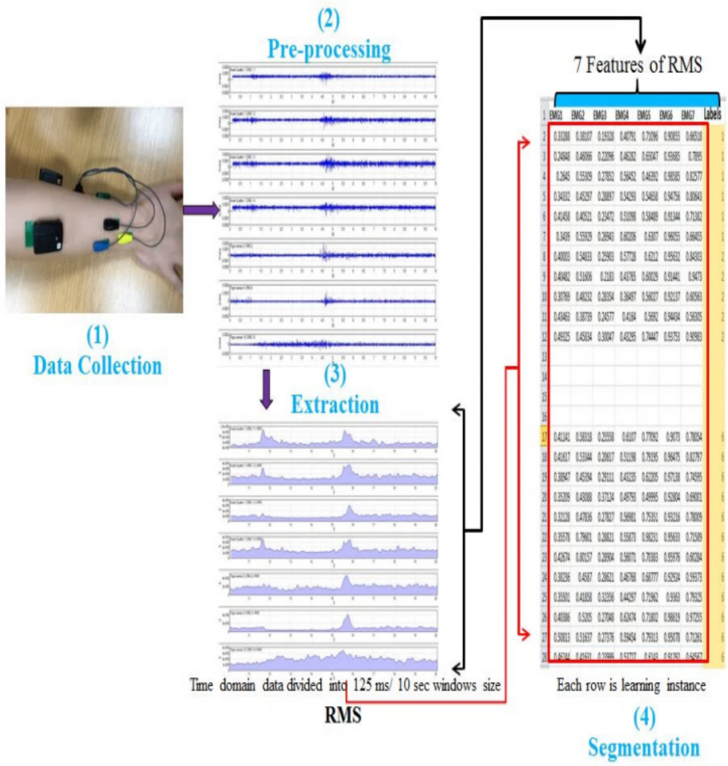

Figure 3:8: The block diagram of proposed data processing. The process comprises four parts: EMG measurement, EMG signal processing, feature extraction, and data segmentation.

3.4 Electromyography (EMG) Data

The muscles' data was collected for each of the three arm conditions with seven channels from each session. All channels were examined at the same time, and the data for each muscle was chosen using a mapping system that allocates a digit number to each muscle (representing electrode). This method was chosen for the examination of targeted muscles because each electrode position and targeted muscle are documented before each session (see figure 3.8)

The primary goal of this chapter is to evaluate the methodology, namely electrode positioning, number of electodes, signal processing methods, and actually observing the sEMG for individual finger could identified for different arm positions. In the discussion, sEMG data from five subjects were analysed for assessment of muscle fatigue and subject influence on data set. Furthermore, because various subjects reflect different levels of muscle contraction, summarising the results of five participants in the same graph is difficult. For example, it was observed that for some subjects, the sEMG signals for EPL and ED muscle were significantly weak compared to other participants, however this does not affect the pattern recongition performance because pattern reconition is not rely on the magnitude of sEMG signal rather the pattern in the signals. Therefore, the results for subject 1 were shown in figures to avoid misrepresentation, with the exception of the figures in the discussion that compare participant influence. However, the figures represented for subject 1 are the average data from five trials. In Chapter 4, the major comparisons between participants, processing methods, classification approach, and electrode number were presented.

3.4.1 Objects Grasping Trials

The data for this study were obtained with seven sensors on the forearm of five able-bodied subjects while they grasped three items, as illustrated in figure 3.9. The crosstalk signal would be significantly reduced with smaller electrodes and a shorter inter-electrode spacing. With the exception of movement artefacts such as wrist rotation caused by the same subject, same muscles, and various experimental approaches, the noise is steady. The muscle behaviours for grabbing three different objects were similar for each trial. The similarity is that a peak has occurred along with active muscles. However, the muscles' combination of grasping ball and cylinder is more powerful than pinch grasping. Participants applied limited fingertip force because flexor digitorum profundus muscle is predominant in the first two grasping types. The variation of EMG amplitude during object grasping tasks was significantly smaller than finger manipulation tasks. The reduction of EMG amplitude could be attributed to stability and control over the force required to hold the objects.

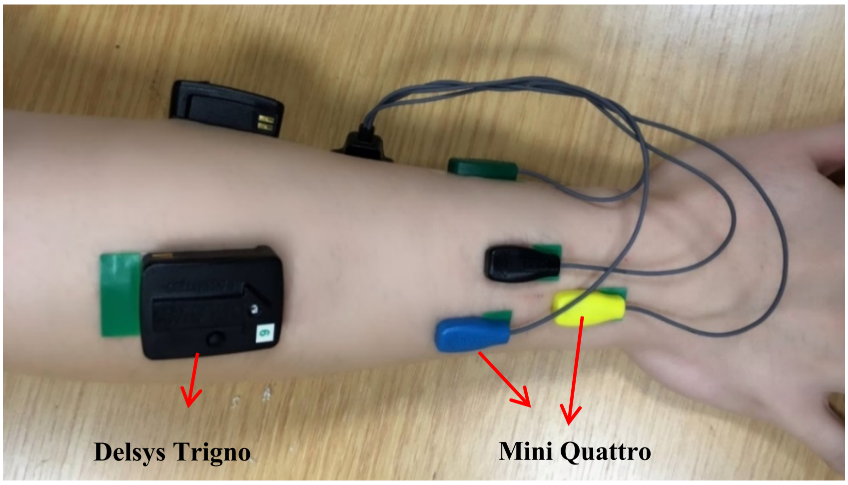

Figure 3:9: Electrode placement on the right forearm. The Quattro sEMG sensor pairs were distributed: over extensor pollicis Brevis muscle (CH1); over extensor digitorum muscle (CH2); over flexor digitorum profundus (CH3); and over flexor digitorum superficialis.

It is suggested that there is a strong relationship between sEMG signals and force. While forces in muscles increases, so do the sEMG signals. This is because there is influence from other muscles, also referred to as cross-talk [206]. This impact may be an issue in biomechanical research or rehabilitation studies since it might mislead therapy and create a misunderstanding of diagnosis. However, in the case of pattern recognition, this may not result in a misleading conclusion. However, electrodes must be placed above specific muscles in order to take exact measurements and evaluate muscle function in relation to identical activities.

Throughout the trials, flexor muscles were seen to be more active for all trials, and this was owing to the anatomical nature and accessibility of the muscles under consideration. The second peak was noticed following the first peak because the extensor digitorum (ED) muscles contracted when extending the fingers while the flexor muscles relaxed (as seen in figure 3.10).

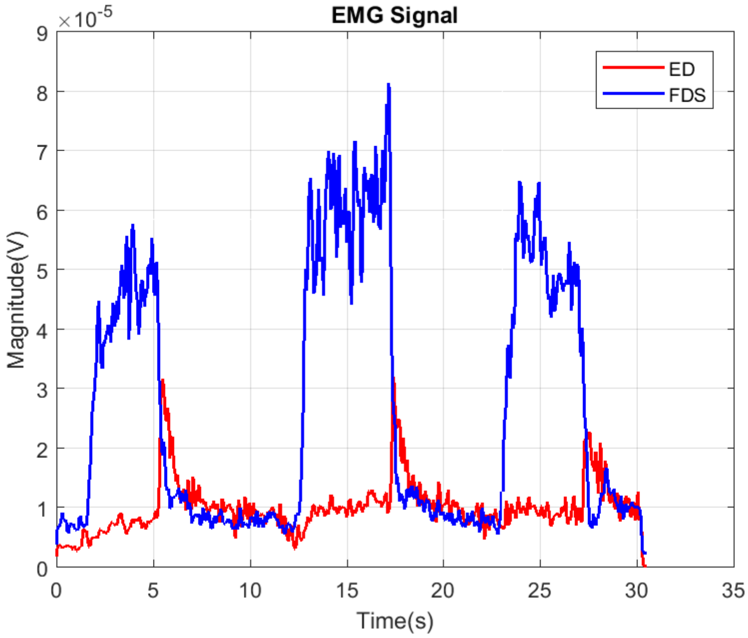

Figure 3:10: Flexor and extensor muscles composition (MAV value) during pinch grasping trials while the participant's arm is in horizontal positions.

During the trial, flexor digitorum profundus (FDP) and flexor digitorum superficial (FDS) muscles were predominantly active during the initiation and maintaining the PIP and DIP joint functions. Maximum activation occurred around full force grasping. During the pinch grasping, the extensor indices activation was dissimilar in ball grasping or cylindrical grasping trials. This was with the exception of large activation of the number of fingers and muscles. The extensive activation during object contacting and the second peak after releasing the grasping suggested that the participant's muscles are relaxed in the initial phase of movements. Notable, muscle activation time for the extension is significantly less than flexion activation time; this is because the subject applied force around three seconds.

When the subject hand is in a rest position, there is a force balance between intrinsic and extrinsic muscles. As suggested from studies [207], [208], we know extrinsic muscles are responsible for forceful grasping, flexion, and extension of the MCP, DIP, and PIP joints; therefore, when there is an intention of nerve, the balance is lost and force from extrinsic muscles are predominant. Carpi muscles are in charge of wrist extension and were not examined during the trial as we maintain minimum action in wrist rotation. For the object grasping in almost all tests, the pollicis muscles are more active as they apply force at the joint for abduction and extension of the thumb. Figure 3.11-3.13 demonstrates the right arm's muscle compositions during three objects grasping: ball grasping, cylinder grasping, and pinch grasping.

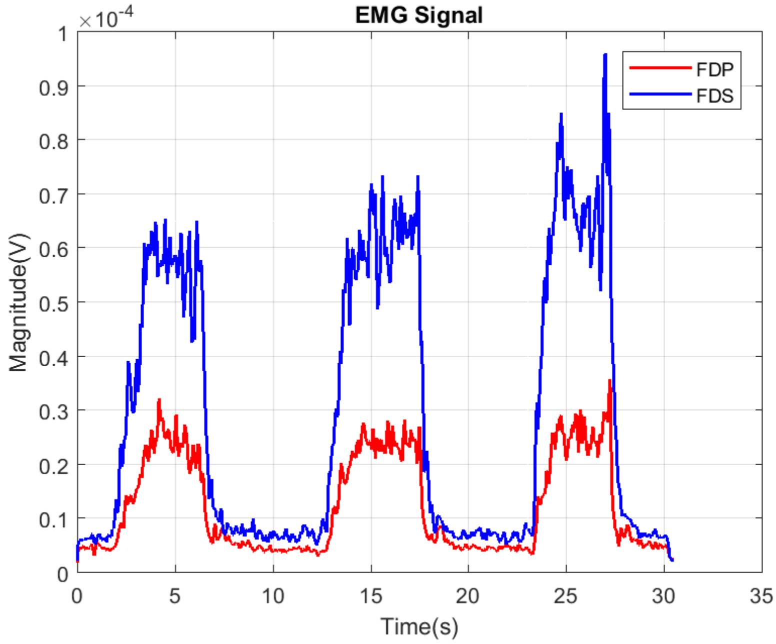

Figure 3:11: Muscles composition during ball grasping trials. The figure represents the MAV value of flexor digitorum profundus (FDP) and flexor digitorum superficialis (FDS) while the subjec's arm is horizontal.

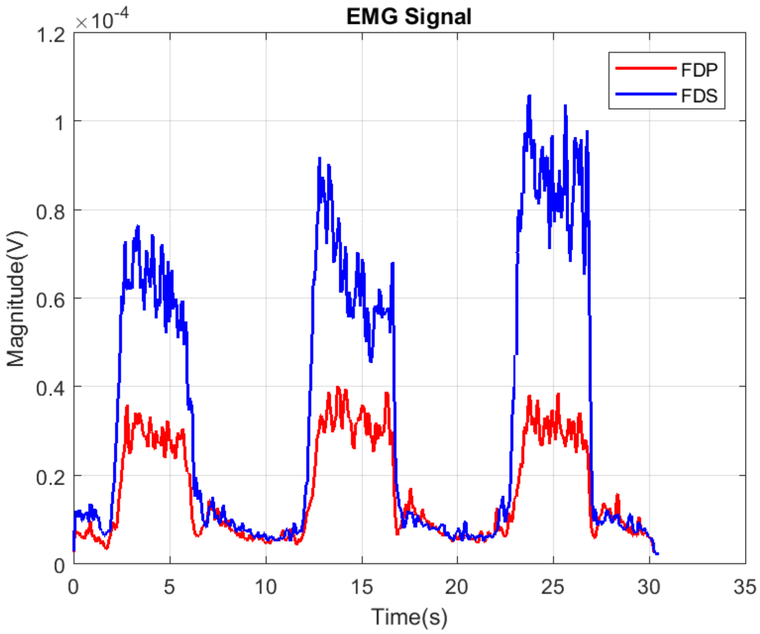

Figure 3:12**:** Muscles composition during cylinder grasping trials. The figure represents the MAV value of flexor digitorum profundus (FDP) and flexor digitorum superficialis (FDS) while the subject's arm is horizontal.

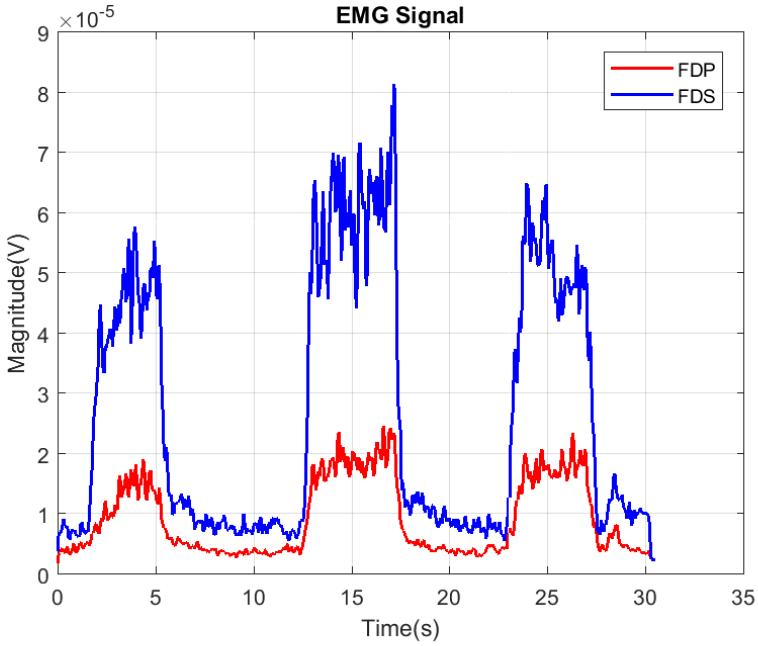

Figure 3:13: Muscles composition during pinch grasping trials. The figure represents the RMS value of flexor digitorum profundus (FDP) and flexor digitorum superficialis (FDS) while the subject's arm is horizontal.

Three scenarios were developed to test whether changes in elbow angle (forearm position) elicited EMG amplitude during object gripping and flexion and extension of individual finger motions. First, we looked at hand muscle EMG activity when the participant held the presented items (ball, cylinder, and pinch) in three distinct forearm postures (as shown in figure 3.4). We completed the trials on the same subject to guarantee that any EMG signal variations were caused by arm position and not by separate individuals. We asked the participant to repeat the identical pressures and finger trajectories as much as feasible.

Figures 3.14-3.16 demonstrate the EMG signals of the flexor digitorum profundus (FDP), flexor digitorum superficialis (FDS), and flexor pollicis longus (FPL) alter considerably with different arm postures ($p < 0.001$). This suggests that the arm posture of able-bodied participant influence muscle distribution. Some muscles, such as the brachioradialis, are placed in the forearm's posterior region and allow wrist flexion and extension. This research does not look at the biceps and triceps muscles in charge of forearm flexion and extension, respectively, from the shoulder to the elbow. Although physiological variations in the upper extremities may occur from subject to subject, resulting in differing muscle group compositions, EMG data demonstrated strong reproducibility across movement cycles for all trials and motions. Figure 3.14-3.16 depicts the change in muscle composition throughout three distinct arm positions: horizontal on the table, vertically upright, and vertically down.

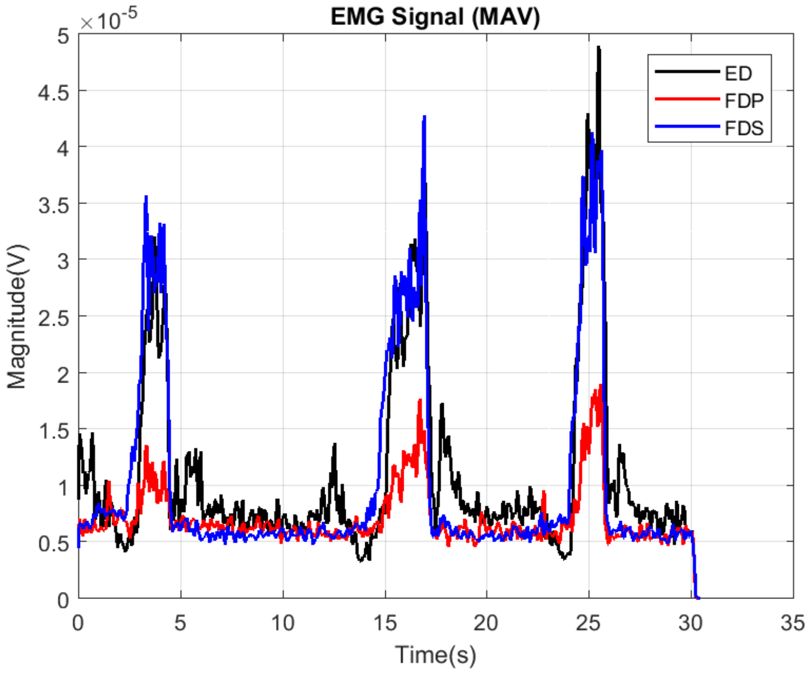

Figure 3:14**:** Flexor and extensor muscles composition during ball grasping while subject's arm was horizontal on the table. Data represents the MAV value of flexor pollicis longus (FPL), flexor digitorum superficialis (FDS) and flexor digitorum profundus (FDP).

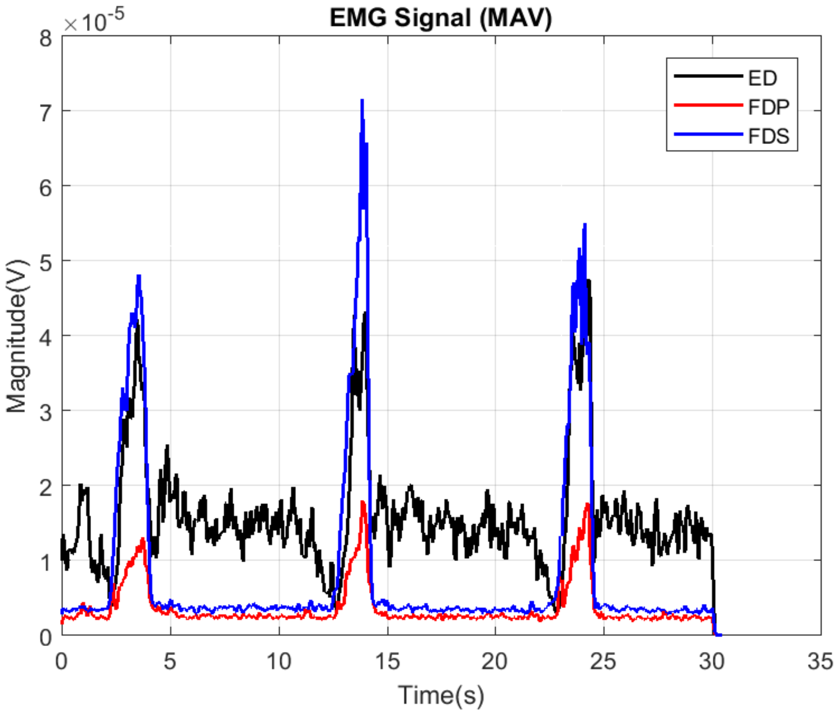

Figure 3:15: Flexor and extensor muscles composition during object grasping while subject's arm was vertically up position. Data represents the MAV value of flexor pollicis longus (FPL), flexor digitorum superficialis (FDS), and flexor digitorum profundus (FDP).

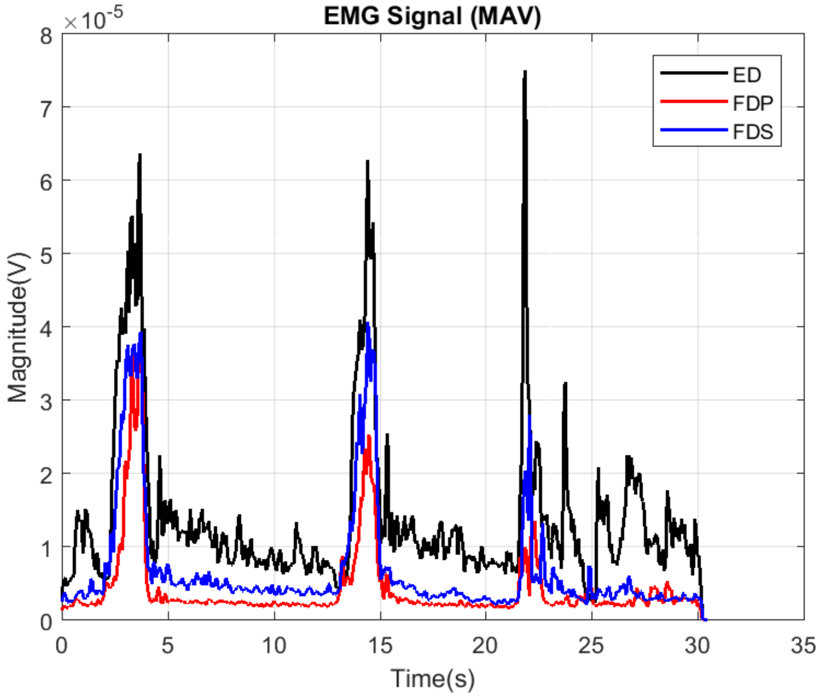

Figure 3:16: Flexor and extensor muscles composition during object grasping while subject's arm was vertically down position. Data represents the MAV value of flexor pollicis longus (FPL), flexor digitorum superficialis (FPS), and flexor digitorum profundus (FDP).

3.4.2 Finger Manipulation Trials

The trials for seven sensors followed a similar pattern to the object gripping studies. Because the participants were instructed not to apply force to the fingertips, the muscle activation amplitude for moving individual fingers is less intense than that for grabbing the items. When compared to object grabbing, the variance in EMG amplitude for finger manipulation was substantial. The same strategy was taken in all cases; the subjects were asked not to rotate their wrist, as it would be expected in real amputation conditions. Extensor muscles were more engaged during phases than object gripping trials (see Figure 3.17). The highest level of activation occurred near the end of finger flexion. Peak activation of the extensor pollicis longus (EPL) and extensor digitorum (ED) occurred around extension beginning, allowing fingers to be extended.

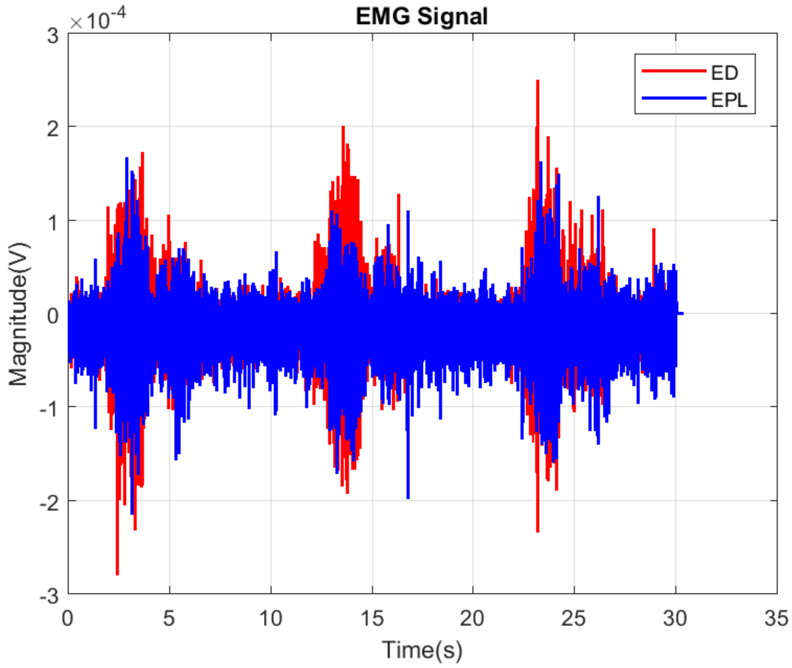

Figure 3:17: Raw EMG signal composition during ring finger flexion and extension while subject's arm was in the table (horizontal position). Data represents extensor digitorum (ED) and extensor pollicis longus (EPL).

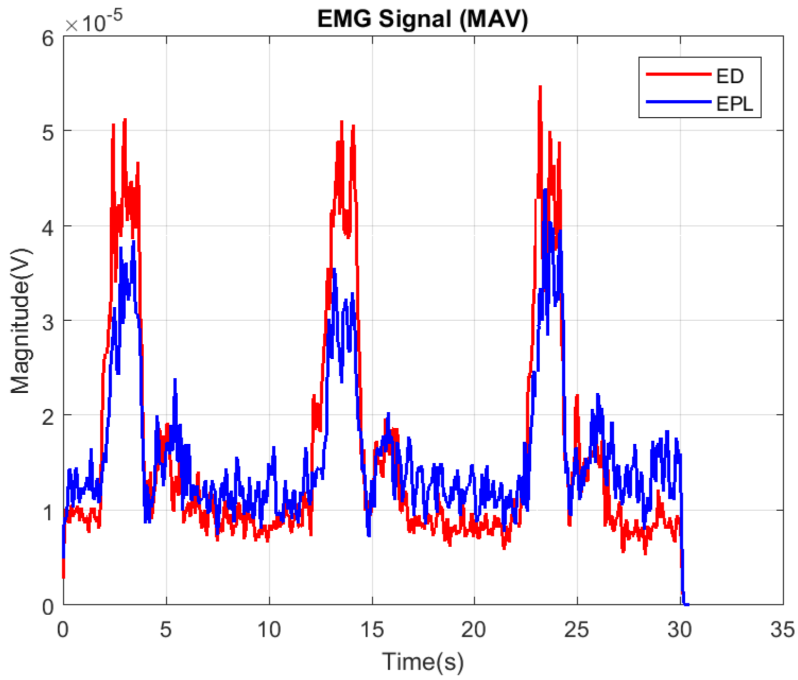

Figure 3:18: Representation of MAV values of ring finger flexion and extension.

As shown in the figures, it was impossible to investigate the beginning and sequencing of finger digits. Furthermore, the graphic does not indicate which finger joint flexion occurs first. Figure 3.19 demonstrates that when flexion is commenced, the extrinsic muscle group plays a significant part in executing the flexion of the MCP, DIP, and PIP joints for a short period of time, whereas the extensor muscle remains tense for a longer period. The statistical data show that the average EMG amplitude is larger for ring movements than for thumb flexion.

According to Figure 3.20, the extensor pollicis longus (EPL) muscle most influences finger EMG amplitude. The research also shows that there is no significant difference in identification ability amongst extrinsic muscles ($p = 0.7390$); however, a significant difference between trials was observed (p =0.0001).

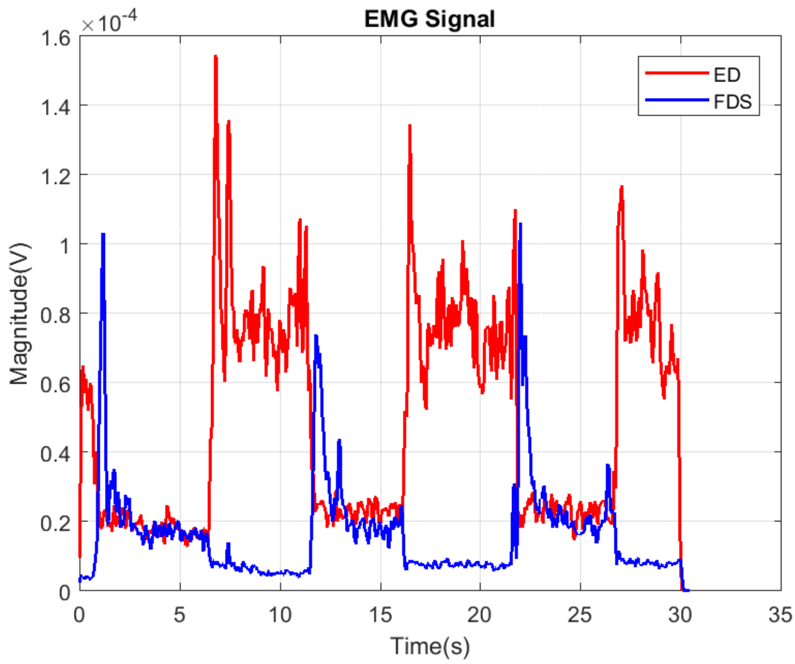

Figure 3:19: The sEMG value representation of flexor and extensor muscles during ring manipulation. RMS results for Extensor Digitorum (ED) and Flexor Digitorum Superficialis (FDS) while the subject's arm was in the horizontal position.

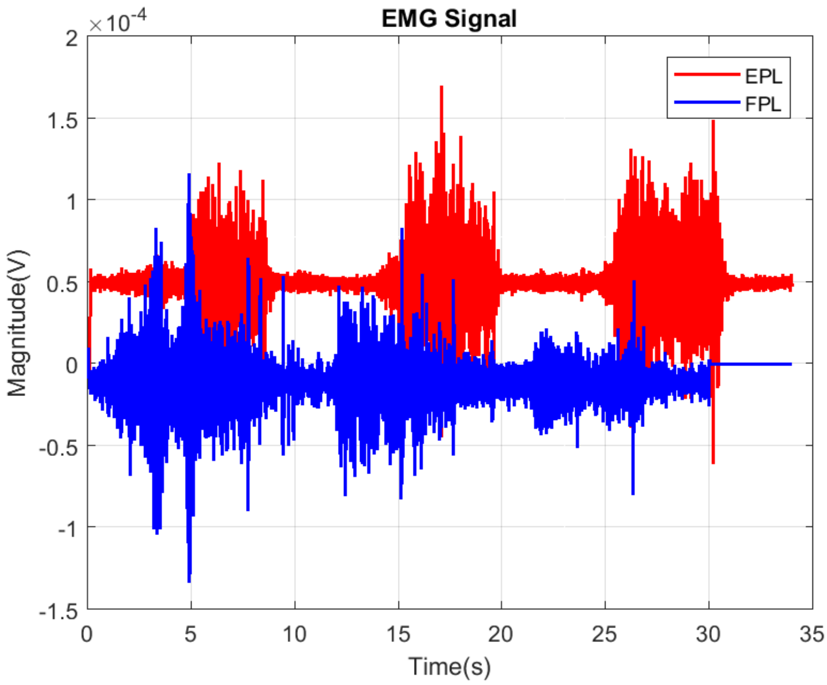

Figure 3:20: Extensor and flexor muscle behaviours during thumb abduction while subject's arm was horizontal on the table. Data represent the RMS value of sEMG signals.

The same approach was used to investigate the influence of arm postures on EMG levels and motion identification performance as it did for object grabbing. The same scenarios were tested again to see if changes in elbow angle affected the amplitude of EMG activity during finger flexion and extension. We examined the EMG activity of hand muscles while the participants moved individual fingers in various forearm postures. We completed the trials on the same subject to guarantee that any EMG signal variations were caused by arm position and not by separate individuals. We requested the participants to repeat the identical pressures and finger trajectories as much as possible. Flexor muscle activations show that EMG muscle activation levels do not change considerably with arm position (as seen in figure 3.21-3.23). During single finger manipulation trials, the average EMG amplitude of flexor muscles in the horizontal position was found to be lower than in the vertical and downward positions.

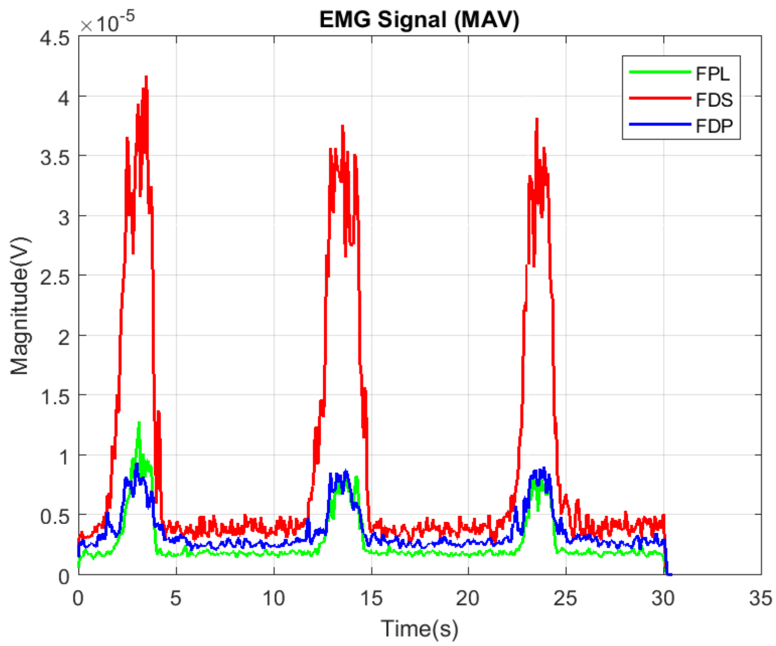

Figure 3:21: The demonstration of MAV values of flexor pollicis longus (FPL), flexor digitorum superficialis (FDS), and flexor digitorum profundus (FDP) while ring finger flexion in horizontal arm position.

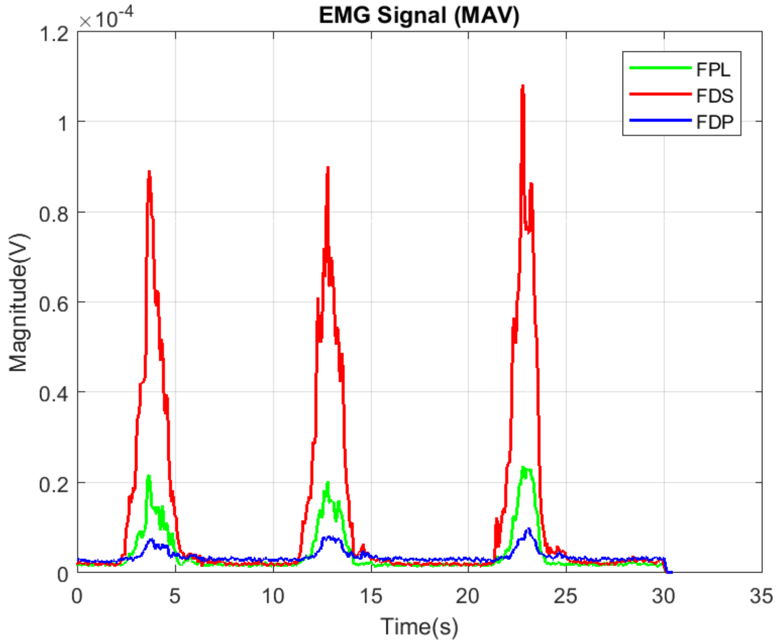

Figure 3:22: The demonstration of MAV values of flexor pollicis longus (FPL), flexor digitorum superficialis (FDS), and flexor digitorum profundus (FDP) while ring finger flexion in arm upright position.

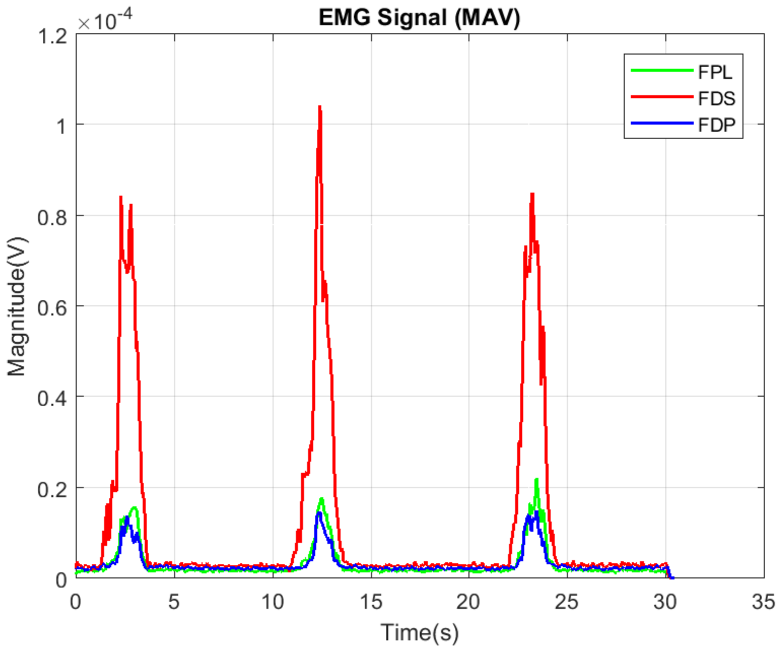

Figure 3:23: The demonstration of MAV values of flexor pollicis longus (FPL), flexor digitorum superficialis (FDS) and flexor digitorum profundus (FDP) while ring finger flexion in arm vertical down position.

Almost the same muscle patterns were observed in the examination of extensor muscles during varied arm postures. When the participant's arms were in a vertical posture, the activation of the extensor pollicis longus was greater than that of the extensor digitorum. The comparison of figures demonstrates that in the observed action, the muscle fibres had a biphasic form with the identical electrode setup. The phases were reflected in the direction of muscular membrane alterations, as stated in the literature. Muscle amplitude is influenced by the diameter of the muscle fibres, the distance between active muscles, and the acquisition point. Figures 3.24-3.26 show the composition of extensor muscles during ring finger flexion.

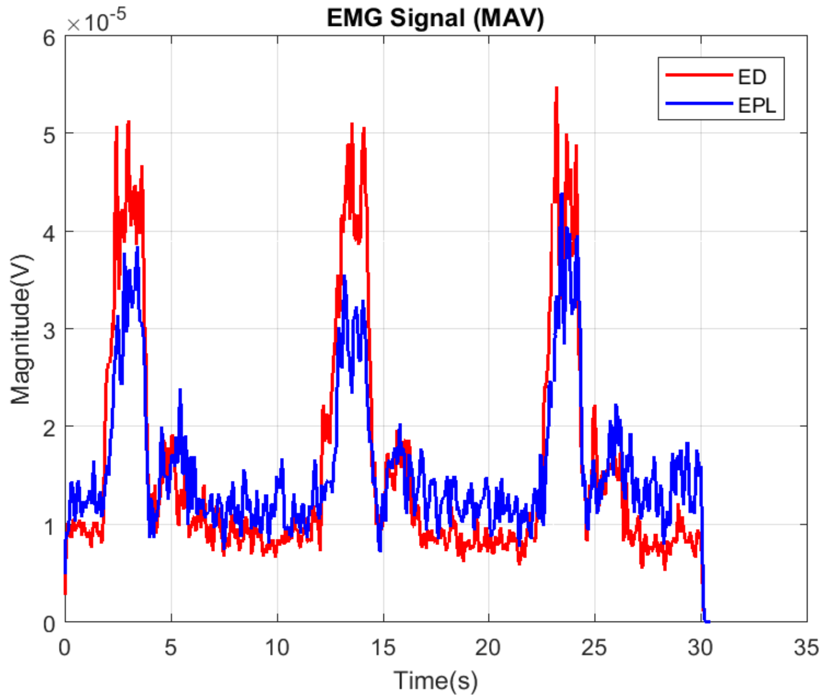

Figure 3:24: The demonstration of RMS values of extensor digitorum (ED) and extensor pollicis longus (EPL) while subject's arm was in the horizontal position.

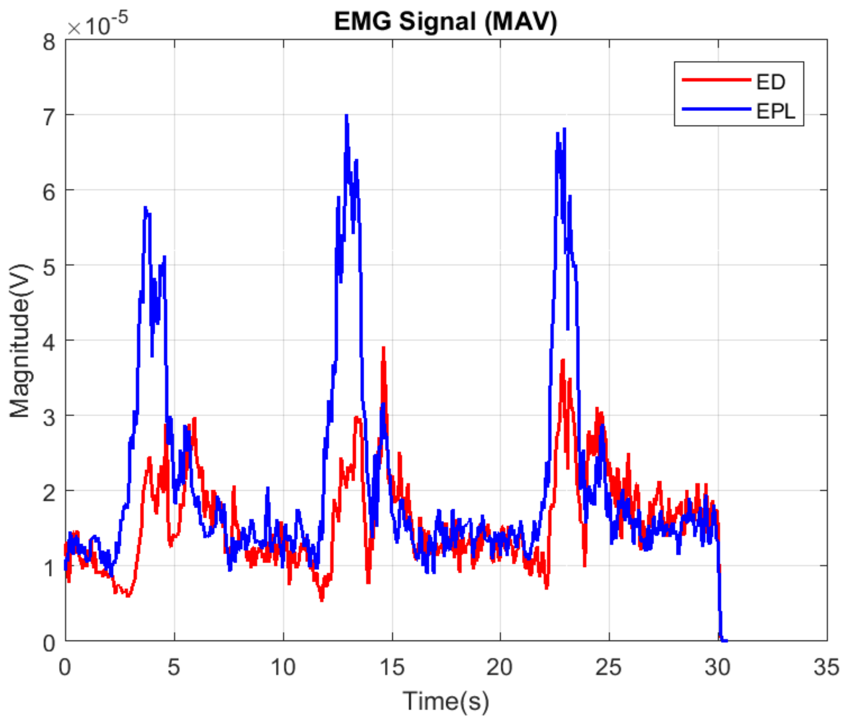

Figure 3:25: The demonstration of RMS values of extensor digitorum (ED) and extensor pollicis longus (EPL) while subject's arm was in the upright position.

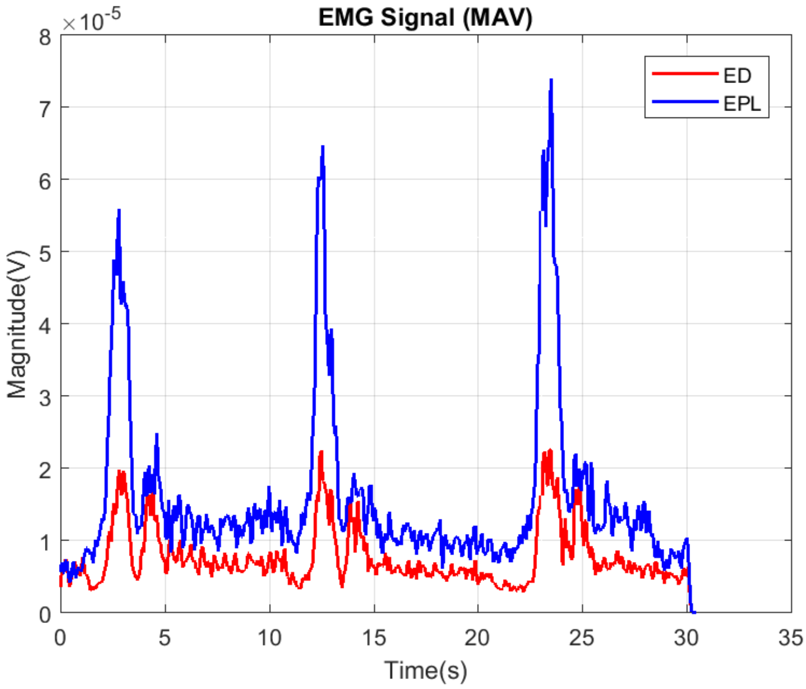

Figure 3:26: The demonstration of RMS values of extensor digitorum (ED) and extensor pollicis longus (EPL while subject's arm was in the vertical down position.

3.5 Discussion

3.5.1 Influence of Arm Mobility

Several studies on able-bodied and amputee people have been conducted to investigate the effects of arm trajectory and, in particular, user mobility on classification performance [209], [210]. According to studies, arm position variation considerably impacts classification performance in offline and offline tests. Various classification approaches have been offered to remove such influences [4],[211]. The user's arm position would unavoidably change while manipulating the number of upper limb motions. Thus, if the user performs an action that differs from the arm posture used for model training, classification performance suffers significantly because the pattern changes. Among other factors, arm position variation has a significant impact on intuitiveness and performance degradation in real-time control. Therefore, it is ultimately one of the major causes for the high rejection rate of EMG control-based prosthesis. Some studies recommended alternative training protocols, such as multilocation setups in which the participants perform a trajectory for collecting data to train the ML model to reduce the effects of arm position volatility. However, it is uncertain if it has the same impact on amputees because they have almost lost a big section of their residual limb; most arm muscles are inaccessible.

Because it has been argued that dynamic hand motions are more reflective of real-time case scenarios, the subjects were instructed to execute five repetitions of multiple finger manipulation in three distinct arm postures to examine the impact of arm mobility on classification performance (see Figure 3.4). Other research [166], [212] have demonstrated a comparable experimental protocols.

The effect of arm position on classification performance was calculated after removing the mean baseline EMG and then normalising the EMG amplitude values by respective hand motions. Classifiers were trained using time-domain features, as previously reported. The final assessment (see Figure 3.27) demonstrates that the classification performance for RMS with SVM is 87.4 % when the subject's arm is vertical downwards and 81.2 % when it is horizontal, with a 6.2 % difference. The average classification for the ANN using RMS was 85.8 % when the subject's arm was vertical downwards and 87.2 % when the subject's arm was upright; the difference is 1.4 %. These findings show that, whereas arm position dramatically modifies muscle shape and EMG amplitude value, it has no significant effect on certain classifiers' performance such as ANN but significant effect on LDA and k-NN in three distinct arm positions ($p = 0.3692$).

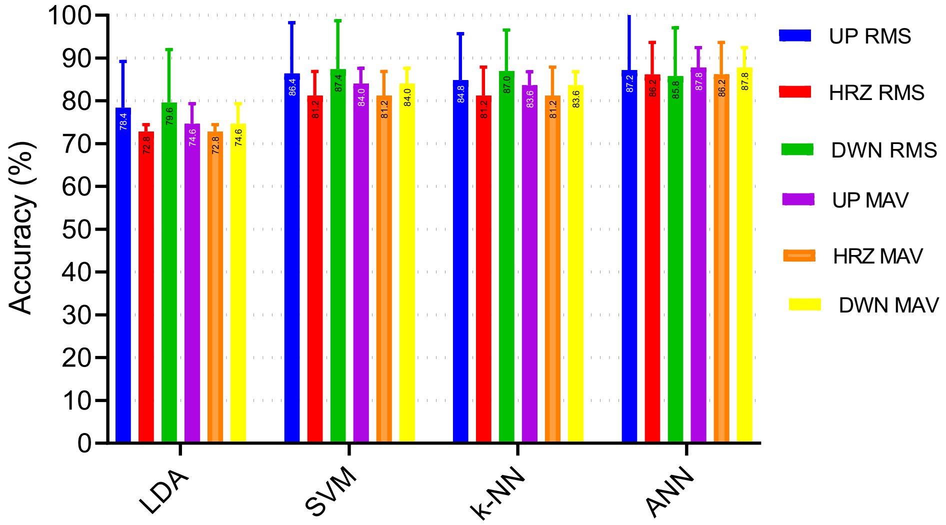

Figure 3:27: The classification performance of four classifiers and two arm positions for objects grasping for RMS and MAV features in 125ms windowing size. (DWN) represents arm vertically in down positions and (UP) in the upright position (HRZ) horizontal

The evaluation for finger manipulations reveals (see Figure 3.28) that RMS classification performance with SVM was 81.6 % while the subject's arm was upright and 80.25 % when it was vertical down, a 1.35 % difference. The average classification in the ANN with MAV was 79.8 % when the subject's arm was upright and 79.4 % when the subject's arm was vertical down. These findings suggest that, with the suggested electrode orientation, arm position has no tangible effect on classification performance for some classifiers for finger manipulation. This could be due to the fact that there is no fingertip force for each individual finger, hence it does not greatly alter EMG patterns.

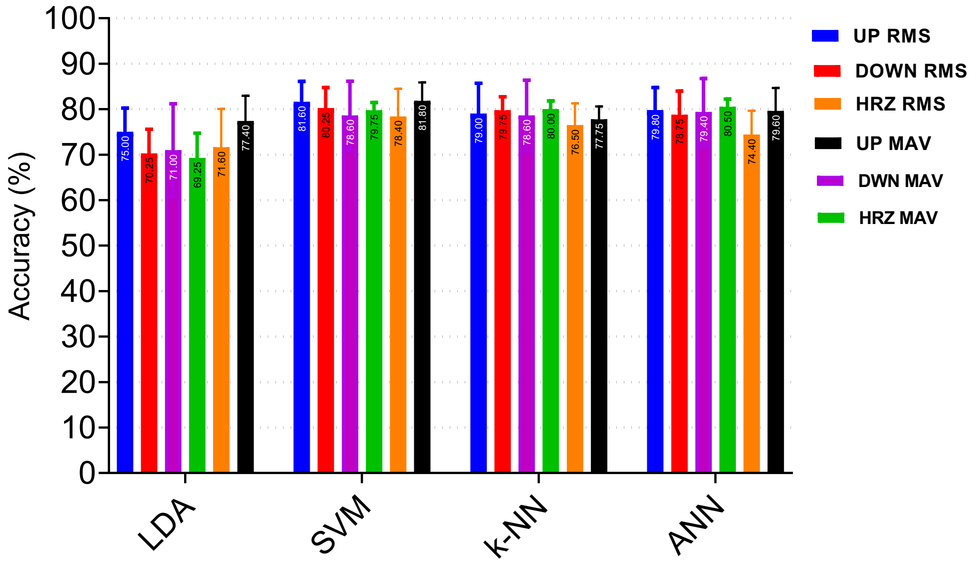

Figure 3:28: The classification performance of four classifiers and two arm positions for finger manipulation for RMS and MAV in 125ms windowing size . (DWN) represents arm vertically in down positions and (UP) in the upright position (HRZ) in horizontal position.

Yang *et al.* [209] have investigated the effects of arm position change on amputees using traditional single positioning and multilocation configurations. They have claimed that using multilocation to improve motion completion rate considerably reduce the influence of arm position changes (almost 8%). Gu *et al.* [116] have reported that, the model trained with arm mibility protocol significantly increase pattern recognition performance, it has been discovered that the traditional (single position) arm position has a motion completion rate of 64.6 %, which is 8.7 % lower than the multilocation arm position for real-time control.

Similar research has been conducted in [212] and [213]. In these studies, a dynamic motion collection procedure has been followed for the able-bodied participants, and the classification accuracy for the k-Nearest neighbour classifier was reported as 68-72%. Therefore, the subject mobility has been reported to have significant effects, about 8.98% degradation on motion classification performance.

3.5.2 Muscle Fatigue and Influence of Individuals

Several studies have demonstrated good accuracy for multiclass motion detection in electromyographic control-based prostheses [86],[112],[187]. Even though the offered approaches achieved high-performance levels of more than 90%, prosthesis users are still unable to sustain continuous motion detection in real-time and experienced long-term usability concerns.

The effect of experiment repetition that indicates the muscle fatigue influence is displayed in figure 3.29. There were statistically significant differences between trials based on RMS feature classification error change (2.35-6.09%). The comparison between each repetition shows some differences, but that does not particularly prove muscle fatigue effects. The experiment did not show a further decrease in the last experiments; on the contrary, the classification error decreased. This improvement in classification performance may be attributed to the fact that the participant performed the series of experiments several times and trained his muscles, leading to muscle contraction level adaptation. However, because of the small number of people employed in the trials, it is difficult to generalise the results. The statistical differences were observed for different features and classifiers and presented in Appendix C

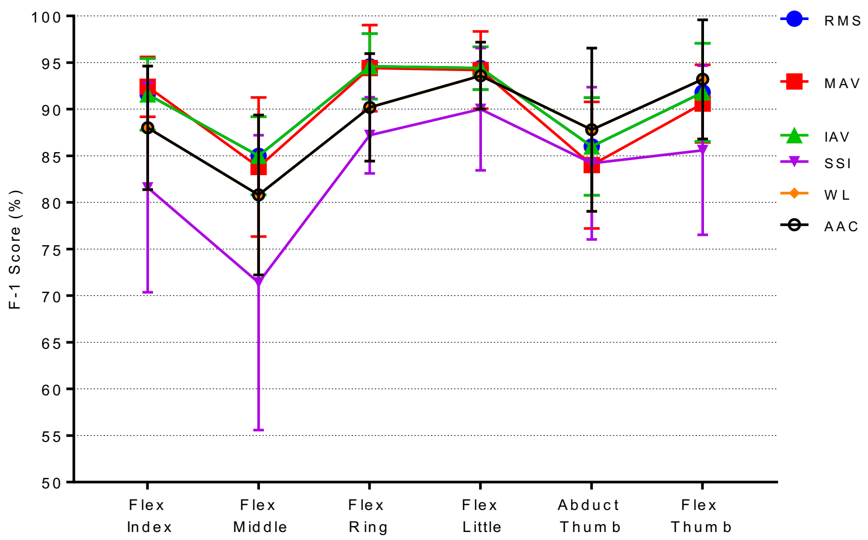

Figure 3:29: Classification performance of SVM with six features. The movement repetition has different classification accuracy.

The results indicate that (see Figure 3.30) there was no correlation between subjects and their pattern recognition performance ($p < 0.0001$). This significant variation implies that, while the signals may give some consistency across multiple individuals, they may also generate some unwanted overshoot at different finger locations for different participants. This might also imply that the levels of EMG signals alter over time, possibly as a result of electrode shifting. As a result, it is undesirable for practical application of the myoelectrical control system.

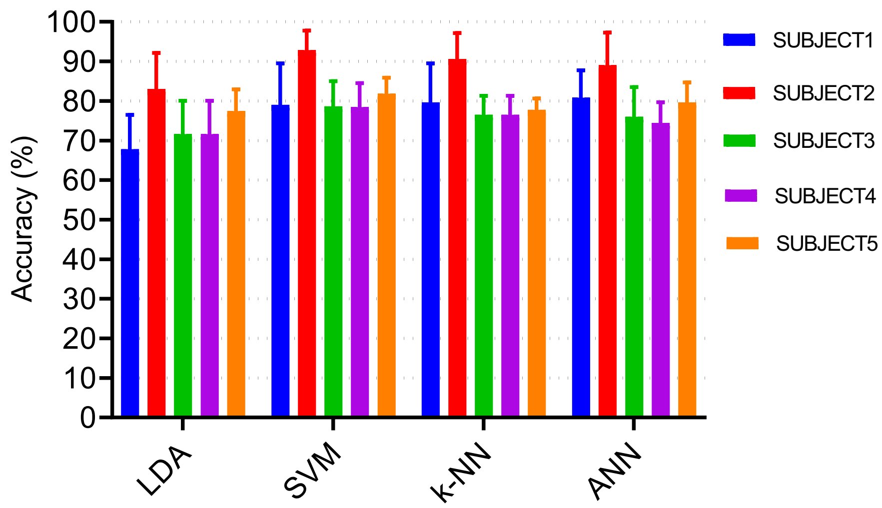

Figure 3:30: Summary result for offline analyses in the able-bodied subjects. The figure illustrates subjects have significant classification performance differences.

Most studies in the literature collected data on a single day or over a short time, causing sEMG data collected in laboratories to differ from real-time applications. The long-term effects of EMG signals have been reported in a few studies [149], [211]. Phinyomark *et al.* [100] have collected data for 21 days with identical motion sequences and with the same subject to investigate the long-term usage influence on EMG signal. They have also researched the influence of various conditions, such as after some physical activities. In this study, it has been shown that the classification accuracy is not significantly different (~2.45%). This might be owing to subject-to-subject variance in muscle contraction level.

In order to provide a good comparison of prosthetic hand usability in real-time and evaluate convenient acquisition setup, Pizzolato *et al*. [112] have conducted a series of experiments and highlighted that fatigue and subject adaptation do not significantly influence muscular response. However, he acknowledges that there are significant variations with respect to movements and subjects since subjects present different muscular characteristics. Muller *et al.* [214] have used BCI with ten EEG electrodes to evaluate the power decrease in EMG signals. They have conducted a test on an amputee subject for three days, and their results showed that there is power degradation on some frequency almost 4%. Hwang *et al.* [215] have conducted a similar experiment with able-bodied subjects. The outcome of their research indicated muscle fatigue in long-term use; however, they claimed this did not change classification performance significantly.

3.6 Summary

This chapter discusses multifunctional upper limb prostheses based on pattern recognition and their manipulation using sEMG signals. A database containing kinematic and sEMG data from the forearm of 5 able-bodied participants while performing six fingers and three object grasping was created for ML model training. The experimental protocol and analysing techniques were derived from the existing literature. A comparative approach was taken to analayse and discuss the compatibility of methodology with some publicly available datasets such as [86],[112].

The data collection is based on seven sEMG Delsys Trigno electrodes to collect signals for different arm positions in order to extend prostheses functionality. On the same subjects and motions, the muscle contraction levels for targeted electrode allocations were acquired to compare the effectiveness of the electrode allocation approaches using consistent feature engineering and data processing. The data acquisition setup both for targeted and untargeted approaches produced comparable results to early literature [22], [100], [187],[216] . Given the fact that these experiments do not include data from hand amputees, it has been demonstrated that sEMG collected from able-bodied subjects can also be used as surrogate datasets from amputees [191].

Individual finger classification was the focus of the experiments. The investigation results revealed that the combined feature extraction and machine learning methods can achieve higher than 84% accuracy, with only 6% variation between participants. The variation between subjects can be interpreted as additional clinical variables that may have influenced the participant's ability to induce muscle contraction, although the procedures were equal. The results show that there are no significant statistical differences when the number of movement repeats is considered for the same subject ($p = 0.5367$), though there are significant differences when various movements and participants are included (p =0.0044). This is reasonable since muscles change when participants change, resulting in varying muscular force and, thus, alters sEMG signal amplitude.

This chapter also examined the performance of two distinct windowing methods in offline classification accuracy on the collected training datasets. The average accuracy was (87-89%) for 125 ms windowing length and (89-92%) for 300 ms windowing length, which is comparable to some classification accuracy reported by [81], [84]. In trials, the variations between experiment repeats were 4.5 %, but some significant changes occurred, notably in the WL and ACC feature extraction approaches. Nonetheless, the effect appears to be substantial only in a few classification methods, including LDA and k-NN.

The goal of this chapter is to demonstrate the disparities and lack of experimental standards in the literature and provide and validate a sEMG database by independent finger signal categorization using popular classifiers. The database generated reliable results, while effective classifiers reached or surpassed similar research, achieving average accuracy greater than 84%, whereas earlier publicly available databases gained 79.77% and 69.83% for Ninapro DB1 and DB2, respectively.

Although the approach and datasets are comparable to the literature, categorisation inconsistencies can occur due to a variety of circumstances. To begin with, research has shown that the age and gender of the individuals might have a considerable impact on sEMG amplitude. Second, the number of classes and the sampling rate affect the results presented in reference studies. Finally, the number of electrodes and their location on the forearm differ between studies.

Chapter 4 Comparison of Classification Strategies and Feature Extraction Methods for Prosthetic Control

4.1 Introduction

Several signal types were investigated in the preceding chapter to develop more reliable sEMG signal datasets for real-time prosthesis control. In order to maintain a more consistent pattern recognition system, this chapter discusses and tests the developed sEMG database utilising a range of classifiers, feature extraction methods, windowing sizes, and electrode allocation procedures. Besides that, this chapter conducts extensive research to assess the real-life test conditions, such as movement repetitions, signal classification accuracy rate, and ML parameters tuning, to eliminate the effect of these factors and improve the findings.

In recent decades, studies have focused on developing sEMG based control method to differentiate hand and finger movements as accurately as possible. Different numbers of electrodes have been paired with muscles to remap a variety of hand and finger motions. In a simple approach, two electrodes of the EMG signal were analysed for four elbow and forearm motions in [217]. In another study, Huang *et al.* [218] collected sEMG signals for four pairs of surface electrodes to determine seven hand movements. Other studies have researched hand and arm movements predictions with a large number of surface electrodes, such as eight electrodes [219] or even more with 32 electrodes [147]. It is suggested that more muscle information increases prediction accuracy in offline and online trials. However, due to limited skin surface area and the finite number of sensors, it is not feasible to characterise 21 (DoFs) under the control of 29 superficial arm muscles. Therefore, it is suggested that determining new feature extractions with different classification methods could make significant differences in developing prostheses' performance.

Many classification approaches have been presented for motion classification, and as a result, good accuracy results for various features and subjects have been achieved. Using our data sets from various scenarios, we utilised five classification approaches for eight feature extraction methods. Eight time-domain features with two windowing lengths (125 ms and 300 ms with half overlap) were evaluated to investigate the influence of feature sets on the classification of human hand gestures. Larger windowing sizes have been recommended for high classification performance in several machine learning algorithms, such as SVM and

LDA; nevertheless, this causes classifier decisions to be delayed and results in high prostheses rejection rates. Windowing sizes ranging from 50 to 300 ms have largely been documented in the literature [176] . According to studies[100], [187], the best results have been obtained with small incremental windowing sizes. The effect of windowing size on classification accuracy is presented in [216]. The sEMG data were acquired from 5 able-bodied volunteers while they performed six finger and three hand motions with varying arm orientations (as presented in chapter 3).

Although several features and classification algorithms have shown strong classification performance, not all methods are computationally suitable for real-time prosthesis control in clinical application. Recent enhanced approaches enable machine learning systems to rapidly execute user intented motion. However, they lack the precision and accuracy required to perform planned motions on a continual basis. Some experiments in the literature have used unrealistic settings such as sensor number, electrode location, windowing size, and learning parameters, making it impossible to integrate smooth hand motions in an acceptable computation time. The classification performance eight time-domain features for two sampling rates was examined using five prominent machine learning methods with k-folds (k=10) cross-validation for the first goal of this study. In this comparative evaluation, the learning algorithms (SVM, LDA, k-NN, ANN, and LR) were trained and assessed for practical considerations and real-time application utilising sEMG features from all defined circumstances. In addition, we showed the efficacy of classifier performances and derived features in terms of amputation level and different number of subjects. This chapter discusses the implications of windowing length, electrode placement, electrode number, and learning parameter on classification accuracy, as well as their possible influences on real-time control.

4.2 Statistical Analysis of Machine Learning Methods

With eight feature methods and five popular classification methods described in section 2.3 and section 3.2, representing a total of 40 combinations and introduced functions, we have achieved successful results regarding motion detection. Some of these features have already been used in some earlier works [22], [95]. The type of feature extraction methods was chosen from the literature [112], [205] that highlight these processing methods are more practical for real-time control since they do not require high computational power. This study demonstrated that six independent finger movements can be differentiated across different experiment sessions and features extraction methods. It presents the accuracy differences between different electrode placements, such as targeted surface and untargeted surface electrode placement. The findings are expressed in terms of accurately classified finger motions. The findings revealed the difficulty in identifying separate finger activities caused by the anatomical anatomy of the human arm muscular system. The resutls revealed a disparity between real-time and offline control in the literature.

According to limited study on individual finger motion detection, with some differences from earlier literature, above 80% accuracy with same data sampling frequency and methodology is suitable for real-time control of multifunctional prostheses and movement recognition [151]. The number of classes, the length of windows, sEMG feature extraction methods, machine learning classifiers, and the number of subject and electrode placement approaches all influence classification accuracy. Variable combinations were investigated, and the impacts of variables were statistically presented in this chapter to develop intuitive prosthetic control.

All statistical data were generated using statistical and Machine Learning Toolbox and functions in MATLAB 2017a (MathWorks, Natick, USA). All statistics were generated using the functions that were provided in toolbox. The effects of subjects and different trials were analysed using a two-way analysis of variance (ANOVA) with repeated experiments on each data set. The least square difference (LSD) multiple comparisons were used to examine differences across variants. Statistically significant differences (p<0.05) across models and motions were denoted by a '*', indicating that the average accuracy obtained from different movements and methodologies differs considerably.

4.3 Feature Selection

With the experimental setup described in Chapter 3, EMG datasets were collected to identify the activation pattern and amplitude of muscles from all channels in order to categorise each window. Because it is difficult to classify samples from raw data and to overcome various constraints of raw data, and prevent misclassification, we pre-processed raw EMG signals as described in Chapter 3 section 3.3. Appendix E has a comprehensive mathematical explanation as well as custom-written MATLAB scripts.

4.4 EMG Based Motion Prediction Algorithms

To control prostheses, the information extracted from EMG signals is fed into classifiers, which map a variety of patterns. Thus, classifiers and their parameters must be carefully chosen in order to discriminate the introduced features with high accuracy. Following the acquisition of the ideal parameters and kernels, the trained model is utilised to create a control command for prosthesis in real-time. A range of techniques, varying from deep learning to linear classifiers, have been employed to classify sEMG data. The next subsections provide a complete evaluation of parameters as well as the efficacy of classifiers on pattern recognition.

4.4.1 Approach 1 (Linear Discriminant Analysis)

The prediction accuracy, complexity, and computing cost of classifiers are all related and considerably effective in real-time control. As a result, the choice of classification technique should also be based on computing cost rather than only classification accuracy, especially in embedded real-time control. In this study, linear and non-linear classifiers were compared in order to give valuable insight into the selection of relevant machine learning approaches for pattern classification.

Linear Discriminant Analysis (LDA) is a supervised linear classification approach that has been widely used to classify biological data. The singular value decomposition "svd" was employed as a solution in this investigation since it outperforms both in classification and has benefits on big feature sizes. As discussed in section 2.4.2, this approach has also been applied in several studies for online control of prostheses. LDA is a efficient method for dealing with multiclass supervised classification problems [98]. The optimal recognition rate obtained for this approach for individual fingers and hand gestures is shown below.

The LDA classifier was implemented using eight time-domain features in the first portion of the preliminary analysis, with initial data sets divided 70 % training 30% testing with k-fold (k=10) cross-validation. The feature samples were randomly shuffled until a proportional class number is achieved. F1 scores were used to evaluate the performance of each finger class, whereas accuracy metrics were used to evaluate the performance of each feature. Figure 4.1 depicts LDA's performance for six features of targeted muscle electrode placement. Due to representation concerns, the findings of two periodic features (kurtosis analysis and peak activation level) were not included in this main chapter; however, more information is provided in appendix C. As shown in Figure 4.1, MAV performed best with a mean accuracy of (84 ±3.8) %, whereas SSI performed worst with a mean accuracy of (67±8) %. The two-way ANOVAs test for the three key features RMS, MAV, and IAV indicated no statistically significant differences (p =0.7643). This is most likely because the mathematical differentiation of these features is comparable. There was a significant difference across trials (p =0.0044) and the other features such as SSI, WL, and AAC (p =0.0221).

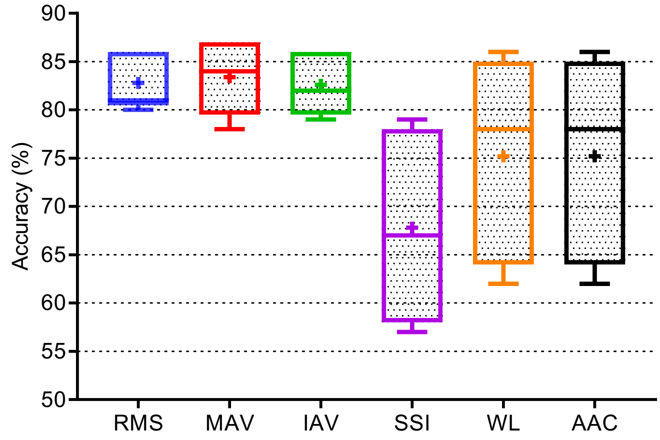

Figure 4:1: Offline classification accuracy of six features for targeted (TR) muscles.

The F1Score of each finger for each targeted muscle is shown in Figure 4.2. Individual finger research yielded the best classification performance for ring finger flexion, with an average (90 ± 5) % identification, and the worst classification performance for middle finger flexion, with an average (72 ±6) percent recognition. Except for the SSI feature, there was a statistically significant categorization difference between ring flexion and middle finger flexion (p<0.0001). These findings are consistent with the anatomical nature of the human arm muscular system, as described in Chapter 3.

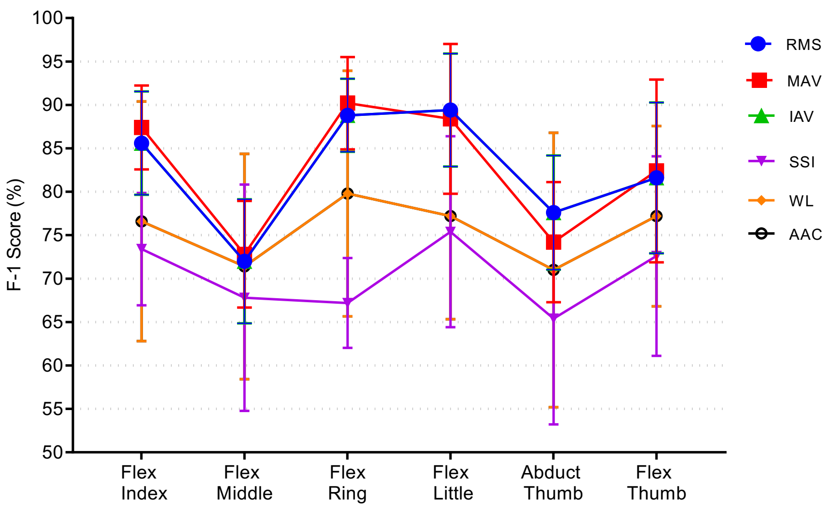

Figure 4:2: Offline prediction performance of six individual fingers motion in targeted (TR) muscle trials

The same parameters with the same windowing size were used to characterise the effects of introducing untargeted muscle electrode implantation. Figure 4.3 shows the accuracy of six features for seven electrodes placed around the arm with the untargeted muscle condition. MAV had the best classification performance (87 ±5) %, with no significant statistical difference across features ($p = 0.97$); nevertheless, the ANOVA test reveals a significant variation between each trials ($p = 0.0025$).

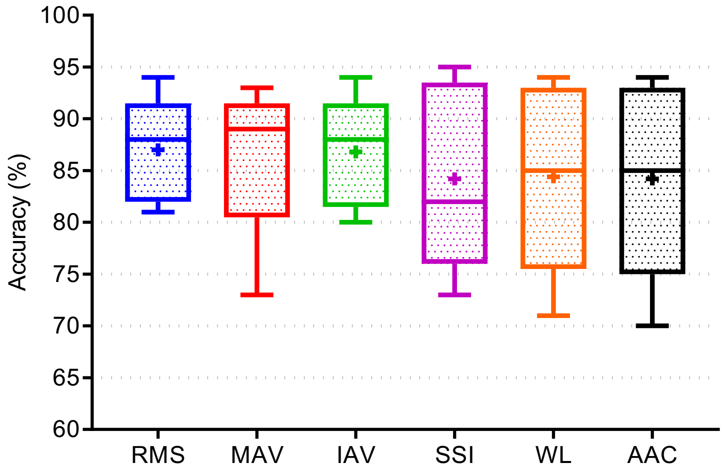

Figure 4:3: The classification accuracy of six features for untargeted (UT) muscles

It was observed that there are no statistically significant differences between six finger movements($p > 0.7684$) for three main features. Similar to targeted muscle investigation, SSI, WL, and AAC features showed slightly lower performance. The examination of the test results and figure 4.4 show that features have similar behaviour while the mean F1Score varies from 95% for ring flexion to 84% for index finger flexion.

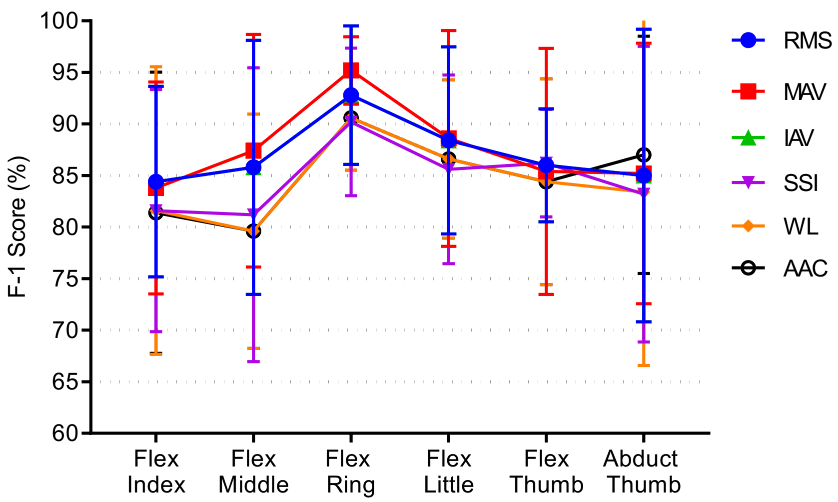

Figure 4:4: Offline prediction performance of six individual fingers motion for untargeted (UT) muscles.

Figure 4.5 shows that the two factors, two levels (targeted/untargeted), and repeated measurements discovered a statistically significant difference between targeted and untargeted electrode placement. The results appear to show that the best performance for the UT strategy over the TR condition is saturated by the performance of the targeted (TR) and untargeted (UT) schemes. When figures 4.1 and 4.3 are compared, statistics reveal that using untargeted muscles improves classification accuracy and delivers improved classification performance by an average of 5% (~83 % to ~88 %).

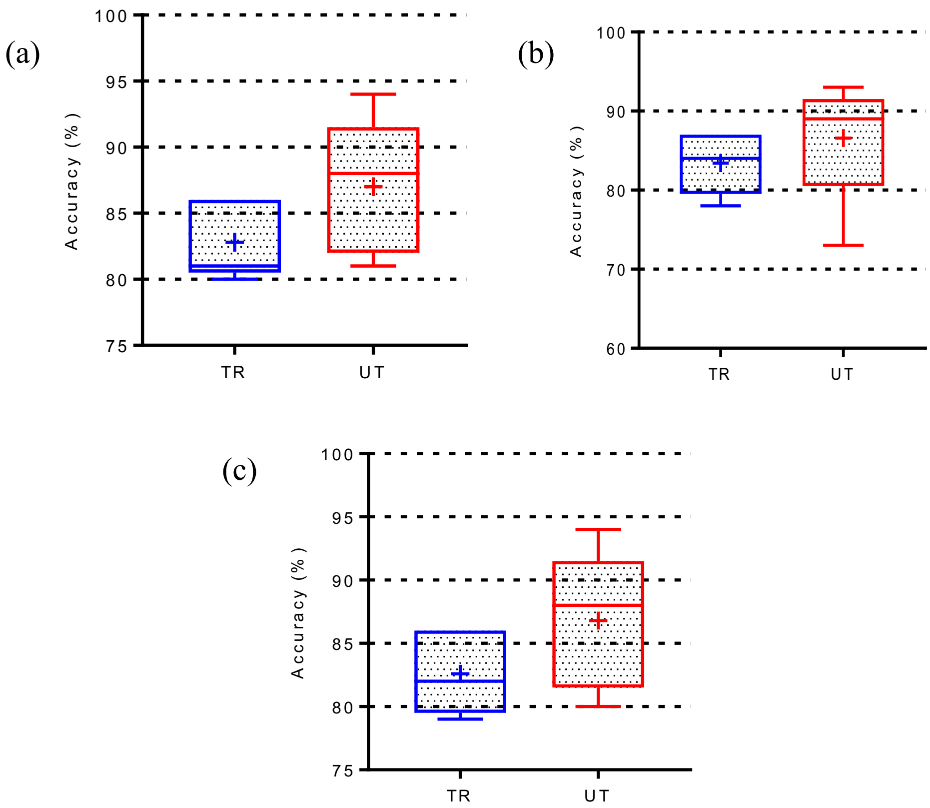

Figure 4:5: Classification accuracy obtained by different electrode placement for TR (targeted) and UT (untargeted): The figures represent (a) (LDA+RMS); (b) (LDA+MAV); (c) (LDA+IAV).

Performance results for recorded data with a windowing size of 300 ms are also included in this section. Despite the good performance of the 125 ms windowing size, it is worthwhile to experiment with different windowing sizes and choose the appropriate real-time control method. The size of the windowing has a considerable influence on the prediction of individual finger motions, according to findings in this study. The pre-processed data sets are fed into LDA in the prediction tasks. Offline accuracy for TR increases by 3% (from 83 to 86%) for RMS (see Figure 4.6). Similarly, the performance of UT for MAV increased by 4%, from 87 to 91 percent (see Figure 4.7). However, the consequences of such advancements must yet be examined clinically in order to completely determine their relevance.

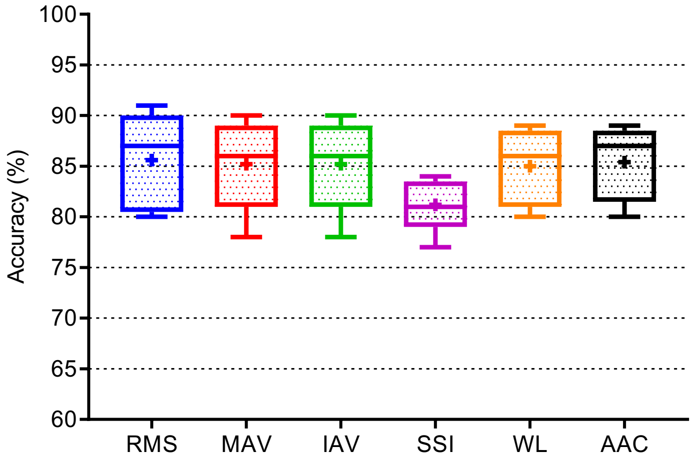

Figure 4:6: Feature extraction performance for targeted (TR) muscles in 300 ms windowing size.

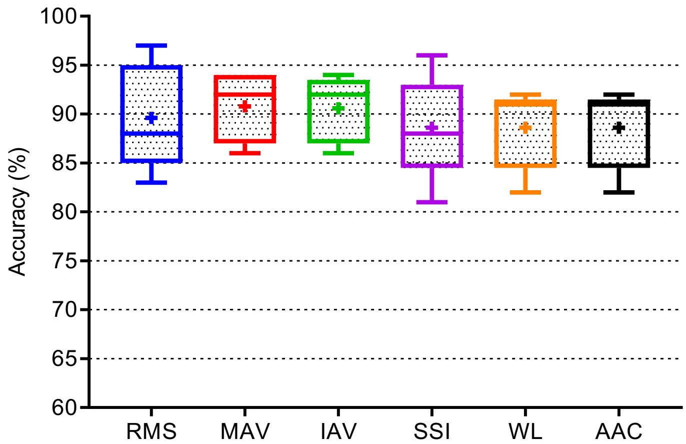

Figure 4:7: Feature extraction performance for untargeted (UT) muscles in 300 ms windowing size.

The results of Linear Discriminant Analysis suggest that this model's capacity to recognise the relationship between EMG data and finger patterns for prosthesis control is satisfactory. It also shows that the RMS and MAV features outperform other EMG features (see Figures 4.6 and 4.7). There is, however, a significant difference between six finger motion detection, which may be insufficient for real-time applications on users. Furthermore, it appears that the higher performance provided by nonlinear SVM kernels and ANN is required to attain acceptable performance for non-stationary EMG signals.

Figures 4.3 and 4.7 demonstrate the averaged classification accuracies obtained with LDA throughout five tests with five able-bodied people; these results are close to early studies presented in [95], [100]. Similarly Bellingegni [99], have achieved 91.9% using six ottobock electrodes with FT features. Mayor *et al.* [199], have achieved far superior signal classification; however, our results present a more realistic scenario because the related paper used mean amplitude value and FD as input features with 400 ms windowing size. According to Daley *et al.* [105], the able-bodied subject group have achieved a higher accuracy rate by (95%). The higher accuracy observed for the subject group could be attributed to a higher number of sensors and more sophisticated electrodes, which may have contributed to the acquisition of more representative sEMG signals. The corresponding accuracies achieved in [97] and [212] were 72% and 81.6%, respectively. Although the model accuracy is a fair comparison, the model parameters and feature sets are valuable information for model employment. Thus, this study decided to employ more straightforward features and windowing sizes to avoid overload signal processing, which causes a significant problem in real-time control.

4.3.2 Approach 2 (Support Vector Machines)

Different combinations of eight feature extraction methods and two electrode placement approaches with varying arm positions were tested by employing the support vector machine (SVM). SVMs are an essential feature in this research for minimising user impacts (training for new instances) and adapting the system to unknown new surroundings and new users because they exhibit somewhat superior performance. The SVM model with efficient coefficient C and kernel was achieved with grid search method. The grid search have identified RBF kernel to determine high accuracy for non-linear dataset, which is specific feature of sEMG signals. Based on the previously described feature extraction settings, other parameters (such as gamma and C) were selected by prior knowledge and user experiences after trials. The subsets were randomly shuffled until an optimal proportionate class accuracy was achieved. As previously stated in section 2.4.3, the SVM approach was employed with Keras in Python 3.5 by utilising open source libraries. The developed platform enables users to configure various regularisation settings and parameters.

This learning approach shown to be robust across the trials and could be employed independently from subjects and sessions. Upon these advantages, the technique is ideal for controlling dexterous prostheses with a high number of active degrees of freedom. In this section, the potential use of SVM and its parameters with different feature extraction methods were evaluated and presented. The figures demonstrate the results of the SVM classifier with six features; because the remaining two characteristics are not practical techniques for biosignal, they were provided in Appendix C for presentation purposes. The proportion of successful categorization between six groups for targeted and untargeted muscle research is shown in statistics for each feature and finger movement. For each activity, the performance metric were calculated independently. The ultimate accuracy provided in offline testing is the mean of the accuracies of five different subjects from five trials.

In terms of recognition performance, statistics show that the IAV feature has the highest rate, with an average accuracy of (91±2.3) %, while the SSI feature has the lowest rate, with an average accuracy of (84±7) %. RMS and MAV characteristics are shown to have the second and third highest recognition accuracy, respectively. The two-way ANOVAs revealed no significant differences between the three main features ($p = 0.8312$); their differences (2.53 %) were nearly identical because the mathematical calculations were similar, but there were significant statistical differences between trials ($p = 0.0266$) and remaining features ($p = 0.053$). Figure 4.8 depicts the experimental findings of offline performance.

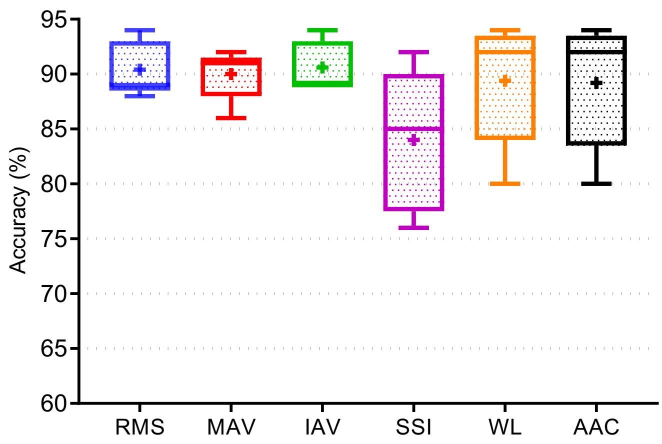

Figure 4:8: The classification accuracy of six time-domain features in 125 ms windowing size for targeted (TR) muscles.

Individual finger analysis (see Figure 4.9) found that ring finger flexion provides the best classification results, with a (95± 3.5) %, whereas pinkie finger flexion outperforms thumb and index flexion (94±2.1). However, the lowest performance was reported in middle finger flexion with (85±4.9) % detection for IAV. These results suggest that the FDS muscle mostly facilitates finger motions while moderately inhibiting them during thumb abduction and flexion.

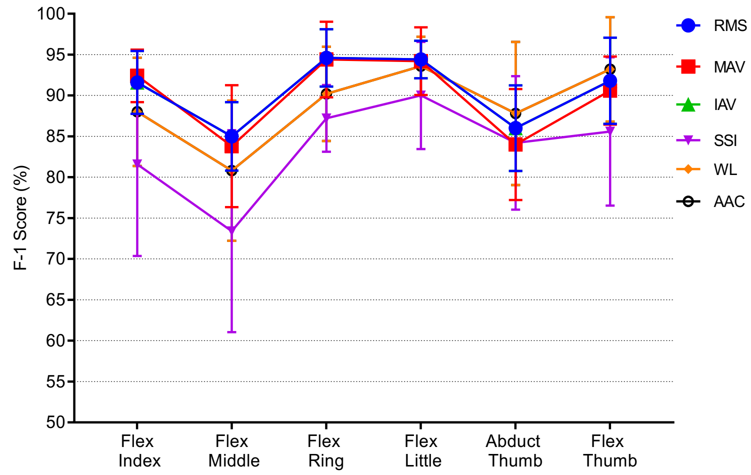

Figure 4:9: Offline prediction accuracy of six individual fingers for targeted (TR) muscles in 125 ms windowing size.

The average accuracy for seven electrodes placed around the arm for individual finger recognition is shown in Figure 4.10. RMS and MAV features were marginally better than IAV in terms of performance among the eight features (89 ±5% vs. 88±7%). The SVM classifier's recognition accuracy rates reduce to a bare minimum (87 ±5) while using the WL feature. For untargeted muscles, there were no statistical changes across key features ($p = 0.8362$), however, statistical differences exist between trials ($p = 0.0001$). Furthermore, there are no significant changes among six finger motions ($p = 0.3558$), with the exception of the WL feature. The mean F1-Score varies from 96 % for flex ring to 87 % for thumb abduction, according to the data analysis in figure 4.10. The analysis of test findings and figure 4.11 reveal that characteristics have similar statistics, and data show similar behaviour in targeted muscle conditions. Furthermore, the recognition rate is distributed consistently throughout the recorder muscles but not uniformly among the types of afflicted fingers.

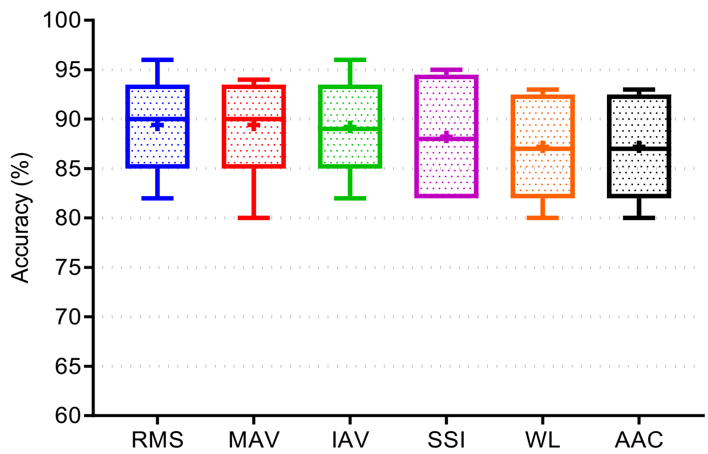

Figure 4:10: The classification accuracy of six time-domain features for untargeted (UT) muscles in 125 ms windowing size.

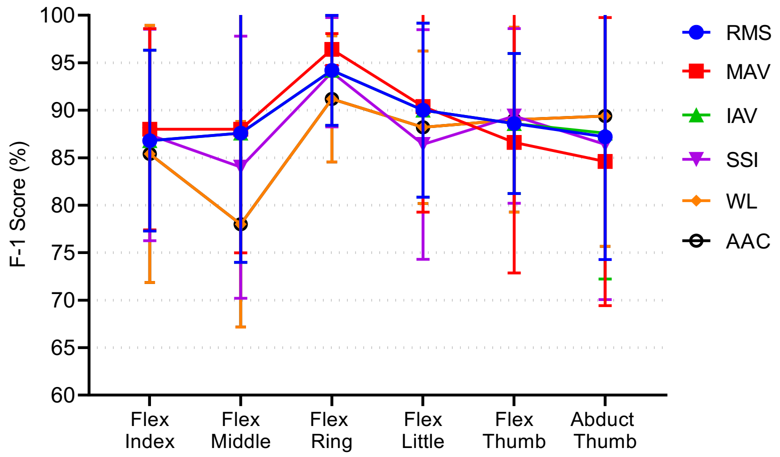

Figure 4:11: Offline prediction accuracy of six individual fingers for untargeted (UT) muscles in 125 ms windowing size.

In the targeted muscles study, the average recognition drops in classification accuracy and generates the best control performance with an average of 2% (~89 % to ~91 %) in comparison to figure 4.8. However, as discussed in section 2.6, the degree of amputation and the feasibility of untargeted muscle implication may compensate for this disparity and provide advantages. Figure 4.12 shows that there is no significant statistical difference between targeted and untargeted electrode placement based on two factors and two levels (targeted/untargeted) repeated measures. On the other hand, the untargeted muscle features used for classification performed slightly worse than the targeted muscle. The new sensory array was put near the motoneuron pool, and the electrodes were adequately scattered, according to these findings.

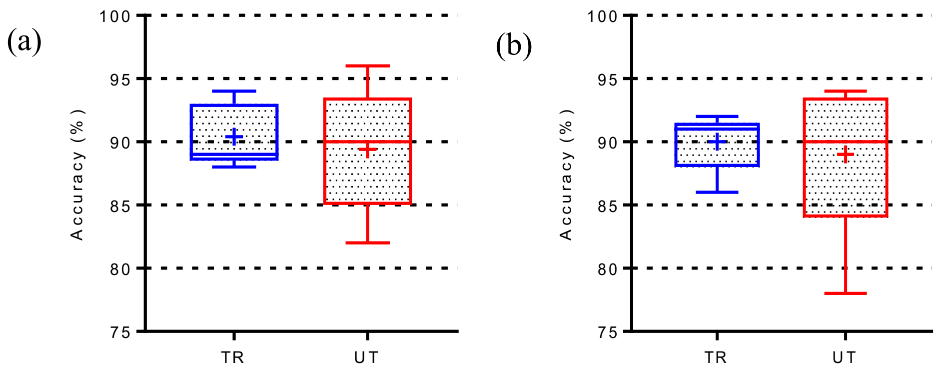

(c)

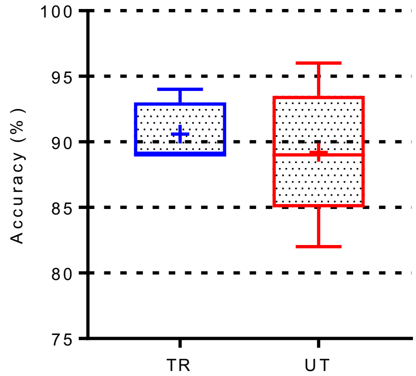

Figure 4:12: Classification accuracy obtained by different electrode placement for TR (targeted) and UT (untargeted) electrode placement: The figures represent (SVM+RMS) ; (b) (SVM+MAV); (c) (SVM+IAV).

Another crucial issue for motion detection is the size of the feature windowing. Using a larger windowing size increases the individual finger's motion recognition accuracy, as previously indicated in the literature. It should be noted that the SVM outperformed the LDA in terms of windowing size despite using the same pre-processing data. In contrast, the magnitude of the recognition rate for SVM is higger than that of LDA. After the data were pre-processed in 300 ms, there was a constant improvement. Figure 4.13 shows that the classification performance of the given six features improved by 3% from 90% to 93.0% for RMS and 2% from 89.0% to 91.0% for MAV.

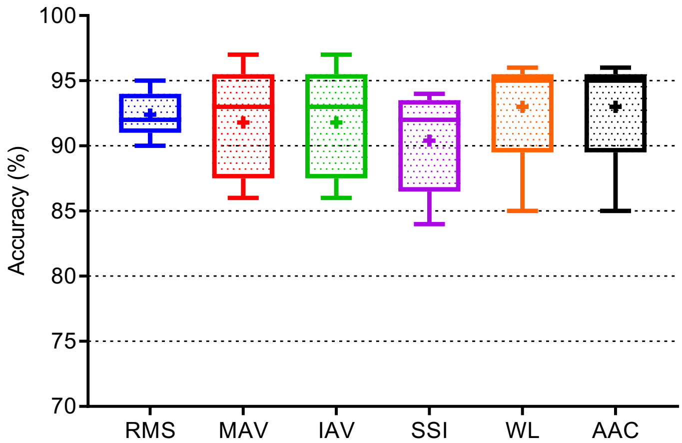

Figure 4:13: Offline performance of six time-domain features for targeted (TR) muscles in 300 ms windowing size.

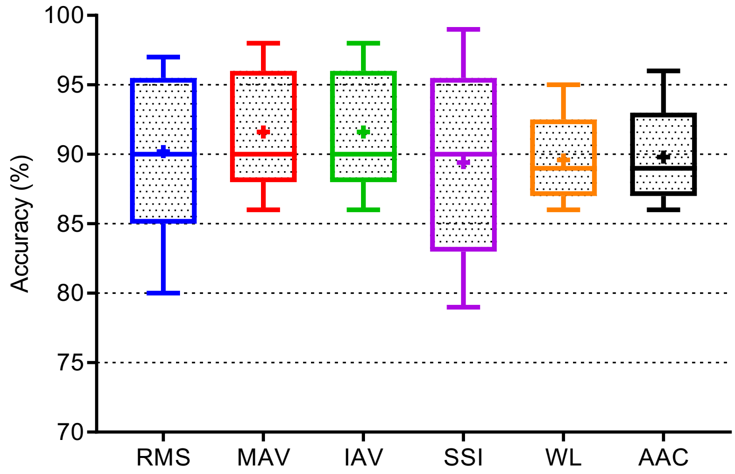

Figure 4:14: Offline performance of six time-domain futures for untargeted (UT) muscles in 300 ms windowing size.

The statistics acquired after data processing by using the SVM approach to features reveal that the data is sufficiently usable, and the classification results are comparable to those published in the literature (e.g., [58], [97], [117]) under similar settings and with a similar number of classes. As presented in [212] the average classification accuracy was attained with six classes is (80.4 %). According to Mayor *et al.* [199], the SVM classification performance for two participant groups (able-bodied and amputees) was 97.6% and 94.3%, respectively. They reported that it was challenging to perform some muscular contractions with the group of amputee participants. Li *et al*. [220] evaluated the performance of SVM with amputee participants, finding that it recognises 11 hand gestures with a 71.3 %. Their investigation, however, contained twelve channels of sEMG signals. Similarly, Al-Timemy *et al.* [221] examined six sEMG channels with 89 %, including nine hand-finger gestures. A comparison between three non-linear classifiers (NLR, SVM and SVM) was carried out in [99]. Their analysis revealed no statistically significant difference between the three methods, with SVM performing the highest performance (93.3%). Despite the fact that the reported papers used comparative test settings, the duration of windows, feature size and data ratio used in segmentation has a significant influence, as accuracy tends to rise proportionally to the length of sEMG data used in model training.

There is a significant disparity in the accuracies obtained by various research. According to Cene *et al.* [187], some studies achieved 99% accuracy regarding the metrics employed, unbalanced data and SVM parameters. However, test conditions' overall performance and representativity are decisive in real-time conditions. In some studies, the FD features are often employed to extract features from amplitude-based metrics to improve accuracy.

In terms of classification outcomes, the analysis also demonstrates that, when compared to other techniques in this study, the SVM method is one of the strongest practical classification approaches. The results show that SMV has a remarkable potential for the real-time control of the prosthesis. This statement was supported by statistical analysis and practical application in Chapter 5.

4.3.3 Approach 3 (k-Nearest Neighbour)

The k-NN approach was used to examine data sets employing eith features extraction methods, two windowing sizes, and two electrode allocation conditions. This method has been shown to be one of the most practical classifiers in the literature for predicting finger motions based on sEMG data [118]. Using cross-correlation between data and the Euclidian distance measure, adequate performance of k-NN classifiers was achieved. The Euclidian distance were used after detailed comparions and also it has been shown to be more appropriate for for regression in TD features. Thus, using prepared data sets, the Euclidian distance between inputs is stored for the EMG pattern with the eight best-related points ($k = 8$), and the output is calculated as the average. The final model was obtained after trying various k values. Although a low degree k value (such as k =2) outperformed in the comparison, it was suggested that this value be avoided because it causes significant variance and a lack of generalisation in the model.

The experimental results for the offline training features are depicted in figure 4.15, which are the average recognition rate of six time-domain features. As indicated in the graph, the IAV feature performed best, with an accuracy of (85-90) %, slightly better than the RMS (84-90) %. The two-way ANOVAs test revealed no significant differences between the three primary features (p=0.2227), but a significant difference between trials (p=0.003). According to the statistics, SSI has an average recognition accuracy of 79 %, which is in line with the worst performance on these tests.

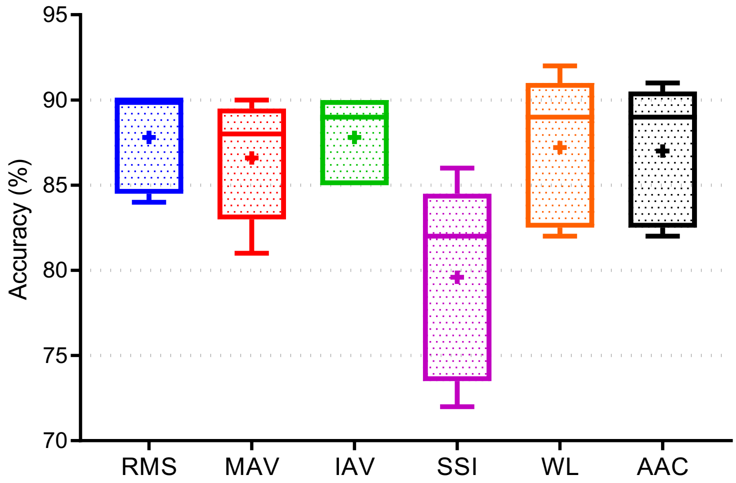

Figure 4:15: The classification performance of six features for targeted (TR) muscles in 125 ms windowing size.

Ring finger flexion had the best average recognition rate for individual fingers (93 ±4.1) %, while middle finger flexion had the lowest performance (81 ±6.36) % (see Figure 4.16). Except for the SSI feature (p=0.0341), statistics revealed no significant variations between individual finger recognition (p=0.2858).

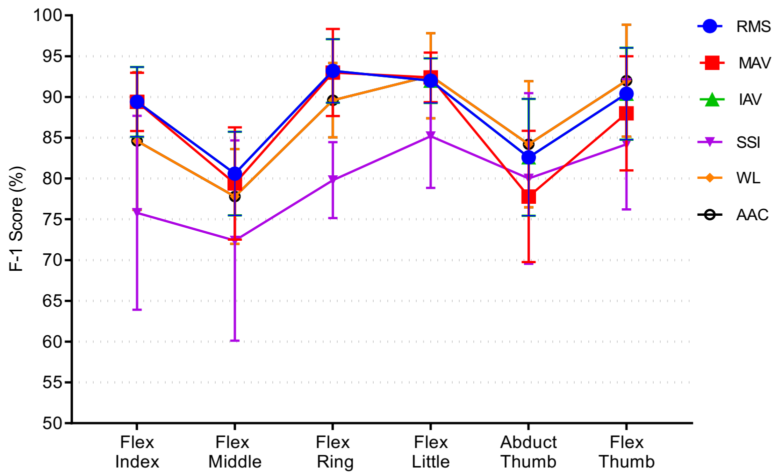

Figure 4:16: Offline prediction accuracy of six individual finger motions for targeted (TR) muscles in 125 ms windowing size.

According to the test results, the average recognition rate for seven electrodes placed around the arm (UT muscle condition) with six movement classes was highest in RMS (89 ±2.55) % and lowest in AAC (85 ±4.62) % for untargeted muscles. Furthermore, there are no significant statistical differences between features (p=0.9985) but slight differences between trials. The examination of test results and figure 4.17 show that characteristics have similar statistics, whereas variable data has similar behaviour in targeted muscle conditions.

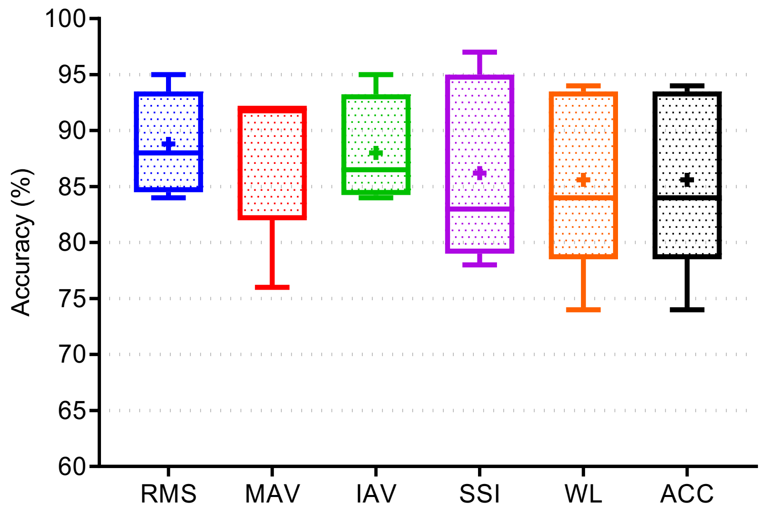

Figure 4:17: Offline performance of six time-domain features for untargeted (UT) muscles in 125 ms windowing size.

However, statistical differences between six finger movements for untargeted muscles occurred, as expected. The ring finger flexion had the highest average recognition rate for the individual finger (93 ±3.78) %, whereas the middle finger flexion had the lowest performance (86 ±9.9) %. Statistics revealed that, with the exception of WL, there are no significant differences in feature extraction approaches (p>0.7834), but there is a significant statistical classification difference between individual finger recognition (p<0.0067). Figure 4.18 displays the relationship between average classification performance and the number of output classes, along with the mean and standard deviation for each class for untargeted muscle.

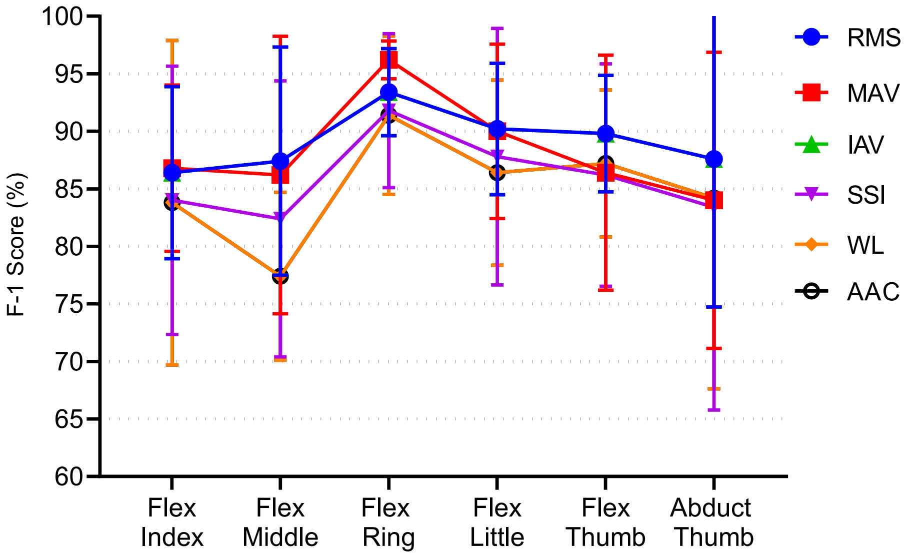

Figure 4:18: Offline prediction performance of six individual fingers for untargeted (UT) muscles in 125 ms windowing size.

In the context of electrode placement, two levels (targeted/untargeted), repeated-measures discovered a statistical difference in k-NN approaches between targeted and untargeted electrode placement, as illustrated in figure 4.19. The performance of motion detection improved when the muscles datasets were switched from targeted to untargeted. From targeted to untargeted muscle inquiry, the average recognition improves offline classification accuracy by 1% (88% to 89 %).

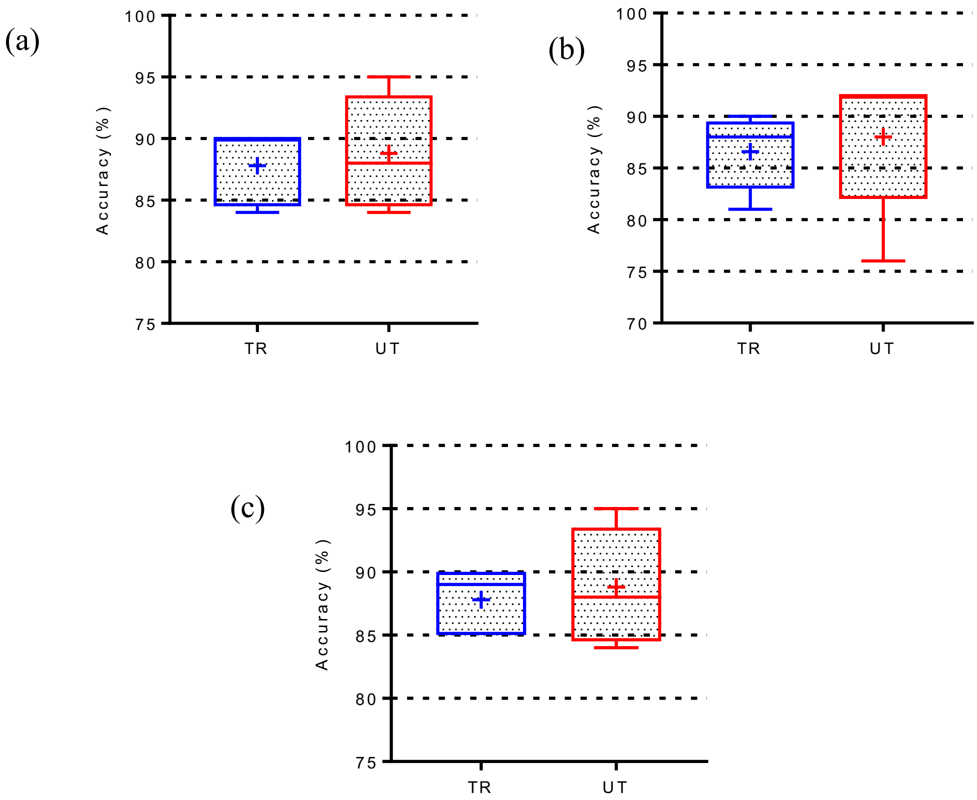

Figure 4:19: Classification accuracy obtained by different electrode placement, targeted (TR) and untargeted (UT): The figures represent (a) (k-NN+RMS); (b) (k-NN+MAV); (c) (k-NN+IAV).

The realistic solutions primarily attributed to data quality and surface recording to study the number of factors that restrict repeatability in pattern recognition and, therefore, on the clinical test of prosthesis control. As previously stated, differing windowing sizes have a major impact on recognition performance without considerably increasing complexity of the ML model. As a result, offline evaluation using the same data sets was used to reduce variability and more fully assess different learning approaches. The same classifier with 300ms windowing size for targeted and untargeted sensory locations was used to enhance finger motion identification and further development. According to the findings, the difference in offline prediction has grown in this scenario, from 87.8 % to 90.6 % for RMS (see Figure 4.20). When the pre-processed data was sent into the classifier, there were minor changes in classifier performance for targeted and untargeted sensory location. Untargeted muscle performance improved from 88% to 91.4 % (see Figure 4.21). As with other classifiers, it is realistic to expect to see a considerable difference between various features.

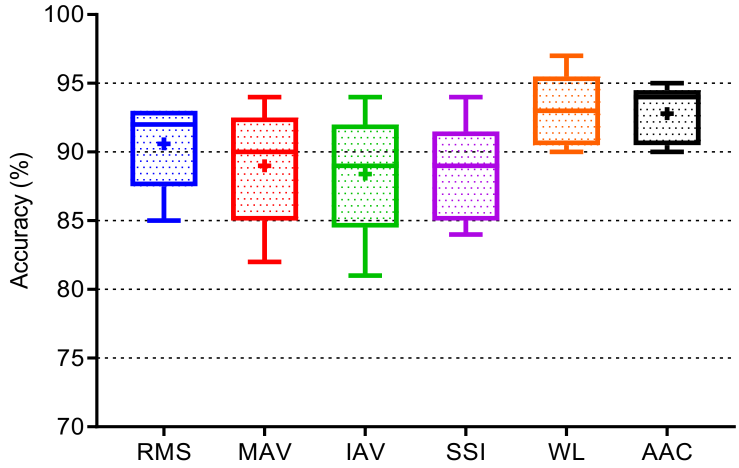

Figure 4:20: Offline performance of six time-domain features for targeted (TR) muscles in 300 ms windowing size.

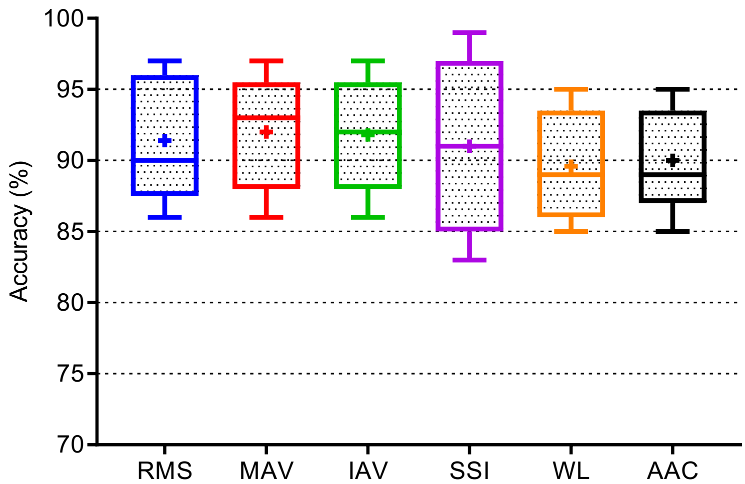

Figure 4:21: Offline performance of six time-domain features for untargeted (UT) muscles in 300 ms windowing size.

In comparison to the articles that employed comparable approach and classifiers, as shown in table 2:2, this research finding for the k-NN was somewhat less accurate but compatible in their baseline considering similar feature size and outperformed the referred research with smaller electrodes and databases. The paper of Rasheed *et al.* [120] had a similar accuracy compared to our method. Kanitz *et al.* [119] have used several classifiers (k-NN, LDA and SVM) to classify a dataset created with sixteen channels from six subjects. Their best results reached 64% using the k-NN method. The performance of k-NN was evaluated with six feature extraction methods in According to their study, the classification rate of all features is above 80%. Similarly, the effect of the arm posture and the weight of the prosthetic device was tested in [222] by employing the k-NN method, and their findings revealed that the socket fitting issue has a significant degradation in classification (almost 24%). In [101], a comparison of k-NN and LDA was made, and the study indicated that k-NN achieved (84.6%) accuracy higher than LDA (81.1 %). Atzori et al. [191] used the k-NN method to compare pattern recognition performance between able-bodied subjects and amputees. Their results indicated that the classification accuracy for the amputee subjects was 62%, which was 15.6% less than the able-bodied subjects.

Because of its simplicity and low training time, the k-NN classifier was employed as a comparison approach. The offline experimental findings show that k-NN performs adequately but somewhat worse than the other mentioned approaches, such as SVM and ANN. However, because it is computationally inefficient for big datasets due to the enormous amount of memory required for sample storage, it appears that other proposed approaches, like as ANN and SVM, are more ideal for their generalisation capacities.

4.3.4 Approach 4 (Artificial Neural Network)

The multilayer ANN is a well-known classification and regression method that has been extensively employed in many pattern recognition and EMG classification. In this study, a three hidden dropout multilayer neural network was adopted for classification and real-time control. The model contains 128 units (nodes) at the hidden layers and the output layer with one neuron for each class to be identified. The number of neurons was determined after a set of trials. The network was trained using "ReLU" activation function in two hidden layers, and the softmax function was used for the output layer. To optimise weights, a back-propagation algorithm with an adaptive "Adam" optimiser was employed. The input and output of the neural network are pre-processed, seven EMG signals from forearm muscles to determine finger/hand motions. The number of hidden units for the model was identified experimentally based on classification accuracy and testing error.

Time consumption is a significant issue for motion detection during training and real-time control. Achieving reasonable motion detection and motion execution time depends on the initial value of the parameters. Therefore in this study, the number of initial parameters and the number of hidden layers was kept as minimum as possible, while the optimum motion recognition was the priority.

The algorithms were developed in Python 3.5 using open source libraries that allow the users to change and decide the optimum parameters for each trial. Since real-time control of a multifunctional hand is our aim, we kept the number of layers and units lower as much as possible due to the number of units and layers corresponding to the complexity and computational cost. For example, in this study, during the ANN training process, it was observed that the optimum training performance generally needs a longer time to train the model. The fastest time of ANN training may be shorter than SVM for some parameters; however, the recognition performance was significantly worse in most features.

A comparison was made for EMG features by performing ANN between the different means of accuracy for the same subjects and data sets. The aim was to show the differences between the four learning models. All samples referred to the EMG signals are features for 125 ms or 300 ms window size in 2 kHz. The main criteria behing windowing size and fature extraction methos are presented in section 3.3. In order to keep the large data sets number for training, the dataset was split for training (70%) and testing (30%). A performance measured by k-fold cross-validation was averaged and compared to detect overfitting problems. Although this approach is computationally expensive, since it is required only in the training process, it offers advantages avoiding wasting a large portion of datasets.

In order to obtain a good generalisation, the training data stages was stopped after 1200 epochs. This number was identified after determining the convergence of training features for some trials. As there is no clear method to identify the number of neurons and layers, several different configurations for satisfying results were tested. All other network parameters, such as weights and biases, were randomly selected in the initial stages.

The training of ANN is often computationally costly, but after a successful training and testing phase, ANN can be presented with a sequence of new samples and find out the intended action in a short time. The network can be retrained and used to implement this model in real-time for new users or calibrate prostheses. Thus, the coefficient numbers can be reduced to obtain a shorter training time with a reasonable performance drop.

The fundamental reason for employing this model was to create an adaptive controller capable of mapping and parameterizing the relationship between neural states and optimal action. According to this assessment, the controller provides an effective way for autonomous control of a dexterous prosthetic hand. A single finger can be controlled continuously with some modifications, and the control parameter can be customised for each grasping pattern. This method could also be integrated with sensory feedback for precise motion detection strategy or sensation. The introduced feedback could categorise sensory information from various sources to decide whether any disturbances are detected, such as slipping or disconnection. With this close feedback, the desired grasping could be updated, and the new position command can be provided. The benefit of this approach could be that the grasping can be established without requiring the user to continually monitor the supplied force on the prosthesis and provide neutral and intuitive control.

Figure 4.22 demonstrates the ANN model's average classification accuracy for six time-domain features with targeted muscle condition. According to the neural network model, the best performance was attained with RMS accuracy ranging from (91-96) %, while MAV came in second with (93-95) %. The SSI and WL characteristics reached recognition accuracy rates higher than 86 and 89 %, respectively. The ANOVA test reveals a statistical difference between trials (p=0.0012). The repeated ANOVA test revealed (see figure 4.22) that there is no significant difference between the three primary features (p=0.3033), however, prediction performance for SSI, AAC, and WL falls to 81.2 %, 83.2 %, and 83.7 %, respectively, similar to other learning approaches.

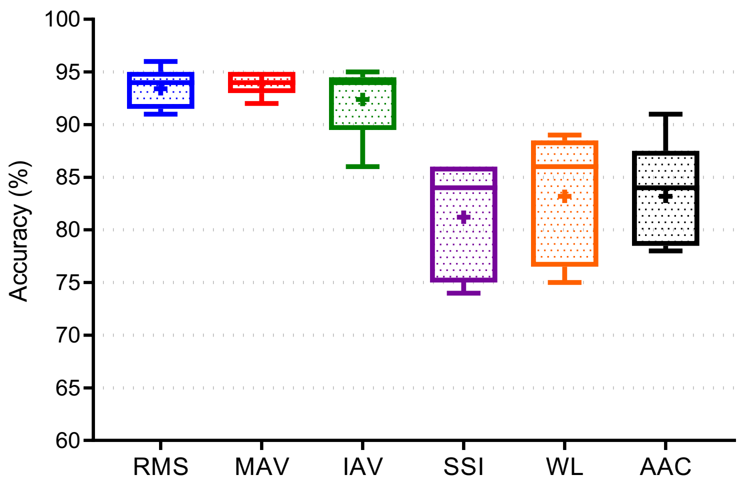

Figure 4:22: The offline performance of six time-domain features for targeted (TR) muscles in 125 ms windowing size.

Regarding sEMG signal classification for individual fingers, it was observed (as seen in figure 4.23) that the ANN successfully classified six finger movements with high success rates. The highest average recognition rate was found for for ring finger flexion (95 ±1.53) %, and the lowest performance was for thumb abduction with an average recognition rate of (90 ±4.53) %. Statistics showed a significant statistical difference between individual finger recognition, especially for SSI features (p=0.027).

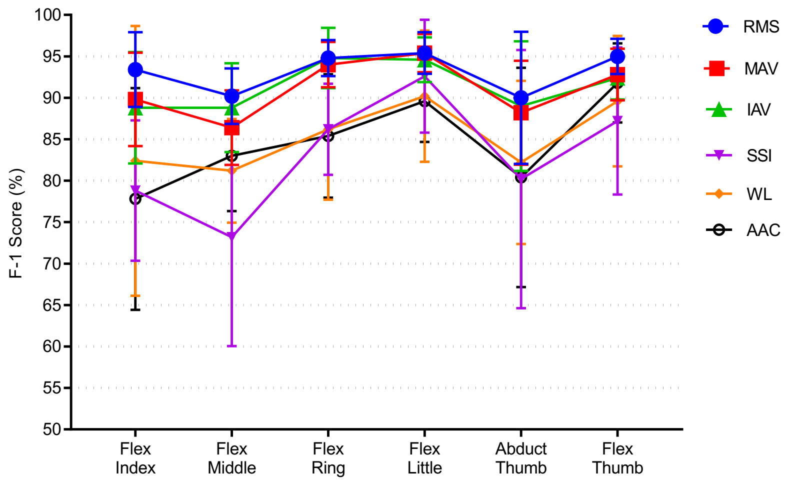

Figure 4:23: Offline prediction accuracy of six individual fingers for targeted (TR) muscle in 125 ms windowing size.

The same ANN model was applied to the untargeted muscle data sets condition. The average accuracy for seven electrodes placed around the arm with six movement classes was reported equal to 89 % for MAV features (see Figure 4.24). There were no significant statistical differences between features (p=0.939), but a significant difference between trials (p =0.0002).

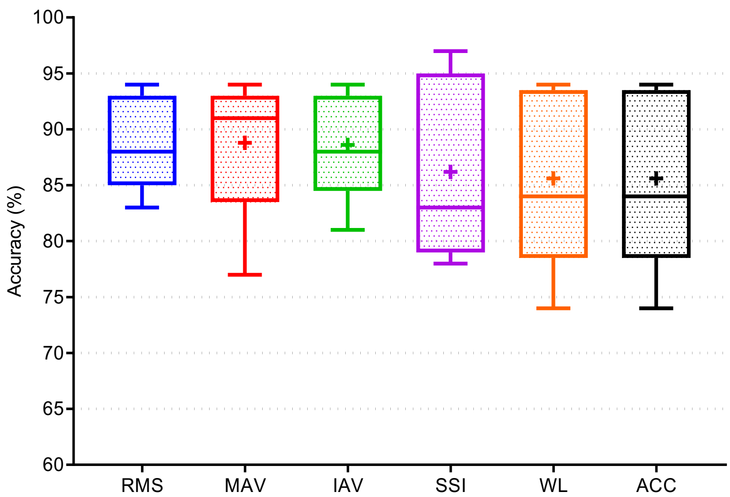

Figure 4:24: Offline performance of six time-domain features for untargeted (UT) muscles in 125 ms windowing size.

Statistical differences between six fingermovements recognition were discovered, as ring finger flexion had the highest average recognition rate for individual fingers (93%). Thumb abduction had the lowest performance, with an average of (80.1 ±11) % for MAV features, as shown in figure 4.25.

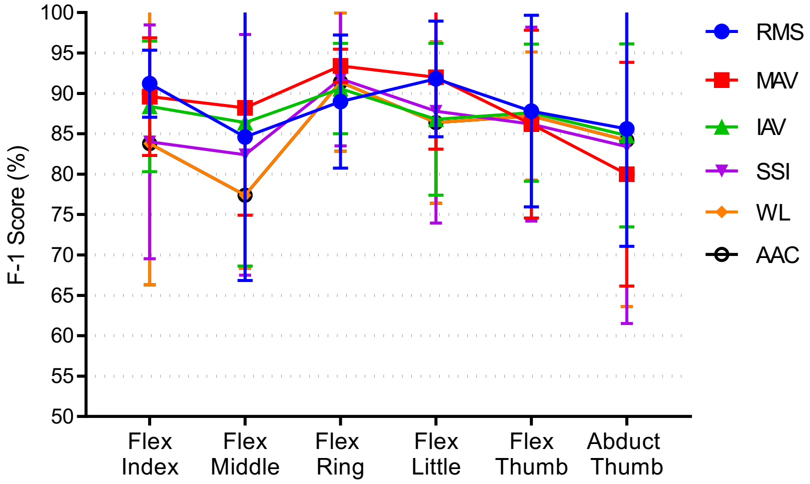

Figure 4:25: Offline prediction accuracy of six individual fingers for untargeted (UT) muscles in 125 ms windowing size.

As a result of comparing targeted and untargeted muscle conditions, repeated assessments revealed a statistical difference between targeted and untargeted electrode placement for ANN, as illustrated in figure 4.26. In the comparions, the feature extracted for the targeted muscle state outperformed the untargeted muscle features.

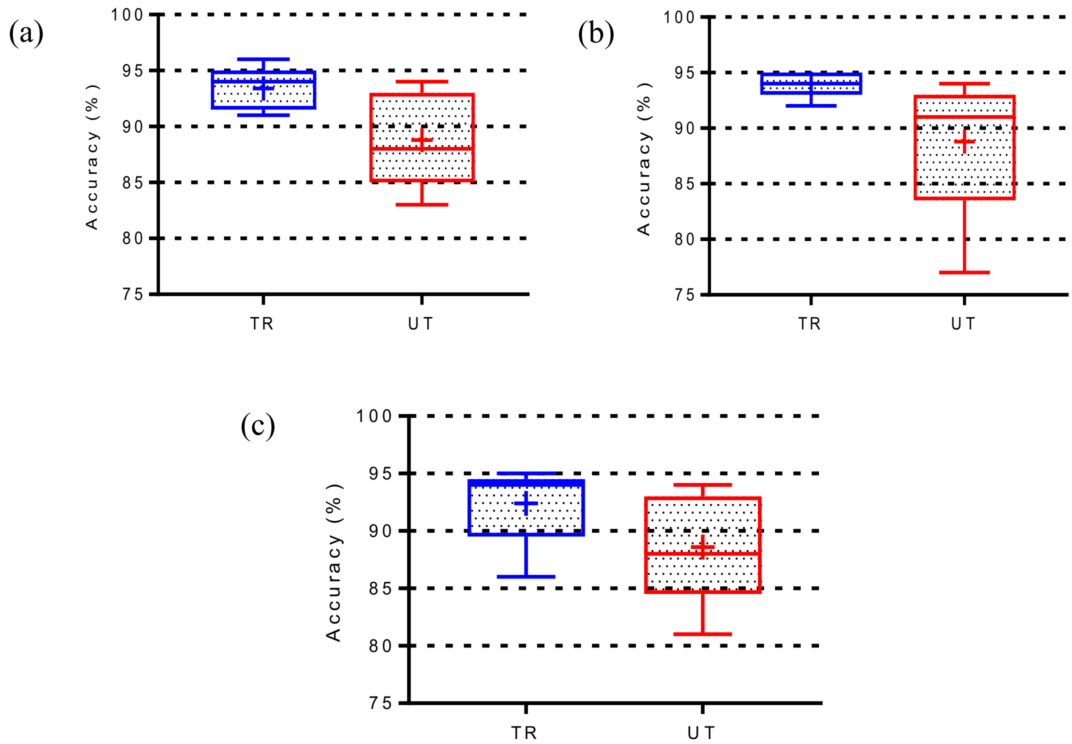

Figure 4:26: Classification accuracy obtained by different electrode placement targeted (TR) and untargeted (UT): The figures represent: (a) (ANN+RMS); (b) (ANN+MAV); (c) (ANN+IAV).

The comparison between figure 4.22 and figure 4.24 showed that the average motion recognition increases in classification and provides the best performance with an average of

(~89% to ~93%) in targeted muscles. However, as described in section 2.5, the level of amputation and practicality of untargeted muscle implication may compensate for this difference and offer advantages because the feature extraction and electrode shifting in the long term may cause some delay and misclassification in targeted muscle conditions.

The ANN maps large data sets as input vectors and sets to maximally separate between outputs variables/classes at a high level. The default parameters of ANN as used for 125 ms were used with 300 ms winndowing size for comparison. As expected, accuracy decreased for all features since ANN performs better with large data sets. The performance of ANN for individual finger motion recognition in 300 ms showed that motion differentiation is 88.20% for RMS and 87.40% for MAV. These results show that poor classification performance occurred with large windowing sizes since these results are lower than 125 ms windowing size. Figures 4.27 and 4.28 show data sets' performance in 300 ms for TR and UT muscle conditions.

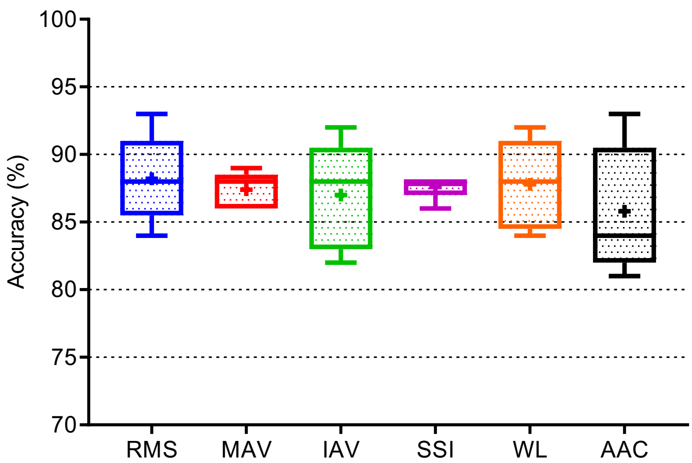

Figure 4:27: Offline performance of six time-domain features for targeted (TR) muscles in300 ms windowing size.

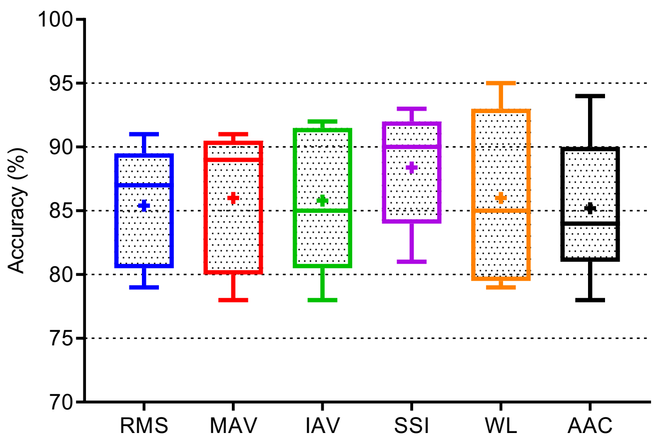

Figure 4:28: Offline performance of six time-domain features for untargeted (UT) muscles in 300 ms windowing size.

With seven channels, an average accuracy of >95% for nine movement classes problem was achieved across five able-bodied subjects in 125 ms windowing size (see figure 4:22 and 4:24), whereas for 300 ms windowing size, seven EMG channels provided >84% accuracy for individual finger movements (see figure 4:27 and 4:28). Those findings are an improvement compared to earlier research by Chunk *et al.* [223], in which six classes of finger motions were categorised using 8 EMG channels with 85 % accuracy for able-bodied subjects. When the number of channels increased to 8 for able-bodied subjects the classification performance reached to 95 % in [117]. Zhai *et al*. [224] had achieved similar results compared to findings in this study. The authors employed CNN and SVM methods to classify the NinaPro database; their results have reached an average of 78.8%. Kuzborskij *et al.* [225] have compared the performance of seven feature extraction methods and five classifiers in three windowing sizes using the same database. Their findings demonstrated that no classifier-feature-window combination exceeded 80% accuracy, but was sufficiently close. In [226] the ANN approach was used to do a complete evaluation of classification performance in terms of subject number, windowing size, number of channels, and various movements. Their results revealed that the best performance was 76 %.

ANN has been utilised in a variety of approaches to investigate various decoding paradigms that interpret human motor intent from nerve signals and control prostheses in real-time. Luu et al. [174] have collected data from amputees' peripheral nerves and compared deep learning performance to traditional machine learning approaches. They stated that their average classification performance with CNN and RNN algorithms reached 99 % accuracy. In [17], a similar strategy was adopted. Deep neural networks were employed by Fukuri et al. to control a prosthesis in real-time. They used a closed feedback control system and achieved a classification accuracy of >90% for ten motions. They reported that the healthy subjects who received feedback had higher accuracy than those who did not receive feedback.

The comparative experimental results suggest that data size has a significant effect on the performance of ANN since large data sets can lead to the highest recognition accuracy rate among two windowing sizes. Although NN took more time for training than SVM, it takes less time at testing and real-time control. Furthermore, similar accuracy behaviour shows that untargeted muscle conditions can perform as well as targeted muscle conditions. Therefore, using different electrode implementations should be made, not based on classification performance but on practicality, repeatability, and socket fabrication. Consequently, it appears to be clear that ANN offers significant advantages when control of individual fingers with large dataset is expected. However, the practical implementation has to be assessed in a standalone test, in which users are introduced to control devices in their daily lives.

4.4 Discussion

The significance of datasets and learning algorithms in pattern recognition for EMG-based prosthesis control was discussed in this chapter. EMG signals have an important role in a variety of applications, including rehabilitation devices, prosthetics, and the diagnosis of neuromuscular disorders. Various filtering methods have been used in the literature to obtain high accuracy and eliminate artefacts. As a consequence, the goal of this research was to develop appropriate data processing and ML algorithms for EMG signals in order to obtain precise real-time control while maintaining an acceptable computational time for real-time control.

The results of machine learning techniques and feature extraction methods for individual finger movements are summarised in each subsection. Through statistical analysis, the average RMS recognition rate for ANN was (93.4 %), higher than SVM (90.4%), k-NN (87.8%), and LDA (82.8%). Similar results were observed for MAV features as the performance of ANN was (94%), higher than SVM (90%), k-NN (86.6%), and LDA (83.4). The average classification performance of the four approaches is depicted in Figure 4.29.

Although targeting muscle condition enhances classification accuracies marginally for some machine learning techniques such as ANN (88.8 %) and SVM (89.4), the targeting surface does not offer an advantage in LDA (87 %) and k-NN (88.8 %) approaches, as shown in Figure 5.30. Due to the importance of repeatability and socket manufacturing, instead of placing such electrodes over specific muscle bellies, it can be simplified as in the second (untargeted) condition by ranging sensors symmetrically throughout the forearm's circumference. A valid comparison should be made according to experimental conditions and pattern recognition methods; however, it is practical to compare these results with some early studies such as [102], [117].

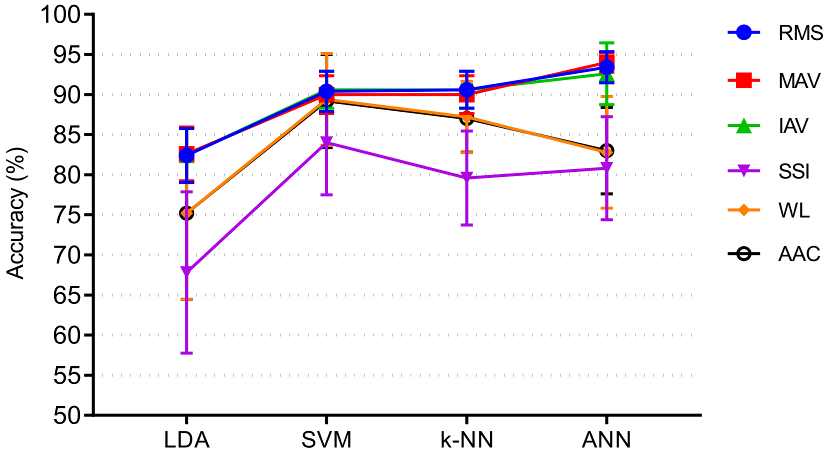

Figure 4:29: Average classification accuracy by different learning approaches for targeted (TR) muscles in 125 ms windowing size.

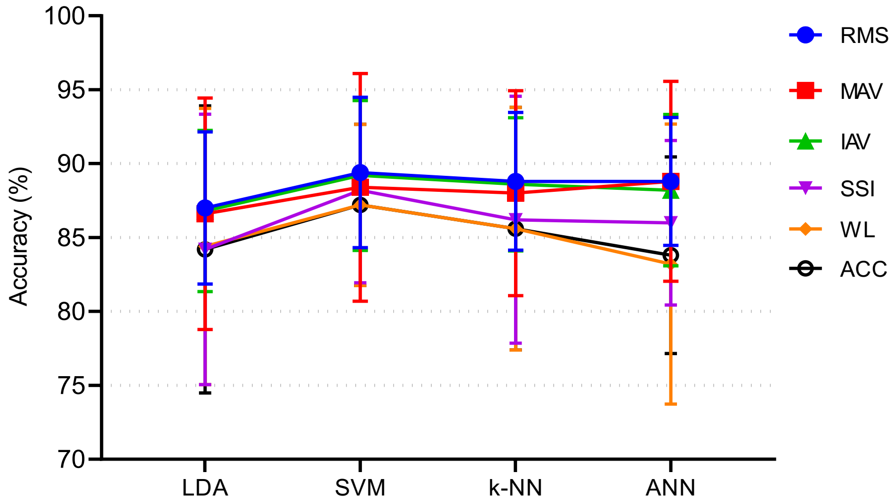

Figure 4:30: Average classification accuracy by different learning approaches for untargeted (UT) muscles in 125 ms windowing size.

The findings indicated that the combination of ANN and RMS is a more accurate choice for classifying individual finger movement than the other three models. Although SVM and ANN achieve comparable recognition accuracy rates during the training phase, ANN achieves superior accuracy and practicality in online tests with larger data sets. Furthermore, the SVM needs the user to carefully pick the training samples for each iteration and does not provide generalisation for all data sets, resulting in longer time consumption and delays in real-time control.

The second purpose of this chapter is to evaluate the several common machine learning algorithms on sEMG data with appropriate electrode placement in targeted and untargeted muscle circumstances. In all cases, there were no statistical differences between the three key characteristics MAV, IAV, and RMS. The first conclusion that can be derived from these results is that the feature extraction techniques can give enough muscle synergy since high accuracy was attained by using the provided feature extraction methods. Individual finger classification in 300 ms windowing size has obtained a high motion identification rate for both targeted and untargeted muscle conditions. Figure 4.31 shows how the performance of LDA (90.8 %), SVM (91.6 %), k-NN (92 %), and ANN (86 %) compares to previous research (e.g., [112], [216]). Figure 4.32 demonstrates that for the targeted muscle (TD) condition LDA (85.2 %), SVM (91.8 %), k-NN (89 %), and comparable classification behaviours were achieved with ANN(87.4 %). Despite methodological variations in some literature, such as the number of sensors, subject group, and processing technique, the results are equivalent to [22] and [187].

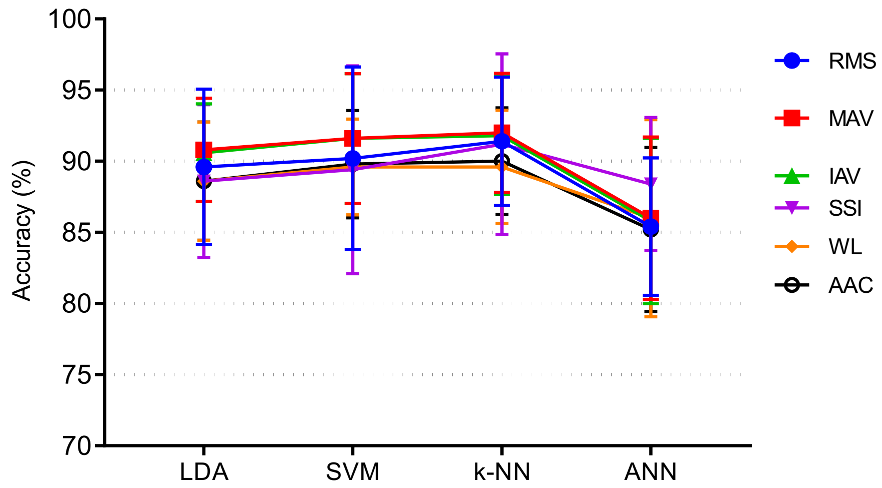

Figure 4.31: Offline performance of four classification methods for untargeted (UT) muscle in 300ms windowing size.

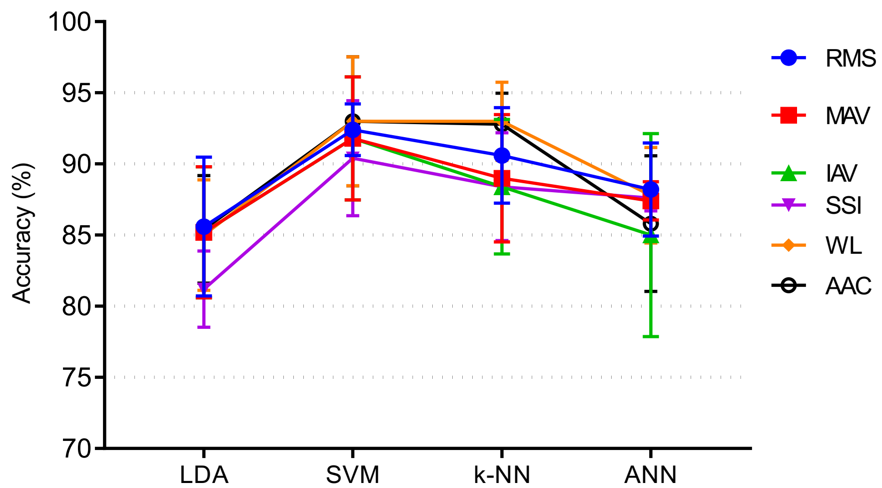

Figure 4.32: Offline performance of four classification methods for targeted (TR) muscle in 300ms windowing size.

The final goal of chapter was to assess the general applicability of such approaches and to confirm statistical variations in classifiers among users. The possibility of making it portable for real-time clinical studies, verification in everyday living activities (ADL), and future industrial exploitation since real-time application of new methodologies was analysed. The effectiveness of these four machine learning algorithms for individual finger motions using EMG signals from healthy subjects were compared. In this chapter, the impact of data sets including typical sampling rates and windowing sizes (125 ms and 300 ms) on a range of hand and finger actions in various arm orientations was also tested. Except for ANN, the given findings reveal that when the windowing size was reduced from 300 ms to 125 ms, the classification performance of all suggested feature sets declined dramatically. These results show that a small windowing size does not give enough signal information for accurate LDA, SVM, and k-NN classifiers. Almost all of the literature has come to the same conclusion: big windowing size outperforms traditional ML methods except ANN. A complete comparison of different windowing sizes can be found in [112] [187].

This investigation also suggests that in comparing 6-7 sensors placements for targeted and untargeted muscles, the motion detection performance for all features decreased significantly ($p<0.001$) by reducing the number of sensors. This drastic result for these features could be explained because of the loss in signal content and fall in required minimum information. Also, despite time-domain features achieved high accuracy (91-86%), when using 125 ms windowing and 300 ms windowing, some of the features significantly decreased the accuracy, such as WL, AAC PEK, KUR features (more comparison of features are presented in Appendix C). Phinyomark *et al*. [102] have evaluated the influence of feature extraction methods on pattern recognition for able-bodied subjects and have reported a similar conclusion. The decreased performance for these features could be an insufficient number of data points in each analysing window. Theoretically, they have a different mathematical definition as their benefit depends on windowing size. It was suggested in [216] that performance is susceptible to the chosen parameters and indicated that the number of data points to be as large as possible for practical implementations, especially for nonlinear classifiers such as ANN methods.

The findings in this study suggest that the approaches, based on proposed parameters and methodology, can identify finger motions and is capable of predicting intended hand patterns with high accuracy. The process is presented to be robust and can be implemented to recognise independent finger motions. With this classification performance, the strategy is ideal for controlling the high degree of freedom prostheses.

4.5 Summary

In this chapter, a combination of eight time-domain feature extraction methods and four classifiers, with two different windowing lengths and two electrode placement approaches, were investigated to recognise human hand motions using sEMG signals as inputs. The comparative experiment results demonstrated that features extracted from RMS and MAV could lead to the highest recognition accuracy in both 125 ms and 300 ms windowing length, while RMS seems more practical for real-time implementation with an overall 2% higher recognition performance than MAV. For classification methods, although artificial neural networks (ANN) perform better for 125 ms windowing size than SVM in offline learning, SVM seems more accurate than ANN in 300 ms windowing size. However, since SVM requires a longer time for training than k-NN and LDA, The real-time implementations may lead to some training progress delays. Consequently, the combination of SVM with RMS is recommended when the highest accuracy is required. On the other hand, ANN with RMS may provide higher and stable motion detection if absolute real-time performance is necessary.

The experimental result for able-bodied subjects showed a similar pattern during all trials; however, more sensors, such as seven sensors placement, offer significantly higher classification accuracy than six sensor placements. This effect seems significant, except for SVM. Therefore, when choosing the number of sensors, care should be taken as it could have more influence in real-time control.

Since some earlier studies suggested that offline classification results do not have an accurate correlation with real-time performance, a detailed evaluation and validation of this physical prototype methodology are necessary. Therefore, to improve the robustness of practical applications and reduce delays in real-time applications, a windowing size of around 65-125 ms in feature extraction with ANN will be ideal. Thus, a small segment of increment is suggested to improve accuracy and response time. In order to assess the performance of the combined system, these methods are applied to the real-time system in the following chapters for robot control.

Chapter 5 Mechanical Design and Performance Evaluation of Socket Prototype against EMG Signals Variation

5.1 Introduction

EMG-based pattern recognition is a favoured sensing modality for prosthetics control because it provides sufficient information directly related to muscle activity and provides natural and intuitive control. It is, nevertheless, sensitive to noise and artefacts generated by environmental changes. However, precise electrode allocating to specific muscles for each experiment is not straightforward, and it necessitates the use of supplementary equipment/procedures, such as ultrasound guidance or specific experiences. Although allocating electrodes to specific muscles improves performance for some linear pattern recognition algorithms, such as LDA and k-NN, this complex medical procedure may be unnecessary if a pattern recognition approach is established in which signal amplitude is not decisive.

Implementing a wearable embedded system in the real-time prosthesis is difficult due to the lack of an interface for amputee bio-signal collection and adequate computing power for motion detection. Number of custom-designed and commercial sockets have been employed to evaluate prostheses performance from the standpoint of prostheses users. It is, however, impossible to evaluate all of the aforementioned factors at the same time in order to determine a successful data acquisition and training session. A practical, uniform and standard data acquisition technique are highly desired when applying pattern recognition-based control in practice. It was proposed that a data collection methodology synthesising dynamic muscular contraction, dynamic arm posture, and tolerance to non-stationary signals could generalise data for daily life [209].

The sEMG electrodes were placed on the surface of selected muscle areas in the early chapters, as it is a common approach in the literature. Following a detailed examination of electrode placement and its impact on motion detection in chapter 4, it was discovered that the targeted muscle approach does not provide a significant advantage for pattern recognition but rather causes human error in the sEMG dataset since precise electrode allocation for each trial is complicated.

In this chapter, a bypass socket was developed to test a new sensory modality with proposed pattern recognition methods presented in chapter 4. The bypass socket is built with three major features: It allows for data collection while maintaining direct access to the main muscles of the forearm for sEMG. It provides a wide range of movements for real-time functional assessments and standardises electrode placement for the users.

Because it facilitates data collection from the main area (approximately 5 cm from the elbow), this technique ensures a consistent setup for all patients, and it is applicable for a large number of transradial amputees. Although electrode placement around the forearm circle may not provide the optimal signal acquisition approach for hand motion detection, it can provide a reasonable approximation to pattern recognition in real-time.

Furthermore, the use of a bypass socket, which minimizes electrode displacement and improves classification performance, allows dynamic arm position tests to be conducted without compromising pattern recognition performance. The findings of comparison revealed that the protocol with a new socket and dynamic arm position produced the highest performance (89%) compared to the targeted muscle condition. The results indicate that it is not necessary to include particular EMG variations in model training to obtain robust pattern recognition; rather, datasets from different conditions with standard training can give superior real-time control for multifunctional prostheses. A similar consideration appear in some early studies [199], [227]. Rather than associating electrodes to specific muscles as in traditional control, this method was used to recognise signals from all muscles uniformly. Furthermore, for some users, this is the only option because their stump prevents the electrode being allocated anywhere else.

According to the findings of this chapter, incremental learning and new electrode allocation with bypass socket are effective in maintaining a stable level of performance. Following that, the approach was improved and used in chapter 6 to control a prosthetic hand with an embedded control system and feature extraction in online tests.

5.2 Socket Design and Learning Framework

Translating prostheses studies into practice has proven to be difficult due to the limitations of commonly used laboratory performance metrics [228]. The majority of the studies used data from able-bodied people's targeted muscles to assess classification accuracy; however, the vast majority of amputees lack access to these muscles. This unrealistic, unrepeatable technique leads to significant classification errors in pattern recognition for various reasons, including the lack of muscles, the volatility of patterns over time, and poorly acquired training data [37]. Another critical issue about sEMG is the electrode shifting during participant motion execution, and this appears to be most significant, particularly during the reach and grasping tests.

The capability of my-electrical prosthesis has been measured using pattern recognition accuracy performance with static arm postures. Despite the fact that the majority of the subjects had reasonably high scores in the offline test, their clinical validations differed greatly because real-life conditions necessitate system integration and dynamic arm manipulation for prostheses [229].

When the figures in Chapter 4 were compared, it was discovered that the subjects could do the same thing with untargeted muscles, if not slightly better. Such issues with targeted muscles were discussed in Chapter 4, and the same techniques proposed in that chapter was improved in a practical setting with bypass socket in this chapter. Furthermore, because the majority of classification errors occur when the arm follows a dynamic trajectory with targeted muscles, the regression machine can be used to start the classification only when the predicted force is above a threshold. However, because electrode switching and electrode displacement occur at some arm locations, particularly with traditional targeted muscles, this can only be done if the data is standardised at those locations. As a result, the new sensory modality can provide repeatable data collection for each trial, standardise data sets, and give ML methods more flexibility for tuning.

As a result, a set of tests were taken to asses sEMG-based device with a fitting socket to perform clinically relevant procedures. The new untargeted electrode placement with bypass socket for sEMG experiments was designed to imitate the real-life conditions of transradial amputees. The experiment's layout was made to provide the data collection necessary for the participant to perform compensatory grasping and finger manipulation. The motivation behind electrode placement choice was to transmit the signal as intuitive as possible, as practical as possible and reproducible from user to user. With this electrode arrangement, no electrode could isolate a single muscle while ensuring that the most significant input to the data comes from all muscles. Similar methodological approach has been used in [187] and [230]. Furthermore, anatomy studies [231] show that this location in the human arm stores a high concentration of muscle activity associated with hand motions, including palmaris longus, flexor digitorum superficialis, flexor digitorum profundus, extensor pollicis longus, flexor pollicis longus, flexor carpi radialis. The main motivation is creating an experience of every day for users to address the disparity between clinical tests and market expectations. This anticipation influenced this design regarding access to the intact limb, durability, and ease-of-use.

Access to intact limbs: By attaching a bypass socket to the elbow, it was possible to maintain electrodes locked in a sensory array that can handle hefty prostheses for a wide variety of user sizes. The close contact configuration allows for the collection of high-density sEMG signals from extrinsic muscles performing finger and wrist motions. The bypass socket's contact area minimisation is an advantage of this socket over previous designs [165], [232], since it allows the device to be used in the high level of amputation.

Durability: The elbow cuff is inserted into bypass socket, allowing users to freely rotate their arm and shoulder while simultaneously keeping the electrodes in the approximately same spot, reducing electrode movement and thereby stabilising sEMG signals. The bypass socket limits the elbow angle of rotation to a minimum, providing for an adequate range of motion completion for daily living activities. In comparison to classic designs [212], the design decision optimises object manipulation tasks and posture freedom.

Practicality: The overall design allows users and experimenters to be versatile. The 3D printed design enables researchers to adapt the size to certain users and sensors while also allowing them to conveniently switch between individuals. The intimate connection between skin and device allows able-bodied participants to test and evaluate pattern recognition from the perspective of amputee participants, providing a more realistic scenario.

The primary goal of this design was to look into the feasibility of an sEMG based HMI in a relatively near to real-life circumstance. The socket and electrode array was designed to maximise mobility, integration with existing prostheses criteria, and reproducibility of data for ML. In terms of portability, all appropriate number of electrodes were implanted in a bypass socket, making the system comparable to a conventional bionic device and providing a platform for a compatible embedded system, as presented in chapter 6. This assessment is critical because better and faster training could be obtained if the methodology that would best suit amputees is known ahead of time.

5.2.1 Participant

In order to identify hand movements using EMG signals, pattern recognition tests on two able-bodied subjects (males, 26-32 years old) with no known history of neuromuscular disorder were conducted. The number of subjects was determined by two major factors. To begin with, because the socket is custom designed, it was not possible to analyse the link between able-bodied and amputee participants and other factors such as type of limb deficit. Instead, the dimensions of two subjects' forearm were measured, and 3D-printed sockets were built, a similar approach was taken in [165]. Furthermore, the influence of subject numbers on pattern recognition was discussed in chapters 3. The comparative results demonstrated that, while each subject has a different level of muscle contraction, the sEMG magnitude has no significant effect on overall performance. The findings of the offline analysis for the same participants were reported and compared in chapter 4. A detailed analaysis about subjects influence has been presented in [175]. A custom-made socket was designed for the able-bodied subjects in order to provide similar and appropriate training conditions and achieve good performance by removing potential training effects such as electrode installation for each session and electode shifting. Instead of comparing participants' performance, the custom-made socket was mainly constructed to increase dataset quality during repeated tests and improve pracricality.

5.2.2 Experimental Hardware

Single fingers and object grasping activities were recorded using Delsys™ Trigno Wireless System® (model DE2.1, Delsys Inc., Boston, MA, USA). The corresponding sEMG signals were recorded by applying 6 and 7 electrodes to the circumference of the forearm. The signals were sampled at a rate of 2 kHz with baseline noise, then it was amplified (3000) and bandpass filtered in 20-450 Hz. Each electrode is assembled with a self-sufficient rechargeable battery (average 8 hours) and equipped with wireless operational space (40 m from wireless Delsys receiver base station).

The sensor's number was chosen following a thorough analysis of the literature in [22] and [221]. Similarly, Farell *et al.* [37] have compared the effects of varying numbers of electrodes on pattern recognition in a review. Huang *et al* [218] have also claimed that there is no significant difference between targeted and untargeted muscle conditions in the classification performance aspect. The literature results mainly revealed a considerable degradation in classification performance with each incremental decrease in the number of sensors. Although this decrease in the number of sensors is significant, the impact on accuracy was relatively small for high number of sensors [116]. Regarding classification accuracy, it has been suggested that using at least four electrodes is reasonable as employing less than four causes a large decrease in classification accuracy [105]. It is recommended that the quantity of sensor must be kept at least in the range of 4 to 6 to ensure that it does not compromise the detection performance [233]. The compatibility of the sensor controller, the duration of the experiment due to computational power, and the feasibility of using the maximum number of electrodes play key role in number of electrode. As a result, tests were conducted employing a socket that can accommodate maximum 7 electrodes uniformly distributed around the circumference of participants' forearms (similar to [223]). Taking into account the size of electrodes (27x37x13 mm), a maximum of seven sensors might be utilised on the circumference of the adult forearm using this sensory modality.

The custom-designed socket was mainly employed to create the best data gathering environment for amputees. A housing mechanism in the socket and armband was used to place the sensors on the forearm. The elastic armband was worn over the electrodes to keep them adhered to the skin while collecting data. Electrode placement was done with great care since it is a critical stage in data reliability and classification accuracy. As illustrated in Figures 5.1 and 5.2, seven electrodes are evenly spaced around the circumference of the forearm to cover the key regions of the muscles.

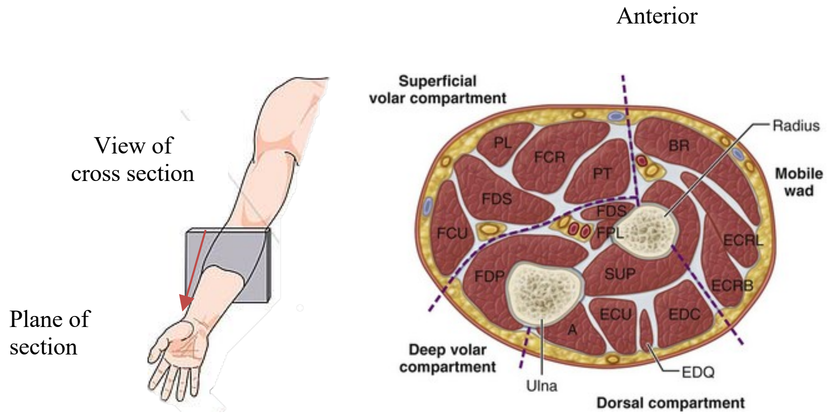

Figure 5:1: Cross-section view of electrode placement location around forearm. The cross-section view is passed into the zone between the elbow and wrist. Electrodes are allocated around the peripheral circle of the forearm.

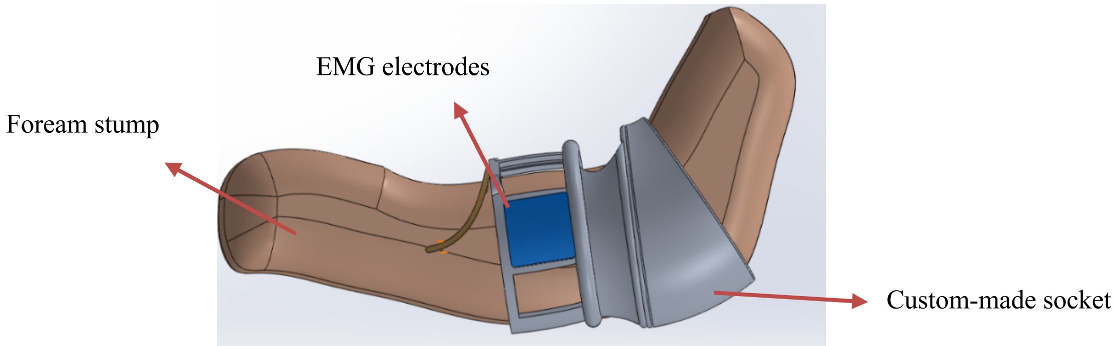

Figure 5:2: Illustration of sensors placed on the residual limb of transradial amputees.

All sensory information was transmitted to the data collection and storing workspace station (Intel i7 @2.6 GHz with Windows). Several experimental conditions influence the quality of signals, such as the location of EMG electrodes, participants, muscle fatigue, and, most importantly, amputation level. To avoid such interferences and to verify the collected data are correlated to performed motions in real life, we simulated the experiment conditions and pre-possessed signals using custom-written MATLAB (MathWorks) codes.

5.2.3 Implementing Experiment Protocol within the Proposed Approach

It has been demonstrated that EMG signals can be altered by a range of factors unrelated to finger posture and movement in real-time situations [234]. Many of these aliasing signals have a significant impact on the quality of EMG signals, interfering with control and classification performance. It has been shown that electromyography (EMG) signals rely on the size and the position of the muscles, and therefore the EMG signal can be weak or strong [235].

The performance and the feasibility of EMG-based control are limited to the intensity and the quality of muscles signals and appropriate electrode placement over correct muscles. In principle, each electrode must be placed accurately on the muscle's belly according to early studies. However, this approach is problematic since the displacement of electrodes must always be in the same location. Therefore, it reduces the number of users to a specific group who have these muscles and makes these prostheses almost infeasible for Transradial and Transhumeral users. Besides this, physical conditions such as the users' weight can always cause electrode shifting, and the design always needs adjustment. Because the targeted muscles are close together, a detailed evaluation of their structure and precise EMG sensor placement are required. Due to the close proximity of the muscles, the individual experiment over the flexor carpi radialis would detect the undesired signal of activity from the flexor digitorum. As a result, the perception of the signal provided by hand gestures is always contaminated by internal and external variables, reducing prediction accuracy.

A number of papers employ different aspects of dynamic arm modularity [215], [236]. Paskett *et al.* [165] have examined the feasibility of controlling a multifunctional prosthesis with non-stationary sEMG signals collected from a dynamic system and suggested that in order to achieve an effective controller, the synergies should be obtained in a standardized feature space. Significant progress has been made in alternative data recordings such as TMR and iEMG concerning some fundamental questions regarding optimization of control architectures for prostheses control [174]. The simulation of complex arm postures showed that extreme arm posture changed muscle configuration significantly and suggested standardized data collection leads to better motion execution performance and generalization [98], [237]. Hwang *et al.* [215] have validated the approach on subjects and stated that mixture dynamic data collection with robust sensory modality could best account for smoothness and reliability.

In this chapter, seven EMG sensors (Delsys, model DE2.1) were distributed on the participants' right arm's circumference with a designed bypass socket to reduce electrode shifting, improve classification performance as it resists elbow rotation and provide consistency for input data. This uniformly distributed electrode allocation has been shown to be efficient in some other studies [223] [227]. Castellini *et al.* [227] claimed that an amputee subject had achieved 95% accuracy with this new electrode arrangement, which is in line with some results from able-bodied subjects.

The considerable variations between different sensor placements in each trial cause significant classification degradation, therefore, in traditional appraoches, the system must be retrained from scratch on a regular basis. This chapter proposes incremental learning with more standartised data collection, which updates with modest portion of the training data and allows for signal adaptation. As a result, this approach will improve and standardise electrode localisation for participants, swiftly convert biosignals, and improve ML model performance.

This placement's general purpose is to provide a realistic data acquisition and record as many different muscles as possible, since conventional targeted electrode placement does not cover the participant's stump with the short remaining arm. Due to wrist rotation not being possible for amputees, the wrist was fixed during trials to reduce the wrist rotation effects. These conditions were tested by comparing the motions detection performance of able-bodied participant with socket and non-socket conditions.

The participants were sitting in front of a table with residual limb stabilised in a comfortable position. The participants were asked to perform the introduced finger and hand motion as naturally as possible, ensuring that only the desired finger moved by stabilising the wrist and rest of the fingers during each trial. The participants were also instructed not to apply force in the finger points as that would not be possible for amputees. The participants were ensured that they had a comfortable hand position with a designed platform for unforced biosignal during the experiments. The subjects were told to concentrate on completing motions rather than exerting forces. After being briefed on the nature and expected outcomes of the tests, the volunteers agreed to take part in the trials. The individuals were asked to perform three objects gripping and six single finger motions: thumb and finger flexion/extension. Thumb abduction and adduction were also assessed. The movement sets were chosen from the robotic and rehabilitative literature [81], to address the most common hand manipulations in everyday life activities.

Throughout the trials, a second computer screen was placed in front of the individuals to display the animated finger activities as well as a timer. Each trial's data was collected five times for a total of ten seconds (3 s holding contraction time) for each participant. The activation time for each motion was derived from literature [81] [238]. The description of finger motion and protocol is given in Figure 5.3. Although there is no consensus on the best data acquisition protocol, the uniform electrode placement has been proven to be effective with the combination of machine learning methods [72], [144] as the signal's high amplitude is not necessary for pattern recognition. Some literature have followed a similar data acquisition and electrode placement [187], [209], [191], with varying number of electrodes and movements.

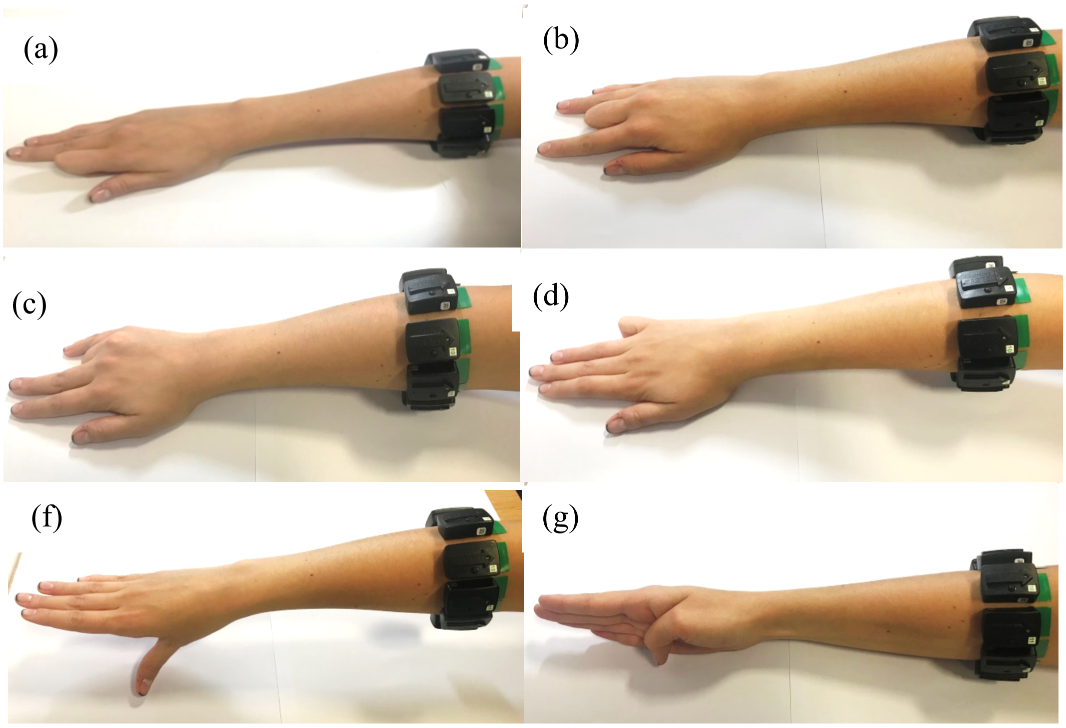

Figure 5:3: Total of six finger motions with Delsys electrode placed around the circumference of the forearm. These fingers are represented as index flexion, middle flexion, ring flexion, little flexion, thumb finger abduction, and thumb flexion.

5.2.3.1 Static Arm Position Effect on Motion Detection

Pattern recognition-based prostheses are utilised to restore basic hand functions and specific finger motions. Most of the study in the literature trains the patterns for various statistical gripping movements, such as executing muscular contraction while the arm is fixed on the table. However, several clinical research have found that training classifiers in a fixed arm posture reduces classification accuracy significantly [97], [182]. This section includes a comparative research on the myoelectrical-based learning strategy that distinguishes gripping and single finger motion intention in different arm orientations in order to produce a more natural and intuitive behavior to prostheses.

This study employed innovative data collection protocol that produce more standardised EMG signal than the traditional targeted muscle-based system since amputees generally have a restricted number of muscles and data collecting locations. Some other invasive methods, such as targeted muscle reinnervation (TMR) [238] or regenerative peripheral-nerve interfaces

(RPNI) [239], can capture more data and give more precise signal detection. These techniques, however, need surgery, induce infection, and are prohibitively costly.

A sophisticated signal processing algorithm was applied in this work to operate high-DOF prosthesis with less EMG data to estimate discrete finger motions. The subjects were set in front of a table during the trials, watching a computer screen with the elbow in three different positions, as shown in Figures 5.4 and 5.5 The individuals were instructed to move their fingers using preset motions while keeping the same wrist angle throughout all trials in the first phase of the experiment. The individuals were requested to hold their arm upright and down during the identical finger motions in the second and third phases. Each finger manipulation lasted 10 seconds, with at least 3 seconds devoted keeping the fingers in flexion. EMG data from three stages of arm orientation were captured, and the same signal processing approach as described previously was used.

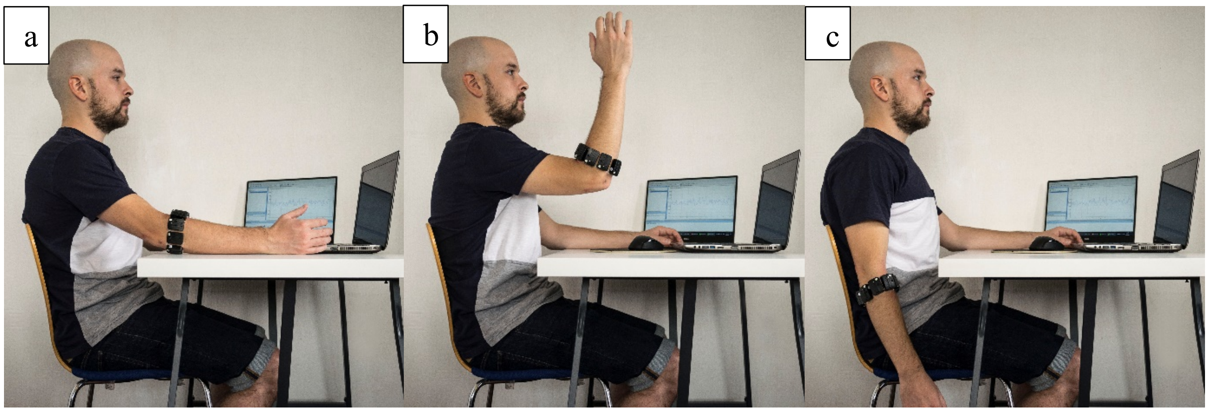

Figure 5:4: Experimental setup showing the positions of arm and electrode placement to perform six finger movements. (a) The arm on the horizontal table position, (b) arm upright, (c) arm up-down (vertical).

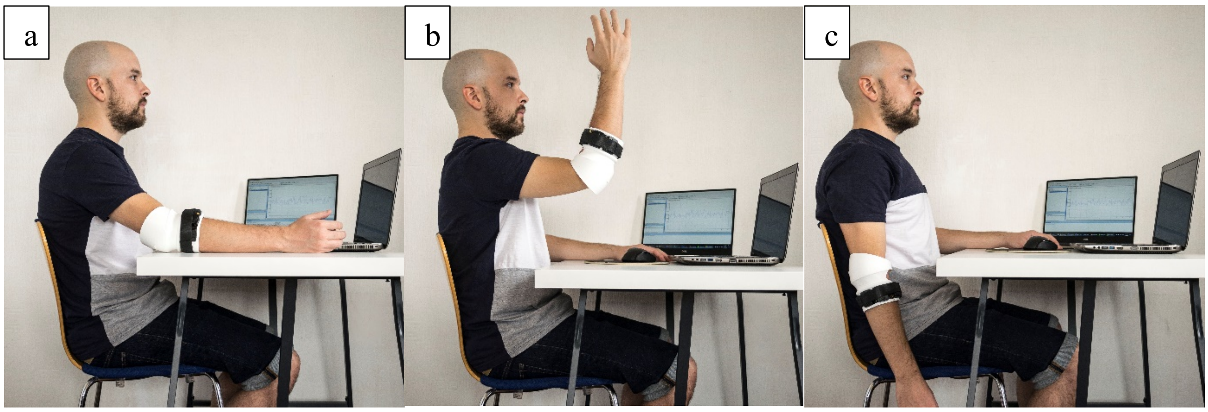

Figure 5:5: Experimental setup showing arm and electrode placement positions with the socket to perform six finger movements. (a) The arm on the horizontal table position, (b) arm upright, (c) arm up-down (vertical).

5.2.3.2 Decoding Hand Motions from EMG during Reach and Grasp Motions

According to amputee studies [240], [241],[180], comfort and functionality are two most important factors in the acceptability of prostheses and assistive devices. To increase comfort and functionality, prostheses should recognise the desired motion immediately in order to provide an intuitive and natural control system. Such methods have been utilised to perform power grabbing and detect static hand movements. However, other studies indicate that it is insufficient to develop a generic control system that distinguishes distinct grabbing and finger actions from limited arm orientation. It has been claimed that it lacks robustness and intuitiveness since natural gripping necessitates dynamic limb postures [97], [182]. Few research in the literature have used able-bodied subjects to identify grasping intentions from EMG signals during reach to grab motion detection [242], [243]. Furthermore, some studies have conducted the same methodology on amputees [209], [244].

To examine the differences between research findings and more clinically relevant outcomes, dynamic variations in limb position was demonstrated in this study. The findings indicated that the training dataset with dynamic arm position might have an effect on the robustness of the myoelectrical-based control. The comparison was conducted by replicating the identical experimental settings with dynamic hand motions for gripping and manipulating the same items. Since the muscular activity and muscle orientation change from static arm positions to dynamic arm positions, the finger and wrist change orientation simultaneously, influencing the EMG amplitude, and so does detection performance. This approach is demonstrated in online validation tests in Chapter 6.

For these experiments, participants were seated in front of a table with their elbow bent about 90 degrees and their hand in a relaxed position with palm downward, and fingers were in a natural, comfortable position (see Figure 5.6 (a)). The participants were instructed to reach and grasp objects with the help of a simulation displayed on a second PC screen. The participants started the arm trajectory as instructed to reach the object and asked to maintain their grasping for at least three seconds before returning to the initial position and then to consider the trial to be completed. Objects were located at three different distances and heights (i.e., 10 cm, 20 cm, and 30 cm). To eliminate the influence of different speeds, the arm trajectory was illustrated on a computer screen and subjects were asked to follow and mimic the same trajectory.

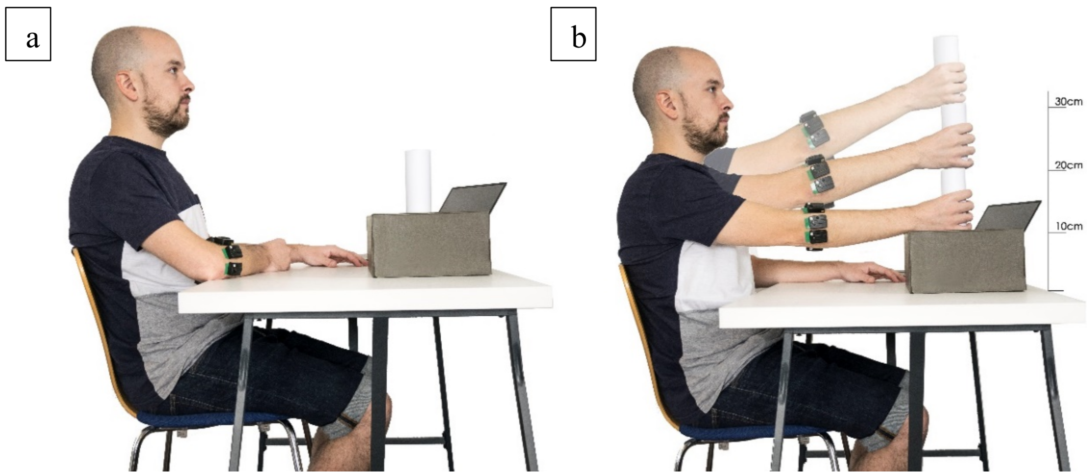

Figure 5:6: Representative of the phases of motion of an able-bodied subject for dynamical hand motions. The experimental setup shows the arm's initial position and the subject performing grasping for three different positions.

The data were collected while subjects performed pre-programmed single finger motions with and without the use of a bypass socket. The retrieved features were then utilised to suit the specifications of the amputee's real-life circumstances. The suggested system, seen in Figure 5.7, consists of a socket and seven sensors. Since this chapter's scope is not necessary to achieve a high level of accuracy but rather to investigate the practicality of electrode placement and the advantage of pattern recognition, the same data acquisition, windowing size, and classifications were used as described in section 4.3. Furthermore, sophisticated real-time performance necessitates a rapid and precise reaction to the user's intention. In order to reduce computational cost, improve the user experience and minimise the cost of the combined system experiments were also conducted with six channels in these trials. The discussion sections provide a full comparison between number of electodes.

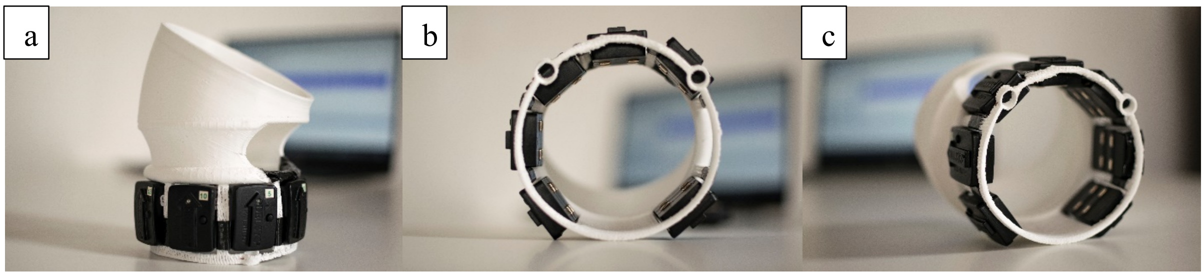

Figure 5:7: Different views of the custom-made socket for electrode placement in the circumference of users.

5.3 Results

This chapter introduces and evaluates a novel data collecting method for hand motion detection using a custom-designed socket. The categorization approach is based on the majority of the research studies mentioned in Chapter 2 and includes pre-processing with two alternative windowing sizes (125 and 300 ms). The time domain characteristics and classifiers utilised in this study are well-known (SVM, LDA, NN, k-NN) and have mostly been used in prior investigations, as discussed in Chapter 3.

The first comparison was made on the number of sensors with six and seven sensors using the identical muscle positioning approach. At the same time, the second comparison of windowing sizes was carried out. It should be observed that in both cases, the data collecting setup and filtering processes are the same. Therefore, motion classification performance should be a qualitative assessment of the dataset. In order to achieve optimum performance, "***Adam***" optimiser and "***grid search*** " were implemented four classification techniques to ensure that the data sets with the embedded system allow the highest detection of single finger motions and hand gestures in real-time. The Adam optimiser determines individual learning rates for each NN parameter and ensures that learning progress is adaptive. It calculates the learning rate for each NN weight by estimating the first and second gradient moments. Grid search, on the other hand, optimises arguments like kernel and gamma of hyper-parameters for the best cross-validation score of SVM. The examination of feature extraction methods reveals that pre-processing is still a substantial factor, even when muscle activation varies. Figure 5.8 depicts the accuracies of seven sensors for six classes of static arm position. Among the six feature extraction approaches, RMS performed the highest performance with an 89 % identification rate, while WL performed the lovest, with an 84.4 % recognition rate. When real-time control is necessary, it is advised that ANN be combined with RMS to offer better and more steady performance. Otherwise, the combination of SVM and three main features (RMS, MAV, IAV) may determine more accurate performance for offline motion recognition. However, the literature review suggests that a high classification accuracy might not secure a good real-time performance, and some sacrifices in offline classification may enhance the real-time performance. The comparison experimental findings demonstrate that offline results are average 5 % more accurate than the online control in all classifiers.

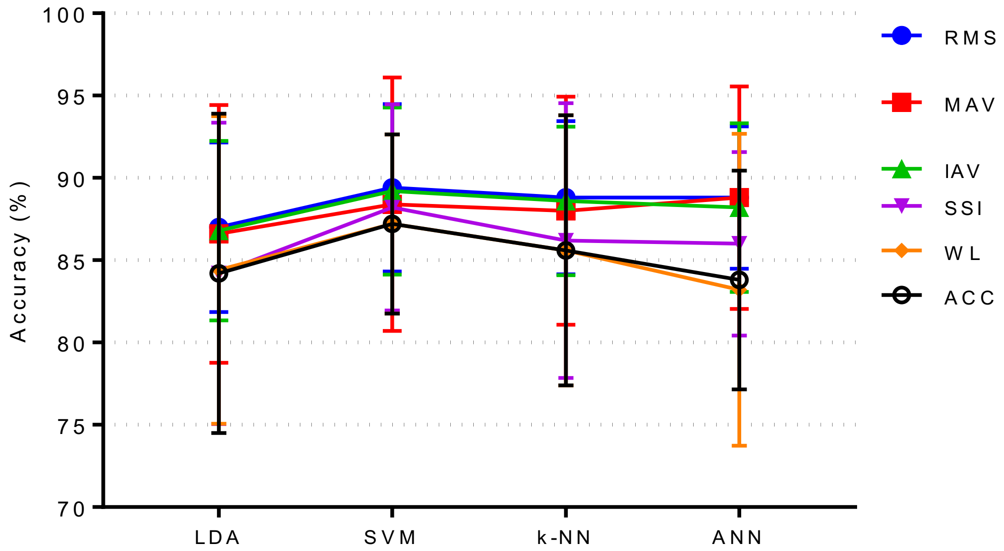

Figure 5:8: Classification performance of four classifiers when using untargeted (UT) muscles in 125 ms window length. The results represent average of five trials for two able-bodied subjects.

The comparison of the same feature shows that SVM demonstrates similar results to k-NN in 300 ms windowing size. The highest classification performance was recorded as (91.4 ± 4.5%) for k-NN, while SVM came in second with average recognition (91.2±6.4).

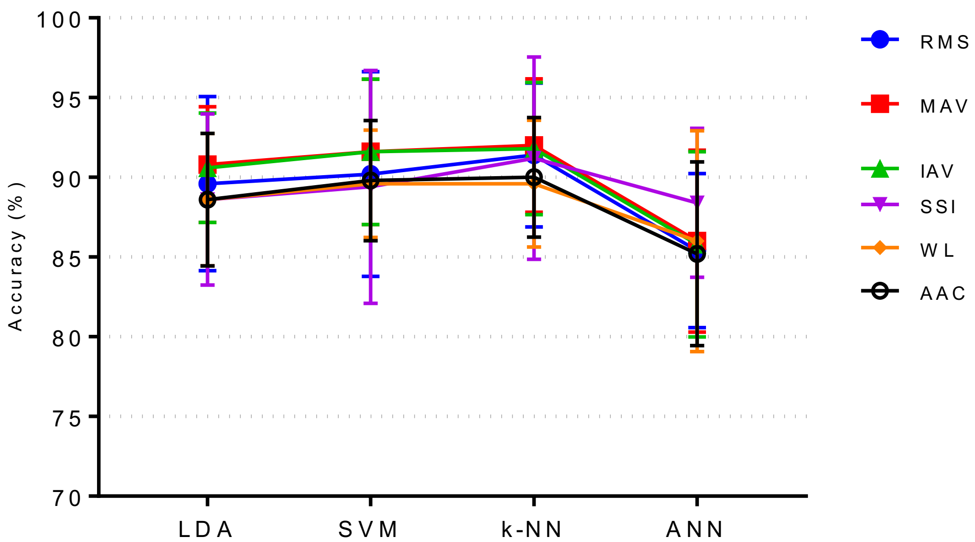

Figure 5:9: Classification accuracy of four classifiers when using untargeted (UT) muscle in 300 ms windowing length. The results represent average of five trials for two able-bodied subjects.

Figure 5.10 shows that classification performance for able-bodied subjects in static arm postures follows a similar trend, with seven sensors providing greater classification accuracy than six sensors. Except for SVM, the number of sensors appears to have a substantial influence on the majority of the classifiers. As a result, while selecting the number of sensors, caution should be made because it will have a considerable impact on real-time control. The highest average classification accuracy with six electrodes was obtained as 90% for SVM, and the highest average classification accuracy for seven electrodes was recorded as 92% with k-NN. Similar results were achieved with some early studies [205],[245].

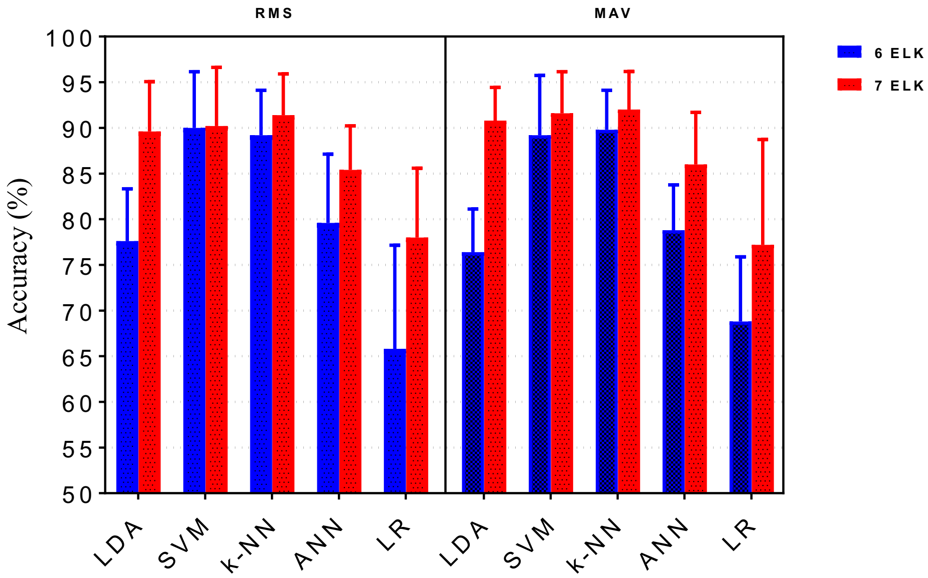

Figure 5:10: Comparison of classifiers and the effect of the number of electrodes in 300 ms windowing length. The results represent average of five trials for two able-bodied subjects.

The classification findings and graphs indicate that sEMG signals and hand motions in the same conditions have a substantial association. Except for one trial, the data revealed no significant changes when the number of motion repeats was taken into account for same the same subject (p =0.2736). Because each participant has different anatomical characteristics, a large disparity between participants for some ML methods were observed. Figure 5.11 depicts the performance of classifiers on the two subjects. It is worth noting that, as seen in the picture, there is no significant difference between the two participants for SVM and k-NN, but significant difference for LR and ANN.

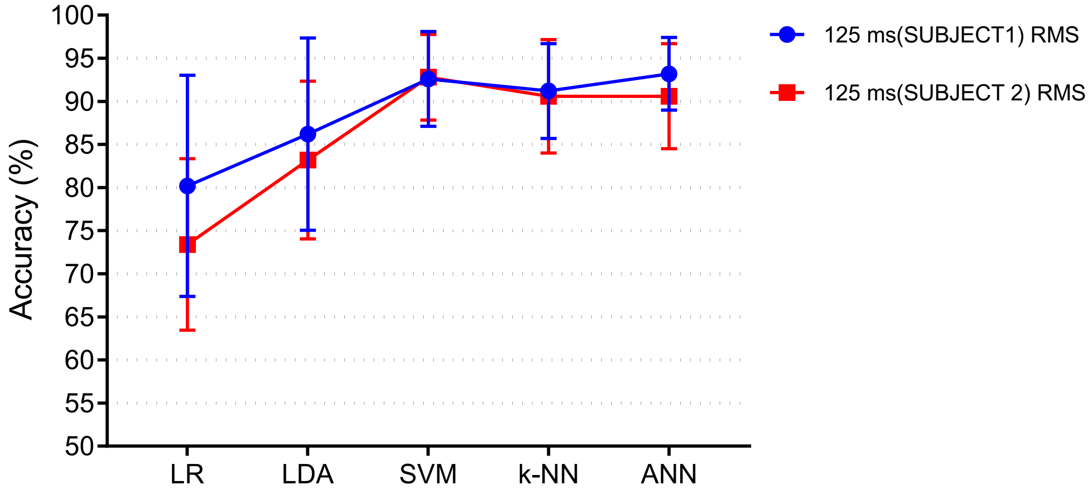

Figure 5:11: The comparison of classifiers between two subjects for RMS features in 125 ms windowing size. The results represent average of five trials for two able-bodied subjects.

Various force patterns result in different average sEMG magnitudes due to muscle stump fitness and objects. Although certain recognition accuracies are quite low among the six movements, including thumb abduction, all average accuracy rates are higher than 88.4 %, with flex index finger motion average rate of 93 %. The average motion recognition performance for six different finger classes is shown in Figure 5.12 when the subjects' arm is in a static posture.

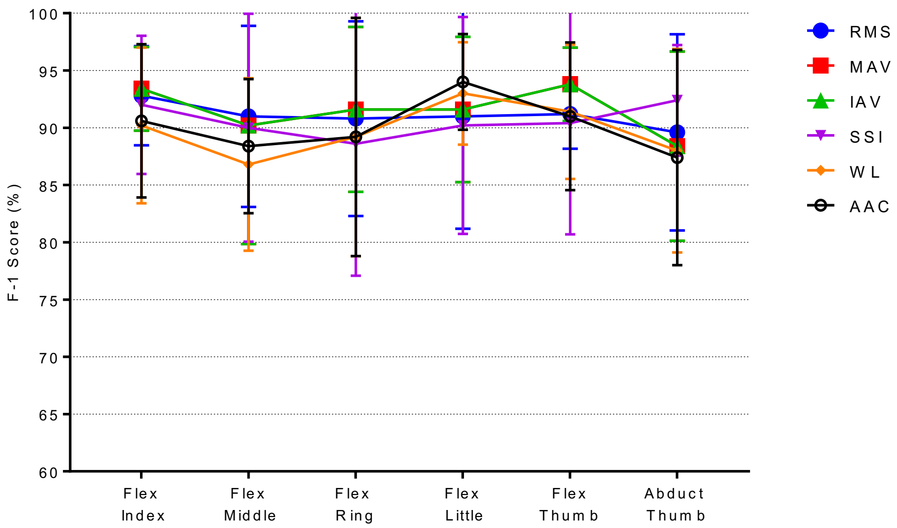

Figure 5:12: The F1 scores of selected finger motions with ANN (125 ms windowing length) while the subjects arm is horizontal. The results represent average of five trials for two able-bodied subjects.

When evaluating alternative windowing sizes, the performance of a bigger window outperforms that of a smaller window for all classifiers except the Artificial Neural Network (see figure 5.14). The artificial neural network (ANN) is thought to be a valuable tool for analysing the cause-effect connection in complicated and large data sets. It is one of the primary characteristics that characterizes deep learning.

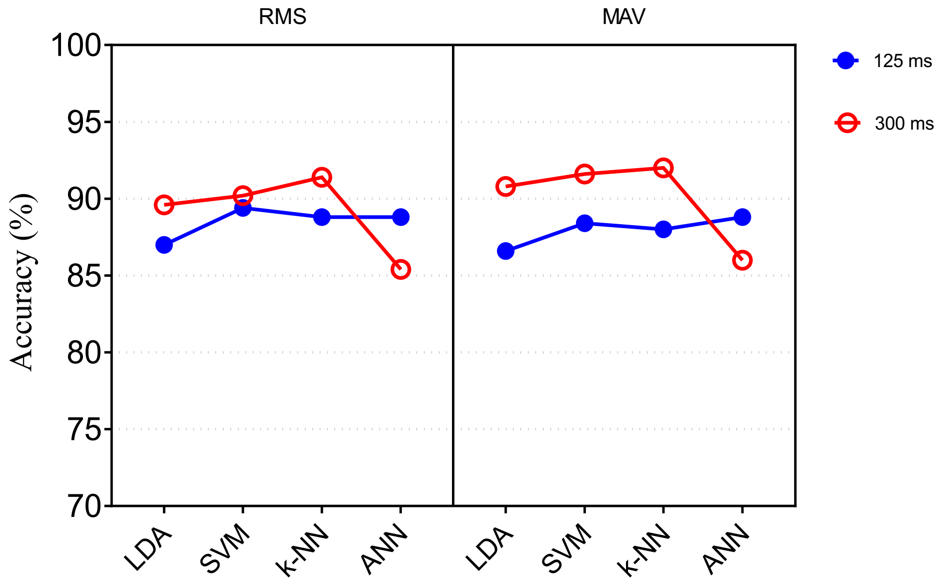

Figure 5.14: The effect of windowing length on classification performance. The results represent average of five trials for two able-bodied subjects.

The offline classification accuracy for previously stated classifiers and features were examined in three distinct static arm positions for object grabbing to analyse the static arm position influence on motion detection, as presented in section 5.2.3.1. Figure 5.15 depicts a combination of six features and five classifiers. The findings reveal that the combination of ANN and AAC achieved the highest recognition rate performance (with an average of 96.4 %), while the combination of LR and SSI achieved the lowest rate (with an average of 79.8 percent). Although there are no significant differences between the three movements in terms of percentage of motion correctly classified ($p = 0.2651$), cylinder grasping outperforms pinch grasping. Ball grabbing, on the other hand, has the lowest performance (see Figure 5.16).

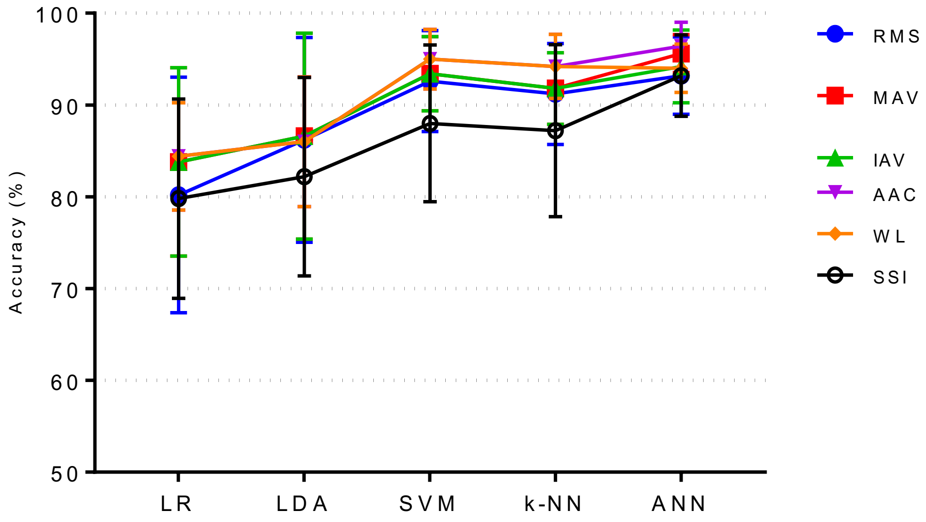

Figure 5.15: Classifiers' performance for six features while the subjects were performing object grasping (cylinder object) with an arm in a horizontal position.

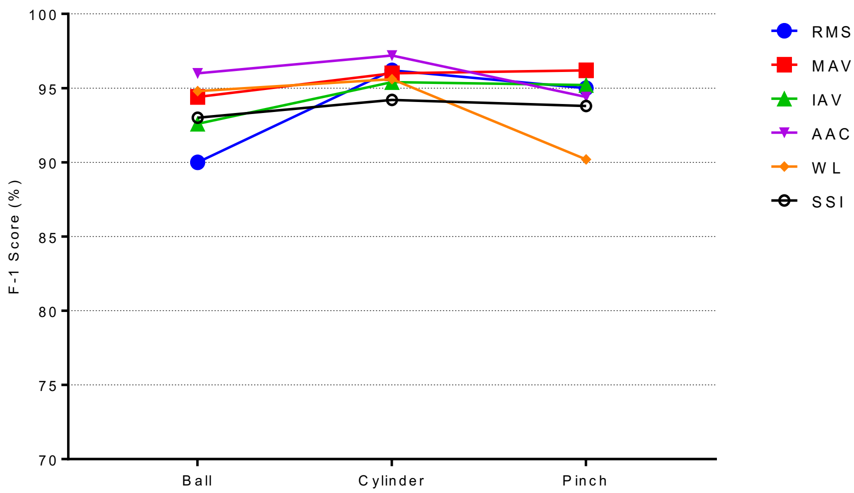

Figure 5.16: Three objects grasping and their standard error while the subjects' arm were in the horizontal position.

For individual finger detection (see Figure5.17), there is no significant difference between three different arm positions ($p = 0.7879$), with the best performance while the arm is in an upright position. For object grasping (see Figure 5.18), there is a significant difference between the three arm positions ($p = 0.0059$), and the best performance was recorded while the arm is in the horizontal position (for SVM 92.8 ±3.8).

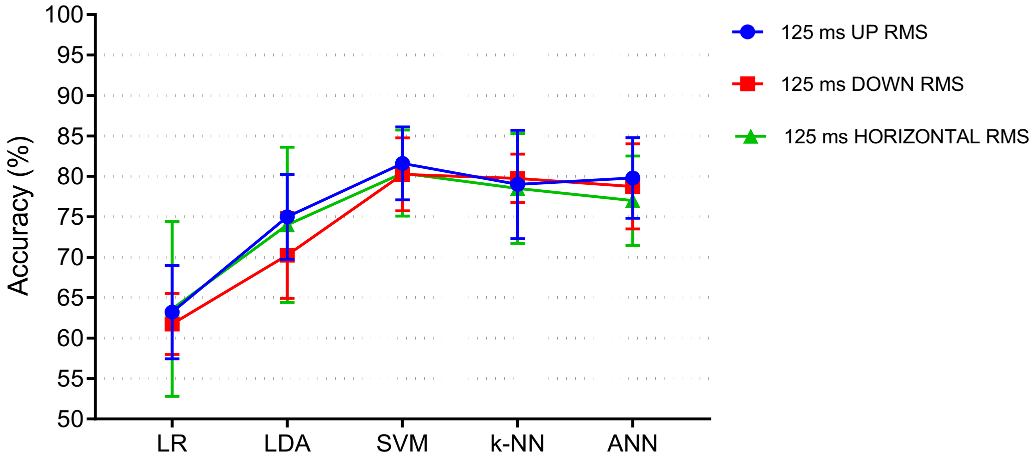

Figure 5.17: Classification accuracy in different static arm positions for independent finger detection. Respectively, the blue line corresponds to the arm in an upright, red line down, and green line horizontal positions.

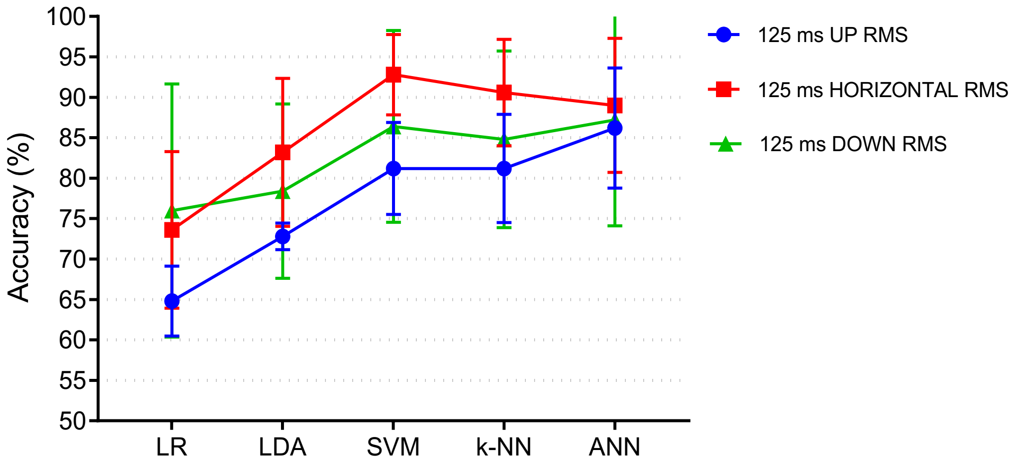

Figure 5.18: Classification accuracy in different static arm positions for object grasping. Respectively, the blue line corresponds to the arm in an upright, red line horizontal, and green line down positions.

As presented in the previous section 5.2.3.2, the performance of fice classifiers were compared for dynamic arm movements (as called reach and grasping). Figure 5.19 shows the average and standard deviation of classification performance for three grasping types during dynamic limb orientation. The accuracy was obtained with no significant differences for ANN and k-NN regarding model accuracy. Compared to static arm positions, it performed a more reliable method as it improved the average classification for ANN from 89% to 91.6%. On average, the classification performance of 92% was obtained for the ANN for all grasping types, which indicate that high classification for some arm position is significantly improved and has a high potential for real-time control.

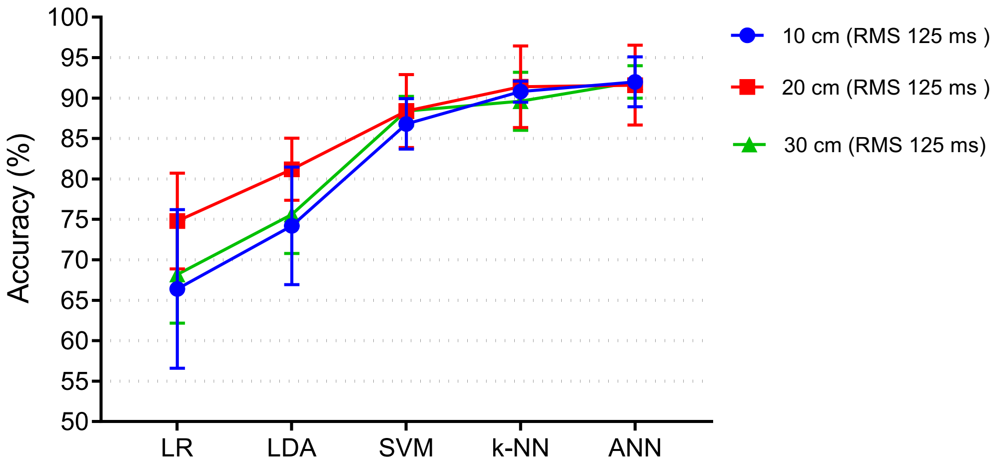

Figure 5.19: Classification accuracy rate in different distances. Respectively, the blue line corresponds to 10 cm, the red line 20 cm distances, and the green line 30 cm distances.

Figure 5.20 shows the averaged across grasping types for six feature and five classifiers for arm travelling to 30 cm. Overall performance for ANN with MAV feature was recorded for ball grasping 94.4%, cylinder grasping 93.6%, and pinch grasping 89.4%, respectively.

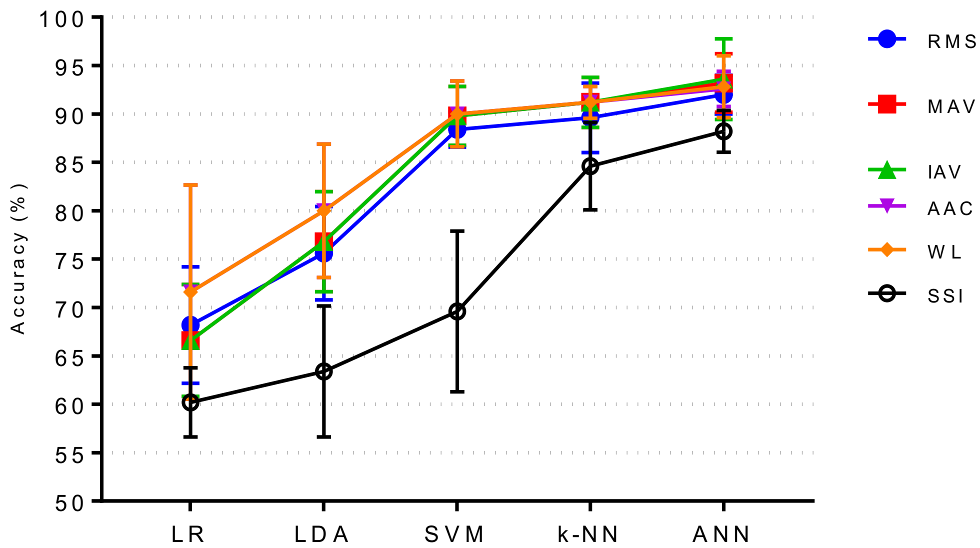

Figure 5.20: Average classification performance for six features and five classifications while arm travelled from the initial position to 30 cm.

Despite some variations from previous research, it is clear that the data collecting, pre-processing, and learning model may be used for real-time motion identification for transradial amputees. It is worth mentioning that, in these experiments reaults are average of five trials for two subjects. The subjects were the same for entire experiments for comparison.

It is suggested that several parameters affect classifiers' performance, such as the capability of amputees to provide movements, the degree of sensation, and the remaining forearm percentage. The influence of experimental conditions such as the effects of the movement's number and user influence, particularly the amplitude changes of sEMG were assessed in this section. One of the important issues for motion recognition is the time consumption for training and offline computation.

5.4 Discussion

Pattern recognition control in electromyography (EMG)-based prostheses has great promise for providing intuitive control. Despite the fact that existing technology for upper-limb prostheses has shown high accuracy (almost >95 %) in offline tests, clinical deployment of prostheses does not yet deliver the same performance. The primary cause for the disparity between academicians' and practitioners' applications is specific variations in setting conditions, such as electrode allocation, muscle contraction variance with varied arm postures, and muscle fatigue.

One of the goals of this research is to look at typical reasons for prosthetic rejection and to offer practical solutions for dexterous prostheses. As a result, an amputee-friendly (realistic) electrode distribution and pattern recognition using various data sets and classifiers were studied. Except for ANN, the results reveal that decreasing the windowing size from 300 Hz to 125 Hz affects the classification performance of all eight characteristics. This study's findings include a comparison of forty-eight features (two windowing sizes with three arm positions), which reveal that with fewer electrodes, the classification performance of all assessed features drops drastically (p <0.0001). The study's primary finding was that classifiers performed considerably better with dynamic arm posture datasets. Because NN works better with big and complex data sets, dynamic arm posture EMGs-based pattern recognition improved robustness against EMG signal fluctuation.

The aim of this section is to discover a suitable collection of sEMG properties that provide superior performance for myoelectric-based control. According to the study, sensors positioned around the circumference of the forearm yielded the best classification performance 87.52±6.25% for seven electrodes and 80.6±8.92% for six electrodes with commonly used EMG features (MAV, RMS, and IAV). With the same number of electrodes, the EMG features with given electrode distribution surpassed existing data sets (sEMG signal from static arm postures) by 4%. The results determined for sEMG when investigating the influence of arm position were similar to those reported in [182], [210], where similarity is the degradation on some particular arm positions (arm down position), despite differences in methodology. Although the classification performance is comparable to earlier research, it differs for two primary reasons. Previous researches examined the classification performance with different hand gestures and wrist motions. This study focused on single finger manipulations and configuration.

Most significantly, past research used a statistical arm position on the table to investigate individual muscles, which is not viable for a substantial majority of amputees. In contrast, this study evaluated alternative arm postures (three static and three dynamic) for superior classifier training in large data sets with varying windowing sizes. In particular, it offers a method for mapping EMGs for reaching and gripping activities. Using this method for real-time applications, the travel distance was also considered forbperforming the preferred grasping. This is more lifelike and resembles a human hand. Despite the fact that no significant difference was detected while conducting motion at varied arm distances and trajectories, it offers a better detection performance while eliminating the impact of EMG reconcentration.

The performance of a non-amputee subjects using a 3D-printed socket, which allowed to conduct and test the prosthesis system from the perspective of amputee was investigated. This unique custom-designed socket and electrode distribution allows a realistic access to adequate forearm muscles without the use of any extra procedures such as ultrasound or medical evaluation. The socket was primarily designed with multichannel arrays in mind, as compared to more sophisticated approaches [246] or commercial prostheses [247]. It preserves intact limb muscle access for sEMG, and it easily adapts to new users.

Therefore, for real-time myoelectrical prosthesis, two feature sets (RMS and MAV) with seven sensors are suggested. Combining these features with the recommended number of electrodes would make the control architecture suitable for functional testing of the entire system on transradial amputees.

5.5 Summary

The study clearly shown that the datasets and electode allocation had a substantial impact on classifier performance in presenting a variety of hand and finger actions. The use of 300 ms window size instead of lower window size results in a drastic reduction in classification error for linear classifiers. In general, the study highlights the potential benefits of a method inspired by the practical execution of utilising electrodes around the circumference of the forearm data sets derived mostly from literature. The results also showed that arm posture had an effect on categorization accuracy. It is recommended that better accuracy can be obtained by using training data from varied arm postures during the training phase.

There are two electrode placement procedures described in the literature. The first is the commonly utilised method of attaching electrodes to specific muscles, which necessitates prior experience and results in humans error with each replacement. The methodology is fully detailed in chapters 3 and 4. As described previously in this chapter, the second technique is to install sensors around the circumference of the user's forearm. In this new sensory modality, electrodes are positioned in an array in a specific spot on the forearm. Although both methods have yielded considerable data for prosthesis control, the second strategy is more practical and consistent since it provides high pattern recognition and allows the prosthesis to be quickly put on and removed. The redesigned socket ensures consistency for each use by employing standard space between each electrode and precise placing on the arm with the unique design (the specifications for the new socket design are presented in Appendix D). This new sensory modality with socket eliminates the user's influence and unifies the experiences.

The primary goal of the tests was to provide a realistic and meaningful assessment of EMG-based control by utilising a new sensory system to optimise electrode localisation. The chapter introduces new tools and advice on selecting the best data gathering process, classifiers, and precise parameters for active prostheses control, with an emphasis on the application and intended outcomes. The findings of the chapter proposed some solutions to a significant problem, the placement of the electrode, which was caused by the various configurations of the amputation stump. The outcomes of this chapter will be used in the following chapter development by extending the analysis to real-time signals and constructing an embedded control unit for pattern recognition in individuals with transradial amputation. The system robustness and reliability will be validated, and the performance of the real-time control will be evaluated using standardised real-time test metrics.

Chapter 6 Validation Test of Robust Control Strategy on Prosthesis Prototype

6.1 Introduction

An intuitive, robust, and multifunctional myoelectric prosthetic hand with a high degree of freedom is an excellent opportunity for upper-limb amputees to regain their daily life activities. Although most advanced prosthetic hands are not even close to human-level dexterity, scientific advancement and early commercially available technologies demonstrate that dexterity may be achieved by analysing real-time electromyography signals (sEMG). According to literature, most of these techniques are based on identical data collecting and processing protocols, as discussed in earlier chapters. Classification, regression, and control algorithms have been developed to understand the intended movement of users. The motion detection results proposed in the literature vary by a large margin to 80-95% accuracy. This accuracy, however, is affected by a variety of factors, including amputation degree, the number of classes, experiment settings, and observed muscles. It is necessary to exhibit empirical investigation in the proposed control strategy to analyse theoretical advancement in the real environment [208], [229], [238].

This chapter presents the outcomes of the proposed technique in real-time conditions and discusses the benefits and drawbacks in detail. It analayses sEMG based pattern recognition using the best-performing machine learning technique ANN and time-domain feature RMS (compare to other tested methods) on a physical prosthesis in a range of real-time evaluation metrics. These two approaches are well-known and have previously been used to control myoelectrical prostheses [17] [187].

This chapter studied the feasibility of operating continuously in real-time despite a range of interferences such as electrical shifting, limb position, and muscle force alterations. This study employed the new sensory modality (discussed in chapter 5) to develop an embedded control for amputees. The embedded pattern recognition architecture was tested in real-time with a robotic hand that can perform six independent finger motions and several hand manipulations. The commonly employed evaluation techniques were used to measure clinical reliability, robustness, and motion recognition accuracy in real-time with object relocation and gripping tests.

6.2 User Online Prediction Strategy

Machine learning techniques have been chosen over traditional control systems for prosthesis due to their superior accuracy, durability, and practicability. The early studies reported high offline classification accuracies for prostheses. However, it has been suggested that the necessary motion detection accuracy for real-time applications has never been achieved.

Obtaining robust control is crucial for extending sEMG-based pattern recognition into real-world applications, as some articles (e.g., [84] [248]) have emphasised. Thus, in order to strengthen the robustness of control architecture, an ML and feature extraction based approach that was proven to be robust to develop such control were tested in this chapter. A wearable embedded prosthesis socket was developed with EMG electrodes to capture muscle contractions and feature extraction algorithms to preprocess biological inputs in real-time. The proposed methodology is believed to play a significant role in developing personalised prosthetic devices at a reasonable cost. The data is collected in real-time, and the motion prediction is executed concurrently with the patient's normal daily activities. The primary advantage of this control architecture in terms of the aforementioned fundamental issues is its intuitiveness and robustness. Unlike previous key pattern recognition studies [116],[156],[95], which remapped hand motions from the wrist or shoulder, this study used the hand's independent fingers to execute the original anatomical motions. Figure 6.1 depicts the suggested prediction model and control for continuous control.

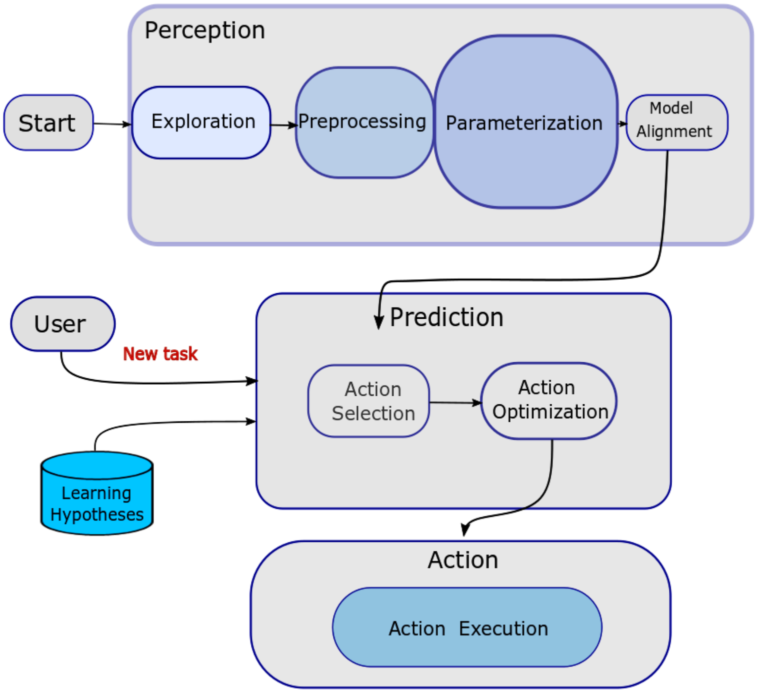

Figure 6:1: Overview of the real-time control architecture. The control system comprises EMG signal acquisition and data processing, motion prediction, and prostheses control.

The suggested control system consists of two segmented control strategies built in the C and Python programming languages. The user can initiate finger positions and operate individual fingers using this control architecture (see figure 6.2), which fills a gap in the numerous existing control methods for transradial amputation. Furthermore, unlike some early prosthetics control methods, this control approach is continuous, similar to human dexterity, thanks to the signal modulation and prediction shifts between movements without requiring a long wait to return to the initial (rest) posture. From the viewpoint of amputees, this is one of the most desired features since it enhances function transfer efficiency [118].

Consequently, the majority of upper-limb amputees may benefit from this non-invasive method, which does not require brain implants or other expensive interfaces like iEMG. This control design has the potential to make next-generation prostheses more natural and intuitive to use for amputees.

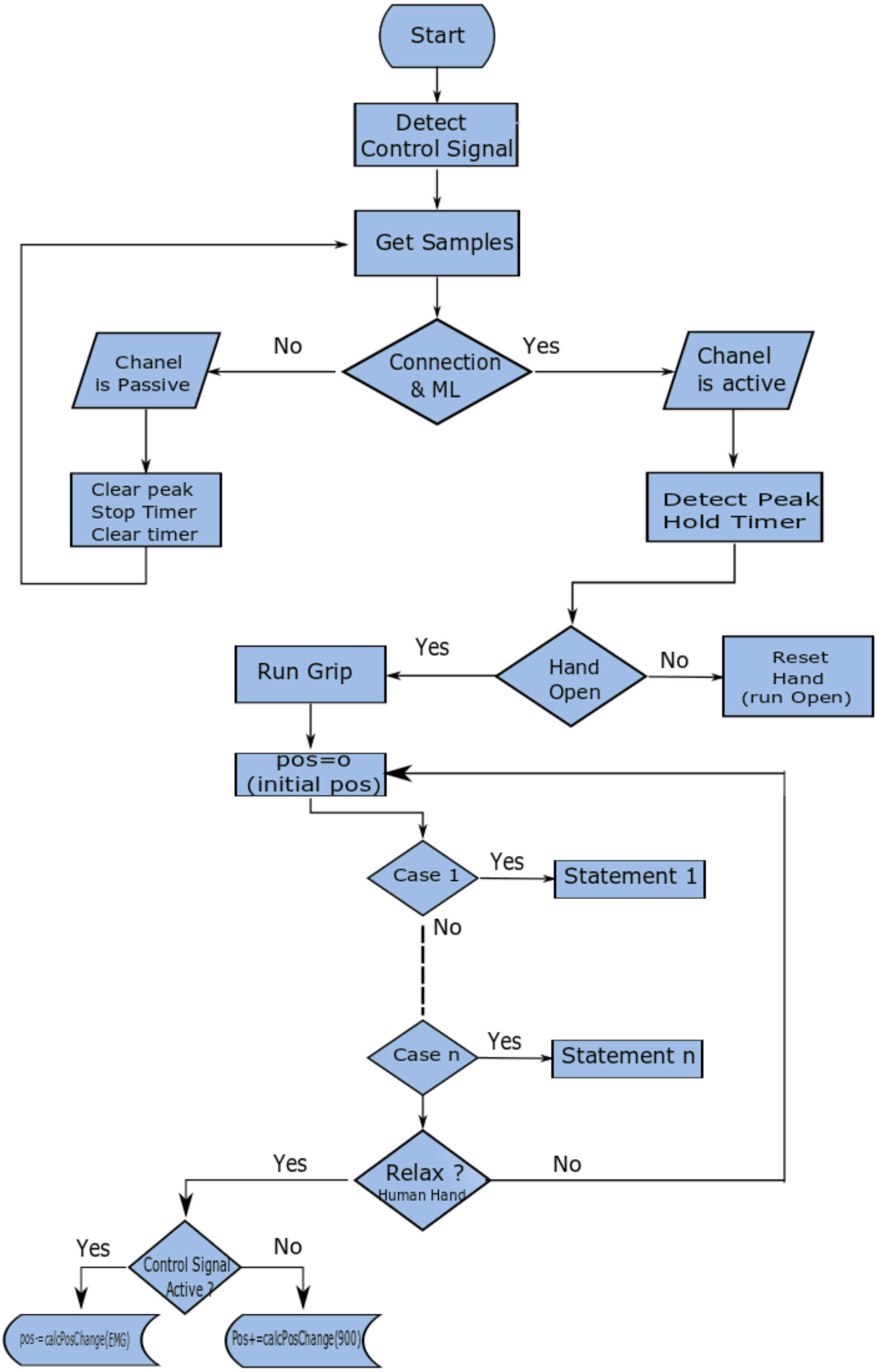

Figure 6:2: The block diagram of proposed data processing and function control. The process is a composition of six parts: sEMG data measurement, signal prepossessing, feature extraction, data segmentation, prediction and control.

6.3 Adaptable Socket Development

One of the advantages of a myoelectrical prosthesis over a regular body-powered prosthesis is that there is no harnessing or reduced body powering. They appear more cosmetic and natural as they do not have cables and straps. However, these prostheses have several drawbacks, such as hefty batteries and a large number of actuators to give high functionality. These prostheses require large number of electrodes to capture signals from targeted muscles in order to activate and operate the prosthesis while preserving skin surface contact. As a result, this association may create discomfort, may not be tolerated by particular user skins, or maybe interrupted by sweating. Maintaining proper contact between electrodes and skin might also be complicated if the prosthesis is not flexible and limb size or shape changes.

Because proper electrode-to-skin contact is critical for recording correct EMG signals for control, a tight socket is required to minimise electrode displacement even if the user changes arm orientation. Although the degree of amputation is important in prosthesis fitting and control, an adequate user interface in socket design is an essential feature of the prosthesis's structure, storing the components and holding the device onto the remaining body part. Nevertheless, determining a well-fitting socket is challenging because the residual limb is frequently of variable shape and size. Hence, several studies [246], [249] have proposed alternative designs to alleviate fitting concerns, such as custom-made sockets and osseointegrated implants (see Figure 6.3).

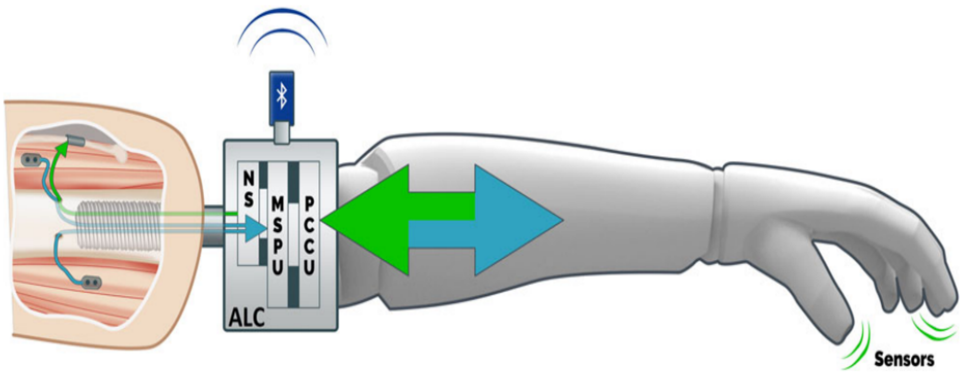

Figure 6:3: A presented embedded system that allows biosignal data acquisition and sensory feedback motor control of prosthesis by [159]. The system has three units: neurostimulator (NS), mixed-signal processing unit (MSPU), and prosthesis control and communication unit (PCCU).

Statistics and surveys of prostheses indicate that 79 % of commercial devices are too heavy [200]. Furthermore, the overall weight of devices has a major influence on the perceived weight of the system. As a result, it is advised that heavy components such as actuators and batteries must be reduced as much as feasible [200]. It is suggested that an ideal socket must be stable while handling several tasks such as slippage, finger manipulation, and soft tissue rotation [250]. Even if the socket is properly designed, keeping a consistent fit over time may be difficult since the form and size of the limb may differ from time to time for the same user. This variation can occur over time and over the course of a day. This is one of the most serious issues with non-invasive EMG-based controlled prostheses. Specific alternative socket designs have been proposed to avoid this physical challenge for control (adjustable electrode housing mechanism) [251].

A surgical alternative method was proposed to circumvent the effects of socket fitting difficulties, such as the effects of volume changes and variations that cause comfort problems. Although this approach solves the majority of fitting issues, there are still challenges in the interface, such as obtaining reliable command signal, processing time, and continuous control. Thus researchers have proposed more direct EMG recording to regulate implanted myoelectrical method [252], [253]. In order to improve the socket comfort and increase acceptance of the device, researchers and prosthetists have developed new materials, production methods such as embedded systems [159], and new sockets to offer customised prostheses by maintaining or adding new functions for the daily life of individuals [160].

This section discusses the development of a wearable prostheses controller based on an improved new sensory modality (presented in chapter 5), intuitive pattern recognition, and a customised control architecture. The robotic hand is controlled directly by a wearable embedded system, which connects wirelessly with sensors and the controller to recognise patterns. The complexity of combining an effective embedded pattern recognition with a control architecture for intuitive user-prosthesis interaction was developed throughout the entire system. A robust feature extraction and data processing (dynamic data collecting) was achieved with less delay using this methodology. The reliability of signal acquisition with suggested approach was improved to eliminate the influence of electrode shifting and electro signal interferences, which degrade the real-time performance of prostheses.

6.3.1 Mechanical Features of Prototype

Myoelectrical-based control prosthesis have been widely researched in order to overcome the limitations of conventional data acquisition methods and meet the demands of all degrees of amputation. Several research projects to improve control methods [103], [160], [254], to enhance the mechanomyography as probing different electrode placement and data processing

[246], to the prospering prosthesis with sensory feedback [35], [64], [164], [255] are ongoing explorations. New approaches increased the cost of the prosthetic hand and thus, increased the rejection rates due to the need to justify their cost quantitively [136]. The summary of upper limb rejection rates, up to 75 per cent, in the past quarter-century with social and technical aspects are given in [12]. The authors have claimed that advances in engineering and technology, materials, battery/charging units, and signal acquisition had decreased the rejection rate.

This research concept was driven by the need for real-time data collection and operation of a dexterous prosthesis for upper body amputees. The empirical data from the able-bodied participant for varied sensor implantation supported the electromyography-based prosthesis socket design. An EMG-based embedded system with external power and a 3D printed and changeable prosthetic hand socket is the main design concept.

In the inertial data collection unit for assessing finger movements, a microcontroller (Chestnut V1.0 PCB) was used to activate motors in the hand palm if the predictions are detected (see figure 6.4). A mini PC (Raspberry Pi 4B) to evaluate signals from electrodes and classify data in real-time is shown in figure 6.4(c). The socket elbow section was particularly designed to ensure accurate data acquisition. The surface and edge of the socket were treated with HTV silicone material to achieve a pleasant fit. The system's total weight, including electrodes and wires, is projected to be 670 g.

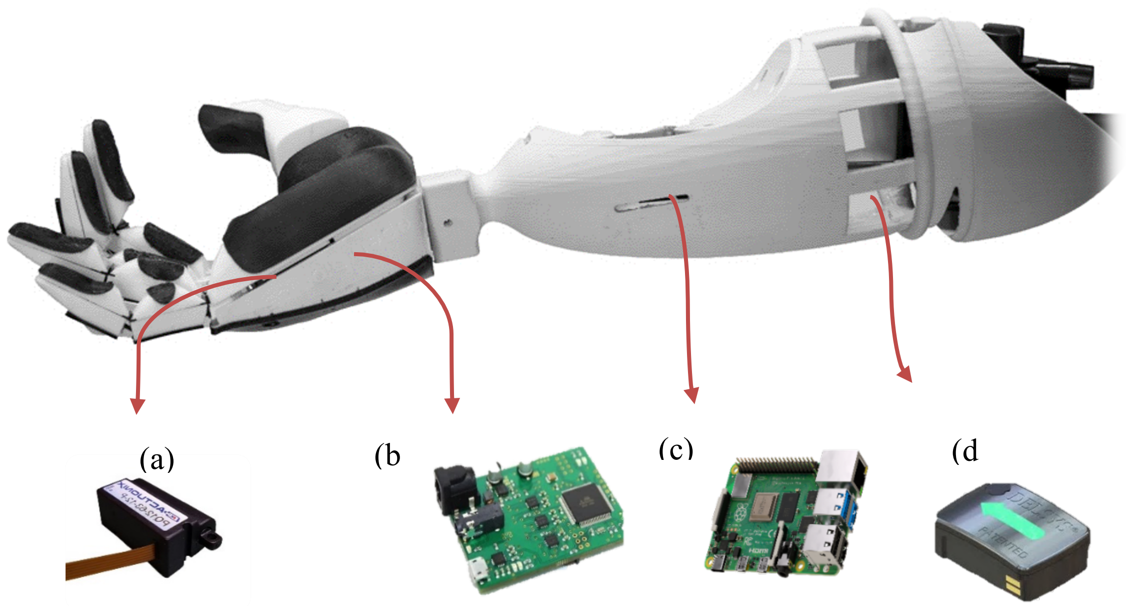

Figure 6:4: The main parts of the system: (a) linear actuator, (b) the mini controller, (c) mini PC, (d) EMG electrodes, custom-made prosthetic socket.

The robotic hand was attached through an ABS plastic socket to the residual limb. To maintain stability, the socket was custom-made for each user out of silicon material, and the outer socket is held to the limb by friction. Commercially available sockets are manufactured of an elastic and long-lasting resin-based material or are supported by carbon fibre. The socket design is equivalent to several commercially available models [40], [256], in terms of size and aesthetics. The socket was built with a 280 cm length and 45 mm radius, corresponding to an adult man's arm size.

The design was developed for two primary purposes. The first reason was that it was desired to have characteristics and a shape similar to a biological human arm. The second was to utilise it as the principal test of the developed control method's real-time performance. Since this study's main motivations are obtaining intuitiveness and robustness, the view was that the embedded control system would improve the data acquisition and real-time control with high accuracy, as new electrode orientation and machine learning algorithms provide better performance with the new sensory modality.

Some research groups tested and validated their control strategy using commercially available sockets and hands. However, It was decided to develop a new socket to analyse the new electrode configuration and embedded ML system for this investigation. The mechanism is divided into two parts: the hand and the socket. The hand part was purchased for testing independent finger's motions since it does not need to be sophisticated if it delivers independent finger motions.

6.3.2 Continuous Data Acquisition System

High performance has been attained in the virtual environment with offline and online data collecting from able-bodied and amputees. However, when users test the entire system in real-time, the system does not deliver the same, or even close to the same, performance. According to studies, offline control has a success rate of 85-95%, whereas online control has a success rate of 65-73% due to the fact that real-world application requires physical equipment and synchronisation. The most significant difficulty encountered by the user is a lack of robustness and adaptability in the embedded system to implement EMG pattern recognition techniques. Thus, issues concerning the adaptability and durability of wearable elements have a significant impact on prosthetic rejection rates.

One of the significant disadvantages of pattern recognition algorithms is re-training for new users and new occasions. Composing training features and producing a new testing feature vector for each user and different arm postures is currently an issue that has to be addressed in this method. Second, there is a lack of a complete device that enables an embedded system to integrate four real-time steps: data acquisition, feature extraction, predictions, and motion execution. It is necessary to process quickly enough (less than 300 ms) to consider the real-time system. Thirdly, as many components in this system do not interact for precise time control, it is not feasible to achieve such a compact system to combine all components and algorithms in an embedded, powerful mini PC [160],[257].

The approach outlined in this work aims to address a gap in the literature by developing an embedded control system. A system for real-time data acquiring, processing, and actuating a prosthetic hand was developed in this chapter. Figure 6.5 displays the suggested system's design, consisting of two major components: a micro PC for data processing and prediction and a mini controller for actuators.

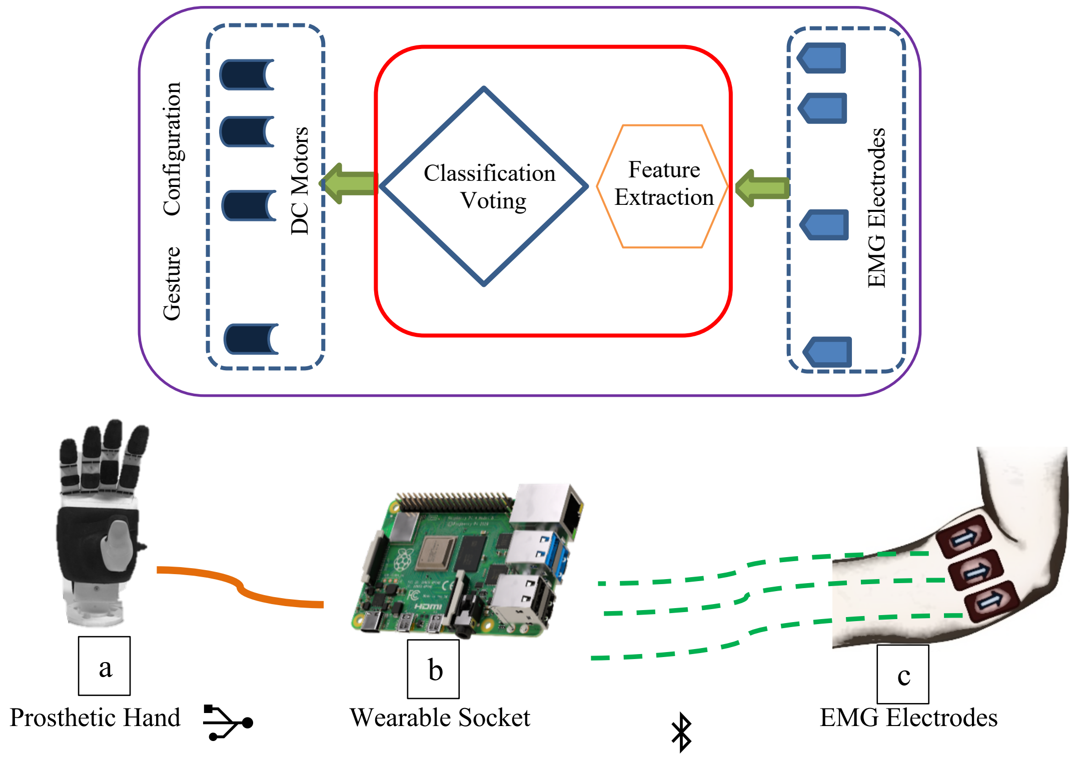

Figure 6:5: The diagram of system architecture for continuous transmission of data to the controller. (c) EMG electrodes around the arm send hand motion to the electronic compartment, (b) custom made socket interface (i) mini PC processing signals and detecting intended motion, (a) prosthetic hand (ii) mini controller for the actuator. The data is transferred from Delsys to the mini PC over Bluetooth, and then by wire from the mini PC to the micro controller through a serial peripheral interface.

The robotic hand holds four linear actuators, a voltage regulator, and wiring components. The Delsys electrodes and Delsys box was used to continuously transmit EMG data to the mini PC in a complete prosthesis. In each window, seven data channels are filtered and cleaned from undesired disruptions. Real-time data is called via Python for model training and prediction through a wireless link between MATLAB and Python programmes. This communication protocol was chosen for its ease of use and versatility to communicate with various host devices. The comunication protocol between components and detailed specifications for sensors are presented in Appendix A.

The interface provides continuous data for new predictions when the finger movements or hand manipulation changes. The controller board was integraed to the system to provide digital signals to each pin of four motors independently by pulse with modulation (PWM). The mini controller's (Chestnut V1.0 PCB) code was written in the Arduino integrated development environment to control each finger via linear motor (PQ12 motors). The setup code runs at the beginning for the initial position for prototype. The main loop continues forever once the Raspberry Pi receives the first message throughout each execution as part of the motion detection. The specifications for the new socket design and commercial parts are presented in Appendix D.

The proposed control mechanism is a key and necessary component of the prosthesis, as well as the most important aspect of this research. It is divided into two stages. The first is a measurement of the participant's muscle activation EMG signals to identify the required pattern. The second step is to simulate the desired movement on the prototype, confirming that the system behaves similarly to an able-bodied user. The first portion is provided in Chapter 4 and 5, covers a variety of topics, ranging from diverse electrode orientation to different feature extraction approaches and machine learning algorithms. This chapter presents the second portion, which serves the control architecture of robotic hand and the validation in real-time. As described in earlier investigations, the suggested control approach has been effectively used to EMG controlled prostheses [160], [212], [248]. This study aims to present and validate our data acquisition and motion detection to maintain more consistent signal acquisition.

The goal was to employ more suitable sensors (e.g., 13E2200, Otto Bock). These are sophisticated sensors that read user input and respond to hand movements. This might allow for faster data recognition and lower computing costs. The data collecting box, like the Delsys system, must be connected to the PC through TCP/IP protocol using the Trigno Control Utility (TCU), which increases processing time. Adding multiple wireless connections increases the likelihood of connection loss and causes synchronisation issues. In doing so, the prototype may not 'drive' the user better, but it will boost intuitiveness and minimise movement response time.

The EMG data were used to develop the control architecture obtained from untargeted muscles in the forearm's circumference. This concept was unlike other commercial prostheses for two reasons. The first approach to determining data from the arm's most dominant muscle, as presented in chapter 3, is the most common approach for some amputation levels. However, this approach is not feasible for transhumeral (above-elbow) and transradial users. Also, it is challenging to maintain the same electrode positions each time of use as it requires precise electrode location, and electrode shifting and crosstalk are most likely. Besides, the aim was to develop the system as minimally invasive to reduce the number of electrodes and, eventually, the prototype's cost for desired control strategy.

The features were obtained in the MATLAB program to identify meaningful information and eliminate unwanted interferences. As previously stated, the high accuracy of motion detection was accomplished in both electrode placement conditions; however, the second strategy, untargeted muscle, was favoured for practical reasons. Throughout development, the prototype's priority was to strengthen the robustness of active powered prostheses without sacrificing their multifunctions.

6.4 Validation Experiments

It is challenging to evaluate the real-time control performance of EMG based prostheses due to the lack of standardisations on data collection, feature extraction and pattern recognition methods. It is difficult to compare different experimental results when varied conditions, such as the number of sensors, classification techniques, diversity of individuals, electrode location, type of limb deficiency, and residual limb length, are taken into account. It was suggested that significant differences between participants and their performances could occur even in the same test conditions, especially considering there are not many multifunctional prostheses available to compare versions.

The accuracy of the classification methods has been used to evaluate the effectiveness of pattern recognition algorithms in most prior research. However, classification accuracy is the capability of recognition algorithms and tools to differentiate different patterns in specific time sequences while the participant manipulates fingers or holds objects. These performance metrics are usually determined after post-processing and regularisation of the EMG signal. Thus they are not a realistic assessment for the real-time performance of electromyographic prostheses. Therefore, it is suggested to employe well established standardised testing protocols on prosthetic hands to see if the residual muscles could still offer accurate real-time prosthesis control using real EMG data. In this study, the object relocation and grasping tests were performed to assess the proposed system's clinical reliability, robustness, and motion recognition accuracy.

The findings of the experiments showed that the robotic hand could successfully display six finger motions and four objects gripping, and the user did not encounter a significant time delay for the control. The control methods demonstrated the capability to predict finger motions and object grasping quantitatively since their predicted motion trajectories have similar forms regarding their intended trajectories from the graphical display. It was discovered that hand gestures could be successfully differentiated across sessions in which electrodes on the arm were replaced, even after several days. Some inconsistencies were discovered due to small shift between the end of some activities and the start of new ones.

6.4.1 Participant Details and Preparation

In this experiemtns data were determined from seven channels of sEMG signals from a human subject while grasping four different objects and manipulating individual fingers (seven electrodes over the circumference of the forearm is illustrated in figure 6.6). The arm and wrist have been constructed to keep rigid using a socket, as these components are frequently unavailable or immobilised in transradial and below elbow amputees. All finger phalanges were manipulated with natural speed while opening and closing the fingers for a total of 10 seconds to establish realistic motion patterns during the EMG analyses. The newly developed adjustable compact socket was used to apply muscle patterns that had been recorded and categorised on the robotic hand.

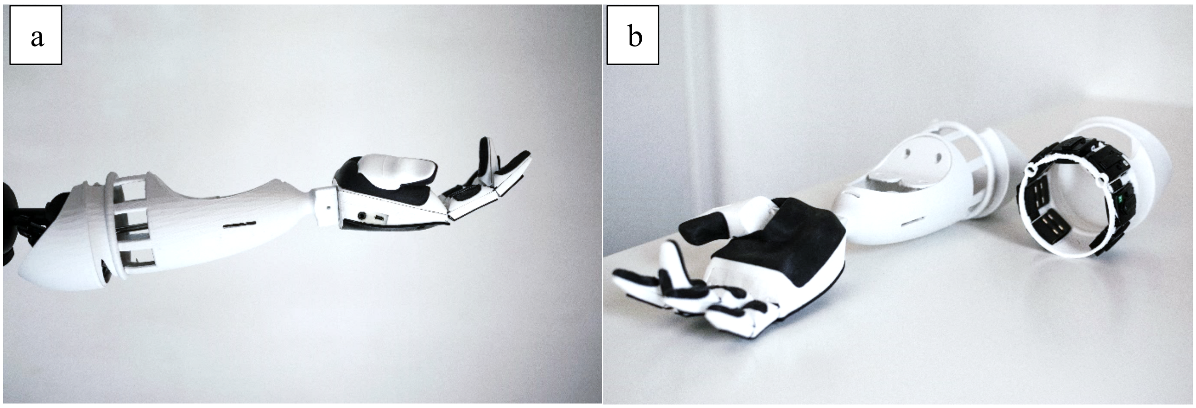

Figure 6:6: Brunel robotic hand (a) and custom-designed socket. The bypass socket (b) is used for able-bodied subjects for data collection and practicality tests.

This work employed two types of EMG datasets to examine the classification performance of six features and five ML models. The first dataset consisted of targeted muscle data collected using seven electrodes. This was the first example, and the complete outcomes are presented in chapters 3 and 5. The second dataset was a novel technique that used seven electrodes along the forearm circumference. The first case was chosen as it is a common approach and has mainly been used in similar research [17], [103], [160]. The second scenario was chosen for practical implementation in order to evaluate if pattern recognition improves differentiation performance while requiring no exact electrode placement. In the experimental setup, seven commercially available Trigno wireless EMG electrodes (Delsys Inc. Boston, USA) were placed around the circumference of the forearm, approximately 5cm distance from the elbow joint. The custom-made housing with electrodes was used for the able-bodied subject to determine the similar condition of amputees. The offline and online evaluation data was collected from an able-bodied subject (male, age 26 yrs.).

The following procedure was used in the first portion of the tests. Before the experiment began, the subject was clearly informed about the objectives of the study. The experimenter recorded trials for model training when the subject had rested and was ready to begin. He manipulated the object as instructed for ten seconds after 3 seconds of rest between each manipulation. In total, the subject repeated each type of grasp and finger manipulations 25 times. In the second part, the subject was asked to determine the initial posture to bring the robotic hand's fingers to the initial position, and then the subject was asked to perform hand manipulations for real-time (online) control of prosthetics. The subject's (able-bodied) arm was inserted into the socket attached to the right arm elbow, as shown in figure 6.6. Each hand manipulation was subjected to a total of 25 real-time tests, equivalent to offline data records.

6.4.2 Data Processing and Feature Selection

Feature extraction is essential to achieve a meaningful set of information that precisely characterise different hand motions in pattern recognition. It is noteworthy, that a variety of feature extraction methods were analysed and presented in chapter 4. In order to obtain the most appropriate feature for this study, a preliminary assessment of different time-domain features in different windowing sizes, was conducted and presented in chapter 5.

Several features could have been used for the real-time control of the prototype. Therefore, the feature with overall high performance and the computationally can easily be applied, is given the first preferences. The overall best-performed feature, root mean square (RMS), was sampled at 2 kHz (0.0005 s sampling period) and bandpass filtered (20-450 Hz) using wireless data transfer method (TCU) from Delsys. The data values were streamed through the data port, and each value contains 4 bytes. The sampling period for each frame is 13.5 ms (0.0135 s). The RMS is accepted to be the most important since it represents the signal's capacity and has been extensively implemented in the field of sEMG based control [235], [248]. The mathematical explanation of all evaluated features is given in Appendix A. The evaluation results and average classification in different comparison conditions such as EMG signals for different electrode placement and various sensors and windowing sizes, are also presented in Appendix C.

Considering one of the main issues in the previous studies, which is to solve the influence of mobility, the EMG data set with different arm postures was trained and tested. It has been suggested that the data set with different scenarios performed better since it includes a more robust approach and tolerates arm mobility [258]. An incremental window analysis approach was used to process EMG signals based on evaluation results and previously reported research. Since each sensor provide 3-axial ACCmmg signals (data of accelerometer), some researchers have also used these data sets as a feature to characterise the hand motion in hand mobility scenarios [211], [213]. For online evaluation, some previous research relied on some high-level features or raw MVC value for each movement; however, this approach was not taken to avoid dimension reduction process by automating signal processing and feature extraction. After correctly labelling the function and obtaining high classification accuracy, system does not need to retrain the classifier for the same user in each operation. Signals will be acquired online, and predictions will be made simultaneously.

6.4.3 Experimental Setups Design

Previous research proposed innovative clinical metrics for evaluating control system performance with virtual systems or by mimicking user performance in a real prosthesis. The virtual reality (VR) system has been used to simulate online manipulation of the prosthesis at various obstruction levels and degrees of freedom. When the classifier predicted the subject's intended move, the virtual human-machine interface was instructed to grab or rest in a custom software interface [26] [252]. The VR system has the substantial advantage of eliminating the need for mechanical implementation and socket design [92], [259]. In some applications, the virtual arms and fingers are intended to move virtual items or order arms into a specific posture [260],[229].

The target achievement control (TAC) test is one of the most often utilised virtual environments for evaluating pattern recognition. Hargrove *et al.* [261], have controlled a virtuall hand prototype using the EMG signal. Similarly Simon *et al.*[260], have used a VR prosthesis to test a myoelectrical control system on a transradial amputee. The test requires the artificial arm to be manipulated within ±5 degrees of the intended posture and a two-second continuing operation time to be considered as successful.

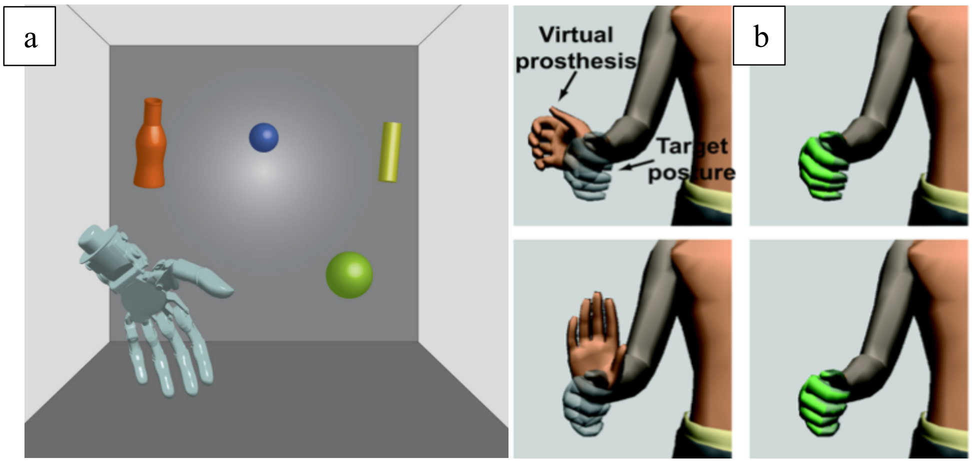

Figure 6:7: The virtual testing and rehabilitation environments; (a) object grasping and manipulation from [26], (b) artificial hand and arm posture control from [260].

Several standardised physical evaluation protocols for prosthesis tests have been devised and adopted. The box and block (B&B) test is the first established method for measuring the performance of the myoelectrical hand [165]. This is the most basic and extensively used test, and it is used specifically for grasping and object handling functional testing. In each round, the user is asked to move as many items as possible from one box to another in 60 seconds, as seen in figure 6.8. (a). The setup only requires limited DoF, focuses on the opening and closing of the prosthesis. The quantity performance metric is the number of blocks transferred successfully [262],[238].

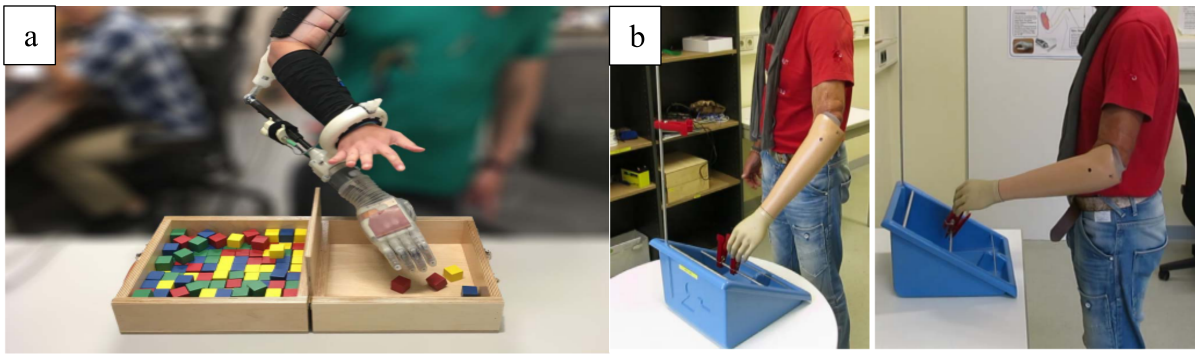

Figure 6:8: Illustrations of (a) box and block test from[165] and (b) clothespin relocation test from[160]

The second most popular test is the clothespin relocation test (CPRT) [263]. A single round test requires users to pick up three pins from a horizontal bar, rotate them, and relocate them in a vertical bar (one at a time), as seen in figure 6.8 (b). The test requires more functionality and DoFs. Such a test has mostly been used in performance evaluation of wrist and fingers, i.e., opening and closing finger and pronation/supination of the wrist. The outcome of the test is the time taken to relocate three pins successfully. The exact evaluation of this test is not limited to a specific time [229],[262].

The bottle/block transfer (BBT) test is the third adopted test established by [103] to evaluate the robustness of the control system while manipulating heavy objects [17]. It requires the prosthesis to move three heavy bottles, 1 L of water (approximately 1 kg) from one location to another, 120 cm distance (see Figure 6.9 (a)). The mission completion time and the number of successfully transferred bottles are the performance outcomes of this test. The modified version of this test is the block turn test. It is a standardised test that requires picking up an object, turning it 90 degrees, and relocating it (see Figure 6.9(b)). The successful completion of a task in a single round in a limited time is the test's outcome metric [103]. The test requires high functionality and arm mobility [262].

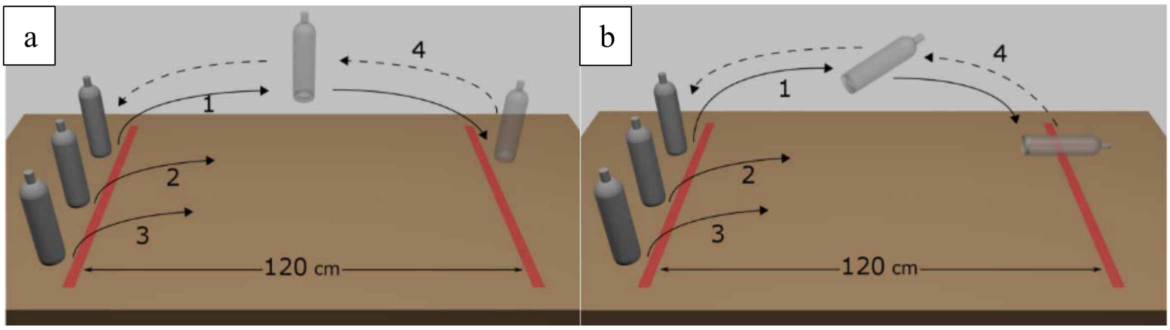

Figure 6:9: The illustration of (a) bottle transfer (b) block (bottle) turn test from [103]

In addition to the assessments mentioned earlier, several more clinical tests and assessments have been conducted with a focus on various purposes and functions. For hand impairment measures, for example, the Southampton hand assessment methodology has been developed. Despite the fact that numerous testing methodologies have been published in the literature, clinical tests are still limited in terms of practicality and functioning assessment.

Aside from the practicality of the VR system, real-time systems offer advantages in that they involve the subject and enable reliable quantity evaluation of performance metrics such as motion completion rate and motion completion time. They also present more realistic settings and a range of limitations. For example, because mechanical and embedded systems require synchronisation of all integrated components, achieving such synchronisation in real-world trials is challenging. Furthermore, because internal and external influences induce significant interferences in the EMG signal, dynamic signal collecting and socket fitting are challenging to maintain.

In this study, the experiments with a real robotic hand and socket were performed immediately after training sessions. The subject was instructed to follow the procedure for each movement on the screen. A multi-degree freedom (DoFs) prosthetic hand that responds to the classifier outputs was connected to the embedded control system [264]. Once the participant performed finger motions, the real-time prediction from the classifier and the motions observed in the robotic hand was recorded until the participant completed the activities. The movement offset was identified as the rest position. Each of six finger motions was randomly presented (on a computer screen), 25 times in each trial for 150 actions. The setup was the same as offline control, but the prosthetic hand outcomes were measured as performance metrics rather than the prediction accuracy of classifiers as presented in [17], [209]. These trials require the robotic hand to mimic the user's finger motion as accurately as possible. The round completion rate and real-time performance were evaluated as outcome measures similar to early literature [160], [169]. Finger motion tests in real-time are presented in figure 6.10.

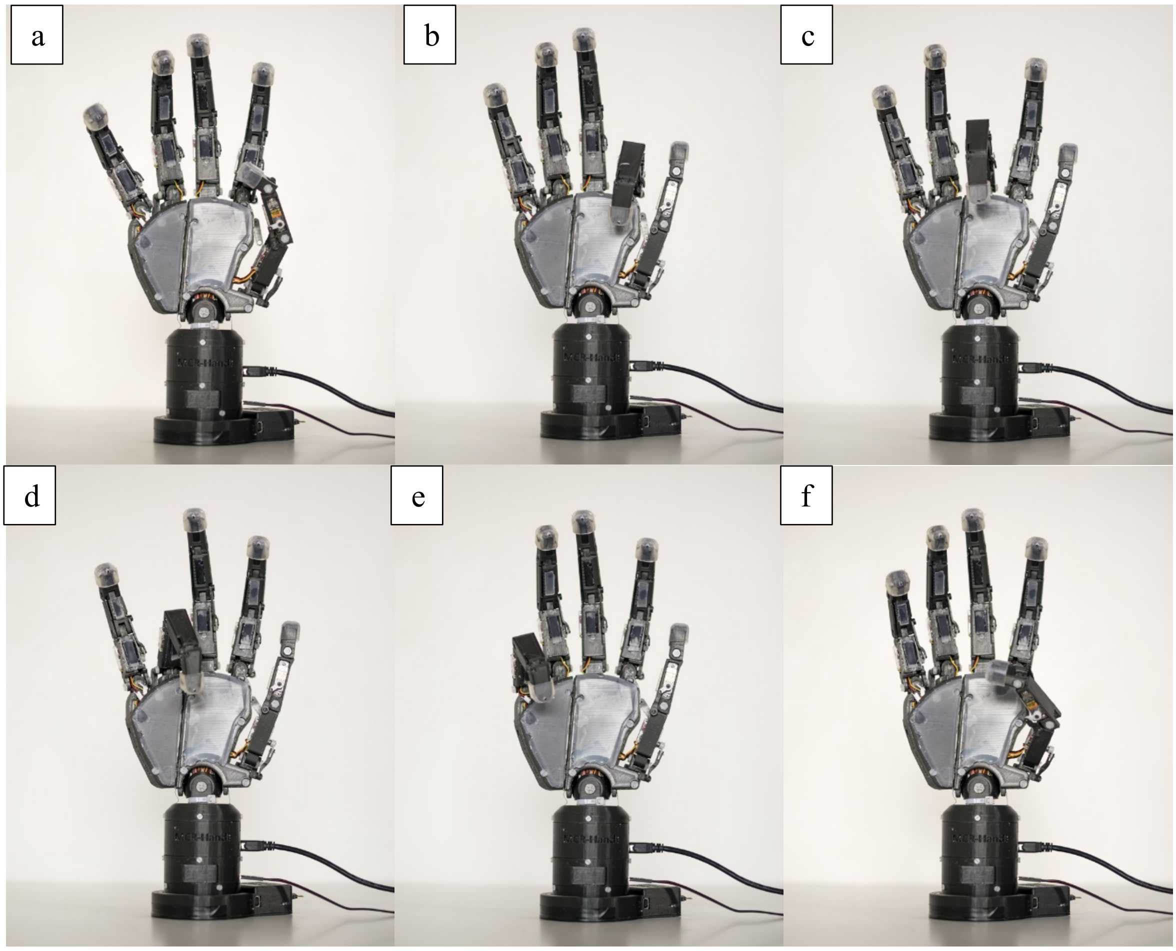

Figure 6:10: Type of finger movement proposed in this study: rest position (a); index flexion (b); middle finger flexion (c); ring flexion (d); little finger flexion (e); thumb flexion (f).

Three online test with varied difficulty levels was used for hand manipulation and object grabbing. The original test called the box and blocks (B&B) [103] is one of the simplest and most commonly used in upper limb prosthesis clinical evaluation. It consists of transferring an object from one location to another, one by one, in a fixed time (usually in one minute). The subject was asked to perform and hold four objects using the proposed control in our modified test. The second test required the participant to control multiple fingers simultaneously 25 times, a total of 100 movements. This test is designed to assess the robustness and continuity of the control when transferring objects. As shown in Figure 6.11, the four most daily used items, representing the four most daily used hand manipulation, were placed on the table. The objects' weight is ignored in the tests as the objects are designed and preferred to be in lightweight materials (see Figure 6.12. The subject was instructed to pick up the object, one at a time, and grasp them for three seconds. The two-performance metrics, including completion rate and average completion time, were determined for each of four grasping actions. This test objectively evaluates the ability to grasp and hold objects in dynamic arm manipulation.

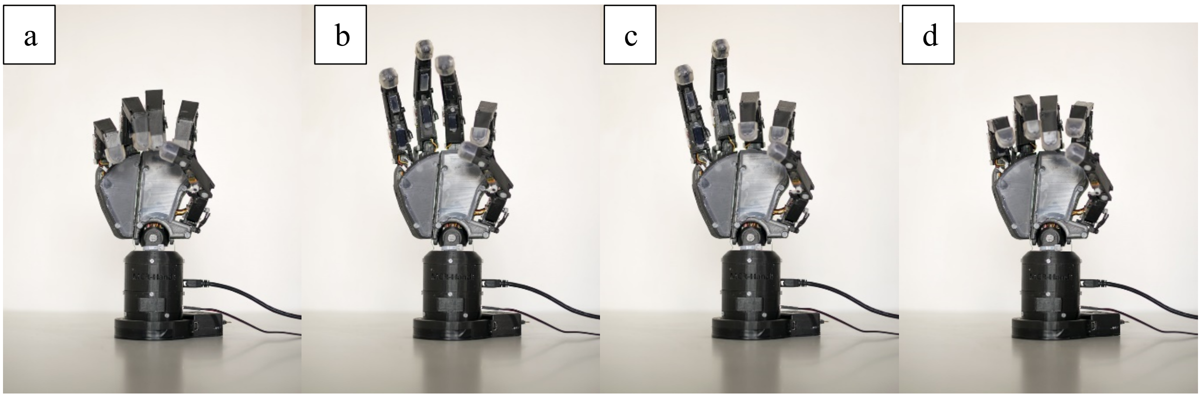

Figure 6:11: Type of object grasping proposed in this study: spherical (a); precision (b); pinch(c); cylinder grasping(d).

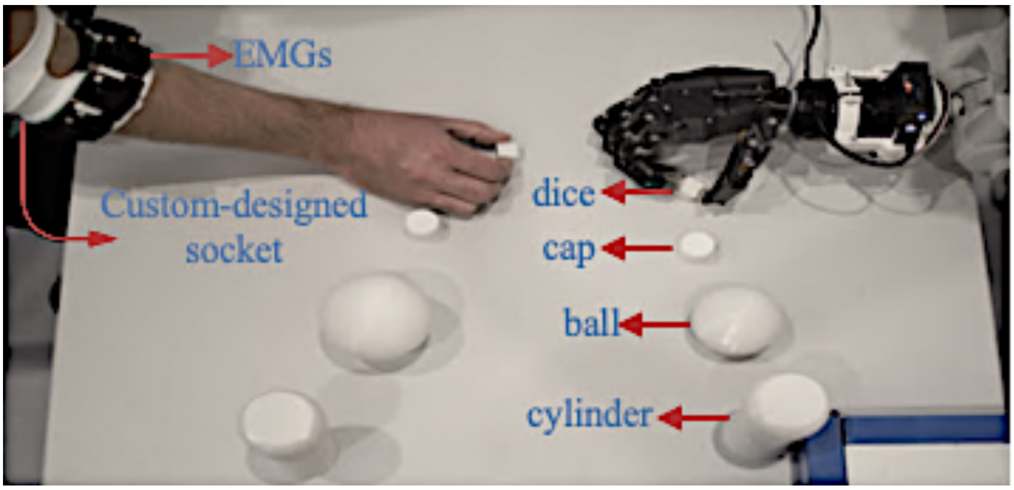

Figure 6:12: Representation of object grasping of the right forearm. The prosthesis was connected to the PC via TCP/IP protocol for recording EMG signals for training and testing.

In addition, for final evaluation, a bottle transfer test was used to test the consistency and continuous control approach (seen in figure 6.13). The most important aspect of this test is that it demonstrates adequate real-time control in various arm postures and path efficiency as presented in [208], [265], [266]. This test could be related to the fact that typical control methods are incapable of producing continuous and efficient control for high-speed systems. Statistically, there is a considerable performance decrease after transitioning from middle to long distances.

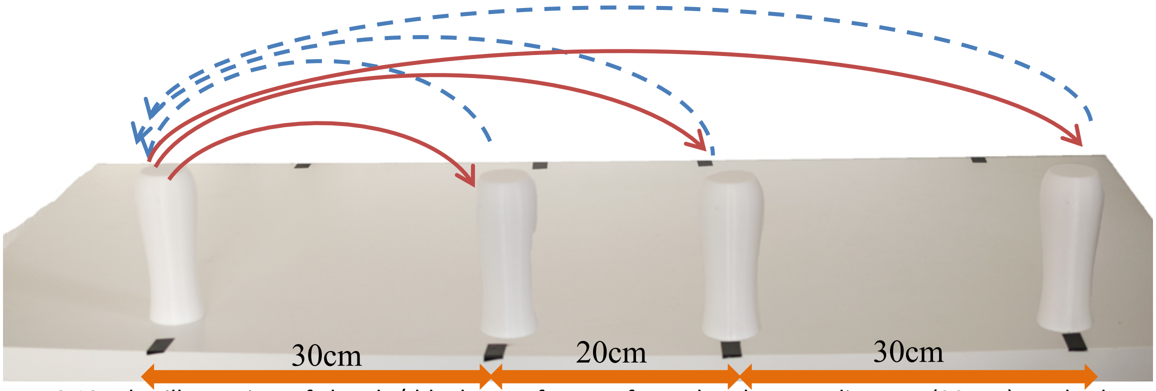

Figure 6:13: The illustration of bottle/ block transfer test from the shortest distance (30 cm) to the longest distance (80 cm)

Before starting the test, the subject was briefed on the concept and outcome of the experiments. The subject was allowed to practice each task as much as was required for familiarisation. After the experiments, each test was subjectively scored with the motion completion rate and mimicking performance over the user performance.

6.4.4 Dynamic Control Method in Real-Time

Myoelectric prostheses operate the actuators based on the user's intended motions predicted by ML algorithms. The motor command signals are delivered based on the highest predicted classes. A filter block in the suggested system was initially employed to derive the relevant part of EMG signals in the defined region (between 20 Hz and 450 Hz) using band-pass filtering to reduce noise and powerline interferences. The process must be fast and accurate in estimating the online EMG signal classes for simultaneous and intuitive control. Therefore, the EMG feature for analysing data and machine learning algorithms should be chosen wisely [267].

Artificial Neural Network (ANN) was used for validation tests because of its practicality and comparatively higher performance in classifying large EMG data than the memory-based SVM classifier. The model was developed and trained using a subset of the retrieved data set (70 %), with the remaining data sets used for testing. To avoid biassed data, overfitting, or underfitting, k-fold cross-validations with (k=10) were used. The k-fold cross-validation method is an iterative technique for evaluating the model's performance with the appropriate data set. The procedure was repeated five times in offline tests (for model training) and average accuracy was claculatead. The optimal parameters then used for real-time control and validation tests. A regression-based approach was employed as an alternative machine learning method to sequence-based algorithms. Details of the regression method and results were presented in section 2.3. This different strategy was adopted to make control architecture more robust and intuitive. This method was introduced and compared to provide simultaneous control in other studies [160], [268].

6.5 Results

In order to evaluate optimal control parameters and gain insight into clinically implementing sEMG based pattern recognition and continuous control of upper prostheses, three real-time performance metrics (motion selection accuracy, motion completion time and reliability) have been introduced and employed by research groups [41], [103], [208]. The myocontrol hand assessment has been broadly divided into two categories, those evaluating system performance based on offline metrics and those based on the online assessment using the virtual system, computer games, or physical tests. With the variety in testing conditions and control algorithms, the offline performance evaluation is mostly made using either classification accuracy or the $R^\wedge 2$ scores, the detail of offline assessment is presented in chapter 4 and chapter 5. However, it has been previously shown that offline results are not offering intuition regarding the feasibility of practical implementations of control methods in real-time [72], [161], [252]. Although algorithms and learning models have achieved peak performance, adapting these models to daily life conditions is not feasible due to various real problems, such as robustness, changes in arm positions, electrode shifting, and skin conditions.

A variety of evaluation metrics have been employed in the literature to examine the performance of prostheses. The model accuracy is the most commonly used model [176], [267], [269], followed by recall [270],[199], precision [19], [223], and accuracy standard deviation per class [271]. These measurements, however, may produce biased results due to two factors: incorrect identification of true positives and unbalanced datasets. Furthermore, because these measures are used to evaluate established algorithms, some of these studies may not be feasible in real-time conditions due to the lack of computational power on prostheses, synchronisation, and processing time. Yanez *et al.* [176] have provided additional analysis on offline metrics.

In order to analyse the theoretical progress in the real environment, it is essential to demonstrate the empirical exploration in the proposed control approach [208], [229], [238]. In the literature, nine real-time evaluation approaches have been offered in [175], [176]. The most popular methods used in clinical tests to determine if prostheses fulfil the minimum acceptable functionality are motion completion rate [260], motion completion time [98], and real-time accuracy [252].

It is critical to evaluate the control architecture in task-related metrics and define statistically significant outcomes to accomplish real-time control. To validate prosthetic outcomes, assessments for the capacity of prostheses test, which evaluates the user's capacity to accomplish a series of tasks and requires physical prosthesis under the control of actual behaviour, were conducted in this section.

6.5.1 Motion Selection Accuracy

The test was devised to assess the efficacy of motion detection capability. It is the proportion of intended movement that is correctly identified in real-time with a prostheses prototype. This accuracy-based metric describes the control system's reliability. It demonstrates how well motor command signals (here represented by myoelectrical signals) can be translated into a correct motion recognition and the control signal for the prosthesis [72]. This performance criterion has been utilised by several researches to assess the capacity of myoelectric control. It provides a qualitative description of the control system, intuitiveness, and motion control while being in use. As a result, the test was used to evaluate the proposed control method and sensory modality reliability. The pre-trained ANN was used with the parameter mentioned above (see section 4.3.4 and 6.4.5) and the RMS feature in a windowing size of 125 ms for the real-time test. Figures 6.14 (a) and 6.14 (b) depict the offline performance of the ANN model over dataset from the able-bodied subject.

(a)

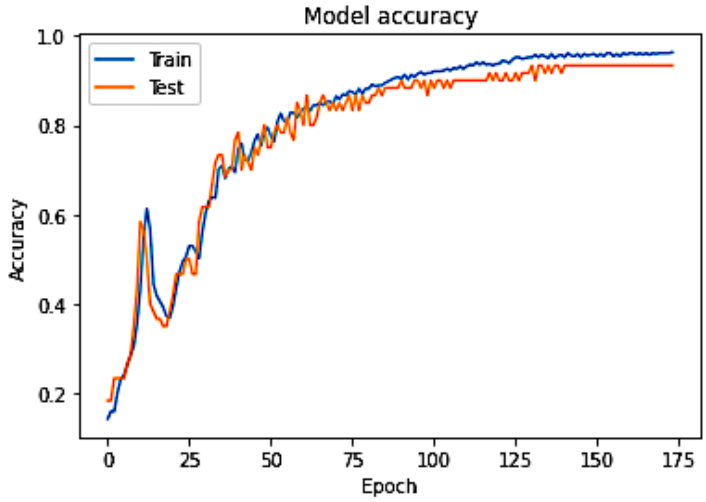

(b)

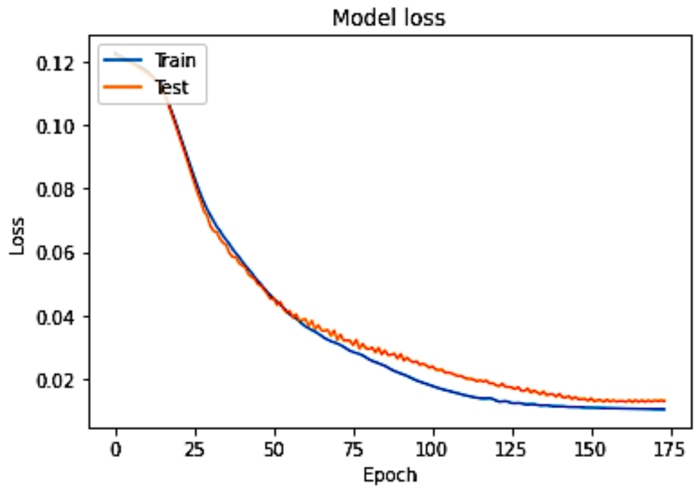

Figure 6:14: The offline performance of the ANN model. The model parameters were used for real-time tests, (a) model accuracy, (b) model loss with 256 iterations.

The accuracy and F1 score derived from true-positive (TP), true-negative (TN), false-positive (FP), and false-negative (FN) have been used to evaluate the classification performance of ML in the literature.

$$\text{Sensitivity}=\text{TP}/(\text{TP}+\text{FN}) \tag{6.1}$$

$$\text{Specifity}=\text{TN}/(\text{TN}+\text{FP}) \tag{6.2}$$

$$\text{Precision}=\text{TP}/(\text{TP}+\text{FP}) \tag{6.3}$$

$$\text{Accuracy}=(\text{Sensitivity}+\text{Specificity})/2 \tag{6.4}$$

$$\text{F1 Score}=\frac{2*\text{Sensitivity}*\text{Precision}}{\text{Sensitivity}+\text{Precision}} \tag{6.5}$$

Confusion matrices were used to quantify the accuracy and F1 score of the ML model on defined datasets. They summarise and visualise classifier precision, and accuracy for each class also provide information about the performance of the models as well as the reliability of parameters. The same evaluation measures have been adopted in the majority of pattern recognition-based prostheses control studies published in the literature, such as [212], [199], [223]. The confusion matrix (shown in Figure 6.15) shows which motion is the most difficult for each evaluation. Notably, it was reported that the subject experienced difficulty when trying to flex the index finger and thumb since thumb flexion predictions were often misclassified as index flexion. The performance of online results obtained during single finger motions is shown in table 6-1. The mean average of pre-collected data is significantly higher than the real-time control performance.

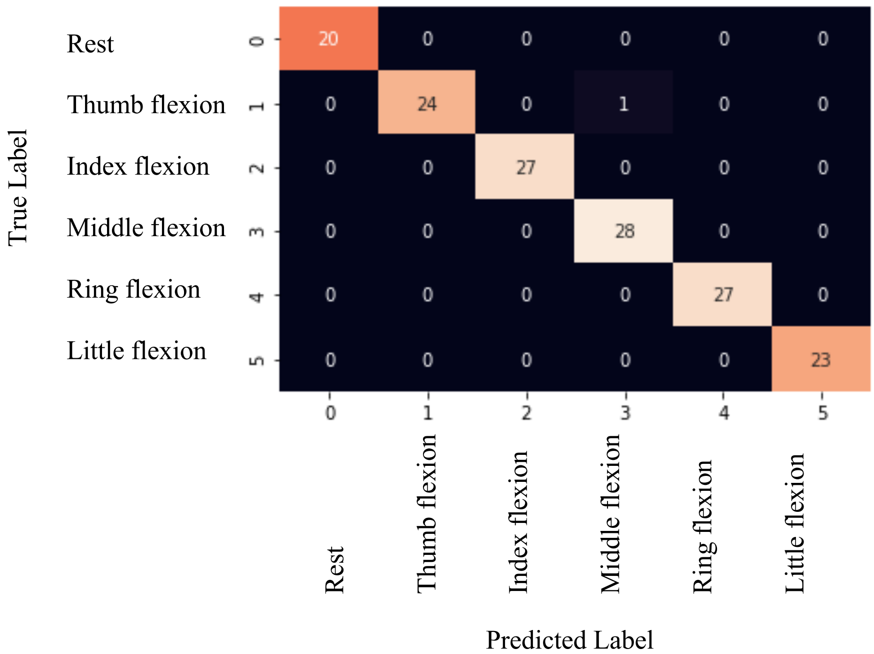

Figure 6:15: The confusion matrix of offline performance for learning model over able-bodied subject while the subject arm is in the table, where each label represents single finger motions. Darker cells indicate the number of incorrect predictions. Each class represents a binary number for practical reasons.

Table 6:1: Performance of Online Tests for Individual Finger Motion Detection

Motions	***Number of Electrodes***	***Motion detection rate (%)***		
		Vertical-Up	Vertical-Down	Horizontal
Rest	7	92	96	92
Thumb Flexion	7	94	92	92
Index Flexion	7	90	88	88
Middle Flexion	7	88	92	92
Ring Flexion	7	90	94	90
Little Flexion	7	94	90	88

In the table, results for single fingers are presented for the online test with the able-bodied participant for three arm postures. The user achieved an average >90% success rate for overall tasks. When comparing the same data and actions with offline accuracy, the table shows that the participant achieved relatively lower success with ~5% differences.

Variations in the user's arm position occur when performing various actions in daily life. The influence is effective on upper limb amputation due to residual muscles that are located in prostheses sockets. A large number of conventional prostheses collect data from the electrodes embedded in the socket. Therefore, these designs lead to displacements on targeted muscles, causes variation in sEMG signals, and affects prostheses' control performance [201]. The implications of different arm positions were presented in chapter 5 for offline tests.

Figure 6.18 demonstrates the average offline performance of data obtained while the user's arm is in a vertical up position. The comparison of Figures 6.16 and 6.17 shows the impact of arm position. High offline performance is generally achieved regardless of the user's arm position from training sessions (e.g., >95% accuracy). However, compared to real-time control performance shown in table 6-1, although a similar trend was observed for all online tests, the performance significantly decreased because non-stationary EMG signals are influenced by arm position.

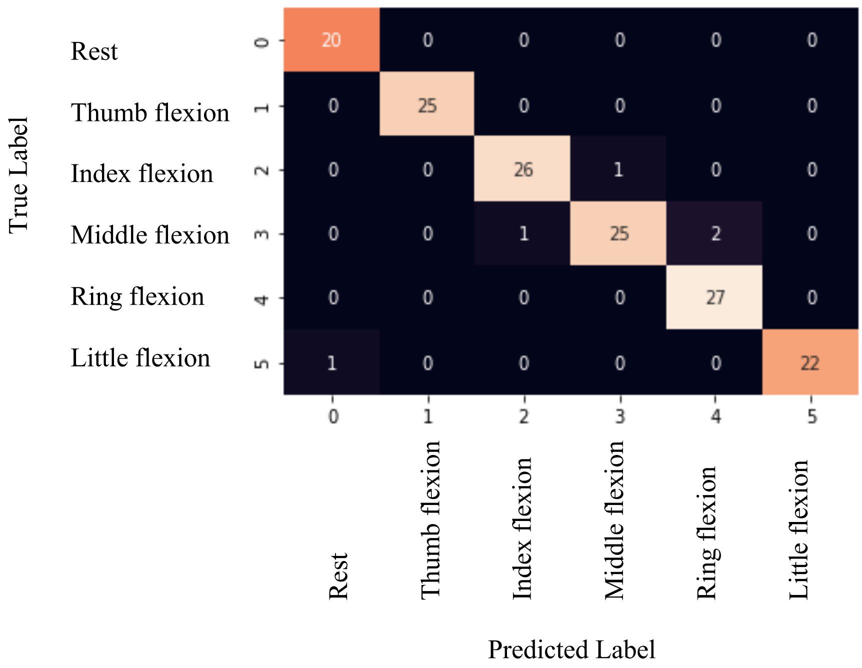

Figure 6:16: The confusion matrix of offline performance for learning model over able-bodied subject while the subject arm is in vertical-up position, where each label represents single finger motions.

The object grasping test was conducted by employing the same machine learning model and parameters. Figure 6.17 shows the performance of the offline model for object grasping tests. In this figure, it was observed that the subject experienced difficulty when trying to perform pinch and precision hand gestures. As shown in the confusion matrix, these two commands were often misclassified with each other. It is a natural result since muscle combinations of these two gestures are very similar and difficult to differentiate. Although collective muscle orientation is expected to perform better, object grasping performance is relatively lower due to arm mobility. For example, the average performance of four patterns for seven electrodes was recorded as 91% (see table 6-2).

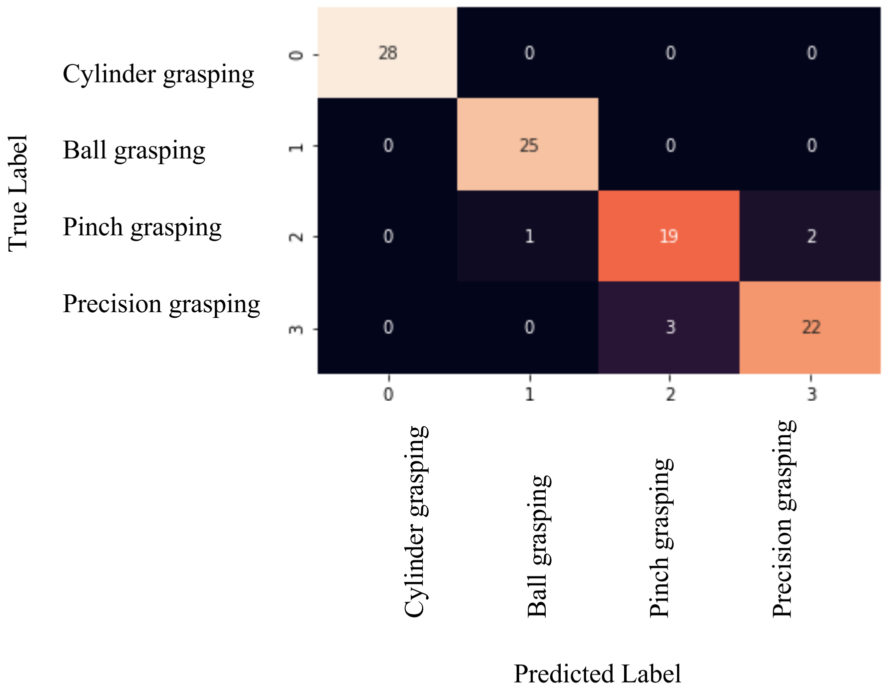

Figure 6:17: Figure 6.17: The confusion matrix of offline performance for learning model over able body subject, where each label represents object grasping; cylinder, spherical, pinch, and precision.

Table 6:2: Performance of Online Test for Object Grasping and Manipulation

Type of motion	***Number of Electrodes***	***Forearm Orientation***	***Motion detection rate (%)***
Cylinder grasping	7	Free	94
Ball grasping	7	Free	92
Pinch grasping	7	Free	88
Precision grasping	7	Free	90

It was found that more accurate control and interaction are possible with longer training time. After several training sessions, misclassification tended to be reduced, and classification performance was improved by ~2%. This could be because the subject can somehow adjust his motions and corrects his sEMG signals. The real-time control experiments also showed that the high misclassification rate occurred in the transition and in the beginning phase of some specific finger motions, such as the thumb's flexion and the index finger's flexion. Commonly, a particular finger will move ahead of another finger, resulting in some crossovers in sEMG samples with the specified window and reduces the classification performance. This may cause a significant problem if a critical and precise execution is required. In order to avoid this problem, a large threshold of sEMG signals can be preferred to improve the quality of training samples.

6.5.2 Motion Completion Performance

This test is established using time metrics to determine the number of successfully completed motions across the entire range of motions in a certain amount of time. It is a test of speed and precision. The time from the beginning to the end of the intended action is used to create the test. If a motion is completed in a reasonable amount of time, it is deemed successful [41], [272]. The tests were designed to show the impact of a variety of variables that influence prosthetics used. The results of this test, for example, demonstrate the control's sensitivity to distinguish between different numbers of motions as well as variations in prosthetic capabilities over time. The test also recommends the system's ability to quantify algorithms on a physical device in a continuous process. In addition, the test was used to determine prototype response time as well as the time delay between user and device.

The experimental results showed that the grasping performance and stability was significantly improved compared to some previous research [165], [189], [190], [259]. Under this combined control method, the prosthetic hand can rapidly grasp objects with 83 % accuracy. It was found that the failure possibility, which was presented as the number of failure times divided by the total transporting times, was considerably reduced. Since the number of successful object transfers is one of the participant's motivations, some object release was observed before reaching the final position. For evaluating the hand functions in daily life, the subject performed the operational tasks several times. Apparently, objects with similar sizes and shapes cannot be differentiated accurately. Nonetheless, dropping possibility is reduced by a long-time training period.

The experimental results for online assessment in the able-bodied subject for bottle/block transfer are shown in table 6-3. The average time to complete the bottle/ block transfer online test for the able-bodied is shown in table 6-3. The time taken to transfer the object was 7±2 s for 30 cm, 8±1 for 50 cm, 10±3 for 80 cm, respectively.

Table 6:3: Precision Results of the Bottle Transfer Test

Distance (cm)	*Time(s)*	*Number of Electrodes*	*Task completion rate (%)*
30	7±2	7	92%
50	8±1	7	82%
80	10±3	7	76%

Pattern recognition requires a sufficiently short time for motion classification and completion with acceptable delay. Strazzulla *et al.* [273] conducted a real-time test and hypothesised that statistical difference occurs between two groups of subjects, naïve and experts. They have achieved a 95.6 % task completion rate in their work and claimed that expert participants completed the task faster than naïve ones. It is suggested that the subject could have performed more adequately with more experience.

Although standard success metrics were used in this study, a comparison with other studies is difficult considering different experimental conditions, equipment, and subjects. Therefore, this study compared results with online TAC, bottle transfer test investigation, and real-time control of five-fingered prostheses [160], [164], [252], [273]. Farrell *et al.* [274] have presented a similar work with online control of object grasping. In that study, the required time for a task is 300 ms and the time given to execute the tasks is 20 s. They have achieved a completion rate of 95 %. In addition to that pattern recognition system in this reseach's combined control architecture, the user has simultaneous control of multi fingers. The learning algorithm provides an additional pattern for individual fingers, which can interfere with other actions such as thumb flexion/ abduction, which mainly engages with common muscles.

The experimental results show that five-finger hand [264], [275], combined with dynamic feature extraction and motion detection, has superiors features regarding dexterity and intuitiveness compared to traditional prosthetics hands [169], [212], [223]. However, due to the robotic hand's surface not being covered with any unique material or fabric, some sliding friction of the contact between fingers and objects is mostly degrading grasping stability.

6.6 Discussion

The real-time validation requires an ML method trained with offline datasets and stores most of the necessary data to repeat pattern recognition, including measurement setups and signal processing methods. Online control provides a continual prediction of desired motions in real-time, which can be used to assess robustness and reliability. Despite the fact that it has been proven to be essential to assess the control system's adaptability genuinely, an assessment of real-time performance is typically deficient in previous studies [252]. As a result, real-time validation tests contains three real-time evaluations that present more realistic assessments of a control method's clinical efficacy. The real-time tests require the participant to perform the instructed actions randomly while analysing the critical success factors listed below.

Selection time is a metric that indicates how long it takes the system to make the first accurate predictions, and it could be used to gauge sensitivity. This study also comprises a time frame for feature extraction, computing time for classification, and motion execution on the prototype. The proportion of required motions that were completed in a specified time is referred to as the *motion completion rate*. *Continuity (robustness);* through trials, it was discovered that the motion completion accuracy and completion time alone is not sufficient to depict the controller's consistency because these two metrics are heavily dependent on algorithms and hardware. As a result, the model prediction performance was also implemented during the motion completion for specificied distances. The tests oucomes are close to reality of real-life conditions. The findings are presented in section 6.4 and discussed in section 6.6.1.

6.6.1 Reliability During the Long-Term Use

The system's reliability with real-time data streaming is one of a key consideration when employing an EMG-based control approach. Standardized motion completion tests were used in this study to assess the control system's long-term reliability. This test was employed because the outcomes of this test are control robustness against a variety of variables such as arm position, changes in sEMG, and system continuity over time. In similar studies [98], [276], the test was used to investigate the clinical resilience and accuracy of pattern recognition on prostheses.

The validation tests were split into two categories based on the sorts of evaluations used in the literature: offline ML metrics and target achievement assessments. Offline measures were used to assess the algorithms competency and compare the results with previous studies. A detailed evaluation of offline and online machine learning-based studies is presented in [98], [112]. According to a research [176], there are three main target achievement tests, and these tests were discovered to be most efficient and been employed in this study. The train and test methodologies differ amongst the researchers, thus, making it difficult to compare the methodology efficiency. Furthermore, given that many publications do not disclose these methods or the entire model structure, one important aspect to evaluate is the importance of the method, repeatability of methodology and average achievements.

During the tests, it was observed that the motion detection accuracy is unreliable over long periods of time (1.5-2 h). Changes in electrode placement, temperature, skin impedance, and some interference between the subject's skin and the electrode, which may interfere with signal quality, are all factors that influence this instability. Even the data acquisition source signal is nonstationary and changes over time. With more sophisticated electrodes and integrated systems, the effects of these variables can be minimised. Furthermore, a self-learning (adaptive model) technique is required for reliable, robust control applications.

The presented control system and robotic hand had no sensory feedback/ sense of touch. Therefore, it was challenging to determine whether the object and robotic hand made contact and the proportion of force applied. Furthermore, the velocity and acceleration profile of the reach and grasp trials were not adequately coordinated with the wrist and shoulder in a synergetic manner since the participant was an able-bodied subject. Although it was not possible to determine how amputees' muscles are preshaped, Hargrove *et al*. [276] have assessed the effect of amputation level and have proposed that a comparable pattern of muscles is presented during reach and grip activities. Similarly, Batzianoulis *et al.* [97], have tested the system performance with eight able-bodied participants and four transradial amputees using three different pattern recognition methods (LDA, SVM and NN). Their findings indicated that there is no significant motion detection differences (only 6%) but device response time. Daley *et al.*[105], have also compared the classification performance between able-bodied subjects and amputees and have claimed that although there is a classification accuracy difference between participants, the classification accuracy obtained from amputee subjects was not significantly affected by the number of electrodes and distribution of electrodes. Young *et al.* [97] have pointed out that the reach and grasp motion is dynamic progress that has a negative impact on the classification performance during the natural coordination of motion. This studies' results complement the approach that the focus is on timing.

In real-time evaluation, it was intended to reduce the time for data processing which cause lower classification performance and leads to a slower device response. Although the combined embedded system is customised to perform specific tasks in real-time, the control architecture was designed mainly to reduce cost and size and enhance prosthesis performance. The total response time for commanding the device is 0.23s, including EMG signal processing, motion recognition with multilayer neural network by the backpropagation algorithm, and commanding the end effector. The proportion of correct predictions is consistent with research highlighting the potential benefits of dynamic data acquisition [209],[277].

Many errors occurring after a certain time implies that the identification rate in the early stages of the movement is very high. Furthermore, some misclassification noticed immediately after or before such motion may be induced by the signal transfer from one label to its successor. On the other hand, significant accuracy degradation was not recorded during the slight signal and arm position changes, which makes it relatively robust and stable.

6.6.2 Limb Posture and Electrode Shifting Effects

In the light of the observed limitation of commercial sEMG based control (such as signal cross-talk, electrode displacement during activities, and changes in muscle synergy), numerous invasive data collection strategies have been devised [66]. Implantable myoelectrical sensors, for example, have recently been used to provide reliable myoelectrical signals. Furthermore, sophisticated pattern recognition and machine learning algorithms have been used to improve the myoelectric prosthesis's robustness, adaptability, and HMI. Overall, the literature revealed that by increasing the datasets with varying hand posture and processing capability of sEMG, the existing barriers to clinical employment might be overcome.

It has been indicated that the singal changes during real-time test due to arm mobility contributes a significant degradation in model performance and repetability. Hargrove et al. [98] have highlighted the performance degradation caused by electrode shifting and sensory modality but indicated that this influence might be reduced by using dynamic arm position during model training. Similar findings have been reported by Fougner *et al.*[236] in relation to changes in residual arm position. Since then, various researchers have emphasised that training a pattern recognition algorithm with dynamic arm positioning helps significantly improve the control scheme's robustness.

To improve prosthetic performance and minimize the associated issues, the system was tested using modified sensory modality with an embedded socket which eliminate arm position variations. An able-bodied subject used myoelectrical pattern recognition with real-time metrics to control a robotic hand in the standardised box/block (B&B) transfer and object grasping tasks. The subject performed the tests with dynamic arm conditions, which causes the muscle alignment to shift dramatically as the arm moves. The results of these complex tests demonstrated that the control algorithms could achieve high prediction accuracy without substantial delay even with dynamic arm postures.

Using human motor control as inspiration, investigated motion detection performance in relation to average muscle activity between different arm orientations led in generalisation over the variability of the EMG data, yielding the classification accuracy. Tables 6-1 shows the outcomes of various arm postures and motion detection rates. There was a substantial link between accuracy groups. Extreme arm postures with mechanical load, on the other hand, were shown to pollute EMG signals and drastically reduce classification accuracy (by 14 %). In comparison to some early investigations [86],[100], the findings show that the novel electrode orientation strategy eliminates the problem of electrode shifting and arm orientation during motion detection.

However, the key challenge with this technology is providing a dependable and adaptable socket for variations in user weight and age. The research indicates that the sensory array appears to be more resistant to limb postures and environmental variables compared to early studies[97], [104]. Although the electrode array and socket design allow the user to conduct a variety of natural motions, the socket, in the user's experience, marginally inhibits the complete extension of the elbow. However, it was not observed to be a barrier to task completion. The new sensory array and electrode location were developed to lower prostheses' cost and enhance practicality and comfort.

6.7 Summary

The practicality of employing the proposed electrode array with simultaneous feature extraction and motion prediction in compact online testing was presented in this chapter. The tests were conducted on the able-bodied subject in some standardised experimental conditions. In order to evaluate the control method in real-time, ANN regression and RMS signal features at 125 ms windowing size with 65 ms overlap were employed. The results showed that it is possible to detect the individual finger and grasping intention accurately. Due to the great accuracy of the motion detection techniques, the ML model and integrated feature extraction approach were validated on a custom-designed socket to test prosthetic devices. The control approach was assessed using a high functional five-fingered robotic hand. These experiments show that this combination of feature selection, number of sensors, and ML model may outperform studies using a greater number of sensors in terms of accuracy and dexterity [97], [223], [212]. The results were compared and proven with some early research to demonstrate the influence of sensor quantity and optimal performance in terms of computational cost and accuracy [92], [278].

Simultaneous and proportionate control of a high degree of freedom is also a major priority in clinical test and device acceptancy, according to some studies [209], [279]. A regression-based real-time control was employed to allow the user to control hand motions without having to use an external switcher to switch between components and motions. Even with non-invasive electrode placement, control became more intuitive and robust as processing performance and accuracy were improved. The implementation of a robust technique with embedded data processing and pattern recognition increased the speed of device response, functionality, and user satisfaction. This could be a feasible alternative to the traditional technique, which embeds electrodes into the prosthesis and uses limited sensors to monitor specified muscles.

One of the main goals of the researchers is to create a hardware and software synchronisation to provide amputees with high dexterity and intuitiveness for prostheses. The embedded dynamic control maps hand synergies and eliminates disturbances such as electrode shifting, limp position, and delays, resulting in robust control of the entire work area and allowing more natural behaviour in the face of unpredictable events.

Chapter 7 Conclusion and Future Works

7.1 Conclusion

This study evaluates the most popular machine learning methods, time-domain features, and different muscle investigations to predict user intention from sEMG signals determined from healthy subjects. It presents an approach to enhance the motion detention performance, computation time and robustness through a systematic evaluation of the pattern recognition system. The proposed control architecture provides potential engineering tools and indicates how to choose the most appropriate classifiers, specific parameters for prosthetic control based on implementation and observed outcomes.

According to the findings of the study, the machine learning-based controller with new sensory modality and embedded control system has a high capability of correctly predicting desired hand motion patterns (92%) accuracy. The sEMG-based control architecture performed a smoother and more natural motion pattern in real-time than standard on/off or sequence-based techniques. These findings suggested that a biologically inspired control strategy might provide considerable advantages in operating multifunctional prostheses by increasing the degree of freedom and classification confidence.

The combination of ML models and feature extraction approaches has been used in the literature with several electrodes to identify multiple classes. Although their immediate results have been reported as successful, the robustness of the suggested systems across sessions without retraining was not evaluated, and a considerable percentage of their motions were dependent on arm and wrist motions (pronation and supination). Thus, because a high degree of freedom and motion independence is necessary in daily living activities, they make the control technique less convenient for prosthesis. In addition having session independence in this study, which makes the system more suitable for amputees' daily usage, the control architecture is more tolerant to wrist rotation and arm mobility, allowing high-precision manipulation of four fingers and the thumb, providing a human-like behaviour to prosthesis.

To address the study problem of robustness and capability to continue to operate despite numerous interferences such as electrode shifting, force fluctuations, and limb posture changes, a regression approach was taken in real-time control. This enabled to maintain continuous control while reducing the impact of variables that impede reliability. A live pipeline between input (EMG signal) to output (robot actions) was employed to improved human-machine interface.

Considering the effect of shifting the arm position in the block transfer test, the integrated data collecting and prediction system demonstrated significant robustness with a low frequency of dropping/failing the objects. Throughout five repetitions of each session, the system continued to provide real-time data within 0.23 seconds. Even with extremely identical movements, the user did not experience a significant performance degradation. It was not possible to investigate if the model can remain stable over a longer period of time (e.g., months) using the same classification model. However, if necessary, the model may be retrained in less than 7 minutes using the new user-friendly electrode modality.

The classification of the myoelectric signal has been recovered using discrete signal decoding from wrist and elbow motions with a restricted degree of freedom in the majority of studies in the literature. However, this research employed a control mechanism that decoded individual finger movements. This considerably increased the intuitiveness and natural control of prosthesis. This strategy allowed differentiating additional tasks and performing them with a high degree of independence. Furthermore, the continuous control allows shifting between the different ranges of motion without triggers or a sequential control strategy.

Then results suggest that by using standard ML methods (LDA, k-NN, SVM, ANN) with optimal parameter and kernels, the created data sets and methodology are competable, as well as motion detection rates are comparable to those found in the literature under similar conditions, i.e., the same number of motions, number of electrodes, and electrode location. The high accuracy of online tests verifies the electrode distribution, data collecting, experimental methodology with the novel socket design, and integrated data transfer/prediction approach. The findings clearly show that the system is highly reliable, since the repetition of the tests has no significant effect on the prediction accuracy rate.

There is a substantial amount of research in the computational field for prosthesis development to enhance the interface for signal acquisition, data processing, and control/learning algorithms to achieve a smarter prostheses and meet user demands. In this study, a control method with a functional socket and a combined data acquisition, in which signal processing (live data pipeline) and motion prediction work together to optimise motion detection in appropriate time was developed. It is a big step toward developing an ideal and affordable prosthetic capable of restoring lost human hand functions. The online block transfer experiments demonstrated that the suggested control mechanism allows users to move items over a wide range of distances in stable manner. In real-time tests, it also offers the gripping of daily living items with high precision (about 88%).

The summary of the key contributions and the novelties of this study are thereof included:

1. Demonstrating that the generic approach with machine learning algorithms and feature extraction methods yielded the best prediction accuracy when using the proposed sensory modality and embedded control system.
2. Controlling a high degree of freedom prosthetic hand solely using sEMG data from upper limb muscles in real-time.
3. Creating a live pipeline between components to deliver real-time data (0.23 sec) and continuously producing human-like behaviour for prostheses with good accuracy (94%).
4. Developing and testing a potential low-cost multifunctional prosthesis control with novel sensory distribution and wearable socket.

7.2 Research Limitation and Area of Improvements

1. The majority of recent studies have evaluated prosthetic performance on intact subjects and assumed that the findings apply equally to amputees [22]. Peerdeman *et al.* [188] conducted a systematic literature review and concluded that the majority of studies only conducted experiments on able-bodied subjects due to the difficulty of recruiting amputated subjects. Previous research has shown that control accuracy for amputees is comparable to that of able-bodied people, if not slightly lower and more unstable [189],[190]. It has been hypothesised that amputees suffer to obtain high accuracy and execute activities on time [191]. It is unclear if this is due to a lack of sensation or a lack of motor control. In [192], Al-Timeny *et al.* collected sEMG data from ten able-bodied and six below-elbow amputees. They achieved 98 % accuracy for able-bodied subjects and 90% accuracy for amputee subjects. It was discovered that the time required to execute activities for intact people increases when the tasks get more complex, from a single finger to combined actions. Furthermore, it has been identified that a small proportion of users who have relatively more active residual muscles have full control experience and successfully deployed the control method with an average of 93.5% in [259]. On the other hand, Atzori *et al.* [191] have conducted experiments with five amputated and 40 intact subjects and have achieved 61.14% with amputee subjects. The literature comparisons have shown that the pattern recognition performance shows significant variety for amputees subject due to some considerable underlying motor control

problems. Therefore, this research can be further improved by undertaking a large number of amputees testing the optimised socket design.

2. Another area that can be invstigated further is close sensory feedback, particularly because it effects the experimental results by obscuring whether or not contact with the object is established. This reseach suggest that the major source of instability was due to lack of sensory/tactile feedback and unresolved friction problem between objects and the robotic hand. As a result, the next goal of this study is investigating innovative smart sensory feedback and materials since it is suggested a sensory feedback will lead to physiological correction and exact relocation of residual muscles.
3. In this study, a bypass socket that holds seven electrodes in an array was designed and tested since the new methodology provides flexibility by alternative data acquisition, requires less maintenance and is more easily wearable than bulky EMG sensors and sockets that are also prone to sweating and electrode shifting. The system was tested on able-bodied people as a first step, but it still has to be improved before it can be tested on amputees. The addition of a wrist rotation function between hand and arm might broaden this method to address the challenge of a large degree of freedom.
4. Furthermore, synchronisation of components such as EMG sensors and the controller is crucial for accurate manipulation. To accomplish effective real-time control, the prototype's servo execution and data processing times must be ideal. Furthermore, the force generated by the robotic hand, particularly while grabbing an object, must be available to prevent the object falling problem. A suitable fingertip force might improve the accuracy of the item grabbing and also block/transfer tests. For example, the digital servo used in our studies has a modest speed (0.3 sec/180 deg at 4.8 V), therefore it takes longer to complete the whole cycle before it receives the new command.
5. A modification of the socket prototype using lighter and more durable materials might lower system weight and enhance the weight-bearing test, which is one of the most common causes for prosthesis rejection. Even though it is outside the scope of this study, optimising the prototype with enough material would be a significant step forward. The long-term goal of this research is to further develop this combination electrode array and socket into a commercially marketable prosthesis.

6. Although data from healthy participants is critical for evaluating devices in this field, a large amputee participant pool might indicate more clearly what is required to build human-level prostheses. Further system testing with broad participant groups would allow enhancements and verify the general applicability of such approaches for completely validation of EMG-based prosthetic hand for daily usage. Possibly a subject pool with more variety, such as diverse ages, sexes, ethnicity, and capacity would be an ideal bublicly open dataset.
7. To avoid the non-stationary surface EMGs and the aforementioned environmental variation issues, implementing a self-learning/ reinforcement learning control strategy that capables of mimicking muscle memory as a result of repetitive tasks would provide a continuous and robust approach to performing output control. Furthermore, in the next phase of this research, the enhancement of the adaptable socket for transradial amputees to elaborate the feasibility of making this device portable for clinical trials and assessment in daily living activities, as well as future industrial exploitation is planed.

7.3 Possible Application Areas of this Research

1. The findings of this study point to the possibility of developing an intuitively operated upper-limb prosthesis. This was confirmed by controlling a prototype with real-time EMG signals transmitted from able-bodied people while performing hand and finger motions. These findings could have ramifications for the technique's robustness, which allows users to control the device effectively in various arm postures with high prediction performance.
2. The findings of this study could be applied to the development of a sensory feedback-controlled prosthesis, in which sEMG signals provide continuous real-time data, and sensory feedback improves object gripping ability. This might be utilised to improve user sensation and natural control of prosthesis by better correcting user movement at appropriate times. A human operator may use the haptic user interface, such as stiffness, to control the robotic hand and provide robot-object contact force to the operator.
3. According to the findings of this study, the integrated real-time system can be successfully applied to a variety of use cases, e.g., in teleoperation,virtual reality and and robotic surgery. The validation results back up the idea that prehensile patterns can be detected with the help of a collaborative mechanical and control system. This

could be useful in rehabilitation centres for therapeutic ways to stimulate paralysed users' hand functions.

4. Some manual procedures performed during and after surgery, such as suturing, sewing up open wounds, and incisions, take time. Furthermore, the surgeon's fatigue may lead to severe consequences for some delicate operations. The automation of surgical procedures has the potential to lower costs while also addressing the lack of surgeons in operating rooms. As a result, the proposed pattern recognition and the intuitive device can assist in mitigating preventable errors. They can be employed as a powerful tool for optimising surgical efficiency and minimising human errors.
5. While humans can efficiently conduct handover activities, there are various challenges when attempting to perform particular human-robot interaction (HRI) tasks using commercial robotic systems. In robotics, intuitive object manipulation, particularly collaboration with humans, is a hot topic. This research demonstrates that it is possible to design an intelligent strategy for natural and intuitive human-robot interaction, precisely grasping and object manipulation. The emphasis of such an approach might be an intuitive tool in the operating room, manufacturing line, or harsh environment of chemical/nuclear plants.
6. The control strategy, signal processing, and motion detection technique used in this study demonstrate the concept of a stable upper-limb prosthesis. Because it improves adaptability to non-stationary and time-dependent signals, the embedded system could be used in clinics with implanted neuroprostheses that connect the Brain-Computer Interfaces (BCIs) system.

7.4 Publications of Research

1. Balandiz, K., Ren, L., Wei, G., (2021). *Motor Learning-Based Real-Time Control for Dexterous Manipulation of Prosthetic Hands* (IEEE Transactions on Neural Systems and Rehabilitation Engineering). Manuscript submitted for publication.
2. Balandiz, K., Ren, L., Wei, G., *Towards Dexterous Manipulation through Motor Learning and Biomechanical Modelling.* (Manuscript in preparation)

Appendices

Appendix A: Delsys Trigno Wireless System

The specification of the Delsys Trigno system and EMGworks software are presented in this appendix. The sensors detailed in this section are used throughout this research. The user's guide, calibration and user interface were extracted is available from [280].

Trigno Avanti Sensors

- *1x EMG, up to 6X IMU (sensor channel)*
- *27x37x13 mm (size)*
- *14 g (mass)*
- *4-8 hours (battery life)*
- *40 m in radio frequency (rf) mode (operating range)*
- *20-450 Hz (EMG Bandwidths)*
- *4370 sa/sec (EMG sampling rate, max)*
- *16 bits (sensor resolution)*
- *750 nV (EMG baseline noise)*
- *11mV/22mV rti (EMG input range)*

Trigno Quattro Sensor

- *4x EMG, up to 6x IMU (sensor channel)*
- *25x12x7 mm (size)*
- *25 g (mass)*
- *2222 sa/sec (sampling rate)*

EMGworks

- *Software Development Kit (SDK)*
- *Application Programming Interface (API)*
- *Real-time synchronisation*
- *Compatible with Python, C#, Unity*

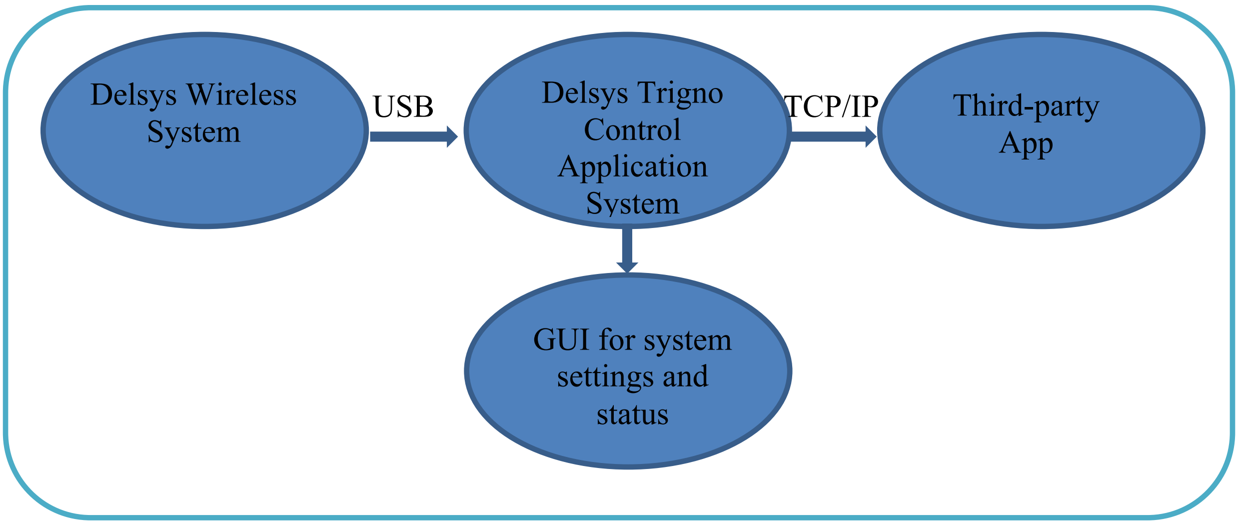

Figure A:0:1: Illustration of data flow and SDK system.

Appendix B: Mathematical Definitions of sEMG Features

In order to remove the artefacts, muscular signals were bandpass filtered and in the range of 20 Hz to 450 Hz using 4th order Butterworth filter. The features were extracted from sEMG signals by employing sliding windows. The following eight-time domain features were extracted from each sEMG signals. It is recommended that the feature sets yield the classification performance and lead differences between very similar motion detection problems or datasets [102]. The theory of filters and specification ranges have been obtained from [194] for the essential digitising process. The filter results are presented in Figure xx to conclude which filters accurately describe the behaviour of sEMG signals.

Mean Absolute Value (MAV) is one the most popular feature extraction methods used in sEMG analysis for prostheses control. It is the average of the absolute value of the EMG amplitude over a specified segment [149]. The EMG signals from every electode can be depicted as a finite time series (X_1, X_2, X_3 …..X_N), where N is the number of specimens examined in the window.

$$MAV = \frac{1}{N}\sum_{i=1}^{N} |x_i|$$

Root Mean Square (RMS) is a derived model of Gaussian random process, which is regarding constant force and non-fatigued contraction[216]. The RMS value of a signal is derived as the square root of the signal's average squared value. It defines a continuous waveform; as the specified window passes the waveform, it sums up each amplitude's square and divides by the frame length.

$$RMS = \sqrt{\frac{1}{N}\sum_{i=1}^{N} x_i^2}$$

Integrated Absolute Value (IAV) is an integrated absolute value of summation of EMG signal in a specified time window of N samples [35].

$$IAV = \sum_{\mathrm{i}=1}^{\mathrm{N}} |\mathrm{x_i}|$$

Waveform Length (W.L.) is the measure of the complexity of sEMG signals[149]. It indicates the cumulative length of a signal wave over the segmented time. The WL calculation's derived values represent a measurement of the waveform's intensity, frequency, and length of time.

$$WL = \sum_{i=1}^{N-1} |x_{n+1} - x_i|$$

Simple Square Integral (SSI) uses the energy of sEMG as a feature. It is the summation of square values of signal amplitude. It commonly employed as an energy index. To avoid noise in the EMG signal, the number of changes between positive and negative gradients between three successive sections is calculated using the threshold function.

$$SSI = \sum_{\mathrm{i}=1}^{\mathrm{N}} |\mathrm{x_i}|^2$$

Average Amplitude Change (AAC) is equivalent to the W.L. feature with averaged wavelength [100]. The time-domain properties can be approximated using AAC.

$$AAC = \frac{1}{\mathrm{N}} \sum_{\mathrm{i}=1}^{\mathrm{N}} |\mathrm{x_{i+1}} - \mathrm{x_i}|$$

Kurtosis (Kurt) is a statistical analysis to characterise the variability of a dataset. It measures if the data is heavy-tailed or light-tailed according to normal distribution. It is a method commonly used for the measurement of symmetric/ periodic signals [281]. It compares the shape of the statistical distribution over the normal distribution. Where $\bar{Y}$ is the mean, s is the standard deviation, Y_i is current specimens and the N is the number of the points.

$$kurt_{EMG} = \frac{\sum_{i=1}^{N} (Y_i - \overline{Y})^4 / N}{s^2}$$

Peak Activation Level (Maximum amplitude) shows the sequence of the time when sEMG is most active. The average peak exceeding the RMS value is calculated. The process analyses and compares each sample to determine the one with greater amplitude.

$$PEK = \frac{||\mathrm{x}||}{\sqrt{\frac{1}{\mathrm{N}} \sum_{\mathrm{i}=1}^{N} {x_i}^2}}$$

Appendix C: EMG Data Classification Performance

Various methods for handling sEMG signals before feature extraction and preprocessing were used to enhance the prediction accuracy and response time of the real-time controller. Initially, the datasets were segmented from raw sEMG signals. sEMG signals were divided by varying windows, then filtered and rectified as feature sets. The five most popular classifiers were employed, and human hand motions were differentiated in sequences. It has been pointed out that the feature sets have a significant influence on classification error [46]. A statement by Farina and Jiang proved that the classification performance degrades by using small segment length (less than 125 ms), which differs from classifier to classifier, cause high bias on features [153]. Studies show that the accuracy increases when windowing length increases from 125 ms to 500 ms due to large windowing size provides additional meaningful information corresponding to human actions. However, a large windowing size causes a certain processing delay and can not be implemented to operate the real-time application. It has been suggested that the response time should be less than 300 ms in order to achieve real-time control for prostheses [143]. To overcome drawbacks associated with segment length and classification methods, we compared the performance of classifiers for various windowing length and feature extraction methods in the figures below.

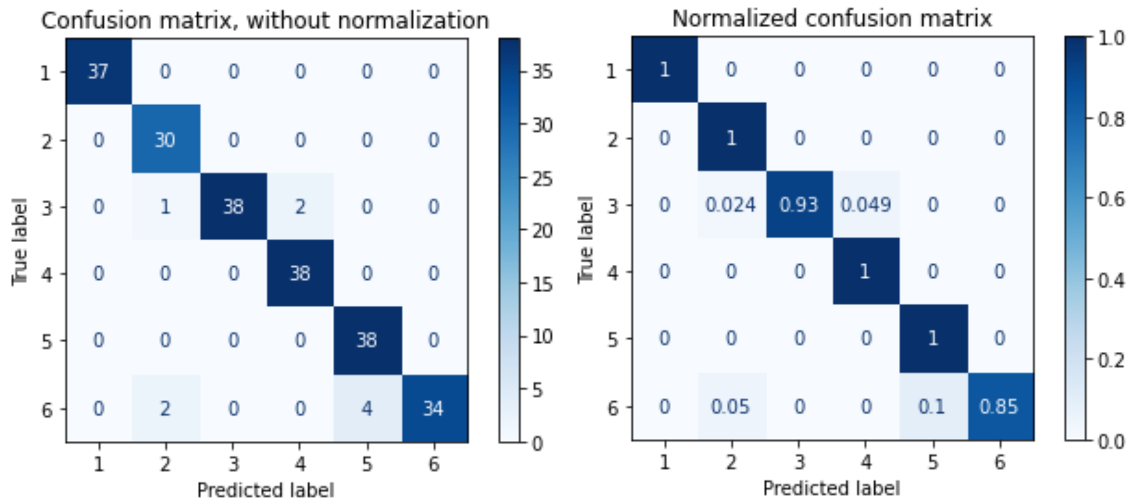

Figure C:0:1: The performance of SVM classifier in 125 ms window for RMS feature.

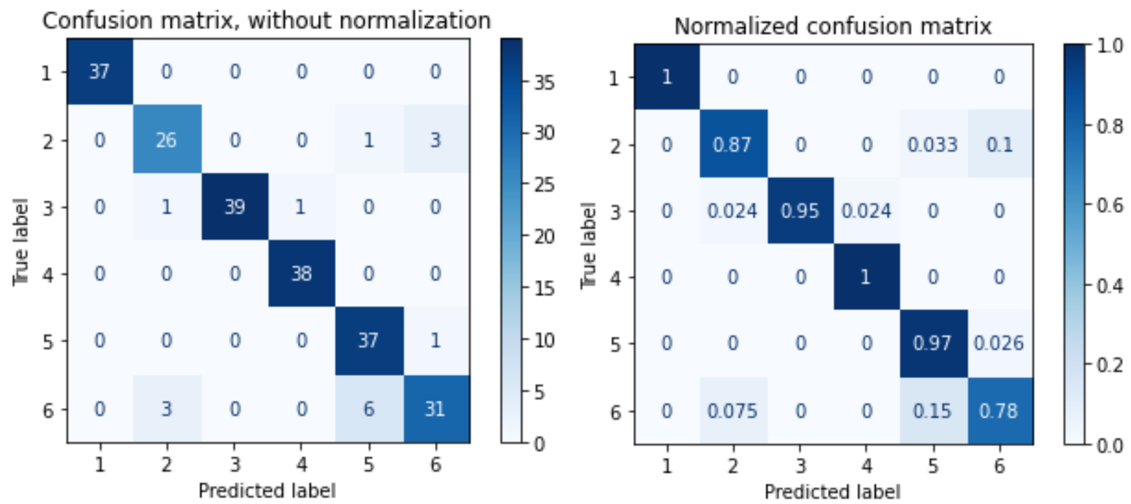

Figure C:0:2: The performance of SVM classifier in 125 ms window for MAV feature.

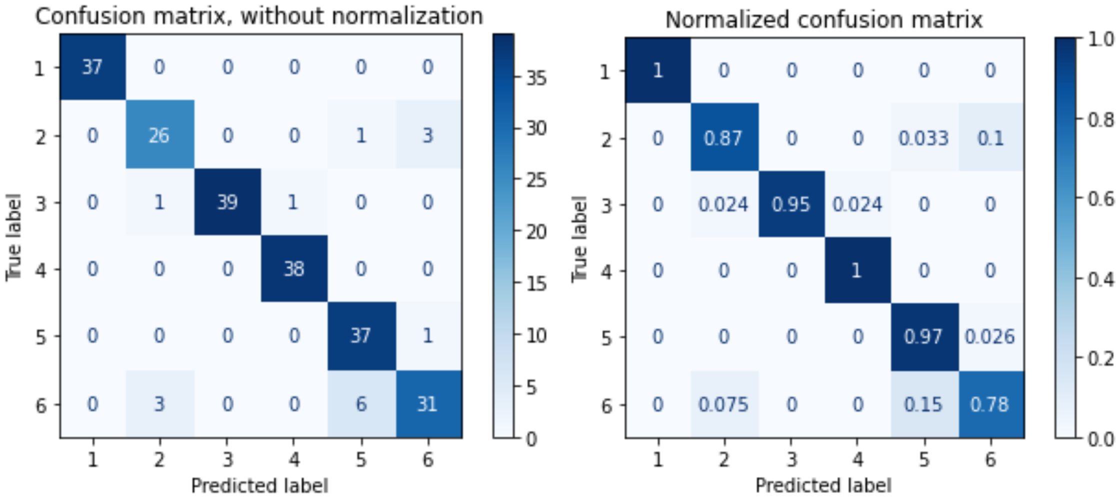

Figure C:0:3: The performance of SVM classifier in 125 ms window for IAV feature.

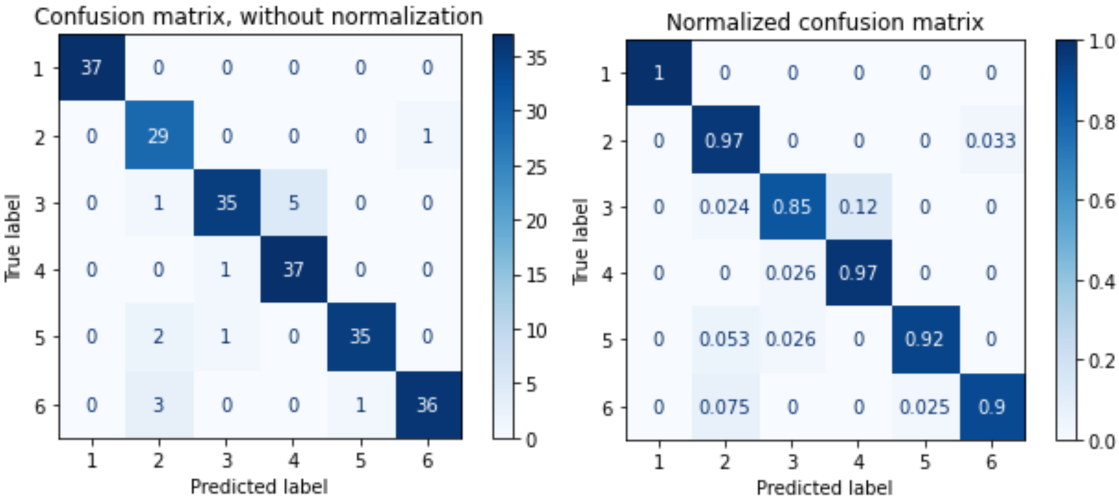

Figure C:0:4: The performance of SVM classifier in 125 ms window for WL feature.

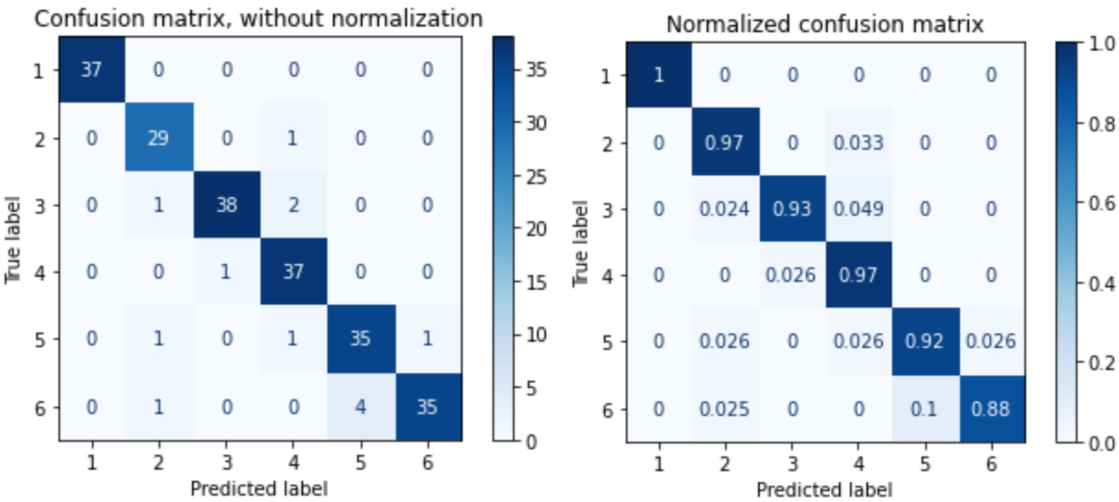

Figure C:0:5: The performance of SVM classifier in 125 ms window for SSI feature.

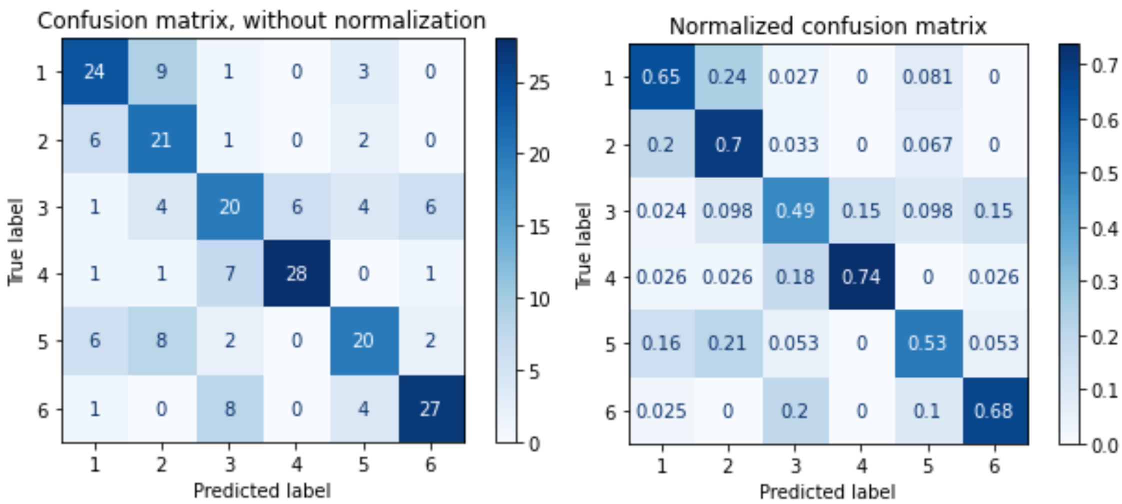

Figure C:0:6: The performance of SVM classifier in 125 ms window for PEK feature.

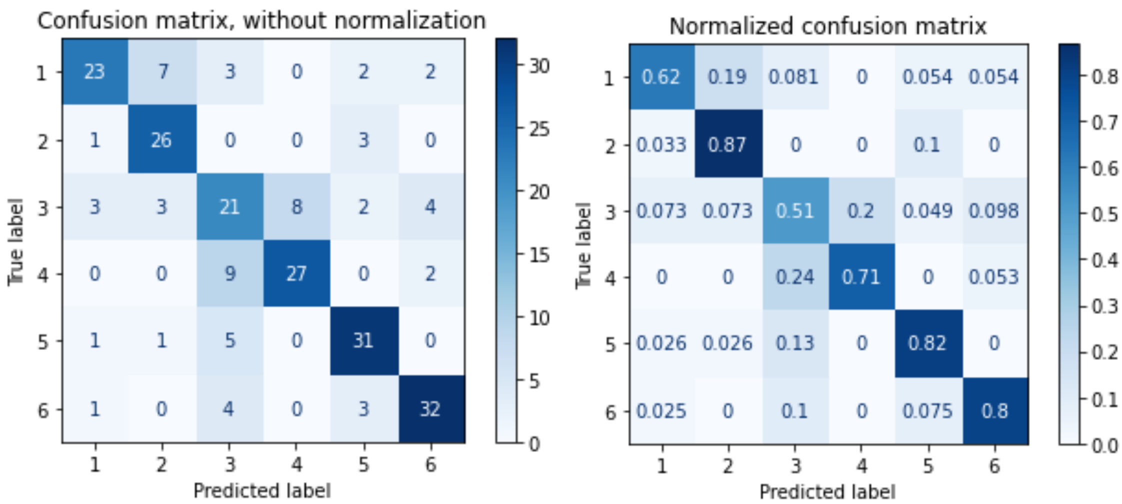

Figure C:0:7: The performance of SVM classifier in 125 ms window for KUR feature.

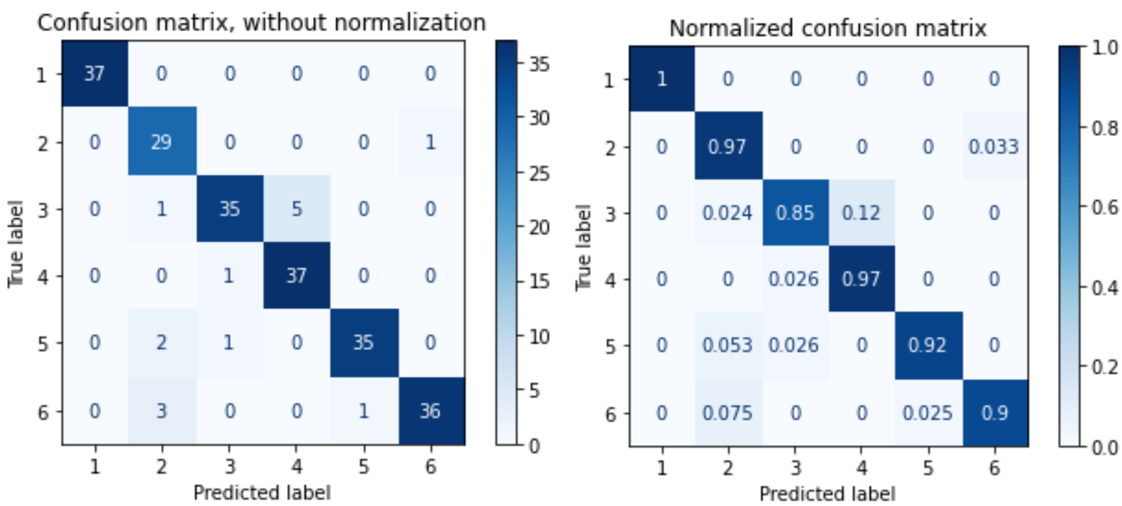

Figure C:0:8: The performance of SVM classifier in 125 ms window for AAC feature.

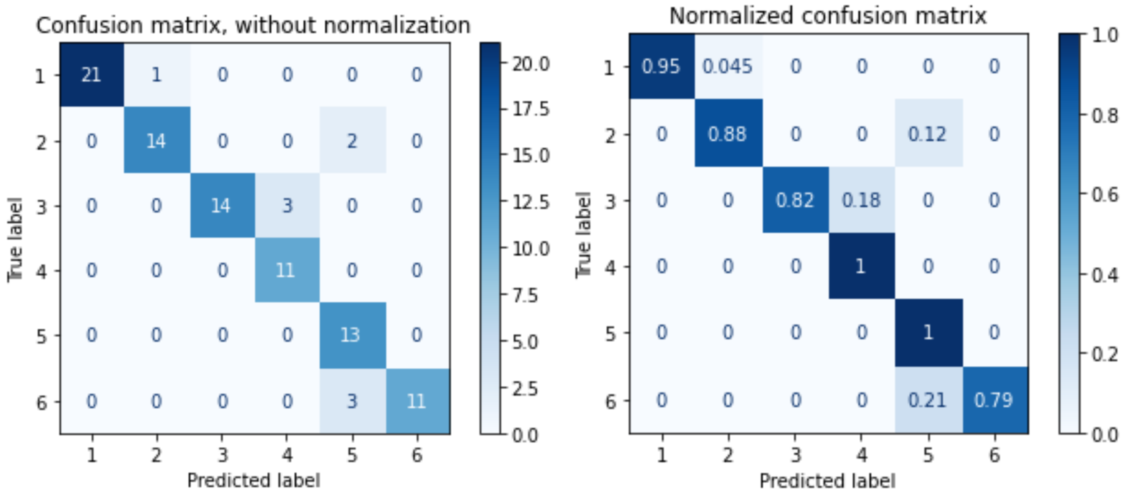

Figure C:0:9: The performance of SVM classifier in 300 ms window for RMS feature.

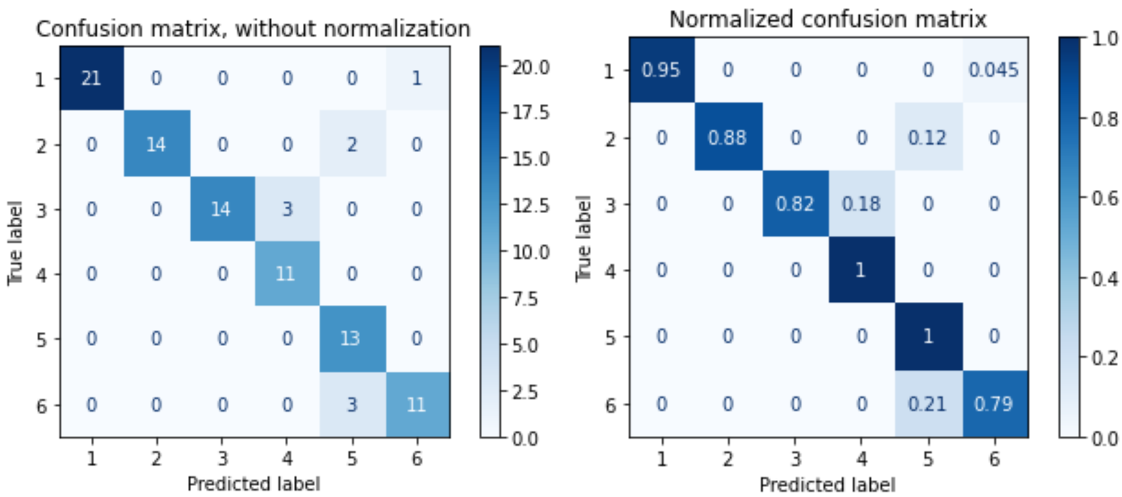

Figure C:0:10: The performance of SVM classifier in 300 ms window for MAV feature.

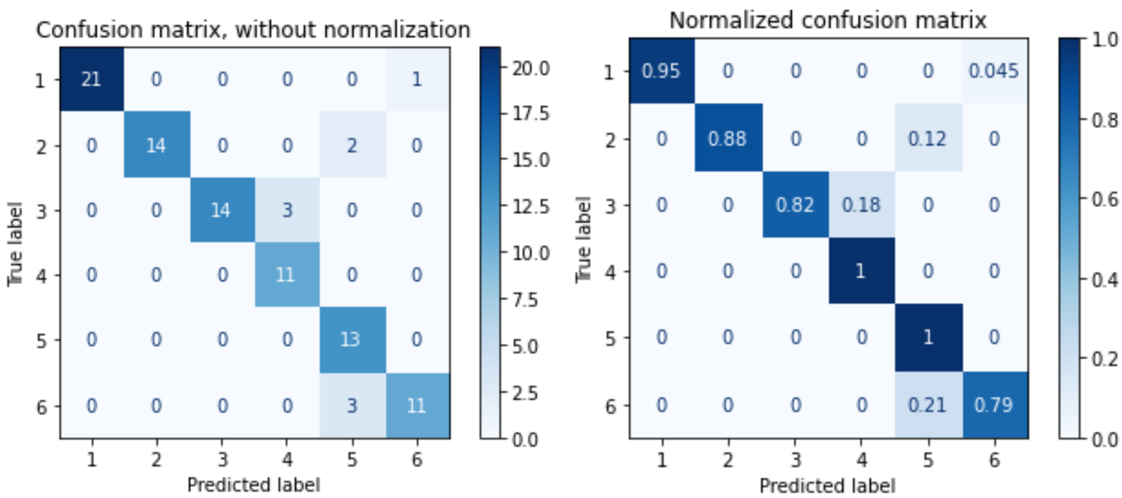

Figure C:0:11: The performance of SVM classifier in 300 ms window for IAV feature.

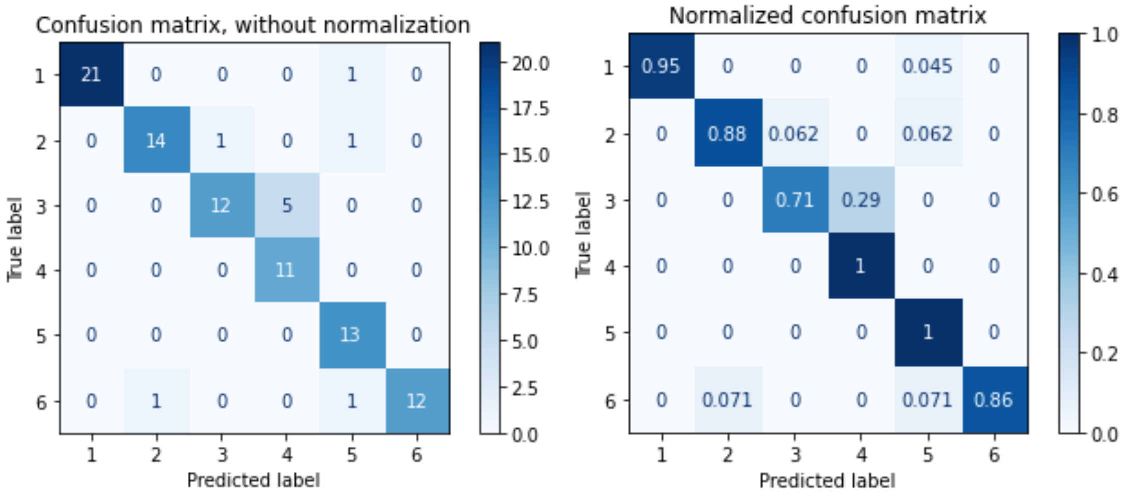

Figure C:0:12: The performance of SVM classifier in 300 ms window for WL feature.

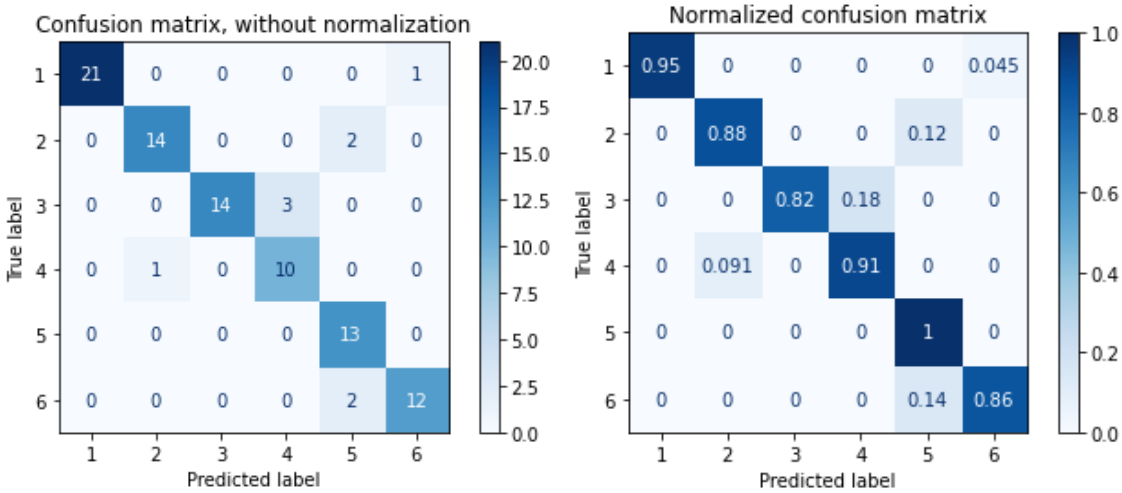

Figure C:0:13: The performance of SVM classifier in 300 ms window for SSI feature.

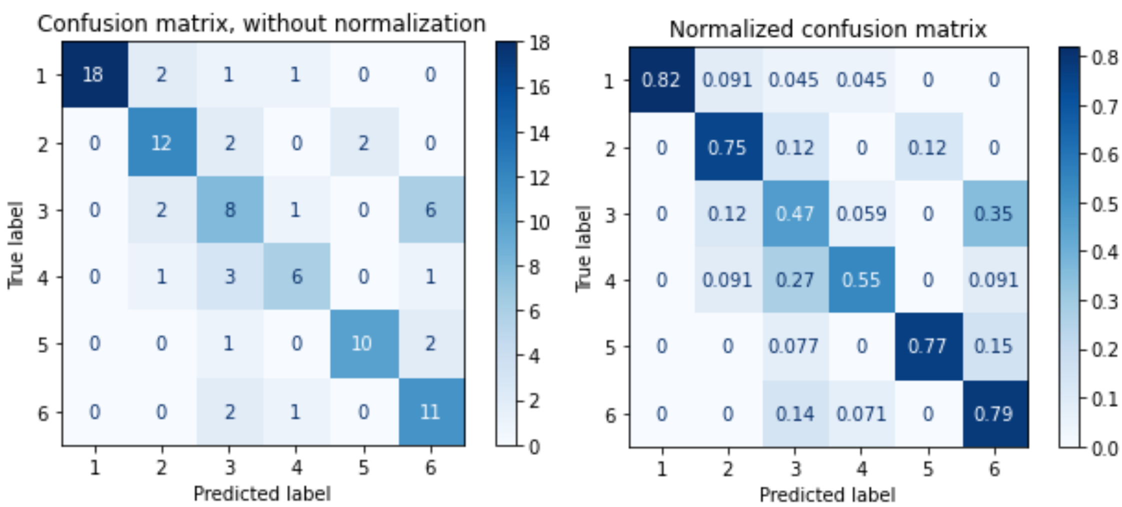

Figure C:0:14: The performance of SVM classifier in 300 ms window for PEK feature.

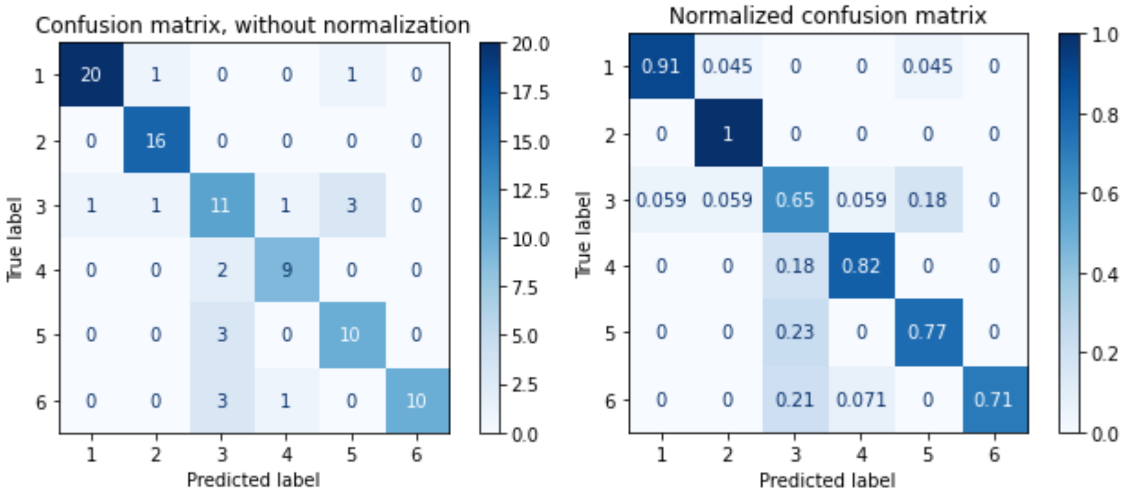

Figure C:0:15: The performance of SVM classifier in 300 ms window KUR feature.

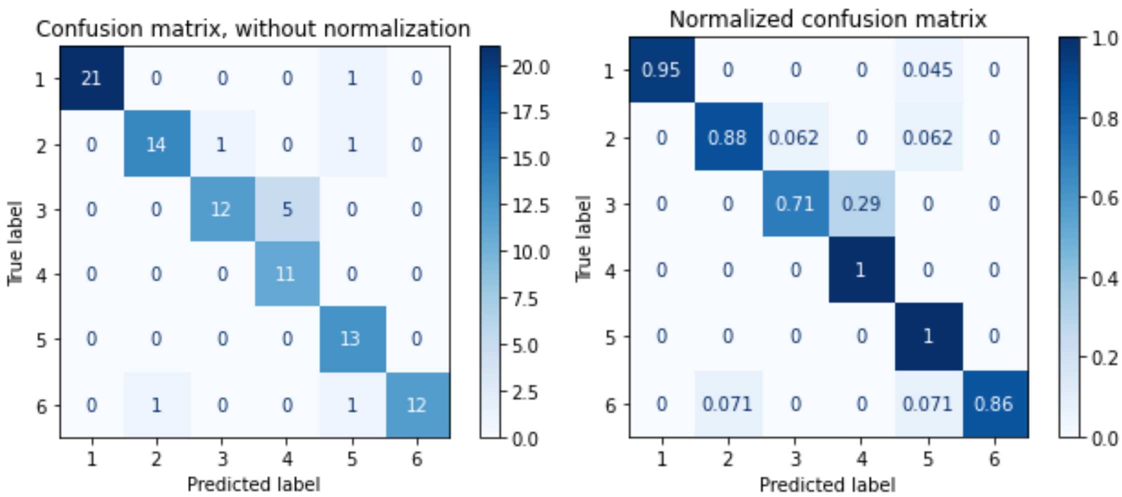

Figure C:0:16: The performance of SVM classifier in 300 ms window AAC feature.

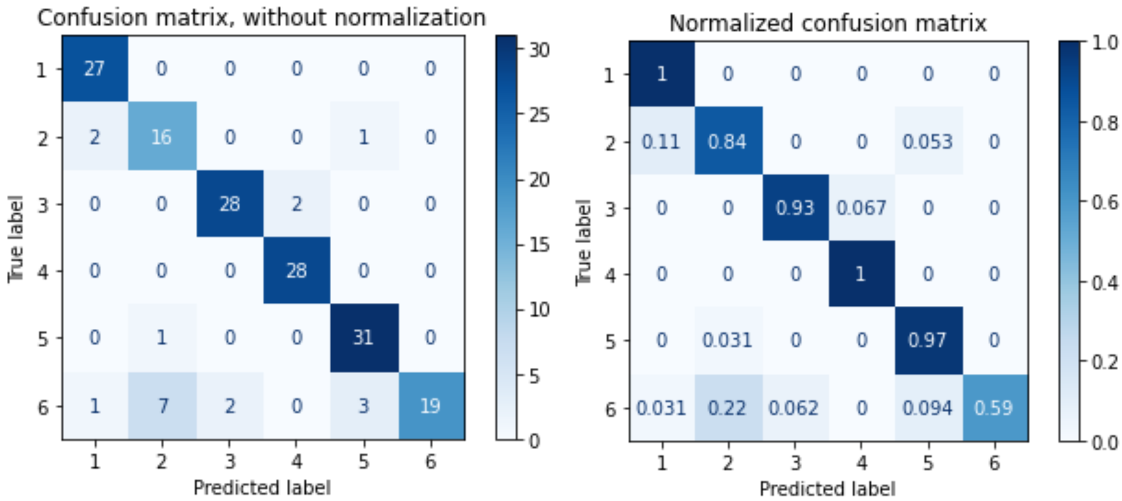

Figure C:0:17: The performance of Logistic regression in 125 ms for RMS feature.

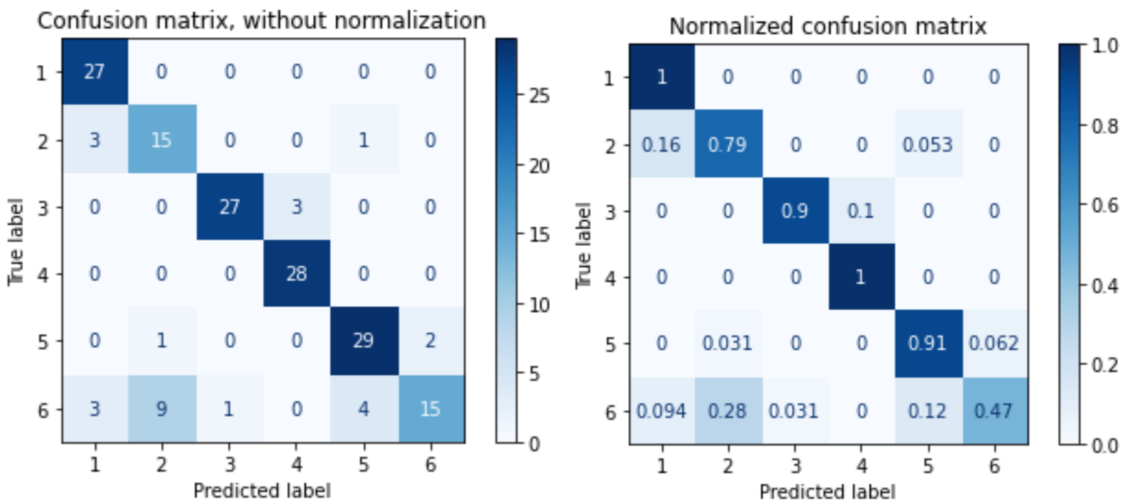

Figure C:0:18: The performance of Logistic regression in 125 ms for MAV feature.

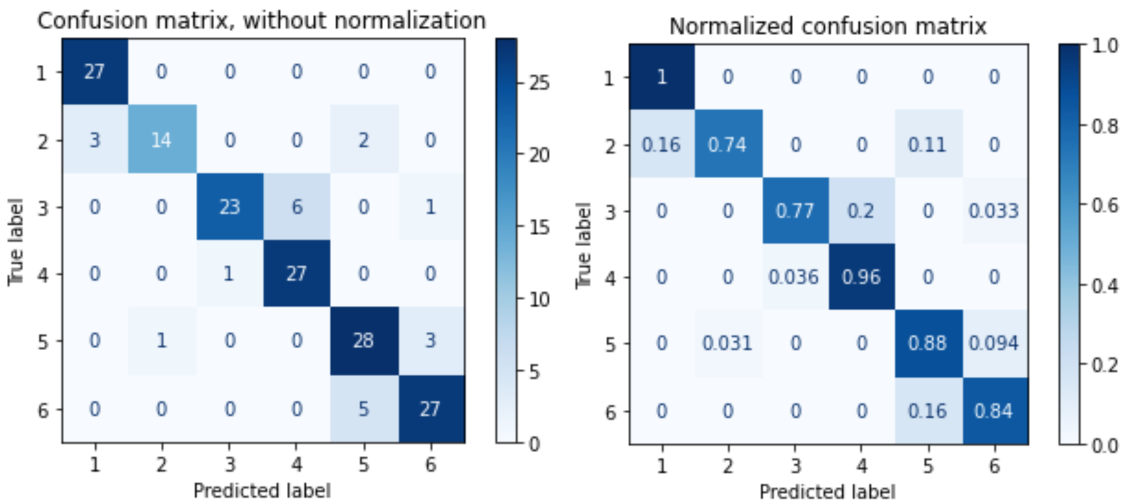

Figure C:0:19: The performance of Logistic regression in 125 ms for WL feature.

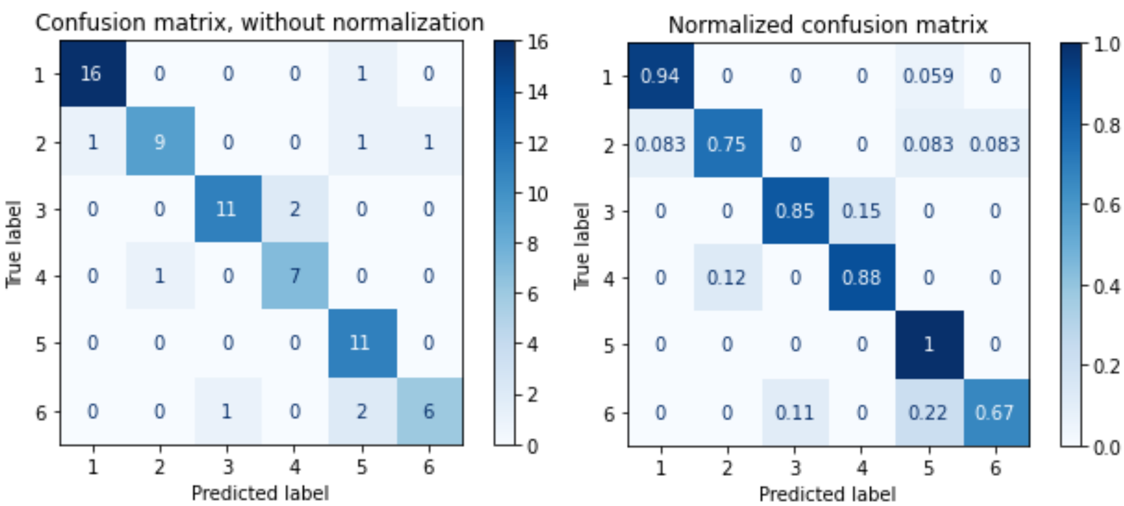

Figure C:0:20: The performance of Logistic regression in 300 ms for RMS feature.

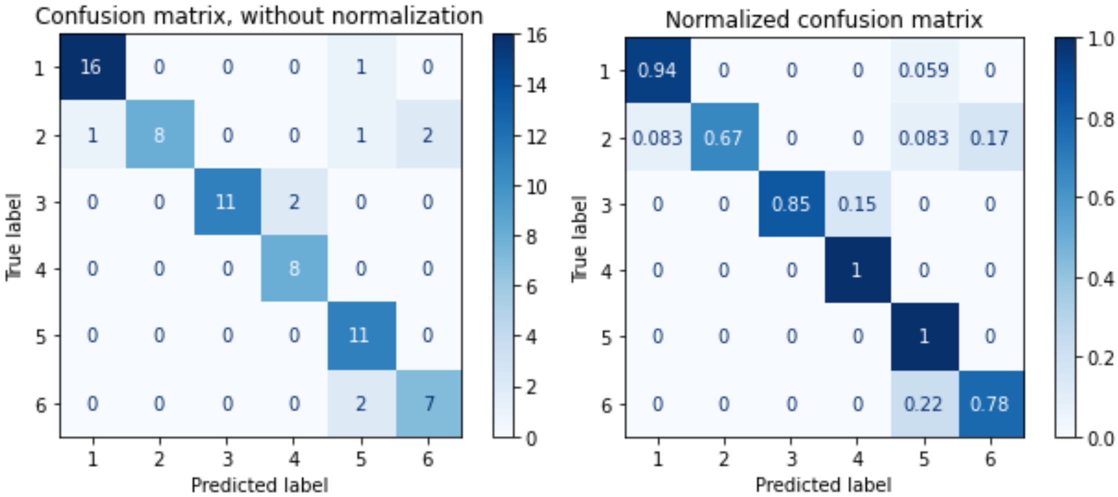

Figure C:0:21: The performance of Logistic regression in 300 ms for MAV feature.

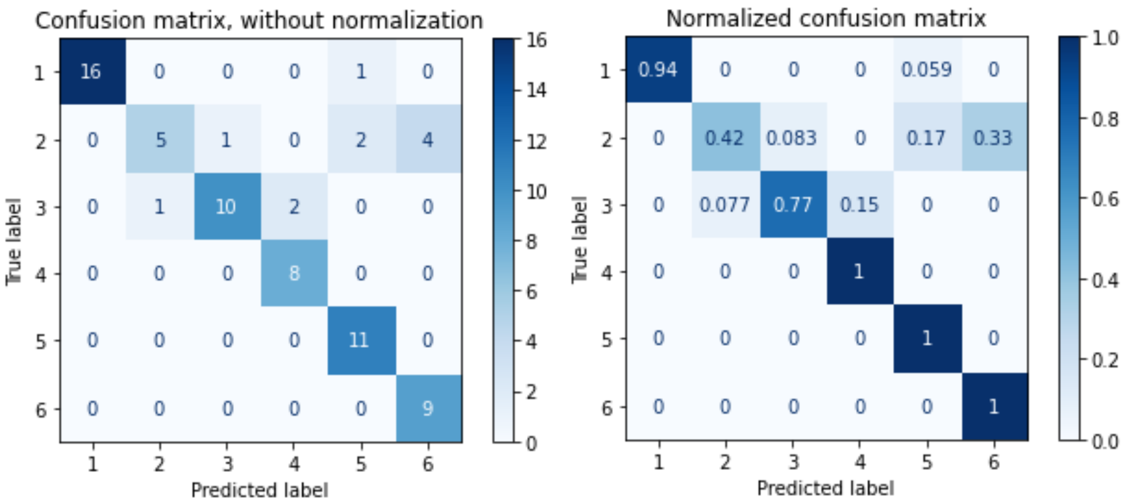

Figure C:0:22: The performance of Logistic regression in 300 ms for WL feature.

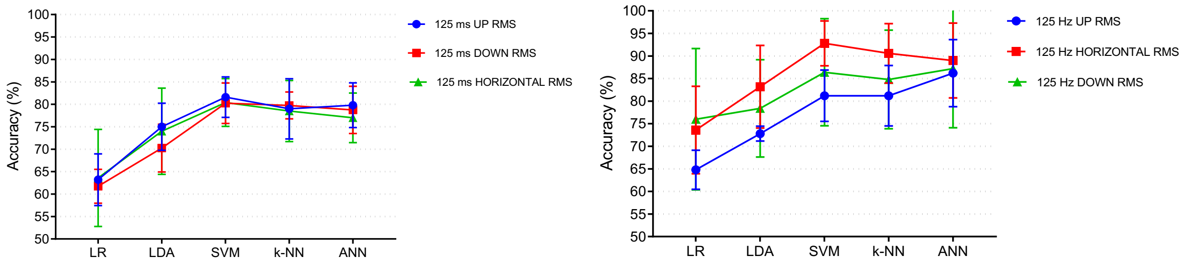

Figure C:0:23: The performance of Logistic regression for (a) finger detection (b) object grasping in 125 ms.

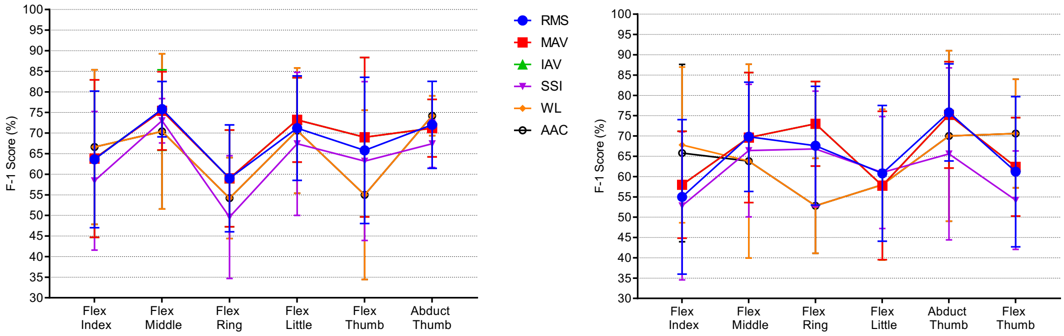

Figure C:0:24: The performance of Logistic regression for individual finger detection (a) in 125 ms, (b) in 300 ms.

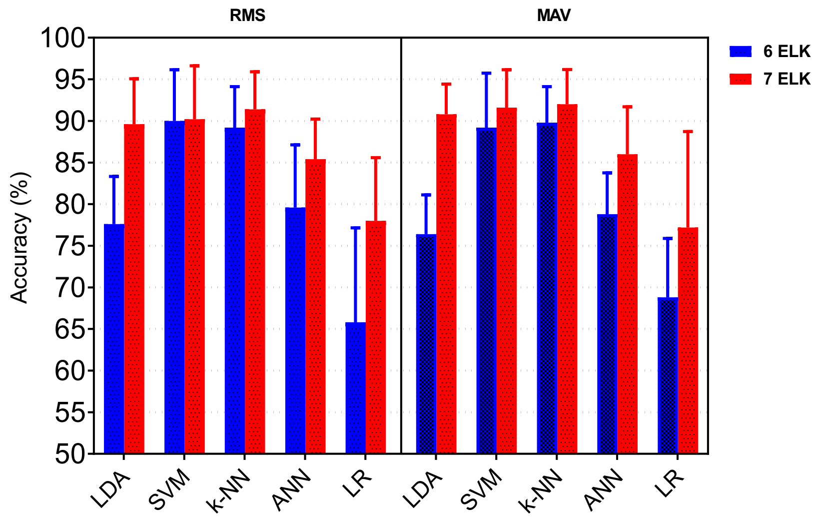

Figure C:0:25: The performance of Logistic regression for six electrodes and seven electrodes in 300 ms.

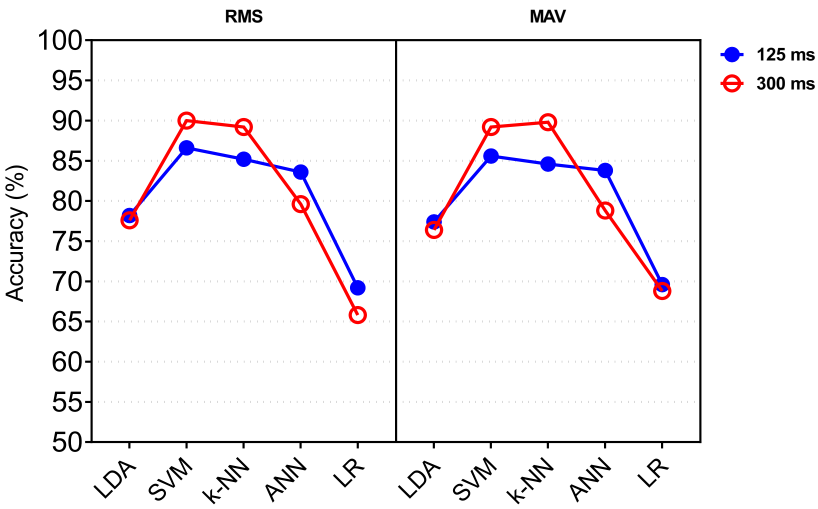

Figure C:0:26: The performance of Logistic regression for 125 ms and 300ms for finger detection.

Appendix D: Prototype Part Specifications and Drawings

Table D:1 presents the details of the prototype part that were used from commercial sources. The CAD drawings of the parts and objects are also presented in this appendix. The socket part includes the control units such as Raspberry pi, battery, control unit chessboard and motors.

Table D:0:1: **Specifications of Commercial Parts.**

Part	Manufacturer	Key Dimension (s)	Qty	Ref.
Dc motors(PQ12)	© RS Components Ltd	15x22x47 mm 18-50 N	4	[282]
Raspberry Pi 4	© R.S. Components Ltd	quad-core Cortex-A72 (ARM v8 85x56 mm 2.4 GHz and 5.0 GHz IEEE 802.11b/g/n/ac wireless	1	[283]
Chestnut V1.0 PCB	© Open Bionics	45X57 mm Arm MO+SAMD21G18A		[284]
Battery	© RS Components Ltd	1,300 mAh, 7.4 V	1	[285]
EMG electrodes (model DE2.1)	Delsys Inc., Boston, MA, USA	27x37x13 mm (size) 14 g (mass) 4-8 hours (battery life)	7	[286]
EMG electrodes	Delsys Inc., Boston, MA, USA	4x EMG, up to 6x IMU (sensor channel) 25x12x7 mm (size) 25 g (mass) 2222 sa/sec (sampling rate)	4	[286]

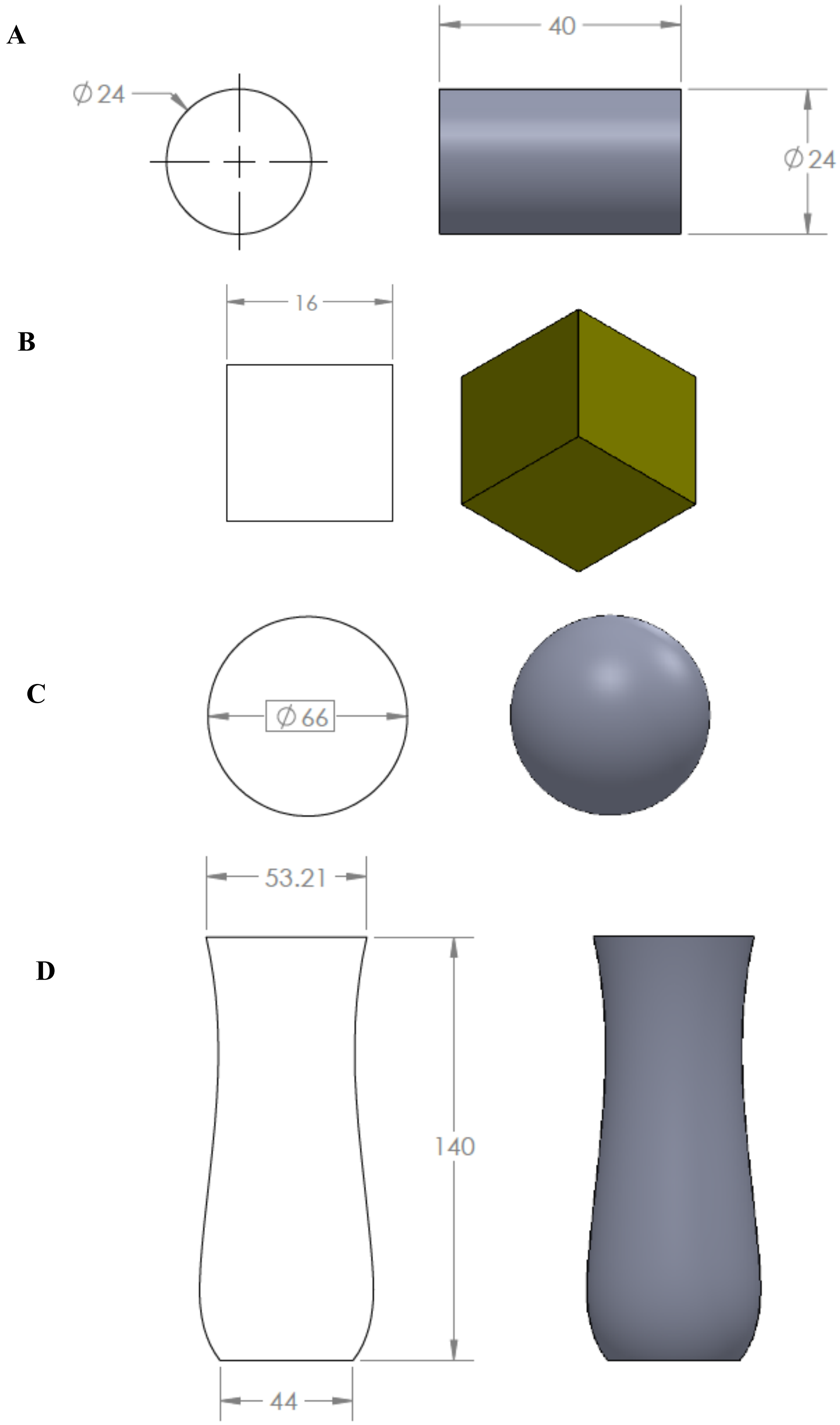

Figure D:1: Specifications of objects used in objects grasping experiments. (A) cylinder, (B) dice, (C) sphere, (D) bottle.

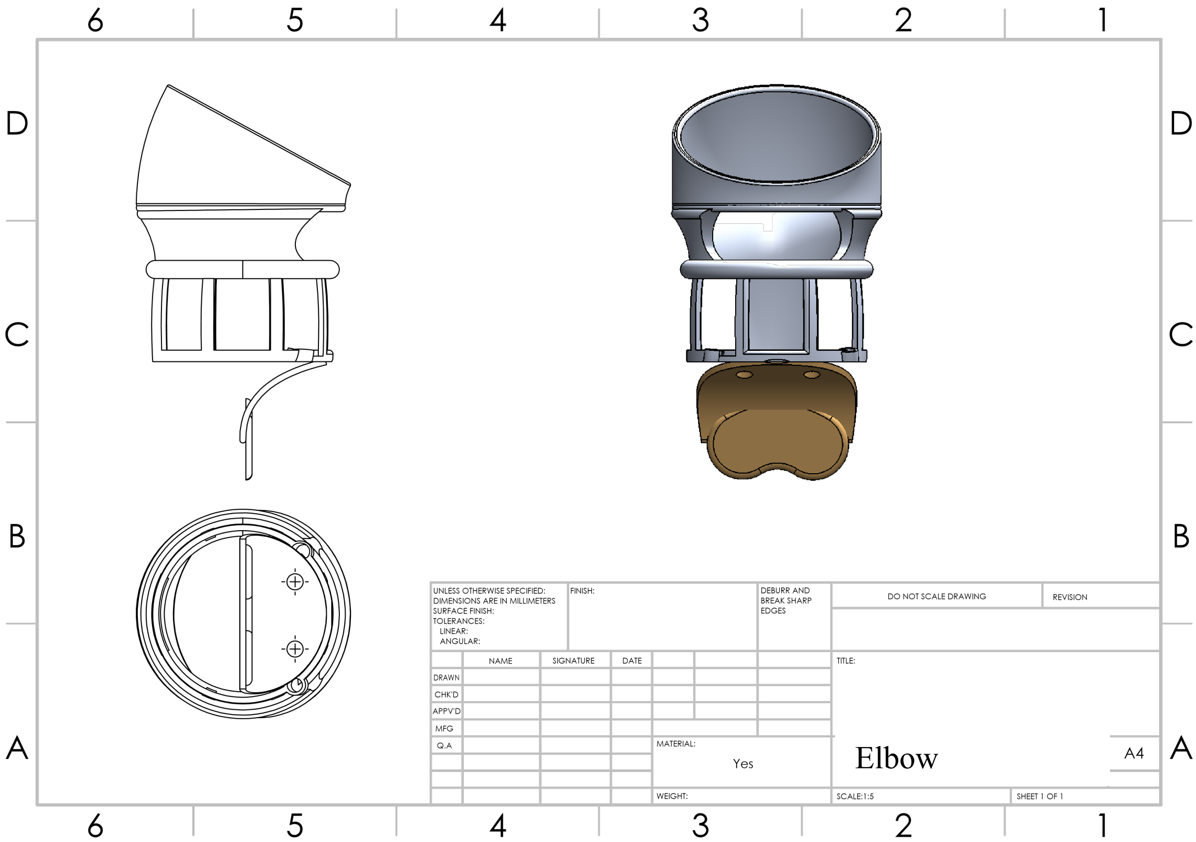

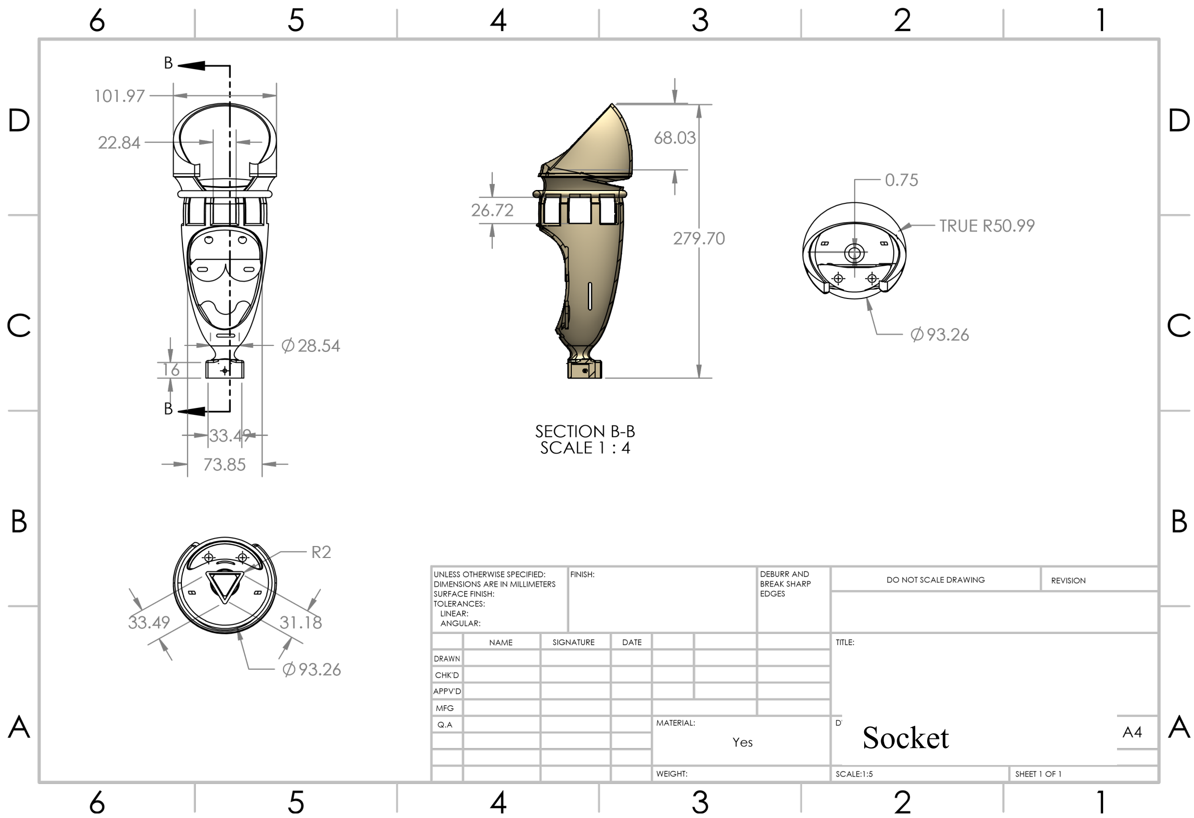

Figure D:2: CAD designs of the socket.

Appendix E: Codes Used in This Study

The Python, Matlab and C codes developed for data processing, prediction and control of prototype in this research are presented in a digital copy. The list of descriptions and shortcuts are given below.

Name	Description
Data Collection_M_EMG	The Matlab scrips to obtain the participant's raw EMG data for finger manipulation and object grasping.
Matlab_Code_MAV	Extracting EMG singal from valid files for feature extraction and to create the input labels.
Matrix_create	Feature creation and labelling for finger manipulation and object grasping.
Graph_matlab	Plotting the raw EMG signals and extracted eighth features.
Func_compress_dw1d	Processing EMG data for DWT features.
Real_time_control	Function for UI. The interface was created to initialise the python function.
My_Real_Time_Prediction	The Matlab script to collect, preprocess data and sent the segmented data to Python for prediction.
k-nn_for_EMG	Python script for k-NN classification. The code was created to call data from the CSV file and score the labels and classifiers.
LDA_for_EMG	Python script for LDA classification. The code was created to call data from the CSV file and score the labels and classifiers.
SVM_for_EMG	Python script for SVM classification. The code was created to call data from the CSV file and score the labels and classifiers.
My_NN_TF_3LAYER_Dropout	Python script for 3 hidden layer ANN classification. The code was created to call data from the CSV file and score the labels and classifiers. The ANN was created in TensorFlow with the dropout method.
Logistic_Regression	Python script for LR classification. The code was created to call data from the CSV file and score the labels and classifiers.
Creating_Dictionary	The python script was written for recording the predicted label for real-time control. The script saves each prediction in a txt file for real-time evaluation.
Server_python	Function to create a TCP/IP server between Delsys box and Python.

Continous_Prediction_SVM	The python script to create a data transfer server between Matlab and Python and predict the hand motions in real-time.
Real-Time_Control	The python script to create an online server between Matlab and Python acquired segments are then predicted and send to the controller to activate the motors.
Servo_Control	The script was written in C language to control servo motors on the robotic hand.
Communication	The script was written in C language to connect the Chesnut board to Raspberry Pi.

Appendix F: The Theory of Machine Learning Methods

1. Liear Discriminant Analaysis (LDA)

Fisher's [287] solution for two classes is provided below in order to gain an understanding of the mathematical operation of linear discriminant analysis. The original method was developed to distinguish two classes, as shown below, and has since been improved to detect multiple classes. The direction vector *w* can be projected onto z space to separate two classes as much as possible, given the samples of two classes C_1 and C_2 from the original equation.

$$z = w^T x$$

Assume m_1 and m_2 are the means of samples form C_1 and C_2 classes. $r^t=1$ if $x^t \in C_1$ and $r^t=0$ if input $x^t \in C_2$.

$$m_1 = \frac{\sum_t w^t x^t r^t}{\sum_t r^t} = w^T m_1$$

$$m_2 = \frac{\sum_t w^t x^t r^t}{\sum_t r^t} = w^T m_2$$

The scatters of samples are;

$$\boldsymbol{s_1^2} = \sum_t (\boldsymbol{w^T x^t} - \boldsymbol{m_1})^2 \boldsymbol{r^t}$$

$$s_2^2 = \sum_t (w^T x^t - m_2)^2 (1 - r^t)$$

To separate means of samples as much as possible $|m_1 - m_2|$ must be maximum and $s_1^2 + s_2^2$ small; therefore, the objective function can be written;

$$J(w) = \frac{(m_1 - m_2)^2}{s_1^2 + s_2^2}$$

rewriting the equation;

$$\begin{aligned}(m_1 - m_2)^2 &= (w^T m_1 - w^T m_2)^2 \\ &= w^T (m_1 - m_2)(m_1 - m_2)^T w \\ &= w^T S_B w\end{aligned}$$

where $S_B = (m_1 - m_2)(m_1 - m_2)^T$ and the sum of scatter around the means can be rewritten as

$$\boldsymbol{s_1^2} = \sum_t (\boldsymbol{w^T x^t} - \boldsymbol{m_1})^2 \boldsymbol{r^t}$$

$$= \sum_t \boldsymbol{w^T} (\boldsymbol{x^t} - \boldsymbol{m_1})(\boldsymbol{x^t} - \boldsymbol{m_1})^{\boldsymbol{T}} \mathbf{w} \boldsymbol{r^t}$$

$$= \boldsymbol{w^T S_1 w}$$

where

$$\boldsymbol{S_1} = \sum_t (\boldsymbol{x^t} - \boldsymbol{m_1})(\boldsymbol{x^t} - \boldsymbol{m_1})^{\boldsymbol{T}} \boldsymbol{r^t}$$

Similarly, $s_2^2 = w^T S_2 \mathrm{w}$ with $S_2 = \sum_t (x^t - m_1)(x^t - m_1)^T (1 - r^t)$ and it concludes as $s_1^2 + s_2^2 = w^T S_W \mathrm{w}$ where $S_W = S_1 + S_2$

The objective function can be written as

$$J(w) = \frac{w^T S_B w}{w^T S_W w} = \frac{|w^T (m_1 - m_2)|^2}{w^T S_W w}$$

Taking the derivation of $J(w)$ with respect to w and setting it equal to zero,

$$\frac{w^T (m_1 - m_2)}{w^T S_W \mathrm{w}} \left(2(m_1 - m_2) - \frac{w^T (m_1 - m_2)}{w^T S_W \mathrm{w}} S_W \mathrm{w} \right) = 0$$

Given that $\boldsymbol{w^T}(\boldsymbol{m_1} - \boldsymbol{m_2})/\boldsymbol{w^T S_w} \mathbf{w}$ is a constant the equation can be concluded;

$w = c S_W^{-1} (m_1 - m_2)$ where c is constant (most of time equal to 1) and w can be calculated.

For multiple classifications;

$$g_i(x | w_i, w_{i0}) = \left\{ \begin{array}{l} > 0 \; if \; x \epsilon C_i \\ \leq 0 \; othervise \end{array} \right\}$$

2. Support Vector Machines (SVM)

As the original equation starts with two classes and each label -1/+1. The sample is $X = \{x^t, r^t\}$ where $r^t = +1$ if $x^t \epsilon C_1$ and $r^t = -1$ if $x^t \epsilon C_2$

$$w^t x^t + w_0 \geq +1 \text{ for } r^t = +1$$

$$w^t x^t + w_0 \leq -1 \text{ for } r^t = -1$$

which can be rewritten as

$$r^t(w^t x^t + w_0) \geq +1$$

and the distance of x^t to discriminant is

$$\frac{|w^t x^t + w_0|}{||w||}$$

which $r^t \, \epsilon\{-1, +1\}$ can be rewritten as

$$\frac{r^t(w^t x^t + w_0)}{||w||}$$

if the determined value is assigned to ρ value which is margine that separates the hyperplance when it is optimal.

$$\frac{r^t(w^t x^t + w_0)}{||w||} \geq \rho$$

In order ot maximize the margin, $||w||$ must be minimum; therefore, the equation can be written as

$$min\frac{1}{2}||w||^2 \text{ subject to } \quad r^t(w^t x^t + w_0) \geq +1$$

To solve the equation, the problem can be rewritten as an unconstrained problem using Lagrange multipliers α^t:

$$L_p = \frac{1}{2}||w||^2 - \sum_{t=1}^{N} \alpha^t[r^t(w^t x^t + w_0) - 1]$$

$$= \frac{1}{2}||w||^2 - \sum_t \alpha^t r^t(w^t x^t + w_0) + \sum_t \alpha^t$$

The equation must be minimised for w and w_0 and maximised with respect to $\alpha^t \geq 0$.

$$\frac{\partial L_p}{\partial w} = 0; \qquad w = \sum_t \alpha^t \, r^t x^t$$

$$\frac{\partial L_p}{\partial w_0} = 0; \qquad \sum_t \alpha^t \, r^t = 0$$

$$L_d = \frac{1}{2}(w^T w) - w^T \sum_t \alpha^t r^t x^t - w_0 \sum_t \alpha^t r^t + \sum_t \alpha^t$$

$$= -\frac{1}{2}(w^T w) + \sum_t \alpha^t$$

$$= \frac{1}{2}\sum_t \sum_s \alpha^t \alpha^s r^t r^s (x^t)^T x^s + \sum_t \alpha^t$$

Which maximise the hyperplane for α^t, subject to constant $\sum_t \alpha^t r^t = 0$ and $\alpha^t \geq 0$

The sets for x^t which $\alpha^t > 0$ are the support vectors and w weighted the sum of training instance for selected support vector are;

$$r^t(w^t x^t + w_0) = 1$$

and it lies with the margin, thus w_0 can be derived from any support vector.

The class can be calculated $g(x) = w^t x^t + w_0$; Chooses C_1if $g(x) > 0$ and C_2 otherwise. Some kernel functions have been proposed to calculate the support vector machine for non-linear and non-separable data [288]. Lets assume the new dimention is calculated from basic functions and mapping from d-dimentional x space to k-dimentional z space, the basic function expension of design matrix is ϕ .

$$z = \phi(\mathrm{x}) \text{ where } z_i = \phi_i(x), i = 1, 2, \ldots . k$$

$$w = \sum_t \alpha^t r^t z^t = \sum_t \alpha^t r^t \phi(\mathrm{x}^t)$$

and the dicrimnat is

$$g(x) = w^t \phi(\mathrm{x}) = \sum_t \alpha^t r^t \phi(\mathrm{x})\, \phi(\mathrm{x}^t)^T$$

$$g(x) = \sum_t \alpha^t r^t \mathrm{K}\,(\mathrm{x}^t, x)$$

Polynomial kernel with d degree and kernel funtion K;

$$\mathbf{K}(\mathbf{x}^{t}, \boldsymbol{x}) = (\mathbf{1} + \boldsymbol{x}^{T}\boldsymbol{x}^{t})^{d}$$

Gaussian (also known radial basis function) kernel;

$$\mathbf{K}(\mathbf{x}^{t}, \boldsymbol{x}) = \mathbf{exp}\left[\frac{|\boldsymbol{x}^{t} - \boldsymbol{x}|^{\,2}}{\boldsymbol{\sigma}^{2}}\right]$$

Sigmoid kernel;

$$\mathbf{K}(\mathbf{x}^{t}, \boldsymbol{x}) = \mathbf{tanh}(\mathbf{2}\boldsymbol{x}^{T}\boldsymbol{x}^{t} + \mathbf{1})$$

3. k-Nearest Neighboror (k-NN)

The k-NN method adjusts the amount of smoothing applied to the data's local density. The amount of smoothing is determined by $k,$ the number of neighbours considered, which is much smaller than N the sample size. Assume that the distance between a and b is $|a-b|$ and that for each x sample is defines

$$d_1(x) \leq d_2(x) \ldots \ldots \leq d_N(x)$$

If x^t is the data point $d_1(x) = \min|x - x^t|$ and if i is the index of the closest sample namely , $i = argmin_t|x - x^t|$, then for second $d_2(x) = min_{i\neq j}|x - x^j|$, therefore the estimeters is

$$\hat{p}(x) = \frac{k}{2Nd_k(x)}$$

To determine a smoother estimate a kernel whose estimate decreases with increasing distance.

$$\hat{p}(x) = \frac{1}{Nd_k(x)} \sum_{t=1}^{N} K(\frac{x - x^t}{d_k(x)})$$

this provides a kernel estimator with an adaptive smoothing parameter $h = d_k(x). K(.)$ that typically takes Gaussian kernel, where K is the number of the outputs.

The multivariate kernel density is used to generalise the given sample with d-dimentional data

$$\hat{p}(x) = \frac{1}{Nh^d} \sum_{t=1}^{N} K\left(\frac{x - x^t}{h}\right)$$

with requirement that

$$\int_{\Re^d}^{N} K(x)dx = 1$$

4. Artificial Neural Network (ANN)

The perceptron is the basic processing element with associated input $x_j \epsilon \Re, j = 1, \ldots, d$ and connection weight $w_j \epsilon \Re$ and output y is defined as;

$$y = \sum_{j=1}^{d} w_j\, x_j + w_0$$

The model is generally weighted with extra bias unit x_0 which is always +1, and w_0 is the intercept value to generalise it. The equation can be rewritten as;

$$y = w^T x$$

where $w = [w_0, w_1, \dots, w_d]$ and $x = [1, x_1, x_2, \dots, x_d]$ are augmented vectors. if the threshould function defined as $s(.)$

$$s(a) = \begin{Bmatrix} 1 & if\ a > 0 \\ 0 & othervise \end{Bmatrix}$$

then it can rewritten as;

$$choose = \begin{Bmatrix} C_1 & if\ s(w^T x) > 0 \\ C_2 & if\ otherwise \end{Bmatrix}$$

The output function can be used to separate the classes; for example, the output value for the sigmoid function is;

$$o = w^T x$$

$$y = sigmoid(o) = \frac{1}{1 + exp[-w^T x]}$$

When more than two classes are present, the output can be summarised as follows:

$$y_i = \sum_{j=1}^{d} w_{ij}\, x_j + w_{i0} = w_i^T x$$

$$y = Wx$$

where w_{ij} is the weight from input x_j to output y_i and W is the $K \times (d + 1)$ weight matrix of w_{ij} for K perceptrons.

The error on a single instance pair with index t, (x^t, r^t) in online learning is

$$E^t(w|x^t, r^t) = \frac{1}{2}(r^t - y^t)^2 = \frac{1}{2}[r^t - (w^T x^t)]^2$$

and for $j = 0, \dots, d$ the online update is

$$\boldsymbol{\Delta w_j^t = \eta(r^t - y^t)x_j^t}$$

Where η is learning rate, which decreases by time for convergence, also known as stochastic gradient descent.

The equations above are for a single perceptron that is unable to discriminate nonlinearity. Input data x is fed into input layer and the activation function propagates the value of hidden layer z_h

$$\boldsymbol{z_h = sigmoid(w_h^T x) = \frac{1}{1 + \exp\left[-\left(\sum_{j=1}^{d} w_{hj}\, x_j + w_{h0}\right)\right]}}$$

The output value y_i is perceptron of the second layer and it takes the hidden unit as it's input.

$$\boldsymbol{y_i = v_i^T z = \sum_{h=1}^{H} w_{ih}\, z_h + w_{i0}}$$

To update multilayer weights for a whole regression sample, where the $(r^t - y^t)$ is the error term

$$\Delta \boldsymbol{v_{ih}} = \eta \sum_{t} (\boldsymbol{r_i}^{\boldsymbol{t}} - \boldsymbol{y_i}^{\boldsymbol{t}}) \boldsymbol{z_h^t}$$

the accumulated backpropagated weight update is

$$\Delta \boldsymbol{w_{hj}} = \eta \sum_{t} \left[\sum_{i} (\boldsymbol{r_i} - \boldsymbol{y_i^t}) \boldsymbol{v_{ih}} \right] \boldsymbol{z_h^t (1 - z_h^t) x_j^t}$$

$\sum_i (r_i^t - y_i^t)\, \boldsymbol{v_{ih}}$ is the accumulated backpropagated error of the hidden unit h from all output units.

5. Principal Component Analaysis (PCA)

To find the orthogonal set of L *linear basis vector* $w_j \epsilon R^D$, and corresponding scores $z_i \epsilon R^L$ and x_i training case;

$$J(W, Z) = \frac{1}{N} \sum_{i}^{N} ||x_i - \overline{x_i}||^2$$

Where empirical mean $\overline{x_i} = W z_i$ subject to W which is orthogonal. The equation can be rewritten as follows;

$$J(W, Z) = ||X - WZ^T||_F^2$$

Where Z is a NxL matrix with z_i in its orthogonal and $||A||_F$ is the Frobenius norm of matrix A and can be defined as

$$||A||_F = \sqrt{\sum_{i=1}^{m} \sum_{j=1}^{n} a_{i,j}^2} = \sqrt{tr(A^T A)} = ||A(:)||_2$$

The optimal solution can be determined by setting the estimate $\widehat{W} = V_L$, where V_L contains L eigenvectors with biggest eigenvalues of covariant matrix which is $\sum = \frac{1}{N} \sum_{i=1}^{N} x_i\, x_i^T$. Which assumes $\boldsymbol{x_i}$ have zero means**.** The variance of projection can be mazimise by $\left||w_1|\right| = 1$; and the cost function

$$J(w_1) = w_1^T \sum w_1 + \lambda_1(w_1^T w_1 - 1)$$

where λ_1 is lagrange multiplier, the derivation of xx equal to zero will give $\sum w_1 = \boldsymbol{\lambda}_1 w_1$ in order to find second direction w_2;

$$J(w_1, z_1, w_2, z_2) = \frac{1}{N}\sum_{i=1}^{N} ||x_i - z_{i1}w_1 - z_{i2}w_2||^2$$

Optimising $\boldsymbol{w_1}$ and $\boldsymbol{z_1}$ gives the similar solution as before and yields

$$J(w_2) = -w_2^T \sum w_2 + \lambda_2(w_2^T w_2 - 1) + \lambda_{12}(w_2^T w_1 - 0)$$

Therefore the second eigenvector with second largest eigenvalue will be;

$$\sum w_2 = \lambda_2 w_2$$

The values continoues in this way for each PCA direction. In most cases, the largest few eigenvalues are much greater than others ($\lambda_1 > \lambda_2 > \lambda_3$). For example, assume m=10, the total variance would be T=100 and λ_1=89, λ_2=6.5….,λ_{10}. This means that the first two directions represent 95.5% of the total variation of data.

References

[1] K. Ziegler-Graham, E. J. MacKenzie, P. L. Ephraim, T. G. Travison, and R. Brookmeyer, "Estimating the Prevalence of Limb Loss in the United States: 2005 to 2050," *Arch. Phys. Med. Rehabil.*, vol. 89, no. 3, pp. 422–429, Mar. 2008.

[2] B. D. Darnall *et al.*, "Depressive symptoms and mental health service utilization among persons with limb loss: Results of a national survey," *Arch. Phys. Med. Rehabil.*, vol. 86, no. 4, pp. 650–658, 2005.

[3] R. F. Weir and D. Ph, "Design of Artificial Arms and Hands for Prosthetic Applications," *Stand. Handb. Biomed. Eng. Des.*, pp. 1–61, 2004.

[4] L. R. Hochberg *et al.*, "Reach and grasp by people with tetraplegia using a neurally controlled robotic arm," *Nature*, vol. 485, no. 7398, pp. 372–375, 2012.

[5] S. Bitzer and P. Van Der Smagt, "Learning EMG control of a robotic hand: Towards Active Prostheses," *Proc. - IEEE Int. Conf. Robot. Autom.*, vol. 2006, no. May, pp. 2819–2823, 2006.

[6] Touch Bionics, "Touch Bionics- Home," *Ossur*. [Online]. Available: http://touchbionics.com/. [Accessed: 02-Jan-2019].

[7] Otto Bock Healthcare, "bebionic | Ottobock US Healthcare." [Online]. Available: https://professionals.ottobockus.com/Prosthetics/Upper-Limb-Prosthetics/bebionic/c/2888. [Accessed: 02-Jan-2019].

[8] P. Ju, L. P. Kaelbling, and Y. Singer, "State-based classification of finger gestures from electromyographic signals," *Icml*, pp. 439–446, 2000.

[9] G. Li, A. E. Schultz, and T. A. Kuiken, "Quantifying pattern recognition-based myoelectric control of multifunctional transradial prostheses.," *IEEE Trans. Neural Syst. Rehabil. Eng.*, vol. 18, no. 2, pp. 185–92, Apr. 2010.

[10] F. Cordella *et al.*, "Literature review on needs of upper limb prosthesis users," *Front. Neurosci.*, vol. 10, no. MAY, pp. 1–14, 2016.

[11] L. C. Smail, C. Neal, C. Wilkins, and T. L. Packham, "Comfort and function remain key factors in upper limb prosthetic abandonment: findings of a scoping review," *Disabil. Rehabil. Assist. Technol.*, vol. 16, no. 8, pp. 821–830, Mar. 2021.

[12] E. Biddiss and T. Chau, "Upper limb prosthesis use and abandonment: A survey of the last 25 years," *Prosthetics and Orthotics International*. 2007.

[13] L. Resnik, M. Borgia, A. W. Heinemann, and M. A. Clark, "Prosthesis satisfaction in a national sample of Veterans with upper limb amputation," *Prosthet. Orthot. Int.*, vol. 44, no. 2, pp. 81–91, Apr. 2020.

[14] T. P. Sheehan and G. C. Gondo, "Impact of Limb Loss in the United States," *Physical Medicine and Rehabilitation Clinics of North America*, vol. 25, no. 1. pp. 9–28, 2014.

[15] G. Ghazaei, A. Alameer, P. Degenaar, G. Morgan, and K. Nazarpour, "Deep learning-based artificial vision for grasp classification in myoelectric hands," *J. Neural Eng.*, vol. 14, no. 3, 2017.

[16] L. Resnik *et al.*, "Advanced upper limb prosthetic devices: Implications for upper limb prosthetic rehabilitation," *Arch. Phys. Med. Rehabil.*, vol. 93, no. 4, pp. 710–717, Apr. 2012.

[17] A. Furui *et al.*, "A myoelectric prosthetic hand with muscle synergy–based motion determination and impedance model–based biomimetic control," *Sci. Robot.*, vol. 4, no. 31, p. eaaw6339, Jun. 2019.

[18] G. Li, "Electromyography Pattern-Recognition-Based Control of Powered Multifunctional Upper-Limb Prostheses," in *Advances in Applied Electromyography,*

Chap. 6, InTech, 2011.

[19] K. C. D. Fu, F. D. Libera, and H. Ishiguro, "Extracting motor synergies from random movements for low-dimensional task-space control of musculoskeletal robots," *Bioinspiration and Biomimetics*, vol. 10, no. 5, 2015.

[20] C. Alessandro, I. Delis, F. Nori, S. Panzeri, and B. Berret, "Muscle synergies in neuroscience and robotics: from input-space to task-space perspectives," *Front. Comput. Neurosci.*, vol. 7, no. April, pp. 1–16, 2013.

[21] I. Delis, S. Panzeri, T. Pozzo, and B. Berret, "A unifying model of concurrent spatial and temporal modularity in muscle activity," *J. Neurophysiol.*, vol. 111, no. 3, pp. 675–693, 2014.

[22] J. Ribeiro *et al.*, "Analysis of Man-Machine Interfaces in Upper-Limb Prosthesis: A Review," *Robotics*, vol. 8, no. 1, p. 16, 2019.

[23] G. H. Kejlaa, "Consumer concerns and the functional value of prostheses to upper limb amputees," *Prosthet. Orthot. Int.*, vol. 17, no. 3, pp. 157–163, 1993.

[24] Ottobock US, "Custom silicone finger and hand prosthetics," 2021. [Online]. Available: https://www.ottobockus.com/prosthetics/upper-limb-prosthetics/solution-overview/custom-silicone-prosthetics/. [Accessed: 10-Jan-2022].

[25] K. J. Zuo and J. L. Olson, "The evolution of functional hand replacement: From iron prostheses to hand transplantation," *Can. J. Plast. Surg.*, vol. 22, no. 1, pp. 44–51, 2014.

[26] A. D. Roche, H. Rehbaum, D. Farina, • Oskar, C. Aszmann, and O. C. Aszmann, "Prosthetic Myoelectric Control Strategies: A Clinical Perspective," *Curr. Surg. Reports*, vol. 2, no. 3, 2014.

[27] "Össur Touch Solutions. Ossur.com." [Online]. Available: https://www.ossur.com/en-us/prosthetics/touch-solutions. [Accessed: 10-Jan-2022].

[28] Ottobock, "Ottobock Michelangelo Prosthetic Hand," *Ottobock.*, 2019. [Online]. Available: https://www.ottobockus.com/prosthetics/upper-limb-prosthetics/solution-overview/michelangelo-prosthetic-hand/. [Accessed: 10-Jan-2022].

[29] "Myo Plus | Ottobock US." [Online]. Available: https://www.ottobockus.com/prosthetics/upper-limb-prosthetics/solution-overview/myo-plus/myo-plus.html. [Accessed: 08-Apr-2020].

[30] M. C. Carrozza, G. Cappiello, S. Micera, B. B. Edin, L. Beccai, and C. Cipriani, "Design of a cybernetic hand for perception and action," *Biol. Cybern.*, vol. 95, no. 6, pp. 629–644, 2006.

[31] A. Gupta, C. Eppner, S. Levine, and P. Abbeel, "Learning Dexterous Manipulation for a Soft Robotic Hand from Human Demonstration," 2016.

[32] L. R. Hochberg *et al.*, "Neuronal ensemble control of prosthetic devices by a human with tetraplegia," *Nature*, vol. 442, no. 7099, pp. 164–171, Jul. 2006.

[33] G. S. Dhillon and K. W. Horch, "Direct neural sensory feedback and control of a prosthetic arm," *IEEE Trans. Neural Syst. Rehabil. Eng.*, vol. 13, no. 4, pp. 468–472, Dec. 2005.

[34] P. M. Rossini *et al.*, "Double nerve intraneural interface implant on a human amputee for robotic hand control," *Clin. Neurophysiol.*, vol. 121, no. 5, pp. 777–783, May 2010.

[35] S. Raspopovic *et al.*, "Restoring natural sensory feedback in real-time bidirectional hand prostheses: supplemental material," *Sci. Transl. Med.*, vol. 6, no. 222, p. 222ra19, 2014.

[36] D. J. Young, B. D. Farnsworth, and R. J. Triolo, "Wireless implantable EMG sensor for powered prosthesis control," *Int. Conf. Solid-State Integr. Circuits Technol. Proceedings, ICSICT*, pp. 2541–2544, 2008.

[37] T. R. Farrell and R. F. f. ff Weir, "A comparison of the effects of electrode implantation and targeting on pattern classification accuracy for prosthesis control," *IEEE Trans. Biomed. Eng.*, vol. 55, no. 9, pp. 2198–2211, Sep. 2008.

[38] P. F. Pasquina *et al.*, “First-in-man demonstration of a fully implanted myoelectric sensors system to control an advanced electromechanical prosthetic hand,” *J. Neurosci. Methods*, vol. 244, pp. 85–93, Apr. 2015.
[39] K. H. Polasek, H. A. Hoyen, M. W. Keith, R. F. Kirsch, and D. J. Tyler, “Stimulation stability and selectivity of chronically implanted multicontact nerve cuff electrodes in the human upper extremity,” *IEEE Trans. Neural Syst. Rehabil. Eng.*, vol. 17, no. 5, pp. 428–437, 2009.
[40] J. A. George *et al.*, “Biomimetic sensory feedback through peripheral nerve stimulation improves dexterous use of a bionic hand,” *Sci. Robot.*, vol. 4, no. 32, Jul. 2019.
[41] T. A. Kuiken *et al.*, “Targeted muscle reinnervation for real-time myoelectric control of multifunction artificial arms,” *JAMA - J. Am. Med. Assoc.*, vol. 301, no. 6, pp. 619–628, Feb. 2009.
[42] S. Tarantino, F. Clemente, D. Barone, M. Controzzi, and C. Cipriani, “The myokinetic control interface: Tracking implanted magnets as a means for prosthetic control,” *Sci. Rep.*, vol. 7, no. 1, pp. 1–11, Dec. 2017.
[43] A. E. Schultz and T. A. Kuiken, “Neural Interfaces for Control of Upper Limb Prostheses: The State of the Art and Future Possibilities,” *PM R*, vol. 3, no. 1, pp. 55–67, 2011.
[44] S. Salminger *et al.*, “Long-term implant of intramuscular sensors and nerve transfers for wireless control of robotic arms in above-elbow amputees,” *Sci. Robot.*, vol. 4, no. 32, p. eaaw6306, Jul. 2019.
[45] L. J. Hargrove, L. A. Miller, K. Turner, and T. A. Kuiken, “Myoelectric Pattern Recognition Outperforms Direct Control for Transhumeral Amputees with Targeted Muscle Reinnervation: A Randomized Clinical Trial,” *Sci. Rep.*, vol. 7, no. 1, 2017.
[46] E. Scheme and K. Englehart, “Electromyogram pattern recognition for control of powered upper-limb prostheses: State of the art and challenges for clinical use,” *J. Rehabil. Res. Dev.*, vol. 48, no. 6, p. 643, 2011.
[47] L. A. Miller, K. A. Stubblefield, R. D. Lipschutz, B. A. Lock, and T. A. Kuiken, “Improved myoelectric prosthesis control using targeted reinnervation surgery: A case series,” *IEEE Trans. Neural Syst. Rehabil. Eng.*, vol. 16, no. 1, pp. 46–50, Feb. 2008.
[48] P. Zhou, N. L. Suresh, and W. Z. Rymer, “Model based sensitivity analysis of EMG-force relation with respect to motor unit properties: Applications to muscle paresis in stroke,” *Ann. Biomed. Eng.*, vol. 35, no. 9, pp. 1521–1531, Sep. 2007.
[49] L. E. Osborn *et al.*, “Sensory stimulation enhances phantom limb perception and movement decoding,” *J. Neural Eng.*, vol. 17, no. 5, 2020.
[50] A. Kostov and M. Polak, “Parallel man-machine training in development of EEG-based cursor control,” *IEEE Trans. Rehabil. Eng.*, vol. 8, no. 2, pp. 203–205, 2000.
[51] T. Yanagisawa *et al.*, “Electrocorticographic control of a prosthetic arm in paralyzed patients.,” *Ann. Neurol.*, vol. 71, no. 3, pp. 353–61, 2012.
[52] G. Schalk *et al.*, “Two-dimensional movement control using electrocorticographic signals in humans,” *J. Neural Eng.*, vol. 5, no. 1, pp. 75–84, Mar. 2008.
[53] A. F. Jackson and D. J. Bolger, “The neurophysiological bases of EEG and EEG measurement: A review for the rest of us,” *Psychophysiology*, vol. 51, no. 11, pp. 1061–1071, 2014.
[54] D. P. McMullen *et al.*, “Demonstration of a semi-autonomous hybrid brain-machine interface using human intracranial EEG, eye tracking, and computer vision to control a robotic upper limb prosthetic,” *IEEE Trans. Neural Syst. Rehabil. Eng.*, vol. 22, no. 4, pp. 784–796, Jul. 2014.
[55] F. Xu, W. Zheng, D. Shan, Q. Yuan, and W. Zhou, “Decoding spectro-Temporal representation for motor imagery recognition using ECoG-based brain-computer

interfaces," *J. Integr. Neurosci.*, vol. 19, no. 2, pp. 259–272, 2020.
[56] H. U. Amin, W. Mumtaz, A. R. Subhani, M. N. M. Saad, and A. S. Malik, "Classification of EEG Signals Based on Pattern Recognition Approach," *Front. Comput. Neurosci.*, vol. 11, no. November, pp. 1–12, Nov. 2017.
[57] M. L. Madeleine, F. ff. W. Richard, and A. K. Todd, "Simulation of Intramuscular EMG Signals Detected Using Implantable Myoelectric Sensors (IMES)," *IEEE Trans. Biomed. Eng.*, vol. 53, no. 10, pp. 1926–1933, 2006.
[58] X. Da and J. Grizzle, "Combining Trajectory Optimization, Supervised Machine Learning, and Model Structure for Mitigating the Curse of Dimensionality in the Control of Bipedal Robots," no. X, pp. 1–17, 2017.
[59] M. C. Jimenez and J. A. Fishel, "Evaluation of force, vibration and thermal tactile feedback in prosthetic limbs," *IEEE Haptics Symp. HAPTICS*, pp. 437–441, 2014.
[60] K. R. Schoepp, M. R. Dawson, J. S. Schofield, J. P. Carey, and J. S. Hebert, "Design and Integration of an Inexpensive Wearable Mechanotactile Feedback System for Myoelectric Prostheses," *IEEE J. Transl. Eng. Heal. Med.*, vol. 6, no. August, pp. 1–11, 2018.
[61] D. J. Weber, M. Hao, M. A. Urbin, C. Schoenewald, and N. Lan, *Sensory information feedback for neural prostheses*. Elsevier Inc., 2020.
[62] N. V. Thakor *et al.*, "Prosthesis with neuromorphic multilayered e-dermis perceives touch and pain," *Sci. Robot.*, vol. 3, no. 19, p. eaat3818, 2018.
[63] F. Clemente *et al.*, "Non-Invasive, Temporally Discrete Feedback of Object Contact and Release Improves Grasp Control of Closed-Loop Myoelectric Transradial Prostheses," *IEEE Trans. Neural Syst. Rehabil. Eng.*, vol. 24, no. 12, pp. 1314–1322, Dec. 2016.
[64] E. D'Anna *et al.*, "A closed-loop hand prosthesis with simultaneous intraneural tactile and position feedback," *Sci. Robot.*, vol. 4, no. 27, 2019.
[65] S. M.A., M. M., D. S., T. F., G. B., and F. D., "Electrotactile EMG feedback improves the control of prosthesis grasping force," *J. Neural Eng.*, vol. 13, no. 5, 2016.
[66] A. L. Ciancio *et al.*, "Control of prosthetic hands via the peripheral nervous system," *Front. Neurosci.*, vol. 10, no. APR, pp. 1–17, Apr. 2016.
[67] S. Lee and C. Lee, "Toward advanced neural interfaces for the peripheral nervous system (PNS) and their future applications," *Curr. Opin. Biomed. Eng.*, vol. 6, pp. 130–137, 2018.
[68] S. Micera *et al.*, "On the use of longitudinal intrafascicular peripheral interfaces for the control of cybernetic hand prostheses in amputees," *IEEE Trans. Neural Syst. Rehabil. Eng.*, vol. 16, no. 5, pp. 453–472, 2008.
[69] J. G. \ CLINE and K., "Functional Separation of EMG Signals Via ARMA Identification Methods for Prosthesis Control Purposes," *IEEE Trans. Syst. Man. Cybern.*, vol. SMC-5, no. 2, pp. 252–259, 1975.
[70] G. Tsenov, A. H. Zeghbib, F. Palis, N. Shoylev, and V. Mladenov, "Neural networks for online classification of hand and finger movements using surface EMG signals," *8th Semin. Neural Netw. Appl. Electr. Eng. Neurel-2006 Proc.*, pp. 167–171, 2006.
[71] R. N. Khushaba, S. Kodagoda, M. Takruri, and G. Dissanayake, "Toward improved control of prosthetic fingers using surface electromyogram (EMG) signals," *Expert Syst. Appl.*, vol. 39, no. 12, pp. 10731–10738, Sep. 2012.
[72] N. Jiang, I. Vujaklija, H. Rehbaum, B. Graimann, and D. Farina, "Is accurate mapping of EMG signals on kinematics needed for precise online myoelectric control?," *IEEE Trans. Neural Syst. Rehabil. Eng.*, vol. 22, no. 3, pp. 549–558, 2014.
[73] L. Hargrove, S. Member, G. Li, K. Englehart, and L. Hargrove, "Principal Components Analysis Preprocessing to improve Classification Accuracies in Pattern Recognition Based Myoelectric Control Corresponding author," vol. 56, no. 506, pp. 1–28, 2009.

[74] F. Sim and P. Mackie, “One and a half centuries—A few moments in the evolution of public health,” *Public Health*, vol. 120, no. 9, pp. 781–782, 2006.
[75] Guanglin Li, A. E. Schultz, and T. A. Kuiken, “Quantifying Pattern Recognition{&}{#}x2014;Based Myoelectric Control of Multifunctional Transradial Prostheses,” *IEEE Trans. Neural Syst. Rehabil. Eng.*, vol. 18, no. 2, pp. 185–192, 2010.
[76] D. Peleg, E. Braiman, E. Yom-Tov, and G. F. Inbar, “Classification of finger activation for use in a robotic prosthesis arm,” *IEEE Trans. Neural Syst. Rehabil. Eng.*, vol. 10, no. 4, pp. 290–293, Dec. 2002.
[77] Y. Huang, K. B. Englehart, S. Member, B. Hudgins, S. Member, and A. D. C. Chan, “Scheme for Myoelectric Control of Powered Upper Limb Prostheses,” *Ieee Trans. Biomed. Eng.*, vol. 52, no. 11, pp. 1801–1811, 2005.
[78] J. Zhao, Z. Xie, L. Jiang, and H. Cai, “Levenberg-Marquardt Based Neural Network Control for a Five-fingered Prosthetic Hand *,” *2005 IEEE Int. Conf. Robot. Autom. Spain*, no. 50435040, pp. 4482–4487, 2005.
[79] A. Soares, A. Andrade, E. Lamounier, and R. Carrijo, “The development of a virtual myoelectric prosthesis controlled by an EMG pattern recognition system based on neural networks,” *J. Intell. Inf. Syst.*, vol. 21, no. 2, pp. 127–141, 2003.
[80] T. Wilcox and A. Hirshkowitz, “NIH Public Access,” vol. 85, no. 0 1, pp. 1–27, 2015.
[81] M. Atzori *et al.*, “Electromyography data for non-invasive naturally-controlled robotic hand prostheses,” *Sci. Data*, vol. 1, pp. 1–13, 2014.
[82] K. Englehart and B. Hudgins, “A Robust, Real-Time Control Scheme for Multifunction Myoelectric Control,” *IEEE Trans. Biomed. Eng.*, vol. 50, no. 7, pp. 848–854, 2003.
[83] C. Jun-Uk *et al.*, “A Real-Time EMG Pattern Recognition System Based on Linear-Nonlinear Feature Projection for a Multifunction Myoelectric Hand,” *IEEE Trans. Biomed. Eng.*, vol. 53, no. 11, pp. 2232–2239, 2006.
[84] F. Palermo, M. Cognolato, A. Gijsberts, H. Müller, B. Caputo, and M. Atzori, “Repeatability of grasp recognition for robotic hand prosthesis control based on sEMG data,” in *IEEE International Conference on Rehabilitation Robotics*, 2017, pp. 1154–1159.
[85] E. E. M. G. Signals *et al.*, “Identi fi cation of Contaminant Type in Surface,” *Ieee Trans. Neural Syst. Rehabil. Eng.*, vol. 22, no. 4, pp. 774–783, 2014.
[86] M. Atzori *et al.*, “Building the Ninapro database: A resource for the biorobotics community,” *Proc. IEEE RAS EMBS Int. Conf. Biomed. Robot. Biomechatronics*, pp. 1258–1265, 2012.
[87] A. Bolu Ajiboye and R. F. ff Weir, “A Heuristic Fuzzy Logic Approach to EMG Pattern Recognition for Multifunctional Prosthesis Control,” *Ieee Trans. Neural Syst. Rehabil. Eng.*, vol. 13, no. 3, pp. 280–291, 2005.
[88] F. K. Lam, Yong-Sheng Yang, F. H. Y. Chan, Yuan-Ting Zhang, and P. A. Parker, “Fuzzy EMG classification for prosthesis control,” *IEEE Trans. Rehabil. Eng.*, vol. 8, no. 3, pp. 305–311, 2002.
[89] O. Fukuda, T. Tsuji, M. Kaneko, and A. Otsuka, “A human-assisting manipulator teleoperated by EMG signals and arm motions,” *IEEE Trans. Robot. Autom.*, vol. 19, no. 2, pp. 210–222, 2003.
[90] A. M. Vögele, R. R. Zsoldos, B. Krüger, and T. Licka, “Novel methods for surface emg analysis and exploration based on multi-modal Gaussian mixture models,” *PLoS One*, vol. 11, no. 6, 2016.
[91] S. Jain, G. Singhal, R. J. Smith, R. Kaliki, and N. Thakor, “Improving long term myoelectric decoding, using an adaptive classifier with label correction,” *Proc. IEEE RAS EMBS Int. Conf. Biomed. Robot. Biomechatronics*, pp. 532–537, 2012.
[92] M. Ison, I. Vujaklija, B. Whitsell, D. Farina, and P. Artemiadis, “High-Density

Electromyography and Motor Skill Learning for Robust Long-Term Control of a 7-DoF Robot Arm," *IEEE Trans. Neural Syst. Rehabil. Eng.*, vol. 24, no. 4, pp. 424–433, Apr. 2016.
[93] Y. M. Zhao, W. F. Xie, S. Liu, and T. Wang, "Neural Network-Based Image Moments for Robotic Visual Servoing," *J. Intell. Robot. Syst. Theory Appl.*, vol. 78, no. 2, pp. 239–256, 2015.
[94] C. R. Rao, "The Utilization of Multiple Measurements in Problems of Biological Classification," *J. R. Stat. Soc. Ser. B*, vol. 10, no. 2, pp. 159–193, 2018.
[95] D. Zhang, X. Zhao, J. Han, and Y. Zhao, "A comparative study on PCA and LDA based EMG pattern recognition for anthropomorphic robotic hand," *Proc. - IEEE Int. Conf. Robot. Autom.*, pp. 4850–4855, 2014.
[96] A. J. Young, L. H. Smith, E. J. Rouse, and L. J. Hargrove, "Classification of simultaneous movements using surface EMG pattern recognition," *IEEE Trans. Biomed. Eng.*, vol. 60, no. 5, pp. 1250–1258, 2013.
[97] I. Batzianoulis, N. E. Krausz, A. M. Simon, L. Hargrove, and A. Billard, "Decoding the grasping intention from electromyography during reaching motions," *J. Neuroeng. Rehabil.*, vol. 15, no. 1, p. 57, Jun. 2018.
[98] A. J. Young, L. H. Smith, E. J. Rouse, and L. J. Hargrove, "A comparison of the real-time controllability of pattern recognition to conventional myoelectric control for discrete and simultaneous movements," *J. Neuroeng. Rehabil.*, vol. 11, no. 1, 2014.
[99] A. Dellacasa Bellingegni *et al.*, "NLR, MLP, SVM, and LDA: A comparative analysis on EMG data from people with trans-radial amputation," *J. Neuroeng. Rehabil.*, vol. 14, no. 1, Aug. 2017.
[100] A. Phinyomark, F. Quaine, S. Charbonnier, C. Serviere, F. Tarpin-Bernard, and Y. Laurillau, "EMG feature evaluation for improving myoelectric pattern recognition robustness," *Expert Syst. Appl.*, vol. 40, no. 12, pp. 4832–4840, 2013.
[101] K. S. Kim, H. H. Choi, C. S. Moon, and C. W. Mun, "Comparison of k-nearest neighbor, quadratic discriminant and linear discriminant analysis in classification of electromyogram signals based on the wrist-motion directions," *Curr. Appl. Phys.*, vol. 11, no. 3, pp. 740–745, May 2011.
[102] A. Phinyomark, R. N. Khushaba, E. Ibáñez-Marcelo, A. Patania, E. Scheme, and G. Petri, "Navigating features: A topologically informed chart of electromyographic features space," *J. R. Soc. Interface*, vol. 14, no. 137, Dec. 2017.
[103] G. K. Patel, C. Castellini, J. M. Hahne, D. Farina, and S. Dosen, "A classification method for myoelectric control of hand prostheses inspired by muscle coordination," *IEEE Trans. Neural Syst. Rehabil. Eng.*, vol. 26, no. 9, pp. 1745–1755, Sep. 2018.
[104] S. Amsuess *et al.*, "Context-dependent upper limb prosthesis control for natural and robust use," *IEEE Trans. Neural Syst. Rehabil. Eng.*, vol. 24, no. 7, pp. 744–753, 2016.
[105] H. Daley, K. Englehart, L. Hargrove, and U. Kuruganti, "High density electromyography data of normally limbed and transradial amputee subjects for multifunction prosthetic control," *J. Electromyogr. Kinesiol.*, vol. 22, no. 3, pp. 478–484, 2012.
[106] a J. Smola and B. Schölkopf, "A tutorial on support vector regression," *Stat. Comput.*, vol. 14, pp. 199–222, 2004.
[107] H. Wechsler, "Learning from Data: Concepts, Theory and Methods, Vladimir Cherkassky and Filip Mulier, John Wiley, New York, 1998," *Int. J. Robust Nonlinear Control*, vol. 10, no. 9, pp. 747–748, Jul. 2000.
[108] T. Hastie, R. Tibshirani, and J. Friedman, *The Elements of Statistical Learning The Elements of Statistical Learning*. 2017.
[109] C. E. Rasmussen and C. K. I. Williams, *Gaussian processes for machine learning.*, vol.

14, no. 2. 2004.

[110] M. Raspopovic, S Capogrosso *et al.*, “Restoring Natural Sensory Feedback in Real-Time Bidirectional Hand Prostheses,” *Sci. Transl. Med.*, vol. 6, no. 222, pp. 222ra19-222ra19, 2014.

[111] C. Castellini, P. Van Der Smagt, C. Castellini, and P. Van Der Smagt, “Surface EMG in advanced hand prosthetics,” *Biol. Cybern.*, vol. 100, no. 1, pp. 35–47, Jan. 2009.

[112] S. Pizzolato, L. Tagliapietra, M. Cognolato, M. Reggiani, H. Müller, and M. Atzori, “Comparison of six electromyography acquisition setups on hand movement classification tasks,” *PLoS One*, vol. 12, no. 10, pp. 1–17, 2017.

[113] B. Crawford, “Real-Time Classification of Electromyographic Signals for Robotic Control,” *Proc. AAAI*, pp. 523–528, 2005.

[114] J. Yousefi and A. Hamilton-Wright, “Characterizing EMG data using machine-learning tools,” *Comput. Biol. Med.*, vol. 51, pp. 1–13, 2014.

[115] A. Subasi, “Medical decision support system for diagnosis of neuromuscular disorders using DWT and fuzzy support vector machines,” *Comput. Biol. Med.*, vol. 42, no. 8, pp. 806–815, Aug. 2012.

[116] Y. Gu, D. Yang, Q. Huang, W. Yang, and H. Liu, “Robust EMG pattern recognition in the presence of confounding factors: features, classifiers and adaptive learning,” *Expert Syst. Appl.*, vol. 96, pp. 208–217, Apr. 2018.

[117] S. Guo, M. Pang, B. Gao, H. Hirata, and H. Ishihara, “Comparison of sEMG-based feature extraction and motion classification methods for upper-limb movement,” *Sensors (Switzerland)*, vol. 15, no. 4, pp. 9022–9038, Apr. 2015.

[118] C. Cipriani *et al.*, “Online myoelectric control of a dexterous hand prosthesis by transradial amputees,” *IEEE Trans. Neural Syst. Rehabil. Eng.*, vol. 19, no. 3, pp. 260–270, Jun. 2011.

[119] G. R. Kanitz, C. Antfolk, C. Cipriani, F. Sebelius, and M. C. Carrozza, “Decoding of individuated finger movements using surface EMG and input optimization applying a genetic algorithm,” *Proc. Annu. Int. Conf. IEEE Eng. Med. Biol. Soc. EMBS*, pp. 1608–1611, 2011.

[120] S. Rasheed, D. Stashuk, and M. Kamel, “Adaptive fuzzy k-NN classifier for EMG signal decomposition,” *Med. Eng. Phys.*, vol. 28, no. 7, pp. 694–709, 2006.

[121] C. I. Christodoulou, P. A. Kaplanis, V. Murray, M. S. Pattichis, C. S. Pattichis, and T. Kyriakides, “Multi-scale AM-FM analysis for the classification of surface electromyographic signals,” *Biomed. Signal Process. Control*, vol. 7, no. 3, pp. 265–269, May 2012.

[122] S. K. Au, P. Bonato, and H. Herr, “An EMG-position controlled system for an active ankle-foot prosthesis: An initial experimental study,” *Proc. 2005 IEEE 9th Int. Conf. Rehabil. Robot.*, vol. 2005, pp. 375–379, 2005.

[123] R. H. Chowdhury, M. B. I. Reaz, M. A. Bin Mohd Ali, A. A. A. Bakar, K. Chellappan, and T. G. Chang, “Surface electromyography signal processing and classification techniques,” *Sensors (Switzerland)*, vol. 13, no. 9, pp. 12431–12466, Sep. 2013.

[124] B. Hudgins, P. Parker, and R. N. Scott, “A New Strategy for Multifunction Myoelectric Control,” *IEEE Trans. Biomed. Eng.*, vol. 40, no. 1, pp. 82–94, 1993.

[125] B. Mahmoudi, E. A. Pohlmeyer, N. W. Prins, S. Geng, and J. C. Sanchez, “Towards autonomous neuroprosthetic control using Hebbian reinforcement learning,” *J. Neural Eng.*, vol. 10, no. 6, 2013.

[126] N. A. N. Bu, “EMG-Based Motion Discrimination Using,” *Science (80-.).*, vol. 21, no. 1978, pp. 113–126, 2003.

[127] Q. Zhang, L. T. Yang, Z. Chen, and P. Li, “A survey on deep learning for big data,” *Inf. Fusion*, vol. 42, no. October 2017, pp. 146–157, 2018.

[128] X. W. Chen and X. Lin, "Big data deep learning: Challenges and perspectives," *IEEE Access*, vol. 2, pp. 514–525, 2014.
[129] A. Hartwell, V. Kadirkamanathan, and S. R. Anderson, "Compact Deep Neural Networks for Computationally Efficient Gesture Classification from Electromyography Signals," in *Proceedings of the IEEE RAS and EMBS International Conference on Biomedical Robotics and Biomechatronics*, 2018, vol. 2018-Augus, pp. 891–896.
[130] H. Shim and S. Lee, "Multi-channel electromyography pattern classification using deep belief networks for enhanced user experience," *J. Cent. South Univ.*, vol. 22, no. 5, pp. 1801–1808, 2015.
[131] W. Geng, Y. Du, W. Jin, W. Wei, Y. Hu, and J. Li, "Gesture recognition by instantaneous surface EMG images," *Sci. Rep.*, vol. 6, no. November, pp. 6–13, 2016.
[132] U. Côté-Allard, C. L. Fall, A. Campeau-Lecoursy, C. Gosseliny, F. Laviolettez, and B. Gosselin, "Transfer learning for sEMG hand gestures recognition using convolutional neural networks," in *2017 IEEE International Conference on Systems, Man, and Cybernetics, SMC 2017*, 2017, vol. 2017-Janua, pp. 1663–1668.
[133] M. Atzori, M. Cognolato, and H. Müller, "Deep learning with convolutional neural networks applied to electromyography data: A resource for the classification of movements for prosthetic hands," *Front. Neurorobot.*, vol. 10, no. SEP, p. 9, Sep. 2016.
[134] R. Laezza, "Deep Neural Networks for Myoelectric Pattern Recognition An Implementation for Multifunctional Control," p. 71, 2018.
[135] P. Xia, J. Hu, and Y. Peng, "EMG-Based Estimation of Limb Movement Using Deep Learning With Recurrent Convolutional Neural Networks," *Artif. Organs*, vol. 42, no. 5, pp. E67–E77, May 2018.
[136] Q. Zhang, R. Liu, W. Chen, and C. Xiong, "Simultaneous and continuous estimation of shoulder and elbow kinematics from surface EMG signals," *Front. Neurosci.*, vol. 11, no. MAY, pp. 1–12, 2017.
[137] S. Negi, Y. Kumar, and V. M. Mishra, "Feature extraction and classification for EMG signals using linear discriminant analysis," *Proc. - 2016 Int. Conf. Adv. Comput. Commun. Autom. (Fall), ICACCA 2016*, pp. 1–6, Nov. 2016.
[138] G. C. Matrone, C. Cipriani, E. L. Secco, G. Magenes, M. C. Carrozza, and M. Chiara Carrozza, "Principal components analysis based control of a multi-dof underactuated prosthetic hand," *J. Neuroeng. Rehabil.*, vol. 7, no. 1, pp. 1–13, 2010.
[139] M. Gabiccini, A. Bicchi, D. Prattichizzo, and M. Malvezzi, "On the role of hand synergies in the optimal choice of grasping forces," *Auton. Robots*, vol. 31, no. 2–3, pp. 235–252, 2011.
[140] M. Santello, M. Flanders, and J. F. Soechting, "Postural hand synergies for tool use," *J. Neurosci.*, vol. 18, no. 23, pp. 10105–10115, 1998.
[141] P. Braido and X. Zhang, "Quantitative analysis of finger motion coordination in hand manipulative and gestic acts," *Hum. Mov. Sci.*, vol. 22, no. 6, pp. 661–678, 2004.
[142] E. Todorov, "Optimality principles in sensorimotor control," *Nat. Neurosci.*, vol. 7, no. 9, pp. 907–915, 2004.
[143] E. K., H. B., and P. P.A., "A wavelet-based continuous classification scheme for multifunction myoelectric control," *IEEE Trans. Biomed. Eng.*, vol. 48, no. 3, pp. 302–311, 2001.
[144] Y. Huang, K. B. Englehart, B. Hudgins, and A. D. C. Chan, "A Gaussian mixture model based classification scheme for myoelectric control of powered upper limb prostheses," *IEEE Trans. Biomed. Eng.*, vol. 52, no. 11, pp. 1801–1811, Nov. 2005.
[145] S. Saponas, D. Tan, D. Morris, and R. Balakrishnan, "Demonstrating the Feasibility of Using Forearm Electromyography for Muscle-Computer Interfaces," in *CHI '08 Proceedings of the SIGCHI Conference on Human Factors in Computing Systems*, 2008,

CHI '08 Pr., pp. 515–524.
[146] M. F. F. F. Lucas, A. Gaufriau, S. Pascual, C. Doncarli, and D. Farina, "Multi-channel surface EMG classification using support vector machines and signal-based wavelet optimization," *Biomed. Signal Process. Control*, vol. 3, no. 2, pp. 169–174, Apr. 2008.
[147] F. V. G. G. Tenore, A. Ramos, A. Fahmy, S. Acharya, R. Etienne-Cummings, and N. V. Thakor, "Decoding of individuated finger movements using surface electromyography," *IEEE Trans. Biomed. Eng.*, vol. 56, no. 5, pp. 1427–1434, May 2009.
[148] J. Vogel, C. Castellini, and P. Van Der Smagt, "EMG-based teleoperation and manipulation with the DLR LWR-III," in *IEEE International Conference on Intelligent Robots and Systems*, 2011.
[149] A. Phinyomark, P. Phukpattaranont, and C. Limsakul, "Feature reduction and selection for EMG signal classification," *Expert Syst. Appl.*, vol. 39, no. 8, pp. 7420–7431, Jun. 2012.
[150] D. S. González and C. Castellini, "A realistic implementation of ultrasound imaging as a human-machine interface for upper-limb amputees," *Front. Neurorobot.*, vol. 7, no. October, pp. 1–11, 2013.
[151] X. Chen and Z. J. Wang, "Pattern recognition of number gestures based on a wireless surface EMG system," *Biomed. Signal Process. Control*, vol. 8, no. 2, pp. 184–192, Mar. 2013.
[152] N. Jiang, L. Tian, P. Fang, Y. Dai, G. Li, and S. Member, "Motion Recognition for Simultaneous Control of Multifunctional Transradial Prostheses," *2013 35th Annu. Int. Conf. IEEE Eng. Med. Biol. Soc.*, vol. 2013, pp. 1603–1606, 2013.
[153] D. Farina *et al.*, "The extraction of neural information from the surface EMG for the control of upper-limb prostheses: Emerging avenues and challenges," *IEEE Trans. Neural Syst. Rehabil. Eng.*, vol. 22, no. 4, pp. 797–809, 2014.
[154] M. S. Fifer *et al.*, "Simultaneous neural control of simple reaching and grasping with the modular prosthetic limb using intracranial EEG," *IEEE Trans. Neural Syst. Rehabil. Eng.*, vol. 22, no. 3, pp. 695–705, May 2014.
[155] I. Kyranou, A. Krasoulis, M. S. Erden, K. Nazarpour, and S. Vijayakumar, "Real - Time Classification of Multi - Modal Sensory Data for Prosthetic Hand Control," *2016 6th IEEE Int. Conf. Biomed. Robot. Biomechatronics*, pp. 536–541, 2016.
[156] J. Ma, N. V. Thakor, and F. Matsuno, "Hand and wrist movement control of myoelectric prosthesis based on synergy," *IEEE Trans. Human-Machine Syst.*, vol. 45, no. 1, pp. 74–83, Feb. 2015.
[157] N. Akhlaghi *et al.*, "Real-Time Classification of Hand Motions Using Ultrasound Imaging of Forearm Muscles," *IEEE Trans. Biomed. Eng.*, vol. 63, no. 8, pp. 1687–1698, Aug. 2016.
[158] G. Shuman, Z. Duri, D. Barbará, J. Lin, and L. H. Gerber, "Improving the recognition of grips and movements of the hand using myoelectric signals," vol. 16, no. Suppl 2, 2016.
[159] E. Mastinu, P. Doguet, Y. Botquin, B. Hakansson, and M. Ortiz-Catalan, "Embedded System for Prosthetic Control Using Implanted Neuromuscular Interfaces Accessed Via an Osseointegrated Implant," *IEEE Trans. Biomed. Circuits Syst.*, vol. 11, no. 4, pp. 867–877, Aug. 2017.
[160] J. M. Hahne, M. A. Schweisfurth, M. Koppe, and D. Farina, "Simultaneous control of multiple functions of bionic hand prostheses: Performance and robustness in end users," *Sci. Robot.*, vol. 3, no. 19, Jun. 2018.
[161] A. Ameri, M. A. Akhaee, E. Scheme, and K. Englehart, "Real-time, simultaneous myoelectric control using a convolutional neural network," *PLoS One*, vol. 13, no. 9, 2018.

[162] B. J. Edelman *et al.*, "Noninvasive neuroimaging enhances continuous neural tracking for robotic device control," *Sci. Robot.*, vol. 4, no. 31, p. eaaw6844, 2019.
[163] R. Meattini *et al.*, "Improving Reliability of Myocontrol Using Formal Verification," *Electron.*, vol. 23, no. 5, pp. 564–571, 2019.
[164] L. Zollo *et al.*, "Restoring tactile sensations via neural interfaces for real-time force-and-slippage closed-loop control of bionic hands," *Sci. Robot.*, vol. 4, no. 27, p. eaau9924, 2019.
[165] M. D. Paskett *et al.*, "A Modular Transradial Bypass Socket for Surface Myoelectric Prosthetic Control in Non-Amputees," *IEEE Trans. Neural Syst. Rehabil. Eng.*, vol. 27, no. 10, pp. 2070–2076, Oct. 2019.
[166] O. W. Samuel *et al.*, "Intelligent EMG pattern recognition control method for upper-limb multifunctional prostheses: Advances, current challenges, and future prospects," *IEEE Access*, vol. 7, pp. 10150–10165, 2019.
[167] D. Yeung, D. Farina, and I. Vujaklija, "Directional forgetting for stable co-adaptation in myoelectric control," *Sensors (Switzerland)*, vol. 19, no. 9, pp. 1–14, May 2019.
[168] J. C. V. Tieck, S. Weber, T. C. Stewart, J. Kaiser, A. Roennau, and R. Dillmann, "A spiking network classifies human sEMG signals and triggers finger reflexes on a robotic hand," *Rob. Auton. Syst.*, vol. 131, p. 103566, May 2020.
[169] J. M. Hahne, M. A. Wilke, M. Koppe, D. Farina, and A. F. Schilling, "Longitudinal Case Study of Regression-Based Hand Prosthesis Control in Daily Life," *Front. Neurosci.*, vol. 14, no. June, pp. 1–8, Jun. 2020.
[170] P. G. Sagastegui Alva, S. Muceli, S. F. Atashzar, L. William, and D. Farina, "Wearable multichannel haptic device for encoding proprioception in the upper limb," *J. Neural Eng.*, vol. 17, no. 5, 2020.
[171] A. Bahador, M. Yousefi, M. Marashi, and O. Bahador, "High accurate lightweight deep learning method for gesture recognition based on surface electromyography," *Comput. Methods Programs Biomed.*, vol. 195, p. 105643, 2020.
[172] J. Fajardo, G. Maldonado, D. Cardona, V. Ferman, and E. Rohmer, "Evaluation of user-prosthesis-interfaces for semg-based multifunctional prosthetic hands," *Sensors*, vol. 21, no. 21, 2021.
[173] K. T. Kim, S. Park, T. H. Lim, and S. J. Lee, "Upper-Limb Electromyogram Classification of Reaching-to-Grasping Tasks Based on Convolutional Neural Networks for Control of a Prosthetic Hand," *Front. Neurosci.*, vol. 15, 2021.
[174] D. K. Luu *et al.*, "Deep Learning-Based Approaches for Decoding Motor Intent From Peripheral Nerve Signals," *Front. Neurosci.*, vol. 15, p. 667907, 2021.
[175] N. J. Jarque-Bou, J. L. Sancho-Bru, and M. Vergara, "A systematic review of EMG applications for the characterization of forearm and hand muscle activity during activities of daily living: Results, challenges, and open issues," *Sensors*, vol. 21, no. 9. 2021.
[176] A. Jaramillo-Yánez, M. E. Benalcázar, and E. Mena-Maldonado, "Real-time hand gesture recognition using surface electromyography and machine learning: A systematic literature review," *Sensors (Switzerland)*, vol. 20, no. 9. 2020.
[177] C. Cipriani, F. Zaccone, S. Micera, and M. C. Carrozza, "On the Shared Control of an EMG-Controlled Prosthetic Hand: Analysis of User–Prosthesis Interaction," *IEEE Trans. Robot.*, vol. 24, no. 1, pp. 170–184, Feb. 2008.
[178] E. Biddiss and T. Chau, "Upper-limb prosthetics: Critical factors in device abandonment," *Am. J. Phys. Med. Rehabil.*, vol. 86, no. 12, pp. 977–987, 2007.
[179] K. Østlie *et al.*, "Prosthesis rejection in acquired major upper-limb amputees: A population-based survey," *Disabil. Rehabil. Assist. Technol.*, vol. 7, no. 4, pp. 294–303, Jul. 2012.

[180] L. Resnik, S. Ekerholm, M. Borgia, and M. A. Clark, “A national study of Veterans with major upper limb amputation: Survey methods, participants, and summary findings,” *PLoS One*, vol. 14, no. 3, pp. 1–24, Mar. 2019.

[181] M. B. I. Reaz, M. S. Hussain, and F. Mohd-Yasin, “Techniques of EMG signal analysis: Detection, processing, classification and applications,” *Biol. Proced. Online*, vol. 8, no. 1, pp. 11–35, 2006.

[182] M. Jochumsen, A. Waris, and E. N. Kamavuako, “The effect of arm position on classification of hand gestures with intramuscular EMG,” *Biomed. Signal Process. Control*, vol. 43, pp. 1–8, May 2018.

[183] M. Isaković *et al.*, “Electrotactile feedback improves performance and facilitates learning in the routine grasping task,” *Eur. J. Transl. Myol.*, vol. 26, no. 3, pp. 197–202, 2016.

[184] E. J. Weiss and M. Flanders, “Muscular and postural synergies of the human hand,” *J. Neurophysiol.*, vol. 92, no. 1, pp. 523–535, 2004.

[185] O. Alizadehkhaiyat and S. P. Frostick, “Electromyographic assessment of forearm muscle function in tennis players with and without Lateral Epicondylitis,” *J. Electromyogr. Kinesiol.*, vol. 25, no. 6, pp. 876–886, 2015.

[186] S. Zhou, K. Yin, F. Fei, and K. Zhang, “Surface electromyography–based hand movement recognition using the Gaussian mixture model, multilayer perceptron, and AdaBoost method,” *Int. J. Distrib. Sens. Networks*, vol. 15, no. 4, Apr. 2019.

[187] V. H. Cene, M. Tosin, J. Machado, and A. Balbinot, “Open database for accurate upper-limb intent detection using electromyography and reliable extreme learning machines,” *Sensors (Switzerland)*, vol. 19, no. 8, p. 1864, Apr. 2019.

[188] B. Peerdeman *et al.*, “Myoelectric forearm prostheses: State of the art from a user-centered perspective,” vol. 48, no. 6, 2011.

[189] M. Connan, R. Kõiva, and C. Castellini, “Online Natural Myocontrol of Combined Hand and Wrist Actions Using Tactile Myography and the Biomechanics of Grasping,” *Front. Neurorobot.*, vol. 14, no. February, pp. 1–16, Feb. 2020.

[190] D. Yang *et al.*, “Experimental Study of an EMG-Controlled 5-DOF Anthropomorphic Prosthetic Hand for Motion Restoration,” vol. 76, no. 3–4, pp. 427–441, Oct. 2014.

[191] M. Atzori, A. Gijsberts, H. Müller, B. Caputo, H. Muller, and B. Caputo, “Classification of hand movements in amputated subjects by sEMG and accelerometers,” *2014 36th Annu. Int. Conf. IEEE Eng. Med. Biol. Soc. EMBC 2014*, pp. 3545–3549, 2014.

[192] A. H. Al-Timemy, G. Bugmann, J. Escudero, and N. Outram, “Classification of finger movements for the dexterous hand prosthesis control with surface electromyography,” *IEEE J. Biomed. Heal. Informatics*, vol. 17, no. 3, pp. 608–618, 2013.

[193] “VMG 30 Virtual Reality Glove - Virtual Motion Labs :” [Online]. Available: https://www.virtualmotionlabs.com/vr-gloves/vmg-30/. [Accessed: 17-May-2021].

[194] G. De Luca, “Fundamental Concepts in EMG Signal Acquisition,” *Delsys Inc.*, no. March, pp. 1–31, 2003.

[195] R. N. Khushaba, M. Takruri, J. V. Miro, and S. Kodagoda, “Towards limb position invariant myoelectric pattern recognition using time-dependent spectral features,” *Neural Networks*, vol. 55, pp. 42–58, 2014.

[196] H. J. Hermens, B. Freriks, C. Disselhorst-Klug, and G. Rau, “Development of recommendations for SEMG sensors and sensor placement procedures,” *J. Electromyogr. Kinesiol.*, vol. 10, no. 5, pp. 361–374, Oct. 2000.

[197] P. Zhou *et al.*, “Decoding a new neural-machine interface for control of artificial limbs,” *J. Neurophysiol.*, vol. 98, no. 5, pp. 2974–2982, Nov. 2007.

[198] I. M. Bullock, J. Z. Zheng, S. De La Rosa, C. Guertler, and A. M. Dollar, “Grasp frequency and usage in daily household and machine shop tasks,” *IEEE Trans. Haptics*,

vol. 6, no. 3, pp. 296–308, 2013.
[199] J. J. V. Mayor, R. M. Costa, A. Frizera Neto, and T. F. Bastos, "Dexterous hand gestures recognition based on low-density sEMG signals for upper-limb forearm amputees," *Res. Biomed. Eng.*, vol. 33, no. 3, pp. 202–217, 2017.
[200] J. T. Belter, J. L. Segil, A. M. Dollar, and R. F. Weir, "Mechanical design and performance specifications of anthropomorphic prosthetic hands: A review," *J. Rehabil. Res. Dev.*, vol. 50, no. 5, p. 599, 2013.
[201] C. Martelloni, J. Carpaneto, and S. Micera, "Characterization of EMG Patterns From Proximal Arm Muscles During Object- and Orientation-Specific Grasps," *IEEE Trans. Biomed. Eng.*, vol. 56, no. 10, pp. 2529–2536, 2009.
[202] J. M. Inouye and F. J. Valero-Cuevas, "Muscle Synergies Heavily Influence the Neural Control of Arm Endpoint Stiffness and Energy Consumption," *PLoS Comput. Biol.*, vol. 12, no. 2, pp. 1–24, 2016.
[203] S. Thongpanja, A. Phinyomark, F. Quaine, Y. Laurillau, C. Limsakul, and P. Phukpattaranont, "Probability Density Functions of Stationary Surface EMG Signals in Noisy Environments," *IEEE Trans. Instrum. Meas.*, vol. 65, no. 7, pp. 1547–1557, Jul. 2016.
[204] A. Burden, "How should we normalize electromyograms obtained from healthy participants? What we have learned from over 25years of research," *J. Electromyogr. Kinesiol.*, vol. 20, no. 6, pp. 1023–1035, Dec. 2010.
[205] S. Benatti, E. Farella, E. Gruppioni, and L. Benini, "Analysis of robust implementation of an EMG pattern recognition based control," in *BIOSIGNALS 2014 - 7th Int. Conference on Bio-Inspired Systems and Signal Processing, Proceedings; Part of 7th Int. Joint Conference on Biomedical Engineering Systems and Technologies, BIOSTEC 2014*, 2014, pp. 45–54.
[206] C. J. De Luca, "S URFACE E LECTROMYOGRAPHY : D ETECTION AND R ECORDING," pp. 1–10, 2002.
[207] J. A. Birdwell, L. J. Hargrove, R. F. Weir, and T. A. Kuiken, "Extrinsic finger and thumb muscles command a virtual hand to allow individual finger and grasp control," *IEEE Trans. Biomed. Eng.*, vol. 62, no. 1, pp. 218–226, Jan. 2015.
[208] L. H. Smith, T. A. Kuiken, and L. J. Hargrove, "Real-time simultaneous and proportional myoelectric control using intramuscular EMG," *J. Neural Eng.*, vol. 11, no. 6, p. 066013, Dec. 2014.
[209] D. Yang, Y. Gu, L. Jiang, L. Osborn, and H. Liu, "Dynamic training protocol improves the robustness of PR-based myoelectric control," *Biomed. Signal Process. Control*, vol. 31, pp. 249–256, 2017.
[210] E. Scheme, A. Fougner, Stavdahl, A. D. C. Chan, and K. Englehart, "Examining the adverse effects of limb position on pattern recognition based myoelectric control," in *2010 Annual International Conference of the IEEE Engineering in Medicine and Biology Society, EMBC'10*, 2010, pp. 6337–6340.
[211] X. Zhang, X. Li, O. W. Samuel, Z. Huang, P. Fang, and G. Li, "Improving the robustness of electromyogram-pattern recognition for prosthetic control by a postprocessing strategy," *Front. Neurorobot.*, vol. 11, no. SEP, pp. 1–15, Sep. 2017.
[212] C. Ahmadizadeh, L. K. Merhi, B. Pousett, S. Sangha, and C. Menon, "Toward Intuitive Prosthetic Control: Solving Common Issues Using Force Myography, Surface Electromyography, and Pattern Recognition in a Pilot Case Study," *IEEE Robot. Autom. Mag.*, vol. 24, no. 4, pp. 102–111, Dec. 2017.
[213] O. W. Samuel *et al.*, "Resolving the adverse impact of mobility on myoelectric pattern recognition in upper-limb multifunctional prostheses," *Comput. Biol. Med.*, vol. 90, no. September, pp. 76–87, Nov. 2017.

[214] G. R. Müller-Putz, R. Scherer, G. Pfurtscheller, and R. Rupp, "EEG-based neuroprosthesis control: A step towards clinical practice," *Neurosci. Lett.*, vol. 382, no. 1–2, pp. 169–174, 2005.

[215] H. J. Hwang, J. M. Hahne, and K. R. Müller, "Real-time robustness evaluation of regression based myoelectric control against arm position change and donning/doffing," *PLoS One*, vol. 12, no. 11, p. e0186318, Nov. 2017.

[216] A. Phinyomark, R. N. Khushaba, and E. Scheme, "Feature extraction and selection for myoelectric control based on wearable EMG sensors," *Sensors (Switzerland)*, vol. 18, no. 5, pp. 1–17, May 2018.

[217] A. Alkan and M. Günay, "Identification of EMG signals using discriminant analysis and SVM classifier," *Expert Syst. Appl.*, vol. 39, no. 1, pp. 44–47, 2012.

[218] H. P. Huang, Y. H. Liu, and C. S. Wong, "Automatic EMG feature evaluation for controlling a prosthetic hand using a supervised feature mining method: An intelligent approach," in *Proceedings - IEEE International Conference on Robotics and Automation*, 2003, vol. 1, pp. 220–225.

[219] D. Yang, Y. Gu, R. Liu, and H. Liu, "Dexterous motion recognition for myoelectric control of multifunctional transradial prostheses," *Adv. Robot.*, vol. 28, no. 22, pp. 1533–1543, 2014.

[220] G. Li, Y. Li, L. Yu, and Y. Geng, "Conditioning and sampling issues of EMG signals in motion recognition of multifunctional myoelectric prostheses," *Ann. Biomed. Eng.*, vol. 39, no. 6, pp. 1779–1787, 2011.

[221] Z. Zhang, X. Yu, and J. Qian, "Classification of finger movements for prosthesis control with surface electromyography," *Sensors Mater.*, vol. 32, no. 4, pp. 1523–1532, 2020.

[222] C. Cipriani, R. Sassu, M. Controzzi, and M. C. Carrozza, "Influence of the weight actions of the hand prosthesis on the performance of pattern recognition based myoelectric control: Preliminary study," in *Proceedings of the Annual International Conference of the IEEE Engineering in Medicine and Biology Society, EMBS*, 2011, pp. 1620–1623.

[223] E. A. Chung and M. E. Benalcázar, "Real-time hand gesture recognition model using deep learning techniques and EMG signals," in *European Signal Processing Conference*, 2019, vol. 2019-Septe.

[224] M. Lebedev *et al.*, "Self-Recalibrating Surface EMG Pattern Recognition for Neuroprosthesis Control Based on Convolutional Neural Network," *Front. Neurosci. | www.frontiersin.org*, vol. 1, p. 379, 2017.

[225] I. Kuzborskij, A. Gijsberts, and B. Caputo, "On the challenge of classifying 52 hand movements from surface electromyography," *Proc. Annu. Int. Conf. IEEE Eng. Med. Biol. Soc. EMBS*, pp. 4931–4937, 2012.

[226] M. Atzori *et al.*, "Characterization of a benchmark database for myoelectric movement classification," *IEEE Trans. Neural Syst. Rehabil. Eng.*, vol. 23, no. 1, pp. 73–83, 2015.

[227] C. Castellini, E. Gruppioni, A. Davalli, and G. Sandini, "Fine detection of grasp force and posture by amputees via surface electromyography," *J. Physiol. Paris*, vol. 103, no. 3–5, pp. 255–262, Sep. 2009.

[228] M. Ortiz-Catalan, F. Rouhani, R. Branemark, and B. Hakansson, "Offline accuracy: A potentially misleading metric in myoelectric pattern recognition for prosthetic control," *Proc. Annu. Int. Conf. IEEE Eng. Med. Biol. Soc. EMBS*, vol. 2015-Novem, pp. 1140–1143, Nov. 2015.

[229] I. Vujaklija *et al.*, "Translating research on myoelectric control into clinics-are the performance assessment methods adequate?," *Front. Neurorobot.*, vol. 11, no. FEB, pp. 1–7, Feb. 2017.

[230] A. Gijsberts *et al.*, "Stable myoelectric control of a hand prosthesis using non-linear

incremental learning," *Front. Neurorobot.*, vol. 8, no. FEB, pp. 1–15, 2014.
[231] M. Gazzoni, N. Celadon, D. Mastrapasqua, M. Paleari, V. Margaria, and P. Ariano, "Quantifying Forearm Muscle Activity during Wrist and Finger Movements by Means of Multi-Channel Electromyography," *PLoS One*, vol. 9, no. 10, p. e109943, Oct. 2014.
[232] L. Haverkate, G. Smit, and Di. H. Plettenburg, "Assessment of body-powered upper limb prostheses by able-bodied subjects, using the Box and Blocks Test and the Nine-Hole Peg Test," *Prosthet. Orthot. Int.*, vol. 40, no. 1, pp. 109–116, 2016.
[233] A. Krasoulis, I. Kyranou, M. S. Erden, K. Nazarpour, and S. Vijayakumar, "Improved prosthetic hand control with concurrent use of myoelectric and inertial measurements," *J. Neuroeng. Rehabil.*, vol. 14, no. 1, pp. 1–14, 2017.
[234] M. Santello *et al.*, "Hand synergies: Integration of robotics and neuroscience for understanding the control of biological and artificial hands," *Phys. Life Rev.*, vol. 17, pp. 1–23, 2016.
[235] C. J. De Luca, L. Donald Gilmore, M. Kuznetsov, and S. H. Roy, "Filtering the surface EMG signal: Movement artifact and baseline noise contamination," *J. Biomech.*, vol. 43, no. 8, pp. 1573–1579, 2010.
[236] A. Fougner, E. Scheme, A. D. C. Chan, K. Englehart, and Ø. Stavdahl, "Resolving the limb position effect in myoelectric pattern recognition," *IEEE Trans. Neural Syst. Rehabil. Eng.*, vol. 19, no. 6, pp. 644–651, 2011.
[237] E. Scheme, K. Biron, and K. Englehart, "Improving myoelectric pattern recognition positional robustness using advanced training protocols," in *Proceedings of the Annual International Conference of the IEEE Engineering in Medicine and Biology Society, EMBS*, 2011, pp. 4828–4831.
[238] J. E. Cheesborough, L. H. Smith, T. A. Kuiken, G. A. Dumanian, L. H. Smith, and T. A. Kuiken, "Targeted Muscle Reinnervation and Advanced Prosthetic Arms," vol. 29, no. 1, pp. 62–72, Feb. 2015.
[239] P. P. Vu *et al.*, "A regenerative peripheral nerve interface allows real-time control of an artificial hand in upper limb amputees," *Sci. Transl. Med.*, vol. 12, no. 533, p. eaay2857, Mar. 2020.
[240] J. Robertson, "Effects of Confidence-Based Rejection on Usability and Error in Pattern Recognition-Based Myoelectric Control Confidence-Based Rejection Threshold and User Error View project Enhancement of muscle and locomotor performance by a series compliance View proj," *Artic. IEEE J. Biomed. Heal. Informatics*, 2019.
[241] L. Resnik, H. Huang, A. Winslow, D. L. Crouch, F. Zhang, and N. Wolk, "Evaluation of EMG pattern recognition for upper limb prosthesis control: a case study in comparison with direct myoelectric control," *J. Neuroeng. Rehabil.*, vol. 15, no. 1, p. 23, Dec. 2018.
[242] M. K. Rand, Y. P. Shimansky, A. B. M. I. Hossain, and G. E. Stelmach, "Quantitative model of transport-aperture coordination during reach-to-grasp movements," *Exp. Brain Res.*, vol. 188, no. 2, pp. 263–274, Jun. 2008.
[243] I. Batzianoulis, S. El-Khoury, E. Pirondini, M. Coscia, S. Micera, and A. Billard, "EMG-based decoding of grasp gestures in reaching-to-grasping motions," *Rob. Auton. Syst.*, vol. 91, pp. 59–70, May 2017.
[244] W. T. Shi, Z. J. Lyu, S. T. Tang, T. L. Chia, and C. Y. Yang, "A bionic hand controlled by hand gesture recognition based on surface EMG signals: A preliminary study," *Biocybern. Biomed. Eng.*, vol. 38, no. 1, pp. 126–135, 2018.
[245] S. Benatti *et al.*, "A Versatile Embedded Platform for EMG Acquisition and Gesture Recognition," *IEEE Trans. Biomed. Circuits Syst.*, vol. 9, no. 5, pp. 620–630, 2015.
[246] M. Ortiz-Catalan, B. Ha˚kansson, and R. Bra˚nemark, "An osseointegrated human-machine gateway for long-term sensory feedback and motor control of artificial limbs,"

Sci. Transl. Med., vol. 6, no. 257, p. 257re6, Oct. 2014.
[247] *The Promise of Assistive Technology to Enhance Activity and Work Participation*. National Academies Press, 2017.
[248] S. Benatti, B. Milosevic, E. Farella, E. Gruppioni, and L. Benini, "A prosthetic hand body area controller based on efficient pattern recognition control strategies," *Sensors (Switzerland)*, vol. 17, no. 4, p. 869, Apr. 2017.
[249] S. Jönsson, K. Caine-Winterberger, and R. Branemark, "Osseointegration amputation prostheses on the upper limbs: Methods, prosthetics and rehabilitation," *Prosthet. Orthot. Int.*, vol. 35, no. 2, pp. 190–200, Jun. 2011.
[250] E. L. Graczyk, L. Resnik, M. A. Schiefer, M. S. Schmitt, and D. J. Tyler, "Home use of a neural-connected sensory prosthesis provides the functional and psychosocial experience of having a hand again," *Sci. Rep.*, vol. 8, no. 1, pp. 1–17, 2018.
[251] J. S. Head, D. Howard, S. W. Hutchins, L. Kenney, G. H. Heath, and A. Y. Aksenov, "The use of an adjustable electrode housing unit to compare electrode alignment and contact variation with myoelectric prosthesis functionality: A pilot study," *Prosthet. Orthot. Int.*, vol. 40, no. 1, pp. 123–128, Feb. 2016.
[252] M. Ortiz-Catalan, B. Håkansson, and R. Brånemark, "Real-time and simultaneous control of artificial limbs based on pattern recognition algorithms," *IEEE Trans. Neural Syst. Rehabil. Eng.*, vol. 22, no. 4, pp. 756–764, 2014.
[253] S. Abbaspour, M. Lindén, H. Gholamhosseini, A. Naber, and M. Ortiz-Catalan, "Evaluation of surface EMG-based recognition algorithms for decoding hand movements," *Med. Biol. Eng. Comput.*, vol. 58, no. 1, pp. 83–100, 2020.
[254] J. Gonzalez-vargas, S. Dosen, S. Amsuess, W. Yu, and D. Farina, "Human-machine interface for the control of multi-function systems based on electrocutaneous menu: Application to multi-grasp prosthetic hands," *PLoS One*, vol. 10, no. 6, pp. 1–26, Jun. 2015.
[255] W. W. Lee *et al.*, "A neuro-inspired artificial peripheral nervous system for scalable electronic skins," *Sci. Robot.*, vol. 4, no. 32, Jul. 2019.
[256] "Improved comfort and adhesion with the SiOCX TR socket system | Ottobock US." [Online]. Available: https://www.ottobockus.com/prosthetics/upper-limb-prosthetics/solution-overview/siocx-tr-socket-upper-limb/. [Accessed: 08-Apr-2020].
[257] D. Yang *et al.*, "Improving the functionality, robustness, and adaptability of myoelectric control for dexterous motion restoration," *Exp. Brain Res.*, vol. 237, no. 2, pp. 291–311, 2019.
[258] C. Ahmadizadeh, B. Pousett, and C. Menon, "Investigation of Channel Selection for Gesture Classification for Prosthesis Control Using Force Myography: A Case Study," *Front. Bioeng. Biotechnol.*, vol. 7, no. December, pp. 1–15, 2019.
[259] N. Jiang, H. Rehbaum, I. Vujaklija, B. Graimann, and D. Farina, "Intuitive, online, simultaneous, and proportional myoelectric control over two degrees-of-freedom in upper limb amputees," *IEEE Trans. Neural Syst. Rehabil. Eng.*, vol. 22, no. 3, pp. 501–510, 2014.
[260] A. M. Simon, L. J. Hargrove, B. A. Lock, and T. A. Kuiken, "Target achievement control test: Evaluating real-time myoelectric pattern-recognition control of multifunctional upper-limb prostheses," *J. Rehabil. Res. Dev.*, vol. 48, no. 6, pp. 619–628, 2011.
[261] L. Hargrove, L. Miller, K. Turner, and T. Kuiken, "Control within a virtual environment is correlated to functional outcomes when using a physical prosthesis," *J. Neuroeng. Rehabil.*, vol. 15, no. Suppl 1, pp. 1–7, Sep. 2018.
[262] S. Amsuess, P. Goebel, B. Graimann, and D. Farina, "A multi-class proportional myocontrol algorithm for upper limb prosthesis control: Validation in real-life scenarios on amputees," *IEEE Trans. Neural Syst. Rehabil. Eng.*, vol. 23, no. 5, pp. 827–836, Sep.

2015.
[263] A. Hussaini and P. Kyberd, "Refined clothespin relocation test and assessment of motion," *Prosthet. Orthot. Int.*, vol. 41, no. 3, pp. 294–302, 2017.
[264] H. Yang *et al.*, "An Affordable Linkage-and-Tendon Hybrid-Driven Anthropomorphic Robotic Hand—MCR-Hand II," *J. Mech. Robot.*, vol. 13, no. 2, Apr. 2021.
[265] J. Gusman, E. Mastinu, and M. Ortiz-Catalán, "Evaluation of computer-based target achievement tests for myoelectric control," *IEEE J. Transl. Eng. Heal. Med.*, vol. 5, no. December, Nov. 2017.
[266] C. Castellini *et al.*, "Proceedings of the first workshop on peripheral machine interfaces: Going beyond traditional surface electromyography," *Frontiers in Neurorobotics*, vol. 8, no. AUG. 2014.
[267] A. K. Mukhopadhyay and S. Samui, "An experimental study on upper limb position invariant EMG signal classification based on deep neural network," *Biomed. Signal Process. Control*, vol. 55, p. 101669, 2020.
[268] F. Leone *et al.*, "Simultaneous sEMg classification of hand/wrist gestures and forces," *Front. Neurorobot.*, vol. 13, no. June, p. 42, Jun. 2019.
[269] W. Li, P. Shi, and H. Yu, "Gesture Recognition Using Surface Electromyography and Deep Learning for Prostheses Hand: State-of-the-Art, Challenges, and Future," *Frontiers in Neuroscience*, vol. 15. p. 621885, 2021.
[270] S. Liang *et al.*, "Identification of Gesture Based on Combination of Raw sEMG and sEMG Envelope Using Supervised Learning and Univariate Feature Selection," *J. Bionic Eng.*, vol. 16, pp. 647–662, 2019.
[271] G. C. Luh, Y. H. Ma, C. J. Yen, and H. A. Lin, "Muscle-gesture robot hand control based on sEMG signals with wavelet transform features and neural network classifier," *Proc. - Int. Conf. Mach. Learn. Cybern.*, vol. 2, pp. 627–632, 2016.
[272] E. J. Scheme, B. S. Hudgins, and K. B. Englehart, "Confidence-based rejection for improved pattern recognition myoelectric control," *IEEE Trans. Biomed. Eng.*, vol. 60, no. 6, pp. 1563–1570, 2013.
[273] I. Strazzulla, M. Nowak, M. Controzzi, C. Cipriani, and C. Castellini, "Online Bimanual Manipulation Using Surface Electromyography and Incremental Learning," *IEEE Trans. Neural Syst. Rehabil. Eng.*, vol. 25, no. 3, pp. 227–234, Mar. 2017.
[274] T. R. Farrell and R. F. Weir, "The optimal controller delay for myoelectric prostheses," *IEEE Trans. Neural Syst. Rehabil. Eng.*, vol. 15, no. 1, pp. 111–118, Mar. 2007.
[275] H. Yang *et al.*, "A low-ccost linkage-spring-sendon-integrated compliant anthropomorphic robotic hand: MCR-Hand III," *Mech. Mach. Theory*, vol. 158, Apr. 2021.
[276] A. A. Adewuyi, L. J. Hargrove, and T. A. Kuiken, "An Analysis of Intrinsic and Extrinsic Hand Muscle EMG for Improved Pattern Recognition Control," *IEEE Trans. Neural Syst. Rehabil. Eng.*, vol. 24, no. 4, pp. 485–494, Apr. 2016.
[277] J. Liu, D. Zhang, X. Sheng, and X. Zhu, "Quantification and solutions of arm movements effect on sEMG pattern recognition," *Biomed. Signal Process. Control*, vol. 13, no. 1, pp. 189–197, 2014.
[278] J. M. Hahne *et al.*, "Linear and nonlinear regression techniques for simultaneous and proportional myoelectric control," *IEEE Trans. Neural Syst. Rehabil. Eng.*, vol. 22, no. 2, pp. 269–279, 2014.
[279] T. S. Davis *et al.*, "Restoring motor control and sensory feedback in people with upper extremity amputations using arrays of 96 microelectrodes implanted in the median and ulnar nerves," *J. Neural Eng.*, vol. 13, no. 3, 2016.
[280] "MAN-025-3-2 Trigno SDK User Guide 1 of 33 TRIGNO™ Wireless System SDK User's Guide," 2019.

[281] L. Zoubek, S. Charbonnier, S. Lesecq, A. Buguet, and F. Chapotot, “Feature selection for sleep/wake stages classification using data driven methods,” *Biomed. Signal Process. Control*, vol. 2, no. 3, pp. 171–179, Jul. 2007.
[282] “PQ12-63-12-S | Actuonix Miniature Electric Linear Actuator - 20% Duty Cycle, 12V dc, 20mm | RS Components.” [Online]. Available: https://uk.rs-online.com/web/p/electric-linear-actuators/2020769/. [Accessed: 16-May-2021].
[283] “Raspberry Pi 4 4G Model B | Raspberry Pi 4 B 4GB | RS Components.” [Online]. Available: https://uk.rs-online.com/web/p/raspberry-pi/1822096/. [Accessed: 16-May-2021].
[284] “Chestnut_PCB/Chestnut Board Data Sheet.pdf at master · Open-Bionics/Chestnut_PCB · GitHub.” [Online]. Available: https://github.com/Open-Bionics/Chestnut_PCB/blob/master/Chestnut Board Data Sheet.pdf. [Accessed: 16-May-2021].
[285] “RS PRO 7.4V Lithium-Ion Rechargeable Battery Pack, 5.2Ah | RS Components.” [Online]. Available: https://uk.rs-online.com/web/p/rechargeable-battery-packs/1449411/. [Accessed: 16-May-2021].
[286] “Trigno® Avanti Sensor - Delsys.” [Online]. Available: https://delsys.com/trigno-avanti/. [Accessed: 10-May-2021].
[287] R. A. FISHER, “the Use of Multiple Measurements in Taxonomic Problems,” *Ann. Eugen.*, vol. 7, no. 2, pp. 179–188, 2011.
[288] N. Cristianini, J. Shawe-Taylor, Subject, M. Learning, Algorithms, and K. Functions, *An Introduction to Support Vector Machines and Other Kernel-based Learning Methods*. Cambridge: : Cambridge University Press, 2000.